INSIGHTS INTO THE ROLE OF ACETYLATION IN *SALMONELLA ENTERICA*: REGULATION OF REVERSIBLE LYSINE ACETYLATION AND THE DETOXIFICATION OF OXIDIZED METHIONINE DERIVATIVES

by

KRISTY LYNN HENTCHEL

(Under the Direction of JORGE C. ESCALANTE-SEMERENA)

ABSTRACT

Protein and small molecule acetylation are widespread in nature. Acetylation can affect the function, activity, or stability of proteins, or alter the structure of small molecules. Acetylation provides an advantageous mechanism for altering activity of the target substrate, allowing for rapid alteration of physiology in response to environmental cues. Many of the enzymes catalyzing acetylation reactions belong to the Gcn5 *N*-acetyltransferase (GNAT) family. The majority of organisms encode around ~25 GNATs and the majority of these enzymes do not have known functions.

In *S. enterica,* reversible lysine acetylation (RLA) of proteins is controlled by a GNAT (Pat) and a NAD^+-dependent sirtuin deacetylase (CobB). RLA control is needed to modify the activity of the AMP-forming CoA ligases, such as the acetyl-CoA synthetase (Acs) enzyme that is required for growth in conditions containing acetate. The first portion of this work describes the identification of a transcriptional regulator, IolR, which activates expression of this system, and integrates the expression with that of the target substrate, Acs. This provided the first example of

the acetylation / deacetylation system and its target being under the control the same transcriptional regulator.

Only one protein acetyltransferase has been identified in *S. enterica* (Pat), and the majority of the characterized GNATs of *S. enterica* acetylate small molecule targets. The second portion of this work characterizes a subset of GNAT enzymes annotated as phosphinothricin acetyltransferases. These enzymes display varying specificity for phosphinothricin, or the closely related analogues methionine sulfoximine and methionine sulfone. This work provided information on how *S. enterica* and organisms respond to and detoxify harmful compounds present in the environment.

INDEX WORDS: acetylation, Gcn5 *N*-acetyltransferase, bacteria, *Salmonella*

INSIGHTS INTO THE ROLE OF ACETYLATION IN *SALMONELLA ENTERICA*: REGULATION OF REVERSIBLE LYSINE ACETYLATION AND THE DETOXIFICATION OF OXIDIZED METHIONINE DERIVATIVES

by

KRISTY LYNN HENTCHEL

BS, Indiana University, 2009

A Dissertation Submitted to the Graduate Faculty of The University of Georgia in Partial Fulfillment of the Requirements for the Degree

DOCTOR OF PHILOSOPHY

ATHENS, GEORGIA

2015

INSIGHTS INTO THE ROLE OF ACETYLATION IN *SALMONELLA ENTERICA*: REGULATION OF REVERSIBLE LYSINE ACETYLATION AND THE DETOXIFICATION OF OXIDIZED METHIONINE DERIVATIVES

by

KRISTY LYNN HENTCHEL

Major Professor:	Jorge C. Escalante-Semerena
Committee:	Diana M. Downs
	Anna C. Glasgow Karls
	Timothy R. Hoover

Electronic Version Approved:

Suzanne Barbour
Dean of the Graduate School
The University of Georgia
August 2015

ACKNOWLEDGEMENTS

I want to thank the faculty members at both the University of Wisconsin and the University of Georgia for their help, support, and valuable advice throughout my graduate studies. I would like to especially recognize my advisor, Dr. Jorge Escalante-Semerena, for being wonderfully supportive and optimistic about my science, and taking the time to help me grow and develop as a scientist. My thesis committee members at both the University of Wisconsin (Dr. Diana Downs, Dr. Paul Weimer, Dr. Nancy Keller, and Dr. Rodney Welch) and the University of Georgia (Dr. Diana Downs, Dr. Anna Glasgow Karls, and Dr. Timothy Hoover) have each contributed to my scientific development throughout my graduate career.

I would also like to acknowledge my undergraduate advisor, Dr. Malcolm Winkler, for providing me with a solid scientific foundation for my graduate work, as well as continuing to support me throughout my graduate career. Under the mentorship of both he and Dr. Smirla Ramos-Montanez I first learned how to approach a scientific question.

Members of the Escalante lab (Dr. Alex Tucker, Dr. Heidi Crosby, Dr. Chi Ho Chan, Dr. Sandy Thao, Ted Moore, Norbert Tavares, and Chelsey VanDrisse) have provided help with technical support, scientific feedback, experimental design, troubleshooting, and data analysis. These individuals have been an invaluable resource and have helped me tremendously. Thank you to all of my colleagues, classmates, friends, and family who have provided encouragement throughout my graduate career.

TABLE OF CONTENTS

Page

LIST OF TABLES

Page

LIST OF FIGURES

Page

CHAPTER 1

INTRODUCTION

OVERVIEW

Acetylation of biomolecules is a conserved mechanism to rapidly modify cellular components in response to environmental cues and metabolic stress [reviewed in (1)]. Acetyltransferases transfer the acetyl moiety, typically from acetyl-Coenzyme A, to a primary amine group of a protein or small molecule. This modification may be removable through the action of a deacetylase. RLA is known to affect the function of diverse cellular processes including regulation of gene expression (2), metabolism (3-6), and cell structure (7). RLA exerts its effects by modulating protein-protein interactions, enzyme activity, DNA and substrate binding, as well as protein stability (8, 9).

Work in this thesis (i.) characterizes the transcriptional regulation of the reversible lysine acetylation system in *Salmonella enterica*, and (ii.) examines detoxification of harmful amino acid derivatives via acetylation.

GCN5 *N*-ACETYTLRANSFERASES

Gcn5 *N*-acetyltransferases (GNATs) are the only family of acetyltransferases that are conserved throughout conserved in archaea, bacteria, and eukaryotes (10-12), and all of the protein acetyltransferases identified in prokaryotes to date belong to the GNAT family (1) (Fig. 1.1A). Although these enzymes have very low sequence homology, they share a high structural

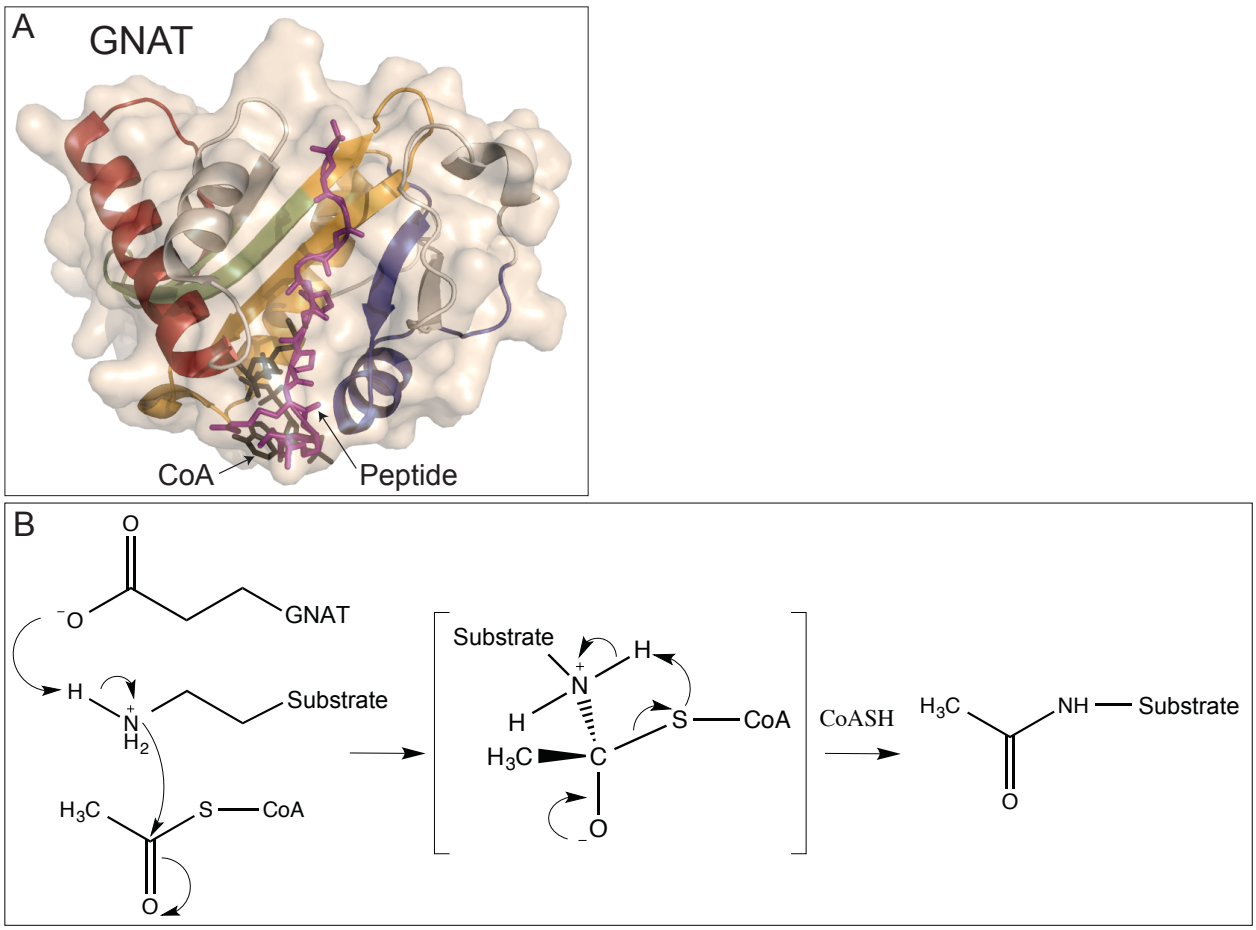

Figure 1.1. Gcn5-related *N*-acetyltransferase structure and mechanism. (A) Structure of *Tetrahymena thermophila t*Gcn5 enzyme bound to Coenzyme A (CoA, black sticks) and a peptide substrate (purple sticks). (B). GNAT reaction mechanism.

homology with the presence of a conserved catalytic fold (10). The core domain is composed of a central β-sheet (six antiparallel strains) which is comprised of four motifs, named A-D (13). The acetylation reaction proceeds via deprotonation of the active site lysine residue of the target substrate by a catalytic glutamate residue of the GNAT, which allows for a direct nucleophilic attack of lysine on the carbonyl carbon of acetyl-CoA (10, 14-16) (Fig. 1.1B)

On average a given organism encodes ~25 GNATs, and many of these enzymes have no known role. Even in well-characterized organisms like *S. enterica*, only half of GNATs have a known function. GNAT enzymes of *S. enterica* have been shown to target primary amines (17, 18), including the *N*-termini of proteins (19, 20), aminoglycoside antibiotics (21), polyamines (22), a nucleotide sugar (23), glutamate (24), toxic aminoacyl nucleotides (25), toxic methionine derivatives (26), and transfer RNAs (27). The only known protein lysine acetyltransferase in *S. enterica* is Pat, (discussed in more detail below) (12, 28).

PROTEIN ACETYATION

Control of protein function by reversible lysine acetylation. Reversible lysine acetylation (RLA) is an important posttranslational modification that allows an organism to quickly and reversibly regulate the activity of proteins, including those involved in transcription, translation, carbon utilization, and stress responses (12, 29-31) by modulating the acetylation state of epsilon amino group of lysyl residues critical for function [reviewed in (1)]. RLA has shown to be a functional system in diverse prokaryotes, including *S. enterica, Rhodopseudomonas palustris*, *Streptomyces lividans, Escherichia coli,* and *Bacillus subtilis* (6, 29, 32-35).

The RLA system controls protein acetylation in *S. enterica* (12, 36, 37), and is comprised of a Gcn5 *N*-acetyltransferase (Pat), and its partner NAD^+-consuming sirtuin deacetylase (CobB). Pat

and CobB work together to modify the activity acetyl-CoA synthetase (Acs), responsible for the conversion of acetate to acetyl-CoA (38) (Fig. 1.2). RLA control of Acs is a widely conserved mechanism and present in bacteria to humans (39). Control of Acs function via acetylation is critical as uncontrolled Acs activity leads to cell death via depletion of cellular ATP pools (33). Acetylation of the conserved active site lysine residue inactivates Acs, while removal of the acetyl moiety by the CobB reactivates the enzyme.

GLOBAL APPROACHES TO IDENTIFY ACETYLATED PROTEINS

Studies examining the total acetylated protein population (the "acetylome") in prokaryotes have been accelerated by recent advances in mass spectrometry-based approaches to enrich for and detect acetylated lysine residues in total protein populations (8). Bacterial acetylomes have been characterized in *E. coli* (40, 41), *S. enterica* (42), *B. subtilis* (34), *Erwinia amylovora* (35), *R. palustris* (3), *Staphylococcus aureus* (43), *Geobacillus kaustophilus* (44), *Vibrio parahaemolyticus* (45), *Thermus thermophilus* (46), *Mycobacterium tuberculosis* (47), and *Mycoplasma pneumonia* (48). In these studies the number of putatively acetylated proteins per organism has ranged from 62-667, providing evidence that acetylation of proteins is prevalent modification in these organisms. The majority of the identified acetylated proteins are involved in central metabolism (40, 43, 45). While these studies provide an important platform for studying the role of protein acetylation, these data have not been experimentally validated to determine if the function of the identified proteins is in fact controlled by acetylation. Validation of these data obtained through global 'omics' approaches is key to improving our understanding of the role of acetylation in prokaryotic cellular physiology.

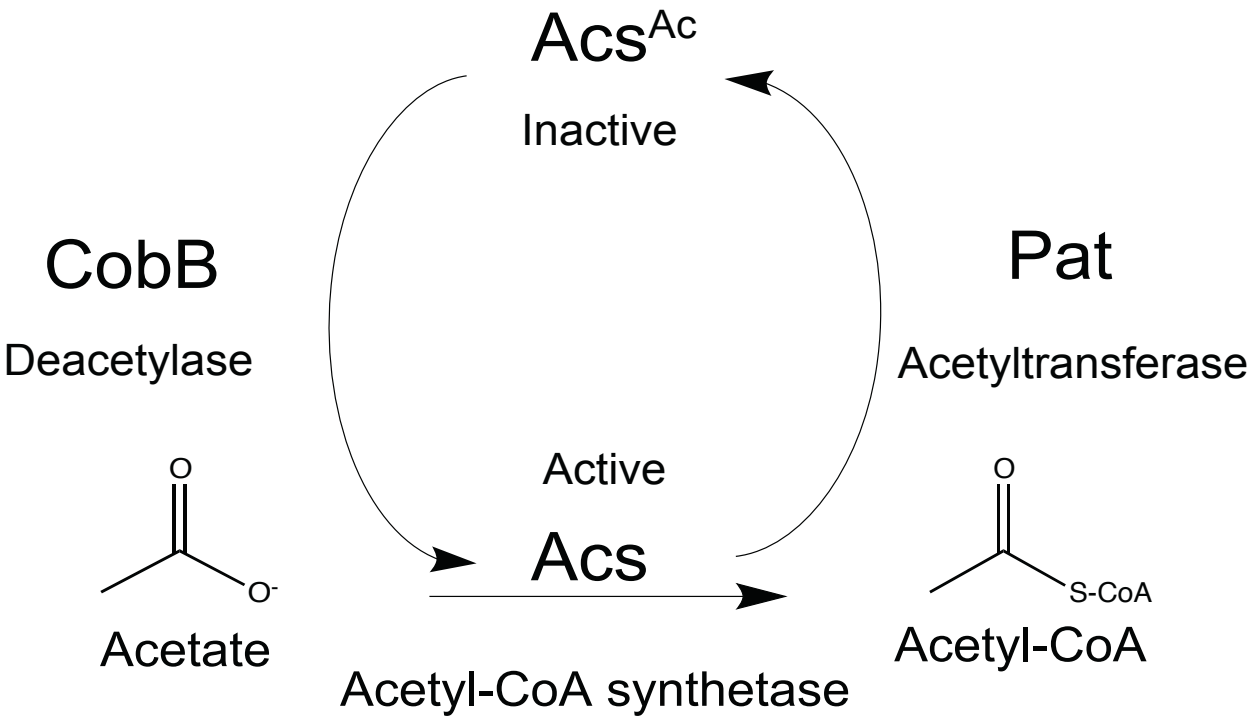

Figure 1.2 Reversible lysine acetylation (RLA) system in *S. enterica*. Activity of the acetyl-CoA synthetase (Acs) enzyme of *S. enterica* is controlled by acetylation. Acs is acetylated (inactivated) by the Gcn5 *N*-acetyltransferase (Pat) and deacetylated (activated) by the NAD^+-dependent sirtuin deacetylase (CobB).

SMALL MOLECULE ACETYLATION

GNATs protect against many types of external and internal stresses (49-51). The majority of characterized GNATs acetylate small molecules including aminoglycoside antibiotics (49), glutamate (24), polyamines (22), aminoalkylphosphonic acid (52), dTDP-fucosamine (23), transfer RNAs (27), toxic aminoacyl nucleotides (25), phosphinothricin (53), and methionine sulfoximine (26, 51). Identification of small molecule substrates for GNATs has been an ongoing challenge in the field.

It could be hypothesized that the diversity of stresses controlled by GNATs correlates with the environment encountered by the organism. Therefore, the relevance of GNAT function to physiology varies between organisms, with respect to not only cellular stresses but also metabolic pathways. For example, *S. enterica* contains ~26 GNATs, *Myxococcus xanthus* encodes ~46 GNATs, and *S. lividans* encodes up to ~70 GNATs. This suggests that perhaps *M. xanthus* and *S. lividans* occupy a more diverse environment than *S. enterica*, while also maintaining a more complex metabolism.

CONCLUSIONS

Acetylation is an emerging field in prokaryotic biology and is advancing by tremendous strides through the use of high-throughput and detailed mechanistic studies diverse organisms. GNATs have been identified in bacteria, archaea, and eukaryotes, and are also highly abundant. Although the physiological role of the majority of GNATs remains unknown, and the elucidation of their function is been an ongoing challenge to physiologists, advances in this area of research will provide valuable insights into the strategies used by cells to cope with metabolic stress.

DISSERTATION OUTLINE

This work focuses on the role of acetylation in the γ-Proteobacterium *Salmonella enterica* and furthers our knowledge of the role of acetylation in cellular physiology. I identified a transcriptional regulator of the reversible lysine acetylation (RLA) system in *S. enterica* and describe how defects in this regulatory system affect C2 metabolism. I characterized the function of a previously unknown *S. enterica* GNAT, MddA, which is responsible for the detoxification of harmful amino acid derivatives. MddA was previously incorrectly annotated as a phosphinothricin acetyltransferase. This lead to the investigation of various putative phosphinothricin acetyltransferases from *Deinococcus radiodurans*, *Geobacillus kaustophilus*, *Burkholderia xenovorans*, and *Bacillus subtilis*, which demonstrated these enzymes have varying substrate specificities for phosphinothricin analogues.

Chapter 2 provides an in-depth literature review on the topic of reversible lysine acetylation. RLA control of proteins affects many cellular processes and is an important mechanism to rapidly and reversibly modify protein function. This literature review presents a close examination of our current understanding of RLA in prokaryotes.

In chapter 3 we report that IolR, a repressor of *myo*-inositol catabolism, activates the expression of genes encoding components of the RLA system (Pat, CobB) in *S. enterica*, and integrates this expression with the target of RLA, the acetyl-CoA synthetase (Acs). Evidence from DNA binding assays and DNA footprinting studies demonstrated that the IolR protein directly regulates *pat* expression. The absence of IolR caused an imbalance in the ratios of Pat and CobB, which in turn affected the level of acetylated (inactive) / unacetylated (active) Acs. These results suggest that transcriptional control of the RLA system is critical and slight changes in protein concentration leads to an imbalance that is detrimental to the cell.

Chapter 4 describes the role of the MddA GNAT in the detoxification of oxidized forms of methionine. Methionine sulfoximine and methionine sulfone inhibited growth of an *S. enterica* Δ*mddA* strain unless glutamine or methionine was present in the medium. Deletion of two amino acid transporters (GlnHPQ and MetNIQ) in a Δ*mddA* strain restored growth in the presence of MSX. A spectrophotometric assay and mass spectrometry were used to show that MddA was responsible for the acetylation of methionine sulfoximine and methionine sulfone. These results show MddA is the mechanism used by *S. enterica* to respond to oxidized forms of methionine, which MddA detoxifies by acetyl-CoA-dependent acetylation.

Chapter 5 outlines the characterization of putative phosphinothricin acetyltransferases using *S. enterica* as a heterologous host to assay for function. Using *in vivo* complementation studies I examined the specificities of annotated phosphinothricin acetyltransferases from *D. radiodurans* and *G. kaustophilus*, and corroborated these results with enzyme studies *in vitro*. Using bioinformatic approaches the specificity of putative phosphinothricin acetyltransferases from *Burkholderia xenovorans* and *Bacillus subtilis* were predicted, and tested *in vivo*. These studies provide method for the rapid characterization of putative phosphinothricin acetyltransferases using *S. enterica*.

REFERENCES

1. **Thao S, Escalante-Semerena JC.** 2011. Control of protein function by reversible *N*(epsilon)-lysine acetylation in bacteria. *Curr. Opin. Microbiol.* **14:**200-204.
2. **Glozak MA, Sengupta N, Zhang X, Seto E.** 2005. Acetylation and deacetylation of non-histone proteins. *Gene.* **363:**15-23.

3. **Crosby HA, Pelletier DA, Hurst GB, Escalante-Semerena JC.** 2012. System-wide studies of *N*-lysine acetylation in *Rhodopseudomonas palustris* reveal substrate specificity of protein acetyltransferases. *J. Biol. Chem.* **287:**15590-15601.

4. **Starai VJ, Takahashi H, Boeke JD, Escalante-Semerena JC.** 2003. Short-chain fatty acid activation by acyl-coenzyme A synthetases requires SIR2 protein function in *Salmonella enterica* and *Saccharomyces cerevisiae*. *Genetics.* **163:**545-555.

5. **Gardner JG, Grundy FJ, Henkin TM, Escalante-Semerena JC.** 2006. Control of acetyl-coenzyme A synthetase (AcsA) activity by acetylation/deacetylation without NAD(+) involvement in *Bacillus subtilis*. *J. Bacteriol.* **188:**5460-5468.

6. **Tucker AC, Escalante-Semerena JC.** 2013. Acetoacetyl-CoA synthetase activity is controlled by a protein acetyltransferase with unique domain organization in *Streptomyces lividans*. *Mol. Microbiol.* **87:**152-167.

7. **Hubbert C, Guardiola A, Shao R, Kawaguchi Y, Ito A, Nixon A, Yoshida M, Wang XF, Yao TP.** 2002. HDAC6 is a microtubule-associated deacetylase. *Nature.* **417:**455-458.

8. **Kim GW, Yang XJ.** 2011. Comprehensive lysine acetylomes emerging from bacteria to humans. *Trends Biochem. Sci.* **36:**211-220.

9. **Xiong Y, Guan KL.** 2012. Mechanistic insights into the regulation of metabolic enzymes by acetylation. *J. Cell. Biol.* **198:**155-164.

10. **Vetting MW, Carvalho LPSd, Yu M, Hegde SS, Magnet S, Roderick SL, Blanchard JS.** 2005. Structure and functions of the GNAT superfamily of acetyltransferases. *Arch. Biochem. Biophys*. **433:**212-226.

11. **Marsh VL, Peak-Chew SY, Bell SD.** 2005. Sir2 and the acetyltransferase, Pat, regulate the archaeal chromatin protein, Alba. *J. Biol. Chem.* **280:**21122-21228.

12. **Starai VJ, Escalante-Semerena JC.** 2004. Identification of the protein acetyltransferase (Pat) enzyme that acetylates acetyl-CoA synthetase in *Salmonella enterica*. *J. Mol. Biol.* **340:**1005-1012.

13. **Neuwald AF, Landsman D.** 1997. GCN5-related histone *N*-acetyltransferases belong to a diverse superfamily that includes the yeast SPT10 protein. *Trends Biochem. Sci.* **22:**154-155.

14. **Rojas JR, Trievel RC, Zhou J, Mo Y, Li X, Berger SL, Allis CD, Marmorstein R.** 1999. Structure of *Tetrahymena* GCN5 bound to coenzyme A and a histone H3 peptide. *Nature.* **401:**93-98.

15. **Yan Y, Barlev NA, Haley RH, Berger SL, Marmorstein R.** 2000. Crystal structure of yeast Esa1 suggests a unified mechanism for catalysis and substrate binding by histone acetyltransferases. *Mol. Cell.* **6:**1195-1205.

16. **Berndsen CE, Denu JM.** 2008. Catalysis and substrate selection by histone/protein lysine acetyltransferases. *Curr. Opin. Struct. Biol.* **18:**682-689.

17. **Hu LI, Lima BP, Wolfe AJ.** 2010. Bacterial protein acetylation: the dawning of a new age. *Mol. Microbiol.* **77:**15-21.

18. **Weinert BT, Iesmantavicius V, Wagner SA, Scholz C, Gummesson B, Beli P, Nystrom T, Choudhary C.** 2013. Acetyl-phosphate is a critical determinant of lysine acetylation in *E. coli*. *Mol. Cell.* **51:**265-272.

19. **Cumberlidge AG, Isono K.** 1979. Ribosomal protein modification in *Escherichia coli*. I. A mutant lacking the *N*-terminal acetylation of protein S5 exhibits thermosensitivity. *J. Mol. Biol.* **131:**169-189.

20. **Isono K, Isono S.** 1980. Ribosomal protein modification in *Escherichia coli*. II. Studies of a mutant lacking the *N*-terminal acetylation of protein S18. *Mol. Gen. Genet.* **177:**645-651.

21. **Davies J, Wright GD.** 1997. Bacterial resistance to aminoglycoside antibiotics. *Trends Microbiol.* **5:**234-240.

22. **Fukuchi J, Kashiwagi K, Takio K, Igarashi K.** 1994. Properties and structure of spermidine acetyltransferase in *Escherichia coli*. *J. Biol. Chem.* **269:**22581-22585.

23. **Hung MN, Rangarajan E, Munger C, Nadeau G, Sulea T, Matte A.** 2006. Crystal structure of TDP-fucosamine acetyltransferase (WecD) from *Escherichia coli*, an enzyme required for enterobacterial common antigen synthesis. *J. Bacteriol.* **188:**5606-5617.

24. **Marvil DK, Leisinger T.** 1977. *N*-acetylglutamate synthase of *Escherichia coli*: purification, characterization, and molecular properties. *J. Biol. Chem.* **252:**3295-32303.

25. **Kazakov T, Kuznedelov K, Semenova E, Mukhamedyarov D, Datsenko KA, Metlitskaya A, Vondenhoff GH, Tikhonov A, Agarwal V, Nair S, Van Aerschot A, Severinov K.** 2014. The RimL transacetylase provides resistance to translation inhibitor microcin C. *J. Bacteriol.* **196:**3377-3385.

26. **Hentchel KL, Escalante-Semerena JC.** 2015. In *Salmonella enterica*, the Gcn5-related acetyltransferase MddA (formerly YncA) acetylates methionine sulfoximine and methionine sulfone, blocking their toxic effects. *J. Bacteriol.* **197:**314-325.

27. **Ikeuchi Y, Kitahara K, Suzuki T.** 2008. The RNA acetyltransferase driven by ATP hydrolysis synthesizes N^4-acetylcytidine of tRNA anticodon. *EMBO. J.* **27:**2194-2203.

28. **Liang W, Malhotra A, Deutscher MP.** 2011. Acetylation regulates the stability of a bacterial protein: growth stage-dependent modification of RNase R. *Mol. Cell.* **44:**160-166.

29. **Thao S, Chen CS, Zhu H, Escalante-Semerena JC.** 2010. *N*(ε)-Lysine acetylation of a bacterial transcription factor inhibits its DNA-binding activity. *PLOS ONE.* **5:**e15123.

30. **Hu LI, Chi BK, Kuhn ML, Filippova EV, Walker-Peddakotla AJ, Basell K, Becher D, Anderson WF, Antelmann H, Wolfe AJ.** 2013. Acetylation of the response regulator RcsB controls transcription from a small RNA promoter. *J. Bacteriol.* **195:**4174-4886.

31. **Lima BP, Antelmann H, Gronau K, Chi BK, Becher D, Brinsmade SR, Wolfe AJ.** 2011. Involvement of protein acetylation in glucose-induced transcription of a stress-responsive promoter. *Mol. Microbiol.* **81:**1190-1204.

32. **Crosby HA, Heiniger EK, Harwood CS, Escalante-Semerena JC.** 2010. Reversible *N*(ε)-lysine acetylation regulates the activity of acyl-CoA synthetases involved in anaerobic benzoate catabolism in *Rhodopseudomonas palustris*. *Mol. Microbiol.* **76:**874-888.

33. **Chan CH, Garrity J, Crosby HA, Escalante-Semerena JC.** 2011. In *Salmonella enterica*, the sirtuin-dependent protein acylation/deacylation system (SDPADS)

maintains energy homeostasis during growth on low concentrations of acetate. *Mol. Microbiol.* **80:**168-183.

34. **Kim D, Yu BJ, Kim JA, Lee YJ, Choi SG, Kang S, Pan JG.** 2013. The acetylproteome of Gram-positive model bacterium *Bacillus subtilis*. *Proteomics.* **13:**1726-1736.

35. **Wu X, Vellaichamy A, Wang D, Zamdborg L, Kelleher NL, Huber SC, Zhao Y.** 2013. Differential lysine acetylation profiles of *Erwinia amylovora* strains revealed by proteomics. *J. Proteomics.* **79:**60-71.

36. **Starai VJ, Celic I, Cole RN, Boeke JD, Escalante-Semerena JC.** 2002. Sir2-dependent activation of acetyl-CoA synthetase by deacetylation of active lysine. *Science.* **298:**2390-2392.

37. **Starai VJ, Escalante-Semerena JC.** 2004. Acetyl-coenzyme A synthetase (AMP forming). *Cell Mol. Life Sci.* **61:**2020-2030.

38. **Wolfe AJ.** 2005. The acetate switch. *Microbiol. Mol. Biol. Rev.* **69:**12-50.

39. **Schwer B, Bunkenborg J, Verdin RO, Andersen JS, Verdin E.** 2006. Reversible lysine acetylation controls the activity of the mitochondrial enzyme acetyl-CoA synthetase 2. *Proc. Natl. Acad. Sci. USA*. **103:**10224-10229.

40. **Yu BJ, Kim JA, Moon JH, Ryu SE, Pan JG.** 2008. The diversity of lysine-acetylated proteins in *Escherichia coli*. *J. Microbiol. Biotechnol.* **18:**1529-1536.

41. **Zhang J, Sprung R, Pei J, Tan X, Kim S, Zhu H, Liu CF, Grishin NV, Zhao Y.** 2009. Lysine acetylation is a highly abundant and evolutionarily conserved modification in *Escherichia coli*. *Mol. Cell Proteomics.* **8:**215-225.

42. **Wang Q, Zhang Y, Yang C, Xiong H, Lin Y, Yao J, Li H, Xie L, Zhao W, Yao Y, Ning ZB, Zeng R, Xiong Y, Guan KL, Zhao S, Zhao GP.** 2010. Acetylation of metabolic

enzymes coordinates carbon source utilization and metabolic flux. *Science.* **327:**1004-1007.

43. **Zhang Y, Wu ZX, Wan XL, Liu P, Zhang JB, Ye Y, Zhao YM, Tan MJ.** 2014. Comprehensive profiling of lysine acetylome in *Staphylococcus aureus*. *Sci. China Chem.* **57:**732-738.

44. **Lee DW, Kim DI, Lee YJ, Kim JA, Choi JY, Kang S, Pan JG.** 2013. Proteomic analysis of acetylation in thermophilic *Geobacillus kaustophilus*. *Proteomics.* **13:**2278-2282.

45. **Pan J, Ye Z, Cheng Z, Peng X, Wen L, Zhao F.** 2014. Systematic analysis of the lysine acetylome in *Vibrio parahemolyticus*. *J. Proteome Res.* **13**:3294-302.

46. **Okanishi H, Kim K, Masui R, Kuramitsu S.** 2013. Acetylome with structural mapping reveals the significance of lysine acetylation in *Thermus thermophilus*. *J. Proteome Res.* **12:**3952-3968.

47. **Liu F, Yang M, Wang X, Yang S, Gu J, Zhou J, Zhang XE, Deng J, Ge F.** 2014. Acetylome analysis reveals diverse functions of lysine acetylation in *Mycobacterium tuberculosis*. *Mol. Cell Proteomics.* **12:**3352-3366.

48. **van Noort V, Seebacher J, Bader S, Mohammed S, Vonkova I, Betts MJ, Kuhner S, Kumar R, Maier T, O'Flaherty M, Rybin V, Schmeisky A, Yus E, Stulke J, Serrano L, Russell RB, Heck AJ, Bork P, Gavin AC.** 2012. Cross-talk between phosphorylation and lysine acetylation in a genome-reduced bacterium. *Mol. Syst. Biol.* **8:**571.

49. **Wright GD, Ladak P.** 1997. Overexpression and characterization of the chromosomal aminoglycoside 6'-*N*-acetyltransferase from *Enterococcus faecium*. *Antimicrob. Agents Chemother.* **41:**956-960.

50. **Wolf E, Vassilev A, Makino Y, Sali A, Nakatani Y, Burley SK.** 1998. Crystal structure of a GCN5-related *N*-acetyltransferase: *Serratia marcescens* aminoglycoside 3-*N*-acetyltransferase. *Cell.* **94:**439-449.

51. **Davies AM, Tata R, Beavil RL, Sutton BJ, Brown PR.** 2007. L-Methionine sulfoximine, but not phosphinothricin, is a substrate for an acetyltransferase (gene PA4866) from *Pseudomonas aeruginosa*: structural and functional studies. *Biochemistry.* **46:**1829-1839.

52. **Errey JC, Blanchard JS.** 2006. Functional annotation and kinetic characterization of PhnO from *Salmonella enterica*. *Biochemistry.* **45:**3033-3039.

53. **Thompson CJ, Movva NR, Tizard R, Crameri R, Davies JE, Lauwereys M, Botterman J.** 1987. Characterization of the herbicide-resistance gene *bar* from *Streptomyces Hygroscopicus*. *EMBO. J.* **6:**2519-2523.

CHAPTER 2

LITERATURE REVIEW - ACETYLATION OF BIOMOLECULES: A WIDESPSREAD STRATEGY FOR THE CONTROL OF BIOLOGICAL FUNCTION AND METABOLIC STRESS[1]

[1]Hentchel. K.L. and J.C. Escalante-Semerena. 2015. *Microbiol. Mol. Bio. Rev.* Accepted. Reprinted here with permission from the publisher.

SUMMARY

Acylation of biomolecules (*e.g.,* proteins, small molecules) is a process that occurs in cells of all domains of life, and has emerged as a critical mechanism for the control of many aspects of cellular physiology, including chromatin maintenance, transcriptional regulation, primary metabolism, cell structure, and likely other cellular processes. Although this review focuses on the use of acetyl moieties to modify a protein or small molecule, it is clear that cells can use many weak organic acids (*e.g.,* short-, medium-, long-chain mono and dicarboxylic aliphatics and aromatics) to modify a large suite of targets. Acetylation of biomolecules has been studied for decades within the context of histone-dependent regulation of gene expression and antibiotic resistance. It was not until the early 2000s that the connection between metabolism and physiology and protein acetylation was reported. This was the first instance of a metabolic enzyme (acetyl-CoA synthetase) whose activity was controlled by acetylation via a regulatory system responsive to physiological cues. The alluded system was comprised of an acyltransferase and a partner deacylase. Given the reversibility of the acylation process this system is also referred to as reversible lysine acylation (RLA). A wealth of information has been obtained since the discovery of RLA in prokaryotes, and we are just beginning to visualize the extent of the impact that this regulatory system has on cell function.

INTRODUCTION

Post-translational Modifications

Post-translational modifications (PTMs) are important for the regulation of protein structure and function (1). These modifications allow organisms to rapidly respond and adapt to changing environmental conditions, forgoing the need to transcribe and translate new proteins by simply

modifying the function of existing proteins. Examples of PTMs include acetylation (2), glycosylation (3), lipidation (4), methylation (5), *S*-nitrosylation (6), phosphorylation (7, 8), succinylation (9), ubiquitinylation (10), adenylylation and phosphocholinylation (11), ADP-ribosylation (12), serine/threonine *O*-acetylation (13), proteolysis (14-16), and others.

Protein acylation is a broadly distributed PTM in prokaryotes. This review focuses on reversible acetyl-CoA-dependent, enzyme-driven protein acetylation, which is broadly distributed in all domains of life. Protein acetylation can occur at the *N*-terminus on the alpha amino group (N^{α} acetylation) or the epsilon amino moiety of lysyl side chains (N^{ϵ} acetylation) (Fig. 2.1). Notably, N^{α}-acetylation can occur co- or post-translationally, alters protein stability, and is typically irreversible (17, 18). In contrast, N^{ϵ}-acetylation can modify protein structure and function, and typically is reversible by a deacetylase (Fig. 2.2).

Discovery of Protein Acetylation

Lysine acetylation was first reported in the 1960's as a modification of the lysine-rich *N*-terminal tails of eukaryotic histones (2). Histones are protein components of chromatin, the compact DNA structure in eukaryotes, and acetylation of these proteins is tightly controlled. Histone acetylation is carried out by histone acetyltransferases (HATs), and is associated with decreased DNA binding due to the loss of interactions between the epsilon amino (N^{ϵ}) group of lysines and the phosphate anions of the DNA strands. Acetylation of the N^{ϵ} group of lysines effectively neutralizes the positive charge of lysine, relaxing histone / DNA interactions, hence providing an opportunity for the transcriptional machinery to decode genes that otherwise would be unavailable (19, 20). In eukaryotes, the tumor suppressor protein p53 was the first mammalian

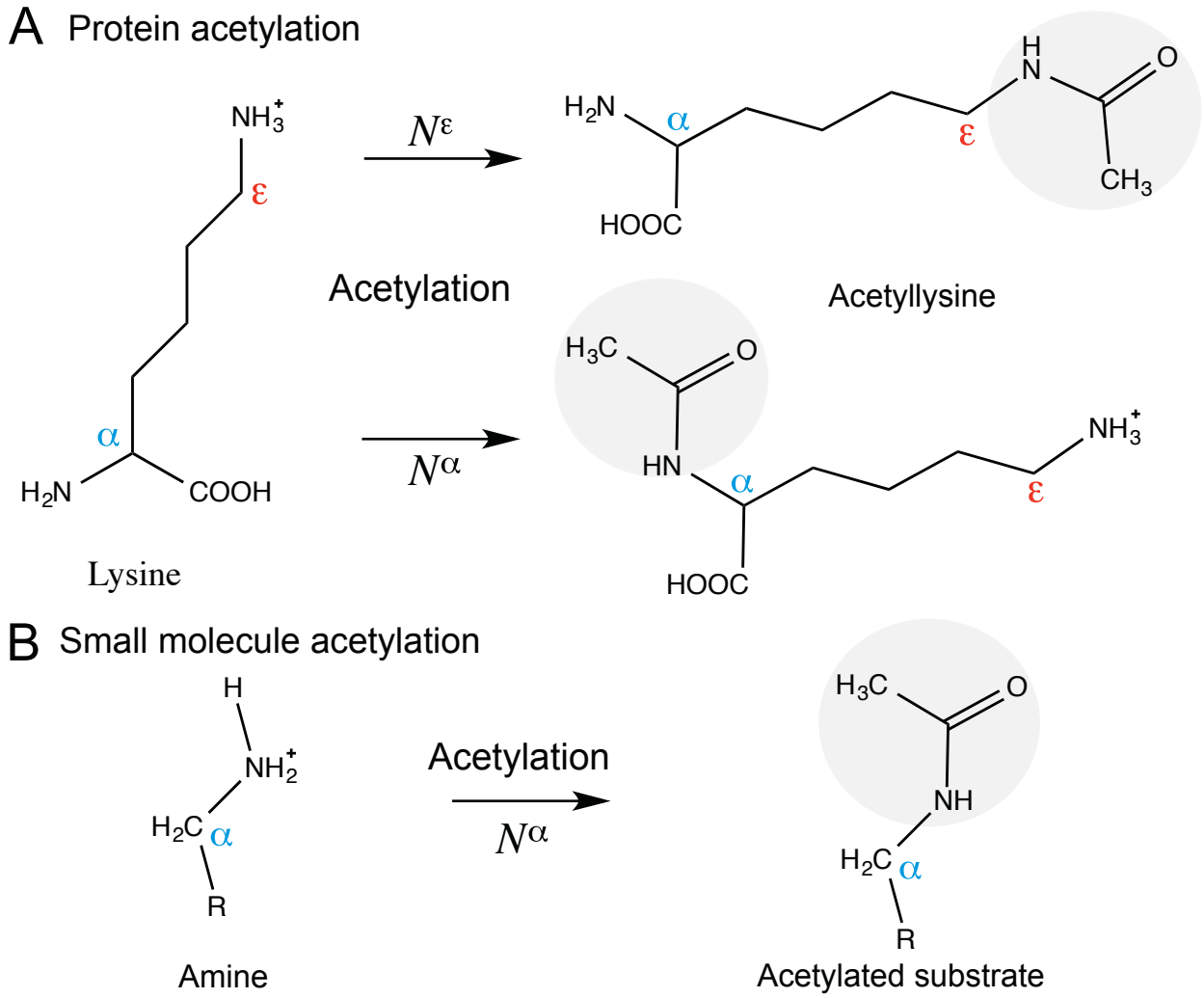

Figure 2.1. **Schematic of N^{ε} and N^{α} acetylation.** Protein acetylation can occur via two methods, (A) acetylation of the ε-amino group of internal lysine residues (N^{ε} acetylation, red) or (B) acetylation of the *N*-terminal α-amino group (N^{α} acetylation, blue). N^{ε}-acetylation occurs post-translationally, can be reversible, and can alter protein structure and function. N^{α}-acetylation occurs co- or post-translationally, is typically not reversible, and alters protein stability.

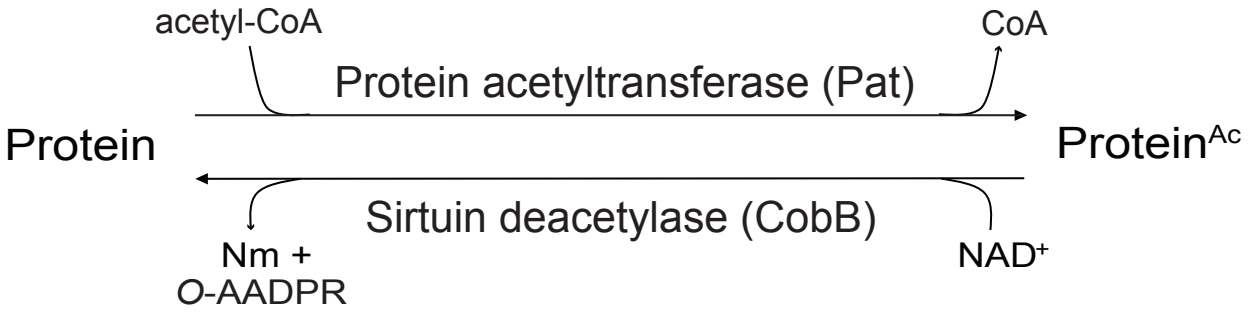

Figure 2.2. Reversible lysine acylation (RLA) schematic. A protein substrate (form 1) is modified by a protein lysine acetyltransferase, Pat (of Gcn5-like *N*-acetyltransferase family, or GNAT), resulting in the acetylated protein (form 2). This modification is reversible, either by a NAD^+-consuming class III sirtuin deacetylase, CobB, or a Zn(II)-dependent protein deacetylase. The sirtuin deacetylase uses NAD^+ as a substrate, not as a coenzyme. Sirtuins modify the carboxyl group of the ribose of the nicotinamide mononucleotide (NMN) moiety of NAD^+, simultaneously releasing nicotinamide (Nm). The resulting by-product is *O*-acetyl-ADP-ribose (*O*-AADPR).

transcription factor shown to be regulated by acetylation (21). Now, there are more than 100 transcription factors have been identified as acetylation targets (22).

As mentioned above, reversible lysine acylation (RLA) was discovered in prokaryotes in the early 2000s (23, 24), and this discovery led to a rapid expansion of the role of acylation, specifically acetylation, in prokaryotic cell physiology. Subsequently, RLA has been observed in bacteria, archaea, and eukaryotes (25), and it is now clear that many non-histone proteins are also post-translationally regulated by RLA.

At present, RLA is known to affect the function of diverse cellular processes including chromatin maintenance (26), regulation of gene expression (27), metabolism (28-31), and cell structure (32). RLA exerts its effects by modulating DNA binding, protein-protein interactions, enzyme activity, substrate binding, and protein stability (33, 34).

Studies have shown that a variety of proteins are regulated by RLA, including the metabolic enzymes acetyl-CoA synthetase (23), phosphoenolpyruvate carboxykinase (35), the M2 isoform of pyruvate kinase (36), phosphoglycerate mutase-1 (37), and the structural protein α-tubulin, a subunit of microtubules (38). Acetylation has been suggested to rival phosphorylation in both its prevalence and diversity of target substrates (39).

LYSINE ACETYLTRANSFERASES

Diversity

There are three classes of lysine (Lys, K) acetyltransferases (LATs, a.k.a. KATs) that catalyze the transfer of the acetyl moiety from acetyl-CoA to the ε-amino group of lysine side chains (Fig. 2.3). These classes of LATs comprise a large and diverse set of enzymes named after their founding member(s), including (i) the Gcn5-related *N*-acetyltransferase family (GNATs, [named

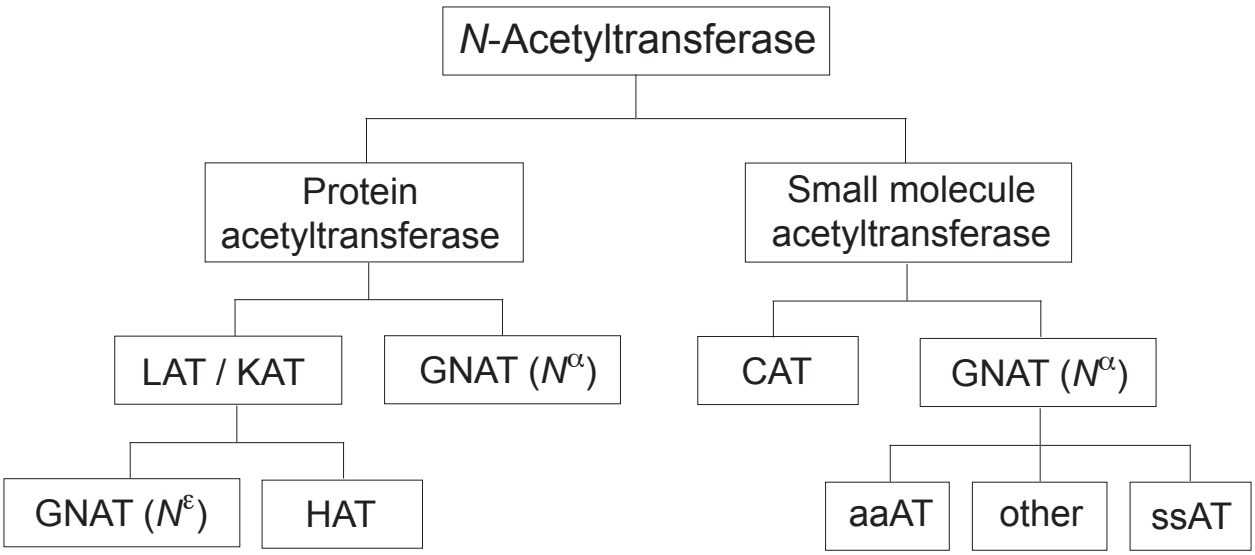

Figure 2.3. **Acyltransferase nomenclature and classification.** Abbreviations: LAT/KAT, Lysine (K) acetyltransferase; GNAT, Gcn5 *N*-acetyltransferase; HAT, histone acetyltransferase; CAT, chloramphenicol acetyltransferase; aaAT, arylamine acetyltransferase; ssAT, spermine / sperimidine acetyltransferase; Other, unclassified acetyltransferase; N^{ε}, acetylation of the epsilon amino group of a lysine; N^{α}, acetylation of the alpha amino group of any *N*-terminal amino acid.

after yeast Gcn5 protein (Pfam 00583)]), (ii) the MYST family [named after human MOZ, yeast Ybf2/Sas3, yeast Sas2, and human Tip60 (Pfam 01853)], and (iii) the p300/CBP family [named after human hp300 and hCBP (Pfam 06466)]. The above-mentioned enzyme families differ in sequence similarity, domain organization, substrate specificity, and catalytic mechanism (40-48). The MYST and p300/CBP families are only present in eukaryotes, while the GNAT family is present in all domains of life.

Conservation of the acetyl-CoA binding domain

Regardless of their mechanistic differences, acetyltransferases contain a conserved core domain which binds to acetyl-CoA through interactions with the pyrophosphate and pantothenate moieties (41, 47, 49-52) [reviewed in (42, 53)]. Neither the adenine base nor the acetyl moiety significantly contributes to binding the core domain. Due to this binding mode, acetyltransferases bind acetyl-CoA with high affinity but low specificity (54, 55), allowing for recognition of various acyl-CoA thioesters as well as free coenzyme A (CoASH). Their specificity is then due to their structurally divergent *N*- and *C*-terminal domains outside of the core domain (49). In some cases, other acyl-CoA thioesters, such as propionyl-CoA and succinyl-CoA, are physiologically relevant substrates (43, 56, 57), and are discussed in more detail below.

Mechanisms of acetylation. The mechanism of transfer of acyl moieties used by the GNAT and MYST families involves a catalytic glutamate residue that acts as a general base, facilitating a water-mediated proton abstraction from the side chain of the substrate lysine (45, 49, 53, 58) (Fig. 2.4). The lysine amine group initiates a nucleophilic attack on the carbonyl carbon of the acetyl moiety of CoA, allowing the direct transfer of the acyl group to the substrate lysine. Members of the MYST family employ either a catalytic mechanism similar to GNATs, or a ping-

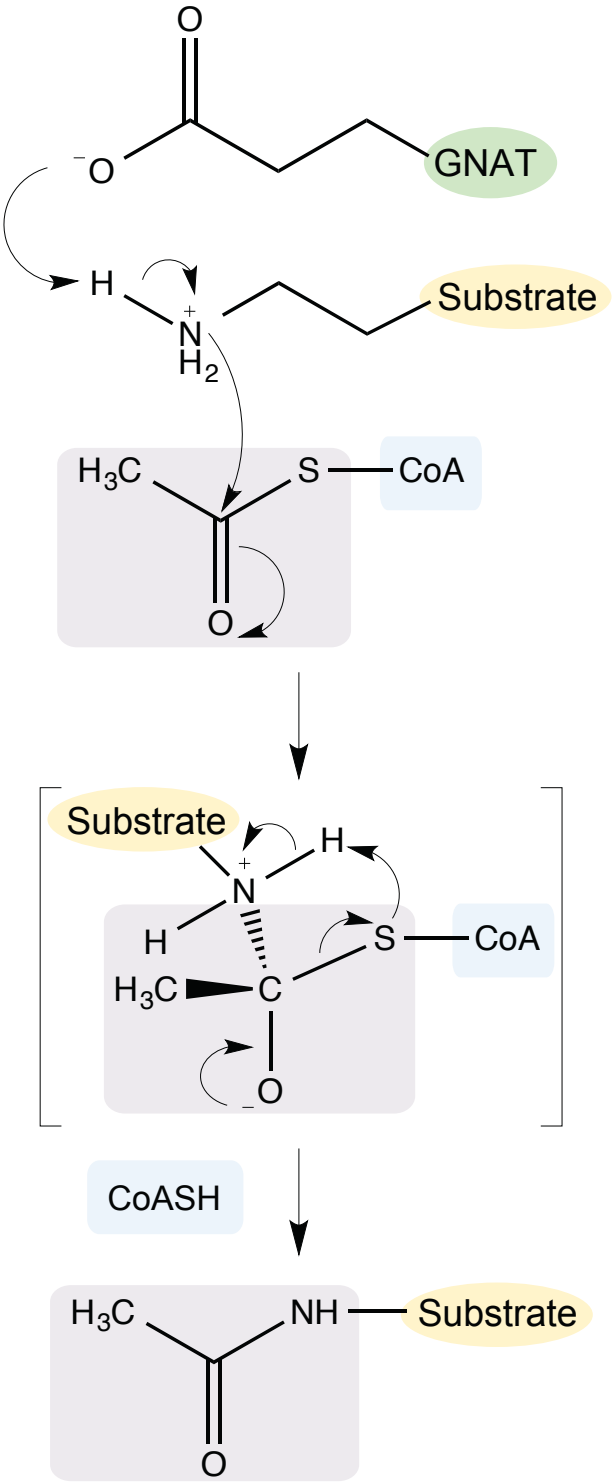

Figure 2.4. Acetylation mechanism of GNATs. The GNAT acetylation mechanism involves a catalytic glutamate that acts a general base, facilitating a water-mediated proton abstraction from the side chain of the substrate lysine. The ε-amino group of lysine performs a nucleophilic attack on the carbonyl carbon of the acetyl moiety of CoA, allowing direct transfer of the acetyl group to the lysine side chain.

pong mechanism (aka double-displacement mechanism) involving an acetylated enzyme intermediate (46). Members of the p300/CBP family are structurally distinct and do not use a catalytic base to initiate the transfer of the acyl moiety (47). Instead, it appears that the p300/CBP family uses a Theorell-Chance mechanism, a sequential mechanism that does not form a stable ternary complex (47).

Bacterial Gcn5-related *N*-Acyltransferases (GNATs)

The GNAT family is conserved among archaea, bacteria, and eukaryotes (24, 53, 59). All known bacterial lysine acetyltransferases identified to date belong to the GNAT superfamily (60). Despite having low sequence homology, GNATs share a conserved catalytic fold, and can acetylate both protein and small molecule substrates (53). The first bacterial GNATs were characterized as aminoglycoside *N*-acetyltransferases from *Enterococcus faecium* (61) and *Serratia marcescens* (62), demonstrating that GNATs acetylate diverse substrates, ranging from histones to antibiotics (2, 62, 63).

Utilization of alternative acyl-CoA substrates. Modifications of the N^{ε} amino group of lysine by propionyl, malonyl, succinyl, and butyryl moieties have also been demonstrated for metabolic enzymes, transcription factors, and histones in both bacteria and eukaryotes (56-58, 64, 65). For example, in *Salmonella enterica*, the activity of propionyl-CoA synthetase (PrpE) is controlled by propionylation (56). Both lysine propionylation and butyrylation have also been identified as reversible modifications that occur on histones (57, 66), expanding the range of GNAT-mediated regulation through their ability to utilize various acyl-CoA substrates.

Overview of GNAT structures. GNATs comprise one of the largest enzyme superfamilies identified thus far (>10,000 members). Dozens of GNATs structures have been resolved and are

available from the RCSB PDB (http://www.rcsb.org/pdb/home/home.do). Despite having low to moderate primary sequence homology, GNATs contain a core catalytic domain that is structurally well conserved (Fig. 2.5A, B). The GNAT domain contains a central β-sheet (six antiparallel strains) composed of four distinct motifs, A (β4, α3), B (β5, α4), C (β1, α1-2), and D (β2-3), which were originally identified by sequence similarity (67). Motif A has the highest conservation and is important for acetyl-CoA binding and catalysis [reviewed in (53, 54)].

Abundance and distribution of GNATs. The number of GNATs present in a given organism varies, with the majority of commonly studied organisms encoding approximately 20-25 GNATs. As an example of the diversity and abundance of GNATs: the Gram-positive, intracellular pathogen *Listeria monocytogenes* encodes ~14 GNATs, the purple non-sulfur α-proteobacterium *Rhodopseudomonas palustris* encodes ~26, and the Gram-positive actinomycete *Streptomyces lividans* encodes ~72 putative GNATs. The majority of these GNATs are uncharacterized, with no known function. Refer to Table 2.1 for an overview of the number of GNATs present in commonly studied prokaryotes. The sheer prevalence of GNATs raises many questions regarding the physiological role and substrate specificity of these enzymes. It could be speculated that the range of GNATs an organism encodes may be driven by the diversity of the environments inhabited.

Diversity of domain organization of GNAT protein acetyltransferases. Protein acetyltransferases of the GNAT family exhibit diverse domain architecture; four of which have been studied and will be discussed (Fig. 2.6).

Type I. The *S. enterica* Pat (*Se*Pat) enzyme, the first enzyme of this type to be discovered (24), has homologues in *E. coli* (*Ec*Pka), *R. palustris* (*Rp*Pat), *Vibrio* species, and cyanobacteria, among others. These *Se*Pat homologues are comprised of two distinct domains, a large (~700

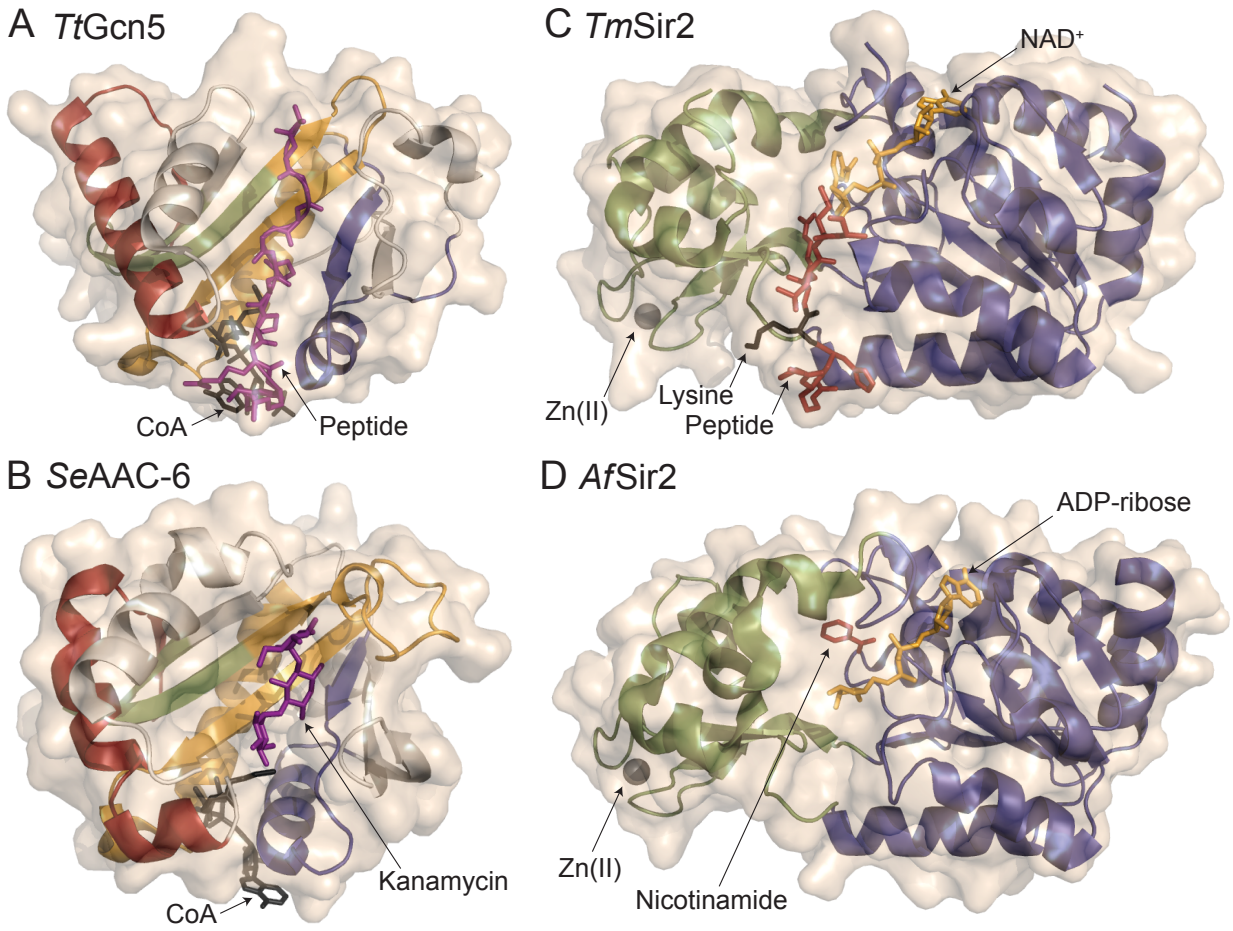

Figure 2.5. **GNAT and Sirtuin structural overview.** GNAT domains are comprised of a central β-sheet and contain four motifs (A, gold; B, blue; C, red; and D, green). Two structures are shown. (A). *Tetrahymena thermophila Tt*Gcn5 is shown with an H3 11-mer peptide substrate (purple sticks). (B). *Salmonella enterica Se*ACC(6') is shown in complex with its substrate kanamycin (purple sticks), and CoA shown in black sticks. Examples of sirtuins structures are shown in panels C and D). These enzymes contain a Rossmann fold domain (blue) and a variable Zn(II)-binding domain (green, with Zn(II) shown as gray sphere). The binding sites for NAD^+ (C, gold) and the acetyllysine substrate (C, red sticks; lysine in black sticks) are located in a cleft between the two domains. The products of the reaction, nicotinamide (red sticks) and ADP-ribose (gold sticks) are shown in panel D. *Thermotoga maritima Tm*Sir2 (panel C) is shown with a peptide substrate (red sticks). The archaeon *Archaeoglobus fulgidus Af*Sir2 is shown in panel D. (A) PDB 1QSN; (B) PDB 2QIR; (C) PDB 2H4F; (D) PDB 1YC2.

Table 2.1. Representative frequency of prokaryotic RLA components

Organism	GNAT	Sirtuin	HDAC
ARCHAEA			
Methanococcus maripaludis	5	0	0
Pyrococcus furiosus	7	1	1
Sulfolobus solfataricus	8	1	3
BACTERIA			
Actinobacteria			
Mycobacterium tuberculosis	19	1	0
Streptomyces coelicolor	72	2	1
Bacteriodetes			
Bacteriodes thetaiotaomicron	8	1	0
Deinococcus-Thermus			
Thermus thermophilus	9	1	3
Firmicutes			
Bacillus subtilis	28	1	1
Clostridium difficile	24	1	0
Geobacillus kaustophilus	9	2	0
Lactobacillus casei	32	1	0
Listeria monocytogenes	14	1	0
Staphylococcus aureus	29	1	1
Streptococcus pneumoniae	22	0	0
Proteobacteria			
Alpha			
Caulobacter crescentus	26	1	3
Rhodopseudomonas palustris	24	1	1
Ruegeria sp TM1040	25	1	2
Beta			
Bordetella pertusis	12	1	1
Neisseria meningitidis	7	0	1
Delta / Epsilon			
Campylobacter jejuni	4	1	0
Helicobacter pylori	11	1	0
Myxococcus xanthus	47	1	3
Gamma			
Erwinia amylovora	19	1	0
Escherichia coli	26	1	0
Francisella tularensis	5	0	0
Haemophilus influenzae	3	2	0
Legionella pneumophilia	18	0	0
Proteus mirabilis	13	1	0
Pseudomonas aeurginosa	22	2	0
Salmonella enterica	26	1	0
Shigella flexneri	21	1	0
Vibrio cholera	31	1	2
Yersinia pestis	14	1	0
Spirochaetes			
Borrelia burgdorferi	1	0	0

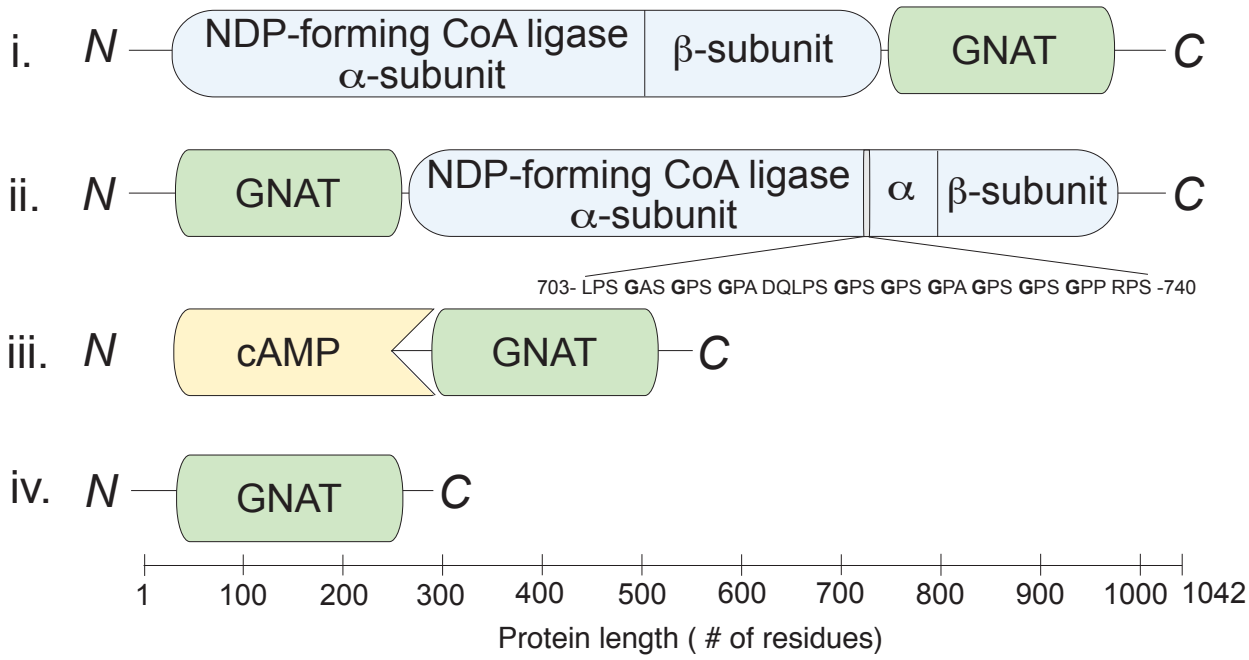

Figure 2.6. **Diversity in the domain organization of prokaryotic protein acetyltransferases.** GNAT protein acetyltransferases characterized to date exhibit different domain organization: (Type I) an *N*-terminal domain of unknown function homologous to an ADP-forming acyl-CoA synthetase domain fused to a *C*-terminal GNAT domain; (Type II) an *N*-terminal GNAT domain fused to a *C*-terminal domain of unknown function homologous to an ADP-forming acyl-CoA synthetase domain, which contains a GPS motif, a 37-aa long, degenerate proline-rich domain typically found in collagen (250); (Type III) a GNAT domain fused to an *N*-terminal cAMP-binding domain; (Type IV) a single GNAT domain.

residues) *N*-terminal domain, and the catalytic GNAT domain (~200 residues) at the *C*-terminus (68, 69). Although the function of the large *N*-terminal domain of Pat enzymes remains largely unclear, insights into its relevance to Pat function have been reported (70, 71). Briefly, results obtained from *in vitro* and *in vivo* analyses of single-amino acid *Se*Pat variants showed that such variants had low enzymatic activity (70). Furthermore, results from recently reported structural work aimed at understanding the substrate specificity of Pat enzymes suggested that in the absence of the large domain of Pat, the catalytic domain of the enzyme inefficiently interacts with its protein substrate (71). Whatever the role of the *N*-terminal domain may be it is likely to also play a role in sensing acetyl-CoA. This conclusion was drawn on the basis of results from isothermal calorimetry experiments, which showed that *Se*Pat binds two molecules of acetyl CoA, one binds to the *N*-terminal domain, the other one to the catalytic domain (70, 72-77).

Type II. *Streptomyces lividans* encodes a protein acetyltransferase (*Sl*PatA) in which the domain order is reversed relative to the domain order observed in *Se*Pat, *Ec*Pka, and *Rp*PatA. That is, in *Sl*PatA the GNAT catalytic domain is located at the *N*-terminus and the large domain of unknown function is located at the *C*-terminus (31). Other members of the actinomycetes, as well as the archaeon *Archaeoglobus fulgidus*, exhibit the same domain organization. Notably, the *Sl*PatA large domain contains a proline-rich region that includes a degenerate collagen-like GPS motif. The role of the degenerate collagen-like GPS has not been established, and the presence of this additional feature of *Sl*PatA may suggest that regulation of this enzyme is more complicated than the regulation other Pat homologues.

The large domains of Type I and Type II Pat enzymes share homology with ADP-forming acyl-CoA synthetases (Pfam 13380) that catalyze the reaction: free acid + ATP + CoA $\rightleftharpoons$ acyl-CoA + ADP + P_i. ADP-forming acyl-CoA synthetases have been characterized in archaea

and protists (75-77). In spite of this homology, no catalytic activity has been attributed to the *N*-terminal domain of Type I or Type II GNAT acetyltransferases (73, 74).

Type III: *Mycobacterium tuberculosis* and *Mycobacterium smegmatis* each encode a two-domain protein acetyltransferase (*Mt*PatA and *Ms*PatA, respectively) in which the *C*-terminal GNAT domain is fused to an *N*-terminal cAMP-binding regulatory domain (discussed in more detail below).

Type IV: Several prokaryotes encoding single-domain GNAT protein acetyltransferases have been characterized. These enzymes are substantially smaller (~200 residues) compared to the large two-domain Pat homologues (~800-1100 residues), yet they appear to perform similar functions. Single-domain GNATs have been identified and characterized in *B. subtilis* (*Bs*AcuA) (30, 78), *R. palustris* (*Rp*KatA) (28), and the archaeon *Sulfolobus solfataricus* (*Ss*Pat) (79). The range of domain architectures and organization in the bacterial and archaeal protein GNATs reveals that lysine acetylation is most likely regulated by diverse signals within these organisms.

A word of caution about nomenclature of Pat enzymes. The reader should be cautioned about the misuse of the 'Pat' abbreviation being used to name acetyltransferases that do not belong to the Type I, Type II, or Type III protein acetyltransferases. Case in point. The 'Pat' enzyme from *Sulfolobus solfataricus* [*Ss*Pat; PDB 3F8K)] is only 160-residues long (73, 74). Such a length is substantially shorter than the typical length of Type I Pat enzymes, which are between 850 and 1100 residues long. The '*Ss*Pat' enzyme actually is a Type IV lysine acetyltransferase.

Known GNAT functions in *Escherichia coli* and *Salmonella enterica.* The model organisms *E. coli* and *S. enterica* encode ~26 GNAT homologues, only half of which have known or predicted functions (Table 2.2). These GNATs target primary amines (80, 81),

Table 2.2. Roles of *E. coli* Gcn5 *N*-acetyltransferases

Protein	Function	Reference
Aat	Leucyl, phenylalanyl-tRNA-protein transferase	(93)
ArgA	Glutamate acetyltransferase	(86)
PanM/PanZ	PanD maturation factor	(14)
PhnO	Aminoalkylphosphonic acid acetyltransferase	(251)
Pka/YfiQ/Pat	*N*-Lysine protein acetyltransferase	(24)
RimI	S18 ribosomal protein acetyltransferase	(89)
RimJ	S5 ribosomal protein acetyltransferase	(89)
RimL	L12 ribosomal protein acetyltransferase	(90)
SpeG	Spermidine acetyltransferase	(84)
TmcA	$tRNA^{Met}$ cytidine acetyltransferase	(88)
WecD	dTDP-fucosamine acetyltransferase	(85)
YhhY	Aminoacyl nucleotide acetyltransferase	(87)
YncA/MntA	Putative methionine sulfoximine/sulfone acetyltransferase	(91, 252)
YafP	Possible nitroaromatic compound acetyltransferase	(253)

including the *N*-termini of proteins (82, 83), aminoglycoside antibiotics (63), polyamines (84), a nucleotide sugar (85), glutamate (86), toxic aminoacyl nucleotides (87), and transfer RNAs (88). Three GNAT enzymes, RimI, RimJ, and RimL, acetylate the α-amine group at the *N*-terminus of ribosomal proteins S18, S5, and L12, respectively (89, 90). The *Ec*YncA homologue of *S. enterica* (*Se*MddA) was recently shown to acetylate and detoxify oxidized methionine derivatives (*e.g.* methionine sulfoximine, methionine sulfone) (91). Pka is the only identified protein lysine acetyltransferase (Pat in *S. enterica*) (24, 92) (discussed in more detail below). Two other *E. coli* GNATs appear to modify proteins through unusual mechanisms. Aat is a leucyl, phenylalanyl-tRNA-protein transferase that modifies proteins targeted for degradation through the *N*-end rule degradation pathway by the attachment of a leucine or phenylalanine to lysyl and arginyl residues. (93, 94). In *S. enterica*, a GNAT homologue known as PanM (formerly YhhK) promotes cleavage and maturation of the *L*-aspartate-α-decarboxylase zymogen (pro-PanD), an enzyme of the coenzyme A biosynthetic pathway (14, 15). PanZ, the PanM homologue in *E. coli* performs the same function in this bacterium (95, 96).

LYSINE DEACETYLASES

N-Lysine protein acetylation is reversible by protein deacetylases (referred to as histone deacetylases, or HDACs (Pfam 08295)). Members of four HDAC families catalyze *N*-lysine deacylation. The related classes I, II, and IV HDACs do not require cofactors and catalyze lysine deacylation via hydrolysis of the acyl group (Pfam 08295) (55, 97) (Fig. 2.7A). In contrast, class III HDACs, commonly referred to as sirtuins (Pfam 02416), are a mechanistically distinct family of NAD^+-dependent deacetylases (97, 98) (Fig. 2.7B). Bacteria and archaea typically encode one to two sirtuin homologues, whereas eukaryotes encode several (59, 99) (Table 2.1).

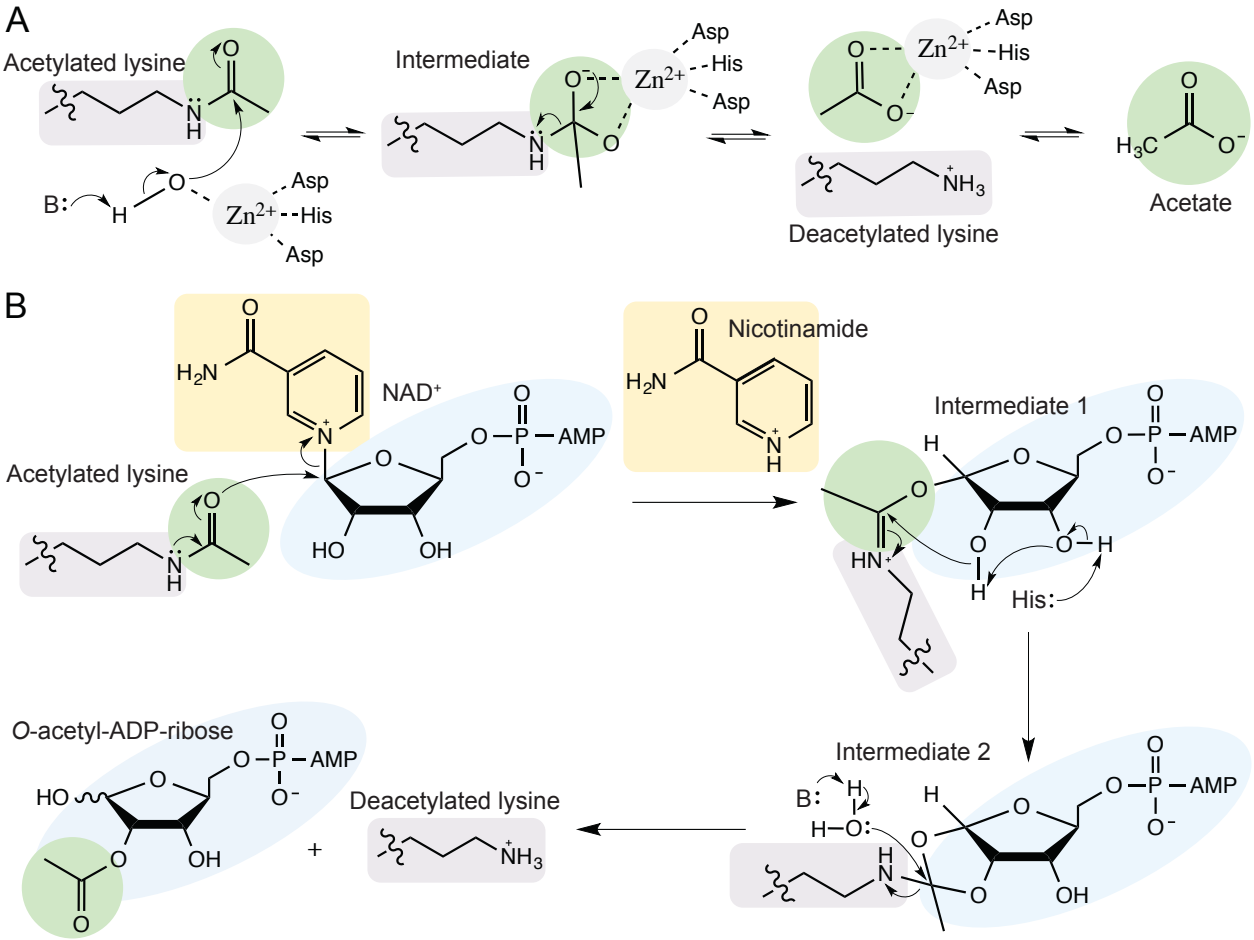

Figure 2.7. **Deacetylation mechanisms of HDACs and Sirtuins.** (A) HDAC-mediated catalysis is mediated by a histidinyl residue, which acts as a general base and in conjunction with the Zn(II) ion, activates a metal bound water molecule for nucleophilic attack of the substrate carbonyl. The products of the HDAC reaction are deacetylated protein and acetate. (B) Sirtuin-catalyzed deacetylation is initiated by binding of NAD^+ to the catalytic site. The formation of an imidate intermediate occurs through a one-step ADP-ribosylation and inversion of configuration. The products of the sirtuin reaction are the deacylated protein, nicotinamide, and an *O*-acyl-ADP-ribose product that is derived by mono-ADP-ribosylation of the removed acyl group.

Zinc-dependent Histone (Lysine) Deacetylases (HDACs)

HDACs belonging to class I, II, and IV families also deacetylate non-histone protein substrates and therefore are referred to as lysine deacetylases [reviewed in (100, 101)]. The core feature of HDAC structure is an α/β deacetylase fold comprised of 8-stranded parallel β-sheet in which conserved residues coordinate a Zn(II) ion required for catalysis. Catalysis is mediated by a histidinyl residue, which acts as a general base and in conjunction with the Zn(II) ion activates a metal bound water molecule that triggers the nucleophilic attack on a carbonyl group of the substrate. HDACs are unique in their ability to catalyze deacetylation of both protein and small molecule substrates (Fig. 2.7). *R. palustris* (LdaA) and *B. subtilis* (AcuC) proteins are examples of bacterial HDACs that deacetylate proteins, and are discussed below.

NAD^+-dependent Sirtuin Deacetylases

Though described as deacetylases, some sirtuins have depropionylase activity (56, 57, 102). In eukaryotes, certain sirtuins have also been shown to have protein desuccinylation (103, 104) and demalonylation (105) activity, and are thought to play a critical role in mitochondrial metabolism [reviewed in (106, 107)]. The ability of sirtuins to deacylate a variety of modifications correlates with the ability of their partner GNAT acetyltransferases to utilize alternative acyl-CoA donors. This provides a mechanism with a wider range of modifications available to the cell to maintain homeostasis under diverse physiological conditions in response to environmental changes.

Sirtuins hydrolyze NAD^+. Due to their requirement for NAD^+, sirtuin deacetylases have garnered a great deal of interest for their ability to 'sense' and respond to NAD^+ levels, which in turn reflect on the cellular energy status (108, 109). Deacetylation is an energetically favorable process and can be catalyzed by the Class I, II and IV deacetylases without cofactors. It is

therefore of interest that sirtuins (Class III) hydrolyze NAD^+ in the course of the deacetylation reaction, an essential metabolic cofactor (110, 111). The resynthesis of NAD^+ from the hydrolysis products requires ~8.2 kcal/mol of energy and is energetically expensive (110, 112). It stands to reason that there is a compelling reason to tie NAD^+ levels to sirtuin activity (i.e. protein acetylation state) (109).

Sirtuin reaction mechanism. Sirtuin deacetylases have an unusual catalytic mechanism that uses NAD^+ not as a cofactor, but as a co-substrate that is cleaved during the deacylation reaction, yielding *O*-acyl-ADP-ribose (*O*-AADPR) (97, 113-116). Sirtuin-catalyzed deacetylation is initiated by binding of NAD^+ to the catalytic site. The formation of an imidate intermediate occurs through a one-step ADP-ribosylation and inversion of configuration [reviewed in (117)] (Fig. 2.7). The inversion of configuration was predicted by the original discovery that sirtuins were enzymes that used pyridine nucleotides as substrates (98). The reaction of the coenzyme B_{12} biosynthetic pathway in *S. enterica* that is also performed by the CobB sirtuin proceeds via a nucleophilic attack inverting the configuration of the *N*-glycosidic bond between the base and the ribosyl moiety of the pyridine nucleotide co-substrate (117). The products formed from the deacetylation reaction are (i.) the deacylated protein, (ii.) nicotinamide, and (iii.) *O*-acyl-ADP-ribose. The *O*-acyl-ADP-ribose by-product is generated through the mono-ADP-ribosylation of the removed acyl group (102, 116, 118, 119).

Physiological importance of *O*-acetyl-ADP-ribose. The physiological role of *O*-AADPR is unknown in prokaryotes, but some information about its metabolism has been reported in eukaryotic systems. In eukaryotes, *O*-AADPR may act as a signaling molecule and may regulate gene silencing, ion channel gating and redox regulation (118, 120). There are several eukaryotic enzymes identified to utilize *O*-AADPR as a substrate including two NUDIX (Nucleoside

Diphosphate linked to X) hydrolases (Ysa1 from yeast; NudT5 from mouse) (121), ADP-ribosyl hydrolase (ARH3, human) (122), and two uncharacterized enzyme activities including an esterase and nuclear acetyltransferase (from yeast and human) (121). These enzymes utilize *O*-AADPR in various ways, generating *O*-acetyl-ribose-phosphate and AMP (Ysa1 and NudT5), acetate and ADP-ribose (ARH3, esterase), or an unknown acetylated product and ADP-ribose (nuclear acetyltransferase). More work is needed to elucidate the role of *O*-AADPR in prokaryotic physiology.

Effect of the NAD^+:NADH ratio on sirtuin function. Both NADH and nicotinamide have been reported to inhibit sirtuin function, and may play a role in regulation of sirtuin activity (123-125). Nicotinamide condenses with an ADPr-like intermediate formed during the deacetylation reaction, which prevents the reaction from moving forward (109), and inhibits sirtuin activity non-competitively at concentrations consistent with physiological nicotinamide levels (30–200 μM) (113, 126-130).

In contrast, NADH competitively inhibits sirtuin activity with reported K_i values in the sub-millimolar to millimolar range, consistent with physiological NADH levels (97, 108, 123, 131, 132). Sirtuin activity varies with the NAD^+:NADH ratio. A high NAD^+:NADH ratio indicates that the cell is efficiently oxidizing NADH back to NAD^+, implying among other things, that a strong proton motive force is being generated under such conditions. A strong proton motive force results in high ATP levels and the concomitant increase in the demand for acetyl-CoA for anabolic purposes. If under such conditions acetate is present in the environment, the cell can activate it to acetyl-CoA using the acetyl-CoA synthetase (Acs), an enzyme known to be under RLA control (discussed further below) (23). Acetylated Acs is inactive, hence, the ratio of acetylated (inactive):deacetylated (active) Acs would be expected to be low when the

NAD^+:NADH ratio is high, since NAD^+ would be available for sirtuin to deacetylate (*i.e.,* activate) acetylated Acs (132). The NAD^+:NADH ratio is known to fluctuate with metabolism, thus changes in this pool of free NAD^+ likely regulate protein acylation state, with deacylation occurring when the NAD^+:NADH is high, and acetylation being favored when the NAD^+:NADH ratio is low.

Overview of sirtuin structures. Three-dimensional crystal structures of sirtuins from all domains of life are available (*e.g., Archaeoglobus fulgidus*, PDB 1YC2; *Thermatoga maritima*, PDB 4BUZ; *E. coli*, PDB 1S5P; *Saccharomyces cerevisiae*, PDB 2HJH; and human SIRT1, 4KXQ; SIRT2, 3ZGO; SIRT3, 4BN4; SIRT5, 3RIY; SIRT6, 3PKI) (Fig. 2.5C, D). Sirtuins are comprised of a catalytic domain that contains a Rossmann fold domain and a variable Zn(II)-binding domain, with divergent *N*- and *C*- terminal regions [reviewed in (133, 134)]. The Zn(II) ion in sirtuins is structurally important and does not contribute to catalysis (135). The binding sites for the nicotinamide and ribose moieties of NAD^+ and the acetyllysine substrate are located in the cleft between the large (Rossmann fold) and small (Zn(II)-binding) domains (Fig. 2.5C, D). This binding cleft allows for substrate selectivity among different sirtuins. Importantly, NAD^+ is oriented opposite to the typical orientation seen with Rossmann fold-containing enzymes, in which the nicotinamide moiety binds to the *N*-terminal half of the β-sheet and the adenine binds to the *C*-terminal half. This orientation reversal ensures the elimination of nicotinamide.

HIGH-THROUGHPUT IDENTIFICATION OF ACETYLATED PROTEINS

Global Approaches for the Identification of Total Acetylated Protein Population

Characterization of the total acetylated protein population (the "acetylome") in a given organism has been accelerated by the development of sensitive mass spectrometry-based methods that detect the precise location of acetylated lysine residues within any given protein pool (33). Such approaches have putatively identified a large number of acetylation targets, many of which appear to be acetylated at several sites. Early studies combined the use of two-dimensional separation of proteins followed by detection of acetyllysine residues by immunoblotting (136). Subsequent studies characterizing the acetylomes of eukaryotes used immunoprecipitation as a way to enrich for acetyllysine peptides present in tryptic digests of a protein pool (137-139). The combined use of anti-acetyllysine antibodies and mass spectrometry are the foundation for the current proteomic methodology used to identify acetylated peptides and proteins (Fig. 2.8A). These global studies have been extended to archaea (*N*-terminal acetylation) (140), bacteria (141-143), plants (144), parasites (145, 146), and humans (147), helping cement the contributions of acetylation to cellular physiology. Such global studies suggest that acetylation controls diverse processes including metabolism, transcription, translation, and cell structure.

Alternative global approaches for the analysis of acetylomes. Proteome microarrays provide an alternate method for identifying the putative targets of acetyltransferases as well as other modifying enzymes. Protein chip technology was first reported in yeast for the analysis of protein kinases (148). Lin *et al* used a similar approach to identify 13 substrates of the NuA4 acetyltransferase, including the phosphoenolpyruvate carboxykinase (Pck1p) enzyme (35). This same experimental method was used in another study to construct a microarray comprised of

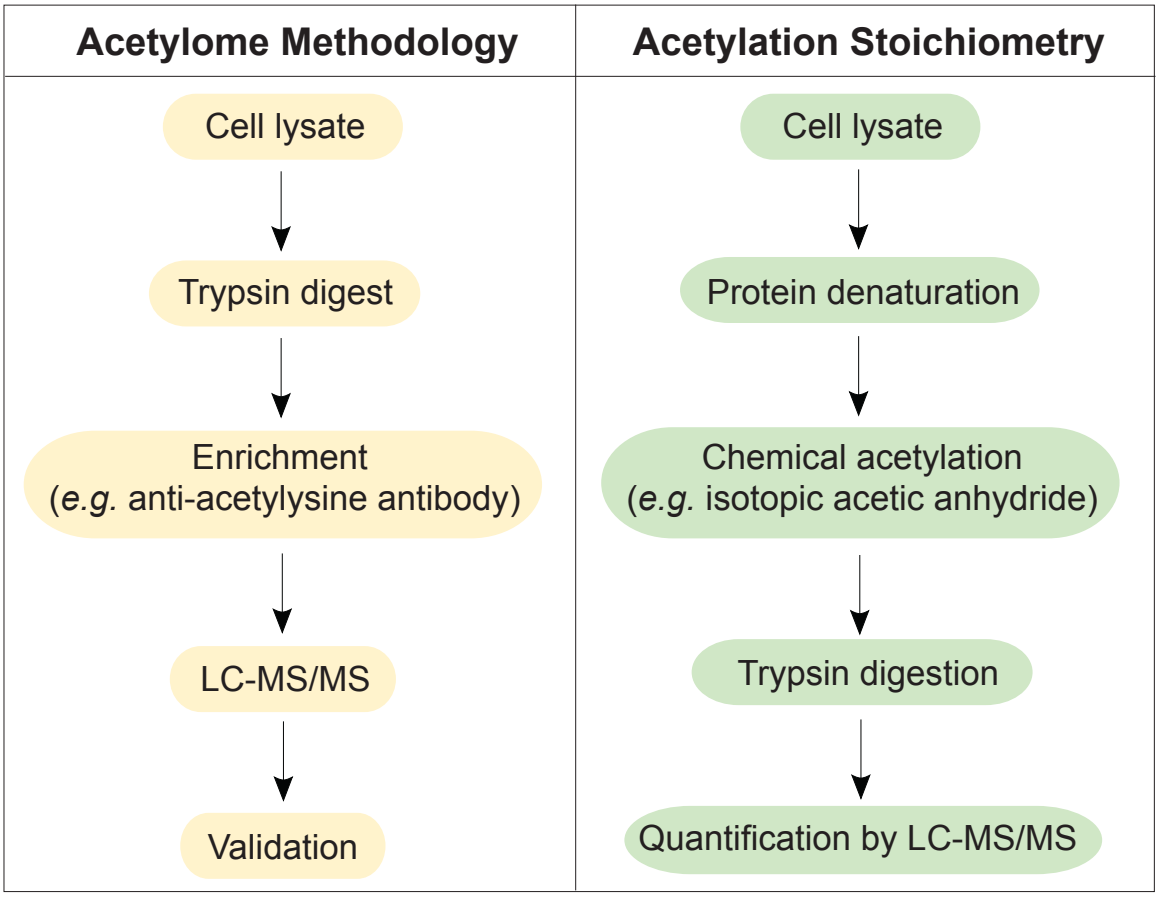

Figure 2.8. Methods for the analysis of acetylomes. (A) A representative workflow of the methodology typically used to determine total acetylated protein from an organism. (B) A representative workflow of a recently described method to determine the level of acetylation of identified acetylated target proteins.

E. coli proteins. These microarrays were probed with the *S. enterica* bacterial protein acetyltransferase (*Se*Pat) enzyme, resulting in the identification of seven substrates, including several transcription factors (149).

Other studies have taken advantage of labeling strategies like Stable Isotope Labeling with Amino acids in cell Culture (SILAC) quantitative mass spectrometry (150). SILAC allows for detection of differences in protein abundance using *in vivo* incorporation of non-radioactive isotope labels. Benefits of this analysis are the identification and quantification of relative differential changes in complex protein samples.

Recent approaches have begun to tackle the problem of the stoichiometry of the level acetylation at individual sites in order to understand the biological significance of acetylation events (151, 152). The first method for determining site-specific stoichiometry of acetylated peptides using no immunoenrichment was used to investigate the acetylome of *E. coli* (151). This was achieved by chemically acetylating unmodified lysine residues using acetic anhydride labeled with stable isotopes to generate an acetyllysine pair and analyzed by mass spectrometry (Fig. 2.8B). In this scenario, proteins endogenously acetylated contain 'light' acetyllysine residues, while proteins modified chemically contain 'heavy' acetyllysine residues. After resolution by mass spectrometry, the stoichiometry is determined by examining the ratio of light to heavy peak areas. By this method the authors identified proteins that use or generate acetyl-CoA, and those involved in transcription and translation, are the most highly acetylated (151).

Bacterial Acetylome Studies

Bacterial acetylomes have been characterized in *E. coli* (141, 142), *S. enterica* (153), *Bacillus subtilis* (154), *Erwinia amylovora* (155), *R. palustris* (28), *Staphylococcus aureus* (156),

Geobacillus kaustophilus (157), *Vibrio parahaemolyticus* (158), *Thermus thermophilus* (159), and *M. tuberculosis* (143), *Mycoplasma pneumonia* (160), and *Streptomyces roseosporus* (161). These studies have identified a range of 62-667 putatively acetylated proteins per organism, with the majority of acetylated proteins involved in central metabolism and translation (141, 156, 158) (Fig. 2.9).

The large number of putative acetylation targets detected by mass spectrometry has raised important questions as to the significance of the detected acetylation events, and how they contribute to cellular physiology. Specifically, it is important to know how these acetylation events occur, at what frequency, and whether they affect protein function or stability. Two independent studies of acetylated proteins in *E. coli* identified 85 and 91 putative acetylation targets (141, 142). Surprisingly, only six proteins acetylated at the same lysine residue were identified in both studies (60). Since then a third acetylome study has been performed in *E. coli* identified 349 acetylated proteins (162). In the related enterobacterium *S. enterica*, Wang *et al* found 191 putatively acetylated proteins, many of which were metabolic enzymes (153). Although experimentally validating some of the results *in vitro*, studies by others groups were not able to reproduce the findings (28).

A combination of mass-spectrometry analysis, *in vivo* genetics analyses, and *in vitro* validation for the Gram-negative photosynthetic bacterium *R. palustris* has yielded the most comprehensive list of *bona fide* acetylation targets to-date (28). In this study, acetylated proteins were identified by tandem mass spectrometry by comparing the acetylome of a wild-type *R. palustris* strain to the acetylomes of strains in which one or more acetyltransferases were absent. Stringent cut-offs were applied to reduce noise by using two different algorithms. Proteins that

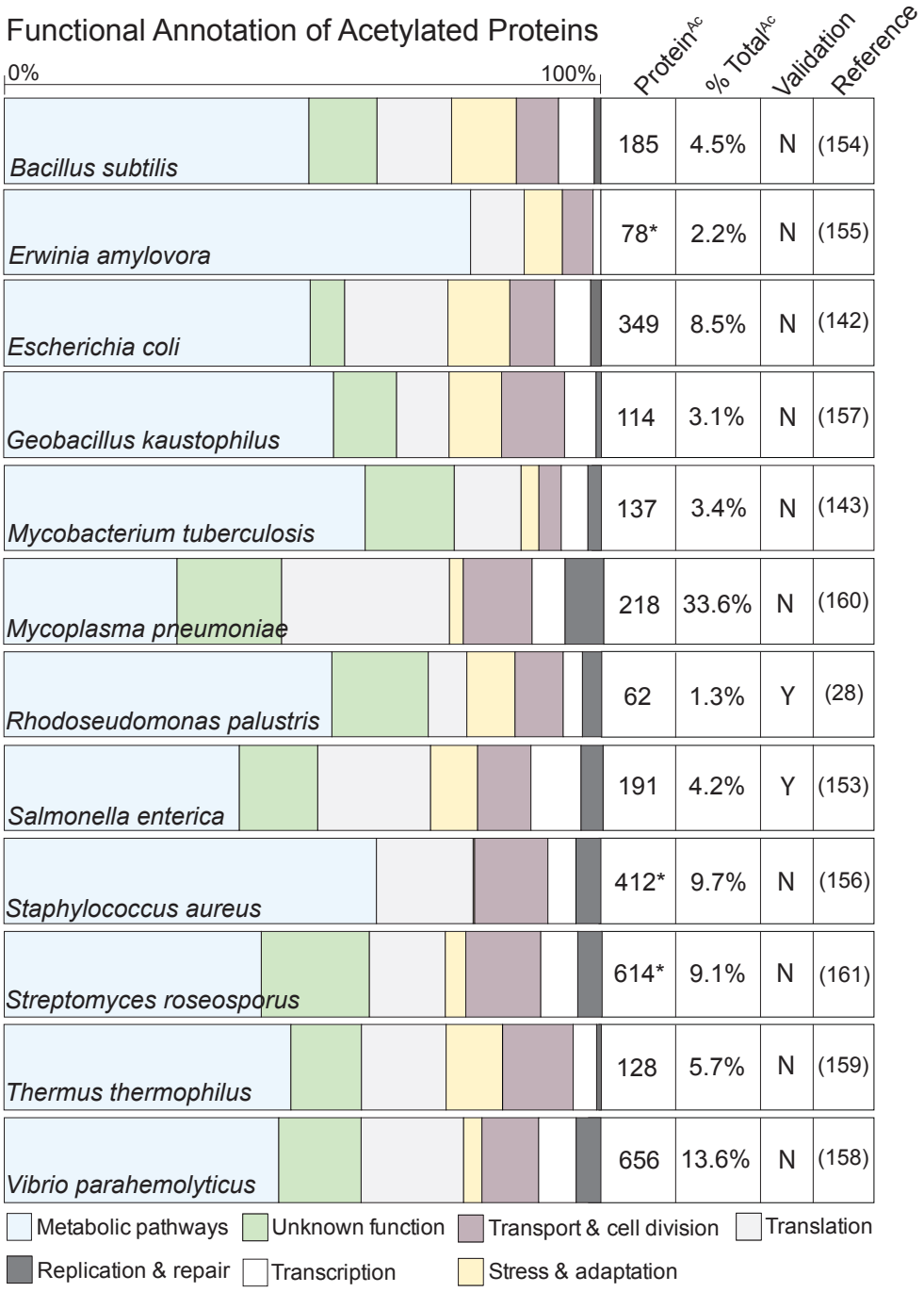

Figure 2.9. Comprehensive overview of bacterial acetylome studies. Functional annotation of identified acetylated proteins from bacterial acetylome studies. Protein^{Ac}: number of identified acetylated proteins; % Total^{Ac}: the percent of acetylated proteins of the entire proteome; Validation: N, no; Y, yes. *Values are different than previously reported; however, the values listed reflect the available data were obtained from supplementary information from the cited references. The percentage scale at the top of the figure should be used to estimate the percentage of acetylated proteins in each of the categories within any given microorganism in the figure.

were identified in this comparison were validated by both *in vitro* and *in vivo* methods. The authors also confirmed that acetylation altered the activity of each of target protein.

Current noteworthy issues in the field. Bioinformatics analyses reveal that protein acetyltransferases are conserved in nearly all reported genomes. This suggests that acetylation is widespread in prokaryotes and eukaryotes, which in turn implies that protein acetylation is not limited to the regulation of proteins involved in DNA maintenance or transcription. The acetylome studies provide a framework for the identification of putative targets of acetylation, but detailed mechanistic studies are needed to validate these proteomics-based results and to demonstrate the findings are biologically relevant. There are several issues that need to be taken into consideration, and are discussed below.

(i) Global, non-enzymatic acetylation by acetyl-phosphate (AcP). Recent work in *E. coli* suggests that global, non-enzymatic, low-level lysine acetylation is also mediated by the reactive, high-energy metabolite acetyl-phosphate (AcP), and that this acetylation event is globally regulated by growth phase and metabolism (81). Weinert *et al* compared the level of protein acetylation from *E. coli* cells at different growth phases using SILAC quantitative mass spectrometry (81). The analysis revealed that the bulk level of protein acetylation was dramatically increased in stationary phase. An increase in protein acetylation was also strongly correlated with an increase in AcP levels. Taken together, these results suggest that AcP may be directly involved in widespread, growth phase-dependent chemical (non-enzymatic) acetylation of *E. coli* proteins. The physiological significance of this phenomenon is not understood (81). Further support for the role of AcP as a non-specific donor of acetyl groups in lysine acetylation in *E. coli* was recently reported (152). Direct acetylation by acetyl-CoA has also been suggested as a mechanism of non-enzymatic acetylation in eukaryotes (163).

(ii) Validation of proteomic approaches. Because of its broad distribution in nature, RLA elicited a great deal of interest amongst biologists eager to define the role of RLA in cell physiology. However, several issues need to be addressed before we understand whether or not the function of specific proteins is under RLA control. Issues that need clarification are:

(a) Non-enzymatic protein acetylation. Chemical, non-enzymatic lysine acetylation can occur when pH is ≥8.0 (151, 164, 165). The autoacetylation activity of some proteins (166) further compounds this problem, leading to reporting of false positive enzyme-driven acetylation. Therefore, multiple controls must be used to distinguish between autoacetylation and enzyme-driven acetylation, namely the reaction substrates with the addition of inactive variants of the modifying acetyltransferase enzyme.

(b) Physiological relevance of multiple acetylation sites. Many of the reported acetylomes identify proteins with multiple acetylated lysine residues (~5-10 in some cases). This information contrasts sharply with observations for validated RLA targets such as acetyl-CoA synthetase (Acs) and other members of the acyl-CoA synthetases (discussed further below), in which the acetylation of a single lysine residue is necessary and sufficient to alter enzyme function (23, 28, 167). Recently, the first validated example of an Acs homologue from *Saccharopolyspora erythraea* that undergoes multiple acetylation events was reported, and the observations were validated *in vitro* and *in vivo* (168). However, of the four original acetylation events, only two were shown to have an effect on enzyme activity, highlighting the importance of *in vivo* and *in vitro* validation. It is imperative to determine the effect that each acetylated lysine may have on substrate binding, catalytic activity, or resistance to proteolytic activity to gain insights into the physiological importance of RLA.

(c) Possible over-representation of central metabolic enzymes. The fact that the majority of acetylated peptides identified are involved in central metabolism, specifically glycolysis, has been perhaps overemphasized. Notably, membrane-associated proteins, proteins present at low levels, or proteins not expressed under the culture conditions tested may represent important groups of targets under the control of RLA which are missed by the current methodology.

(d) Validation. Very limited, and in some cases no validation of results obtained by mass spectrometry analyses has been reported in studies of bacterial acetylomes. Specifically, the function of the proteins identified as acetylation targets have not been analyzed *in vitro* to identify the modifying enzymes, or whether or not acetylation alters protein function or stability. At present, large-scale mass spectrometry results of bacterial acetylomes provide only putative targets until further validation is performed.

VALIDATED REVERSIBLE LYSINE ACYLATION (RLA) TARGETS IN BACTERIA AND ARCHAEA

Discovery of RLA in Prokaryotes

The role of RLA in bacteria, specifically in relation to acetylation of metabolic enzymes, was discovered in *S. enterica*. Refer to Table 2.3 for a to-date comprehensive list of validated RLA targets in prokaryotes. The protein acetyltransferase of *S. enterica, Se*Pat, was first identified as the enzyme responsible for the acetylation and inactivation of acetyl-CoA synthetase (Acs), the enzyme that activates acetate when present in the environment at low concentrations (≤10 mM) (24). Acs belongs to the acyl-CoA synthetase family (Pfam 00501), which convert acetate to acetyl-CoA (24). Acyl-CoA synthetases are ubiquitous across all domains of life (169-171).

Table 2.3. Validated substrates of prokaryotic lysine acetyltransferases

Protein	Function	Reference
Bacillus subtilis AcuA		
AcsA	AMP-forming acetyl-CoA synthetase	(30)
Escherichia coli Pka		
Acs	AMP-forming acetyl-CoA synthetase	(177)
RNase R	Stable RNA exoribonuclease	(68, 92)
RcsB	Response regulator for capsule synthesis	(149)
Mycobacterium smegmatis PatA		
MSMEG_4207	Universal stress protein	(191)
Acs	AMP-forming acetyl-CoA synthetase	(178)
FadD2, FadD4, FadD5, FadD10, FadD12, FadD13, FadD22, FadD35	AMP-forming acyl-CoA synthetases	(192)
Rhodopseudomonas palustris KatA		
Acs	AMP-forming acetyl-CoA synthetase	(28)
PrpE	AMP-forming propionyl-CoA synthetase	(28)
BadA, HbaA, AliA	AMP-forming aromatic and alicyclic acyl-CoA synthetases	(28)
Rhodopseudomonas palustris Pat		
Acs	AMP-forming acetyl-CoA synthetase	(69)
PrpE	AMP-forming propionyl-CoA synthetase	(28)
BadA, HbaA, AliA	AMP-forming aromatic and alicyclic acyl-CoA synthetases	(69)
PimA	AMP-forming pimeloyl-CoA synthetase	(28)
HcsA, FadD, FcsA, LcsA, IbuA	AMP-forming acyl-CoA synthetases that activate mono- and dicarboxylic acids	(28)
Salmonella enterica Pat		
Acs	AMP-forming acetyl-CoA synthetase	(23, 169)
PrpE	AMP-forming propionyl-CoA synthetase	(56)
Streptomyces lividans PatA		
AacS	AMP-forming acetoacetyl-CoA synthetase	(31)
Sulfolobus solfataricus Pat		
Alba	Chromatin protein	(59)

This family of enzymes converts weak organic acids to their CoA thioesters through two half reactions via an adenylated intermediate (see reaction below) (172) (Fig. 2.10A).

$$\text{Acetate} + \text{ATP} + \text{Acs} \rightarrow \text{Acetyl-AMP} + PP_i + \text{Acs} \quad \ldots\ldots\ldots\ldots \text{ Eq. [1]}$$

$$\text{Acetyl-AMP} + \text{CoA} + \text{Acs} \rightarrow \text{Acetyl-CoA} + \text{AMP} + \text{Acs} \ldots\ldots\ldots\ldots\ldots\ldots \text{Eq. [2]}$$

As mentioned above, *Se*Acs is required during growth at low concentrations of acetate (≤10 mM). When the concentration of acetate in the environment is >10 mM, assimilation of acetate occurs via the phosphotransacetylase / acetate kinase (Pta / Ack) pathway (173).

*Se*Acs activity is regulated by reversible acetylation of an active site lysine residue, Lys609 (23). This discovery opened the doors to numerous studies on regulation of metabolic enzymes by acetylation and shifted the focus from regulation of histones by acetylation to acetylation as a means to regulate metabolism and physiology.

*Se*Acs activity was first predicted to be under the control of acetylation was when it was observed that the sirtuin deacetylase (*Se*CobB) was needed in growth conditions in which acetate (10 mM) or propionate (30 mM) was the sole source of carbon and energy (23, 29). In support of this idea, the *Se*CobB protein was shown to deacetylate Acs *in vitro* (23), resulting in reactivation of the Acs enzyme. These findings revealed for the first time that acetylation was a means to modulate activity of a metabolic enzyme (23). The modifying protein acetyltransferase of this bacterium, *Se*Pat, was subsequently discovered by selecting for derivatives of a Δ*cobB* strain that grew on 10 mM acetate (24). Deletion of the protein acetyltransferase (*Se*Pat) in a strain lacking *Se*CobB restored growth on both acetate (10 mM) and propionate (30 mM). *In vitro* studies demonstrated that *Se*Pat could both acetylate *Se*Acs and propionylate the propionyl-CoA synthetase (PrpE) (24, 56).

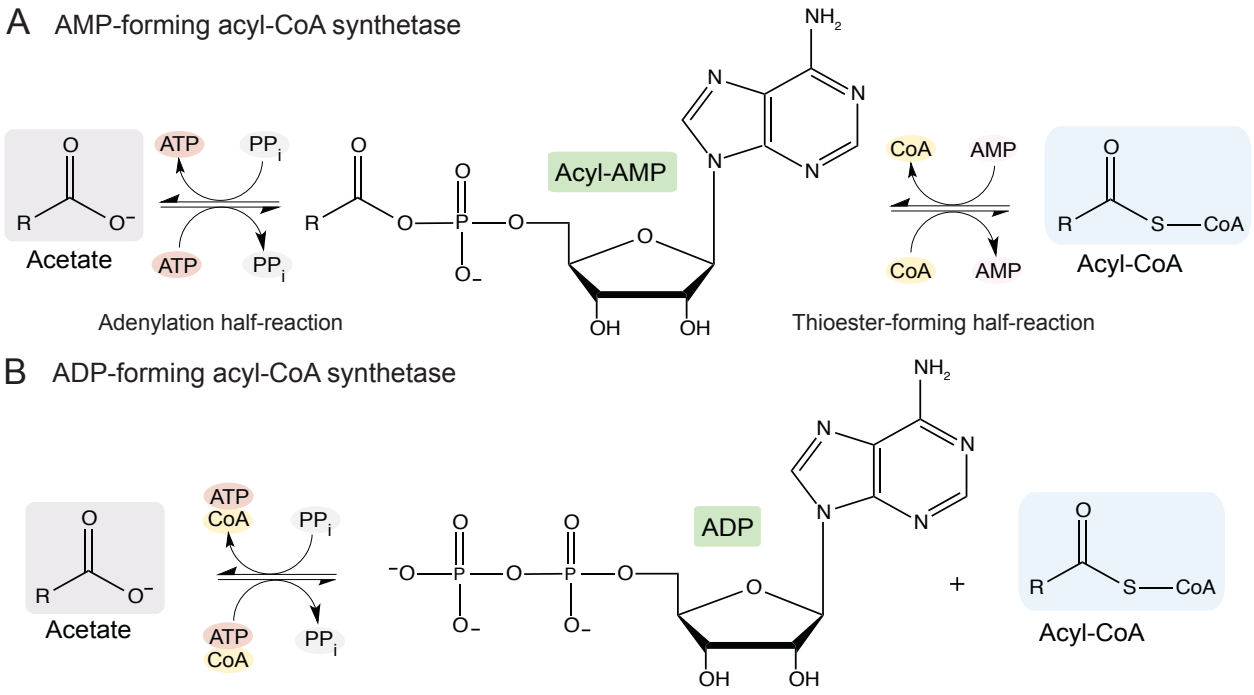

Figure 2.10. **Synthesis of acyl-CoAs by AMP- and ADP-forming acyl-CoA synthetases.** The AMP-forming and ADP-forming acyl-CoA synthetases convert organic acids to their CoA thioesters. AMP-forming acyl-CoA synthetases perform this reaction through two half reactions via an adenylated intermediate (A), while the ADP-forming acyl-CoA synthetase reaction is driven by the energy of hydrolysis of the γ-phosphate of ATP (B).

The acetylated lysine residue (Lys609 in *Se*Acs), is required for adenylylation of organic acids, and is universally conserved in the AMP-forming acyl-CoA synthetases. Acetylation of this lysyl residue prevents adenylylation of the acid substrate and blocks enzyme activity. Thus, *Se*Pat acetylation of the *Se*Acs active site lysine blocks the conversion of acetate to acetyl-AMP (23), the first half-reaction catalyzed by *Se*Acs. It is proposed that the lysyl residue (i) aids in the orientation of the carboxylate moiety of the acid and phosphoryl groups of ATP for the in-line attack, and (ii) stabilizes the transition state through the positive charge interactions (174, 175).

Acetylation of acetyl-CoA synthetase (Acs) is a conserved regulatory mechanism. Since its discovery, it has been shown that RLA controls Acs and other members of the acyl-CoA synthetases via acetylation, and that this regulatory mechanism of metabolism is present in prokaryotes and eukaryotes (29, 176). Acetylation of Acs homologues by *Se*Pat homologues has also been demonstrated in *E. coli* (141, 177), *R. palustris* (69), *B. subtilis* (30), *Streptomyces* spp. (31), and *Mycobacterium* spp. (178). Insight into the need for post-translational control of Acs activity was provided in studies that demonstrated dysregulation of this enzyme caused a severe imbalance in the energy charge of the cell, leading to growth arrest (179). An expanded explanation of these effects is described below.

RLA in Gram-negative Bacteria

Non-acyl-CoA synthetase targets of the *Salmonella enterica* protein acetyltransferase. It has been suggested that *Se*Pat can acetylate a variety of metabolic enzymes, including glyceraldehyde-3-phosphate dehydrogenase (GapA) and isocitrate lyase (AceA), and the glyoxylate shunt regulator isocitrate dehydrogenase kinase/phosphatase (AceK) (153). However, difficulties in reproducing these results by others have been reported (28). These discrepancies

need to be clarified before any conclusions about the involvement of RLA in the modulation of such key enzymes can be validated.

In *Escherichia coli*, the protein acetyltransferase (Pka) alters the fate of RNase R. Results from early studies suggested that the Pat homologue from *E. coli*, *Ec*Pka, acetylated the RNA polymerase alpha subunit; however, results from subsequent analysis failed to confirm this claim (180, 181). A *bona fide* substrate of *Ec*Pka is exoribonuclease RNase R, shown to degrade highly structured mRNA. RNase R is acetylated during exponential phase, destabilizing the protein, making it prone to proteolytic degradation (68, 92). This is the first example of acetylation by a *Se*Pat homologue affecting protein stability and thus enzyme activity. Notably, RNase R cannot be deacetylated by the *E. coli* sirtuin CobB, the only known protein deacetylase in this bacterium, and therefore is not a reversible modification (68).

In *Rhodopseudomonas palustris*, RLA controls the activity of many AMP-forming acyl-CoA synthetases. The role of RLA in the physiology of the purple non-sulfur photosynthetic α-proteobacterium *R. palustris* has been investigated (28). In this bacterium, RLA modulates the activity of enzymes involved in the anaerobic catabolism of aromatic organic acids and other fatty acids. Results from proteomics global analyses indicate that *Rp*Pat acetylates many acyl-CoA synthetases (AMP-forming) in addition to acetyl-CoA synthetase (Acs) and propionyl-CoA synthetase (PrpE), including those involved in activating short-, medium- and long-chain fatty acids and aromatic acids (*e.g.,* BadA, HbaA, AliA, PimA, HcsA, FadD, FcsA, LcsA, and IbuA) (28). It is significant that all of the verified *Rp*Pat substrates from this study were acyl-CoA synthetases. This data strongly suggests that *Rp*Pat may specifically recognize and regulate this class of enzymes via a negative feedback mechanism.

When an *Rp*Pat substrate, benzoyl-CoA synthetase (BadA) was acetylated *in vivo* in the absence of *Rp*Pat, Crosby *et al* predicted the existence of a second *R. palustris* protein acetyltransferase (69). A single-domain GNAT, *Rp*KatA (for K (Lys) acetyltransferase A), was identified based on its limited sequence homology (33% identical over 64 residues within the GNAT domain) to other known protein acetyltransferases. *Rp*KatA also acetylated the conserved catalytic lysine of acyl-CoA synthetases whose substrates included short-, medium-, long-, and branched-chain fatty acids in addition to aromatic organic acids (28, 69). It is noteworthy that although *Rp*KatA has similar enzymatic capabilities as *Rp*Pat (Type I GNAT), it is a much smaller protein comprised only of a catalytic domain (Type IV GNAT).

Insights into the role of *Rp*KatA were obtained by performing mass spectrometry-based proteomics analysis. Briefly, four acyl-CoA synthetases (BadA, AliA, HbaA, and PrpE) were acetylated in a *pat* deletion strain, but no acetylation of these proteins was seen in a *pat katA* double mutant (28). From *in vitro* studies, the authors learned that *Rp*Pat and *Rp*KatA had different substrate specificities for the acyl-CoA synthetases of *R. palustris*. For example, there are two acyl-CoA synthetases, hexanoyl-CoA synthetase A (HcsA) and long-chain acyl-CoA synthetase A (LcsA), which were acetylated by *Rp*Pat but were not acetylated by *Rp*KatA (28). It is not known how *Rp*KatA and *Rp*Pat recognize their substrates or why there is overlapping activity between the enzymes.

In addition to having two protein acetyltransferases, *R. palustris* also encodes two protein deacetylases, a sirtuin deacetylase (SrtN) and a Zn(II)-dependent lysine deacetylase (LdaA). Genetic evidence suggests that both deacetylases play a role in regulating acyl-CoA synthetases in *R. palustris* (28).

RLA in Gram-positive Bacteria

RLA controls acetyl-CoA synthetase activity in *Bacillus subtilis.* In *B. subtilis,* the GNAT *Bs*AcuA (Type IV protein acetyltransferase) is comprised of only a single GNAT domain, and has no significant sequence homology to *Se*Pat (Type I protein acetyltransferase). However, a structure of a *Bs*AcuA homologue resolved from *Exiguobacterium sibiricum* demonstrated that *Bs*AcuA does contain the conserved GNAT domain (PDB 2Q04) (78). *Bs*AcuA acetylates and inactivates acetyl-CoA synthetase A (AcsA) at the conserved catalytic lysine (Lys549) (30). Deacetylation of *Bs*AcsA^{Ac} can occur by either of the two protein deacetylases of *B. subtilis*, the Zn(II)-dependent *Bs*AcuC deacetylase and / or the sirtuin *Bs*SrtN (30, 182).

The genes encoding *Bs*AcuA (GNAT) and *Bs*AcuC (deacetylase) are located within the *acuABC* operon (183), and are divergently transcribed from *acsA* (target). It was initially thought that the *acuABC* operon was involved in acetoin utilization, as deletion of *acuA* caused a growth defect when cells were grown on acetoin (183). However, it has since been shown that the acetoin utilization pathway is encoded by *acoABCLR* in *B. subtilis* (184). At present it is unclear if or how *Bs*AcuB is involved in the *Bs*AcuA- and *Bs*AcuC-dependent regulation of *Bs*AcsA, or if acetoin utilization is either directly or indirectly regulated by acetylation.

Acs from *Streptomyces lividans* is the exception to the Acs acetylation paradigm. Metabolic regulation in actinomycetes, like *Streptomyces*, is of interest because of the diverse natural products they produce (185-188). *S. lividans* encodes a protein acetyltransferase, *Sl*PatA (Type II), which also acetylates AMP-forming acyl-CoA synthetases, including *S. lividans* acetoacetyl-CoA synthetase (*Sl*AacS) and *S. enterica* Acs (31). *Sl*PatA only weakly modified the *S. lividans* Acs homologue. However, it efficiently acetylated the related enzyme, *Sl*AacS, both *in vitro* and *in vivo* (31). Aacs is present in all domains of life, and this work provided the first

example of regulation of its activity by acetylation. Recently, the structure of *Sl*AacS was reported and the structure provided for the first time an ordered view of the 30-residue extension of the *C*-terminus of this type of enzyme, and it was suggested that such an extension may interact with catalytic residues of the *N*-terminal domain (189). A comparison of the *Sl*Acs and *Sl*AacS would provide valuable insights into the determinants that make AMP-forming acyl-CoA synthetases good substrates for the *Sl*PatA enzyme.

*Sl*PatA is the first characterized Pat homologue that does not efficiently acetylate its cognate Acs enzyme *in vitro* (31), suggesting that *Sl*PatA may not be the enzyme responsible for Acs acetylation in *S. lividans*. Alternatively, acetylation of *Sl*Acs by *Sl*PatA may require additional factors that are not required by *Se*Pat and *Rp*Pat for acetylation of Acs orthologues from those organisms, or simply *Sl*Acs is not enzymatically acetylated.

S. lividans encodes two sirtuin deacetylases, CobB1 and CobB2, and a Zn(II)-dependent AcuC-type deacetylase. Work in the closely related *Streptomyces coelicolor* demonstrated that Acs was acetylated and that CobB1 deacetylated Acs *in vitro* (190). However, the acetyltransferase responsible for acetylation of *S. coelicolor* Acs was not identified.

Recently, studies showed that in another actinomycete, *Saccharopolyspora erythraea,* a homologue of the GNAT-related AcuA enzyme from *B. subtilis*, acetylates the *S. erythraea* Acs enzyme at four different positions, and that in a mutant of *S. erythraea* lacking the *Sa*AcuA enzyme, *Sa*Acs is not acetylated at all (168). The *Sa*AcuA enzyme is the first of its class to be experimentally shown to target several residues of an Acs homologue, as described above. Whether AcuA homologues in other actinomycetes are responsible for the single or multiple acetylation of Acs in this class of microorganisms remains to be determined.

In *Mycobacterium spp*. the universal stress protein USP is under RLA control. *M. tuberculosis* and *M. smegmatis* encode unique protein lysine acetyltransferases (*Mt*PatA and *Ms*PatA, respectively). In these organisms, the GNAT domain is attached to a cyclic AMP (cAMP) binding domain (Type III) (178, 191). cAMP allosterically activates *Mt*PatA and *Ms*PatA, enhancing their activity >2-fold (178, 191-194).

*Ms*PatA acetylates a universal stress protein (USP, MSMEG_4207) at a single lysine residue, and acetylation increases in the presence of cAMP (191). The *in vivo* significance of USP acetylation was not tested, likely because the function of most USPs is unclear, but there is evidence suggesting that USPs provide resistance to various stressors [reviewed in (195)].

*Ms*PatA and *Mt*PatA share 57% identity, thus they may have similar substrates, except for USP, which is not conserved in mycobacteria that encode homologues of *Ms*PatA. Based on these findings, Xu *et al* used *Ms*PatA to acetylate whole-cell lysates with or without the acetyl-CoA analogue chloroacetyl-CoA. The authors identified *Ms*Acs as an acetylated protein target of *Ms*PatA (178). Because *Ms*Acs could not be overproduced in *E. coli*, *in vitro* experiments aimed at showing acetylation of *Ms*Acs by *Ms*PatA were not performed (178). Using an alternative approach, the authors purified *Mt*Acs, (76% identical to *Ms*Acs), and demonstrated *Ms*PatA-dependent acetylation of *Mt*Acs at the expected catalytic lysine residue, which abolished *Mt*Acs activity (178). Although the degree of identity between *Mt*PatA and *Ms*PatA is high, there is precedent in the literature of Acs enzymes that are very poorly acetylated by Pat enzymes (*e.g., Sl*Acs). Therefore, in the absence of experimental evidence, it is premature to conclude that *Ms*Acs is a substrate of *Ms*PatA.

An independent study identified eight additional acyl-CoA synthetases as substrates of *Ms*PatA (192). The single protein deacetylase in *M. tuberculosis*, an NAD^+-dependent sirtuin

homologue (MRA_1161, from H37Ra), deacetylated *Mt*Acs and all eight acyl-CoA synthetases *in vitro* (178, 192), suggesting that that this likely constitutes a regulatory system comparable to the RLA systems found in *S. enterica* and *R. palustris* (196). The authors were able to demonstrate that acetylation in *M. tuberculosis* was dependent upon intracellular cAMP levels by examining the acetylation level of known targets in conditions with varying cAMP concentrations. Acetylation of the acyl-CoA synthetase targets was seen only in conditions with higher levels of cAMP (178, 192).

RLA in Archaea

The first studies examining protein acetylation and deacetylation in archaea were performed in *Halobacterium salinarum* (previously *H. halobium*) in which a 2Fe-2S ferredoxin protein was identified to be acetylated at a specific lysine residue (Lys118) (197). While this was the first example of protein acetylation in archaea, no further studies of acetylated proteins involved in processes other than gene expression have been reported.

Acetylation of the *Sulfolobus solfataricus* chromatin protein (ALBA). As mentioned above, little is known about acetylation in archaea, even though many archaeal species have acetyltransferase and deacetylase homologues. Some archaea encode histone proteins similar eukaryotes. However, the archaeal histones differ in that they do not contain the flexible *N*-terminal tails and are not post-translationally modified (198, 199). In addition to histones, archaea have another chromatin protein known as Sso10b or Alba (for acetylation lowers binding affinity). When bound to DNA, Alba inhibits transcription (200, 201).

Investigators discovered that Alba homologues purified from *Sulfolobus* spp. were 84-Da larger in mass than predicted. Because an acetyl group adds 42 Da to the protein mass, it was

suggested that the Alba proteins were acetylated at two sites (200, 202). A Type IV GNAT-family acetyltransferase, *Ss*Pat (single GNAT domain), was identified by homology to *Se*Pat, and was shown to acetylate Alba *in vitro* at Lys16 (59). Subsequence studies showed acetylation of Lys16 decreased the ability of Alba to bind DNA by ~3-fold (59). However, the authors determined that Alba is a relatively poor substrate for *Ss*Pat and that other substrates may exist in *S. solfataricus* (74). Lys16 of Alba was shown to be deacetylated by the sirtuin deacetylase in *S. solfataricus* (Sir2) (200), which increased the affinity of Alba for DNA (200). The control of Alba by acetylation and deacetylation seems to mirror histone regulation in eukaryotes, providing an example of a conserved regulatory process.

RLA Targets Whose Modifying Acetyltransferases are Not Known

A large number of proteins have been reported to be acetylated, but the identity of the modifying GNAT has not been discovered. Two of these examples include the transcriptional regulator RcsB and the chemotaxis response regulator CheY.

In addition to Acs, an *E. coli* proteome array incubated with *Se*Pat (92% identical to *Ec*Pka) and radiolabeled [1-^{14}C] acetyl-CoA suggested that *Se*Pat acetylated several proteins, including the bacterial transcription factor, RcsB (149). RcsB is involved in regulating the expression of genes that affect flagellar and capsule synthesis, as well as cell division (203, 204). Acetylation of RcsB decreases its ability to bind DNA, an effect that is reversed by incubation of RcsB^{Ac} with the sirtuin *Ec*CobB and NAD^+ (149). More recently reported work did not find direct evidence that *Ec*Pka acetylates RcsB in *E. coli*, leaving the identity of the acetyltransferase that modifies RcsB in these bacteria unanswered (205).

The response regulator CheY, involved in bacterial chemotaxis, is predicted to be under the control of RLA (166, 206). While the phosphorylation of CheY has been extensively studied, the effect of acetylation on the activity of the protein is still poorly understood (207-209). Acetylation of CheY inhibits binding to three of its interacting partners, the CheA kinase, the CheZ phosphatase, and the flagellar motor switch FliM protein (166). CheY is acetylated at multiple sites *in vivo* and the majority of the acetylated residues are grouped on the surface of the protein near the *C*-terminus, the region that binds to the protein targets (210).

While there is *in vivo* and *in vitro* evidence that the CobB sirtuin deacetylates CheY, the identity of the acetyltransferase is unknown (209). Previously, acetylation of CheY was hypothesized to occur via either autoacetylation, or acetyl-CoA synthetase-dependent acetylation by some unknown mechanism (206, 211). To date, studies of CheY have been performed by chemical acetylation of the protein using acetic anhydride (208). However, this method does not acetylate CheY to the same extent as what is seen for the protein *in vivo* (166, 206). It is currently hypothesized that there must be a GNAT acetyltransferase responsible for the acetylation of CheY and is yet to be discovered.

GNAT STRUCTURE AND SUBSTRATE SPECIFICITY

Structural divergence of ADP-forming acyl-CoA synthetases. As mentioned earlier, the large domain of Type I and Type II GNATs are homologous to ADP-forming acyl-CoA synthetases. This catalytic mechanism involves a transfer of a phosphate group to a conserved histidinyl residue located within a flexible loop in subdomain 2 (212) (Fig. 2.10B). *Ec*Pka and *Se*Pat have divergent sequences in the flexible loop region and lack the catalytic residue, suggesting that their ADP-forming acyl-CoA synthetase domains may lack enzymatic activity.

Other protein acetyltransferases, like *Rp*Pat, encode the catalytic histidine. Whether or not *Rp*Pat maintains acyl-CoA synthetase activity has not yet been investigated.

***Mycobacterium tuberculosis* PatA is a sensor of carbon quality.** The crystal structure of *Mt*PatA has been resolved in the presence and absence of cAMP, and revealed an intricate regulatory mechanism (PDB 4AVB) (194) (Fig. 2.11). Structural studies demonstrated that *Mt*PatA can exist in either an active or auto-inhibited state (194). In the absence of cAMP *Mt*PatA adopts the auto-inhibited state, in which the *C*-terminal helix (lid) blocks entrance of the protein substrate into the active site of the GNAT domain (PDB 4AVA). In the active state, the cAMP-binding domain is rotated 40° relative to the GNAT domain, causing the inhibitory lid to refold and swing away, exposing the active site cleft (194) (Fig. 2.11). Binding of cAMP stabilizes the active state of *Mt*PatA, enabling acetylation of the target. Acetyl-CoA co-purified with the *Mt*PatA and was present in both crystal structures, demonstrating that it binds tightly to the enzyme and that *Mt*PatA is poised to respond to cAMP levels (194).

Determinants Needed for Recognition and Acetylation of Protein Targets by GNATs

The ternary structure of the *Tetrahymena thermophila* GNAT, *t*Gcn5, in complex with an 11-residue peptide from histone H3 and CoA (PDB 1QSN) (Fig. 2.12A) revealed a constellation of interactions between GNATs and their protein substrates (49) (Fig. 2.12B). Notably, CoA binding to *t*GCn5 triggers structural changes that facilitate its interactions with the protein substrate. From the above-mentioned structure one can see that the role of the catalytic residue (Glu122) is to abstract a proton from the ε-amino group of Lys14 via an ordered water molecule bridging the two residues. Further positioning of Lys14 is afforded by hydrophobic interactions between residues in *t*Gcn5 and methylene groups and the ε-amino of the lysyl side chain.

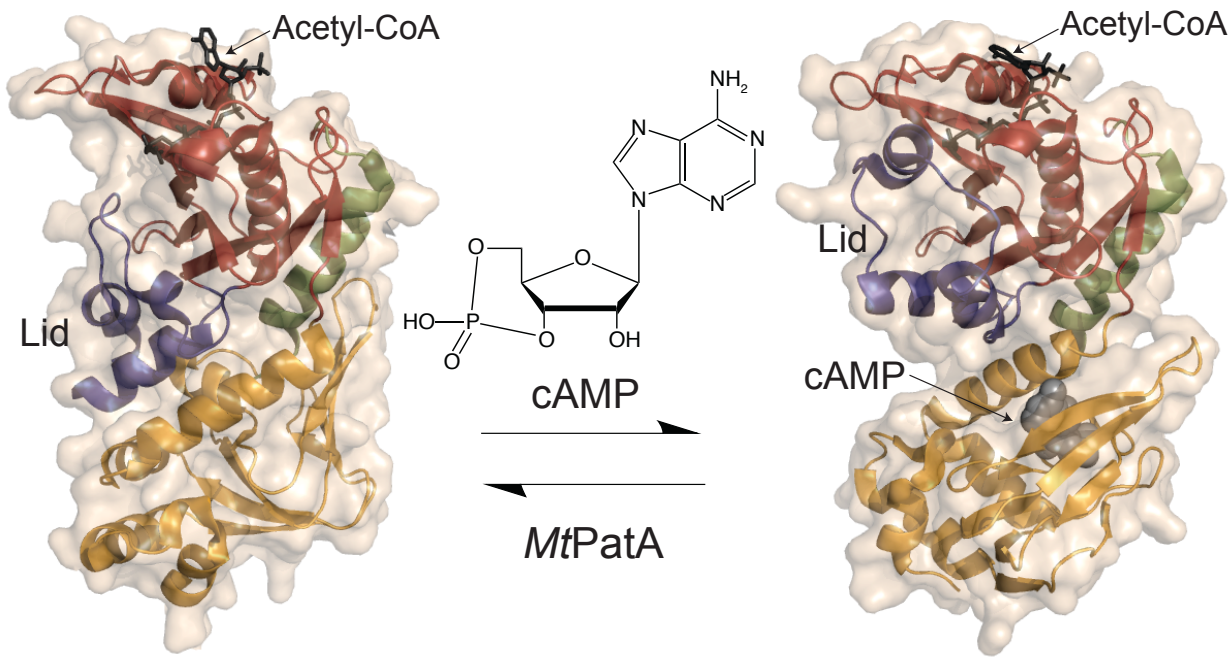

Figure 2.11. Binding of cAMP induces a 40-Å structural change in *M. tuberculosis* PatA. In the absence of cAMP *Mt*PatA adopts an auto-inhibited state, where a 'lid' (blue) blocks the entrance of the substrate to the active site of the GNAT domain (red). In the presence of cAMP, the cAMP-binding domain (gold) rotates 40° relative to the GNAT domain. This causes the lid to swing away from the GNAT domain, exposing the active site cleft. Also shown, acetyl-CoA (black sticks), cAMP (gray spheres), *C*-terminal helix (green). *Mt*PatA structure (PDB 4AVA); *Mt*PatA structure with cAMP (PDB 4AVB).

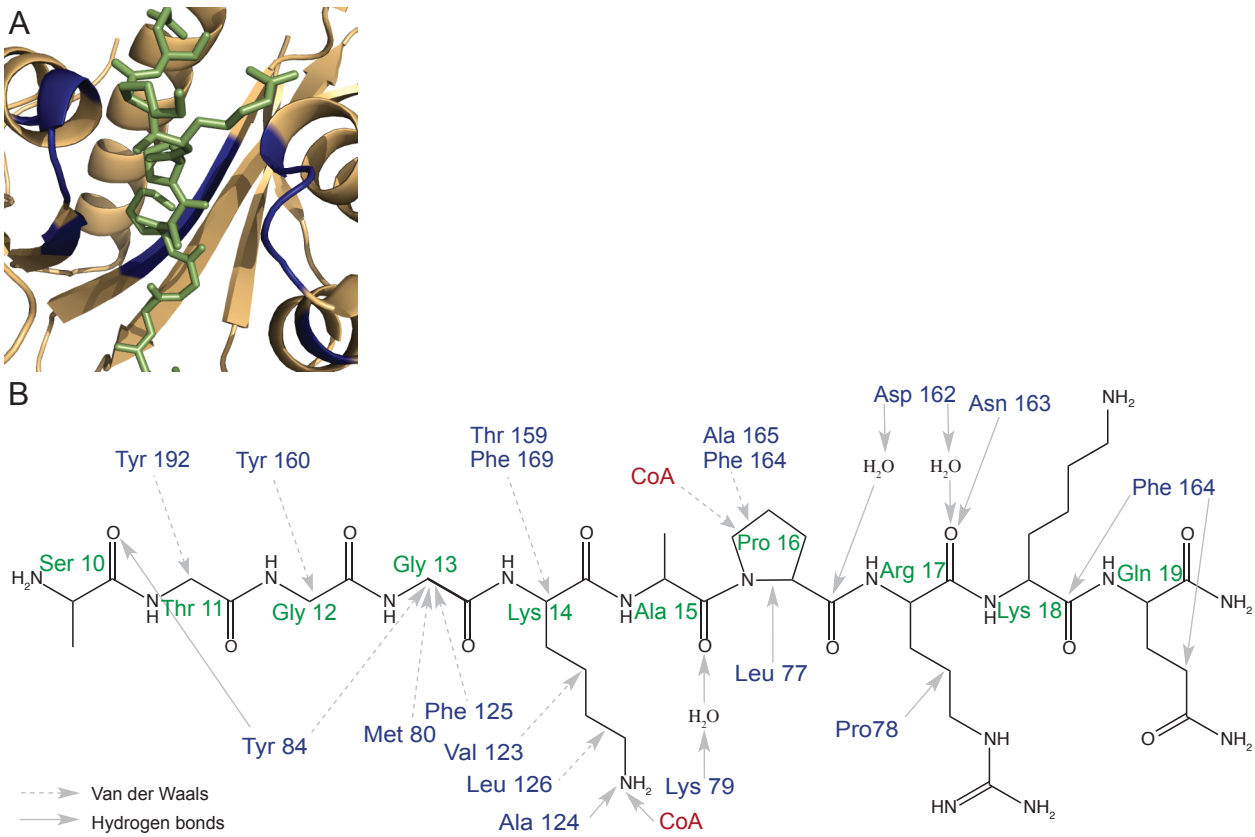

Figure 2.12. Interactions between the *T. thermophila* Gcn5 protein and a peptide substrate. (A) The structure of *t*Gcn5 and a histone H3 11-peptide residue (PDB 1QSN) demonstrated the presence of CoA (not shown) causes structural changes that may facilitate interactions with its protein substrate (interacting residues shown in blue). (B) Molecular interactions of *t*Gcn5 (blue) with the peptide substrate (green) are shown. Modified from figure published in *Nature*; reproduced with permission.

The glycyl side chain next to Lys14 interacts with *t*Gcn5 through van der Waals forces, most likely introducing flexibility into the substrate protein. Binding of the protein substrate to *t*Gcn5 positions the G-**K**-X-P motif of the former in close proximity to acetyl-CoA in the active site of *t*Gcn5. Such position is maintained via interactions between the prolyl side chain and CoA.

Structure of a GNAT:protein substrate complex. Recently, the first structure of a GNAT family member in complex with a protein substrate with tertiary structure was reported (71, 213). The GNAT domain from *S. lividans Sl*PatA (*Sl*PatA^{GNAT}) was crystallized in complex with the *C*-terminal domain of *S. enterica* Acs (*Se*Acs^{CTD}) (71) (Fig. 2.13A). A comparison of the *Sl*PatA^{GNAT}-*Se*Acs^{CTD} and *t*Gcn5-peptide structures revealed (i) a glycine residue (G608) preceding the target lysine (K609) was important for positioning the lysine for interaction with *Sl*PatA^{GNAT} and (ii) a hydrophobic pocket in *Sl*PatA^{GNAT} positioned the lysine side chain (K609) near the catalytic glutamate (E123) of the GNAT (Fig. 2.13B). The interaction surface of the *Sl*PatA^{GNAT}-*Se*Acs^{CTD} acetylation complex was more extensive than the surface observed for *t*Gcn5-peptide interactions, indicating that *Sl*PatA recognizes substrate sequences outside of the flexible loop containing the target lysine (K609). These interactions included complementary ionic interactions of positively charged side chains in *Se*Acs^{CTD} with negatively charged side-chains in *Sl*PatA^{GNAT} (Fig. 2.13C, D). Reversing the charges in either *Se*Acs^{CTD} or *Sl*PatA^{GNAT} significantly decreased interactions between these proteins (71).

Diversity of determinants in the motif containing the acetylation site. All *bona fide* substrates of *R. palustris Rp*Pat are AMP-forming acyl-CoA synthetases and display a high degree of conservation surrounding the acetylation site. A consensus sequence at the site of acetylation can be approximated by the motif PX$_4$G**K** (23, 169) (Fig. 2.14A). The Gly residue preceding the target lysine is conserved in *Rp*Pat substrates, as seen with the *t*Gcn5 substrate

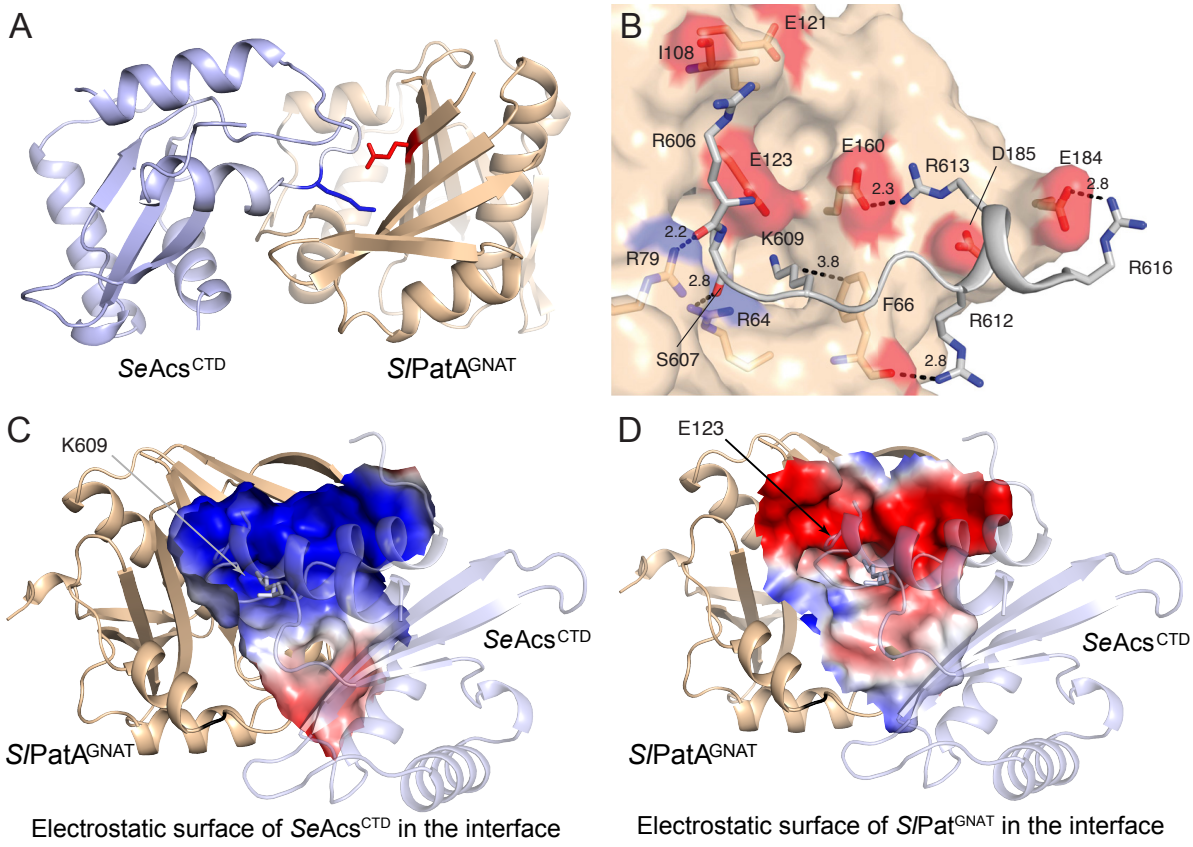

Figure 2.13. Molecular interactions of *S. lividans* PatA^{GNAT} and *S. enterica* Acs^{CTD}. (A) Crystal structure of the interactions between *S. lividans* PatA^{GNAT} and *S. enterica* Acs^{CTD} (PDB 4U5Y). The *Sl*PatA^{GNAT} catalytic residue (E123) is shown in red sticks and the acetylated lysine of *Se*Acs^{CTD} (K609) is shown in blue sticks. (B) Interactions between *Sl*PatA^{GNAT} (surface) and *Se*Acs^{CTD} (sticks). (C, D) Electrostatic potential of the *Sl*PatA^{GNAT}-*Se*Acs^{CTD} surface interface with negatively charged regions in red, positively charged regions in blue, and neutral residues in white. This research was originally published in the Journal of Biological Chemistry. Alex C. Tucker, Keenan C. Taylor, Katherine C. Rank, Ivan Rayment, and Jorge C. Escalante-Semerena. Insights into the Specificity of Lysine Acetyltransferases. *J. Biol. Chem*. 2014; 289:36249-36262. © the American Society for Biochemistry and Molecular Biology.

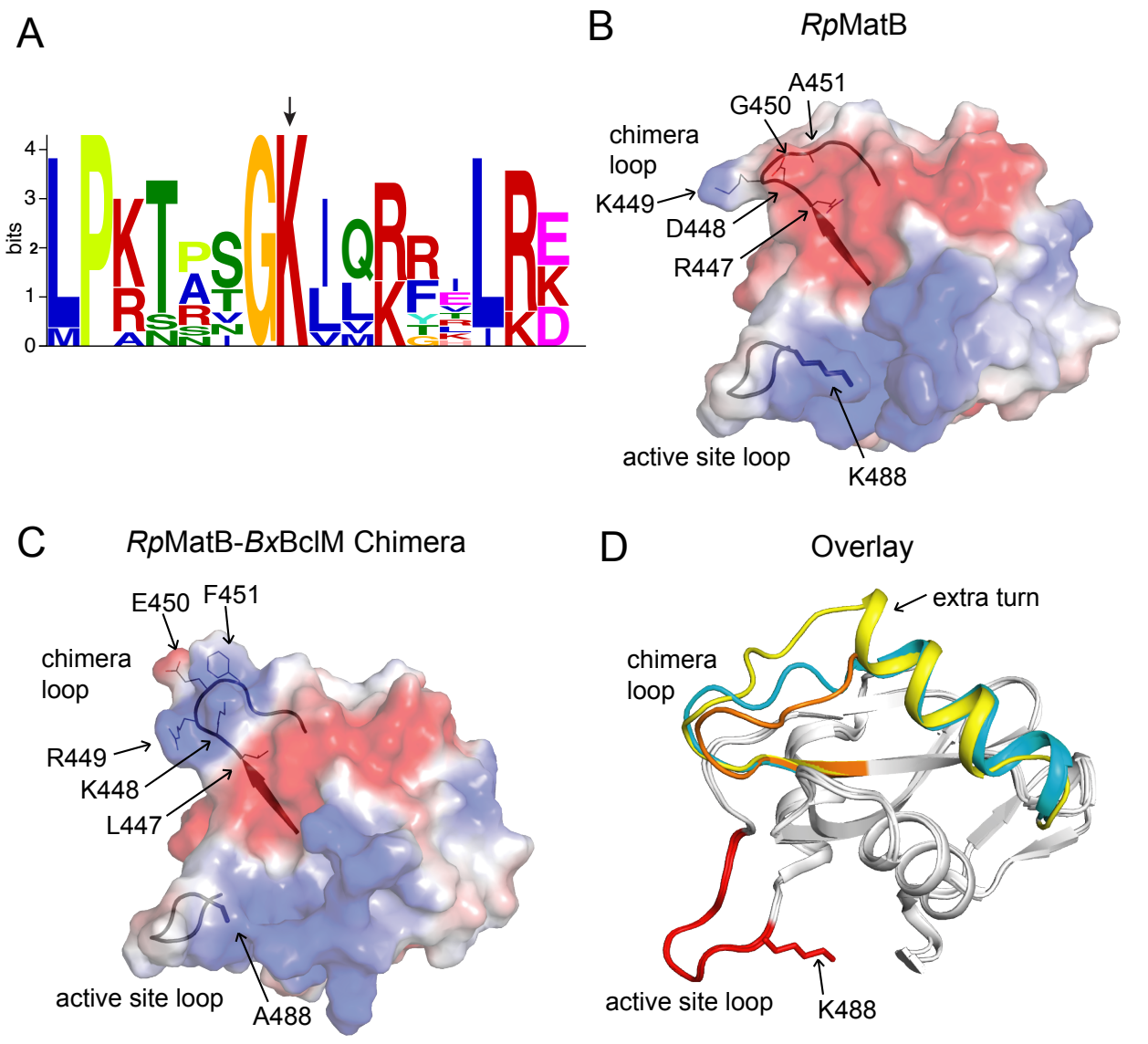

Figure 2.14. Acetylation determinants outside the motif containing the acetylation site. (A) Consensus motif containing the acetylation site (indicated by the arrow) generated from the alignments of acyl-CoA synthetases acetylated by *R. palustris* Pat (*Rp*Pat). The letter height corresponds to the frequency of a particular amino acid residue in that position. (B) The electrostatic potential of the *Rp*MatB (methylmalonyl CoA synthetase), a protein that is not acetylated by *Rp*Pat. The illustration shows negatively charged regions in red and positively charged regions in blue. (C) Electrostatic potential of the *Rp*MatB and *B. xenovorans* BclM (benzoate:CoA synthetase) chimera protein (*Rp*MatB-*Bx*BclM chimera, B3), a protein that is acetylated by *Rp*Pat. The illustration shows negatively charged regions in red and positively charged regions in blue. (D) Overlay of the *C*-terminal domain of the *Rp*MatB-*Bx*BclM chimeras (B1, PDB 4GXQ; B3, PDB 4GXR) aligned with the *C*-terminal domains of *Rp*MatB (PDB 4FUQ), with the *Bx*BclM-derived residues of the B1 chimera in yellow, *Bx*BclM-derived

residues of the B3 chimera in orange, the wild-type *Rp*MatB residues in cyan. The consensus motif containing the acetylation site (PX_4G**K**) is shown in red in the active site loop, with the acetylated lysine residue (K488) shown as red sticks. This research was originally published in the Journal of Biological Chemistry. Heidi A. Crosby, Katherine C. Rank, Ivan Rayment, and Jorge C. Escalante-Semerena. Structural Insights into the Substrate Specificity of the *Rhodopseudomonas palustris* Protein Acetyltransferase *Rp*Pat: Identification of a Loop Critical for Recognition by *Rp*Pat. *J. Biol. Chem*. 2012; 287:41392-41404.

mentioned previously, and may be a common feature of GNAT substrates (49). However, recent results support the conclusion that this motif is not sufficient for acetylation to occur. *Rp*MatB, an acyl-CoA synthetase which activates the dicarboxylic acid methylmalonate to methylmalonyl-CoA (214), contains the PX_4G**K** motif but is not acetylated by *Rp*Pat (215) (Fig. 2.14B).

The term 'acetylation motif' is misleading because it oversimplifies what is encoded in this motif. While it is true that the PX_4G**K** motif identified for AMP-forming acyl-CoA synthetase acetylation targets is necessary for acetylation to occur, it is not sufficient. Alanine scanning of 14 residues surrounding the acetylation site of *Rp*PimA (a *bona fide* substrate of *Rp*Pat) demonstrated that nearly half of them were important for acetylation by *Rp*Pat, whereas only two were required for *Rp*PimA enzymatic activity (23, 28, 167). Interestingly, one acyl-CoA synthetase was identified in *R. palustris* that appeared to evade acetylation through the presence of a leucine residue two positions upstream of the conserved lysine. Changing the leucine to a valine residue restored recognition of the substrate and its acetylation. Collectively, these results emphasize the fact that the presence of the 'acetylation motif' in AMP-forming acyl-CoA synthetases is not a good predictor of a protein being under RLA control.

Using Protein Chimeras to Probe GNAT Substrate Specificities

To investigate *R. palustris Rp*Pat specificity, a series of chimeric proteins in which portions of *Rp*MatB (methylmalonyl-CoA synthetase, not acetylatable) were replaced with the corresponding sequences from known *Rp*Pat substrates (Fig. 2.14C). The *Rp*Pat chimeras were constructed with pimelate-CoA synthetase (*Rp*PimA) or benzoate-CoA synthetase from *Burkholderia xenovorans*, *Bx*BclM (28, 216). Introduction of residues from *Rp*PimA or *Bx*BclM into *Rp*MatB allowed the chimeras, *Rp*PimA-*Rp*MatB and *Bx*BclM-*Rp*MatB to be recognized

and acetylated by *Rp*Pat. Significantly, *Rp*PimA-*Rp*MatB chimeras with *Rp*PimA residues located ~20Å away from the target lysine (K488) allowed *Rp*Pat to recognize and acetylate *Rp*MatB. These data indicated that *Rp*Pat recognizes additional structural elements in protein substrates in addition to the residues immediately surrounding the target lysine, as seen with *Sl*PatA. This information may help account for the substrate specificity of protein acetyltransferases for their structurally diverse substrates.

The three-dimensional crystal structure of the *Bx*BclM-*Rp*MatB chimera identified a loop, (named chimera loop), that is important for recognition by *Rp*Pat (215) (Fig. 2.14D). It seems that the shape and electrostatic potential of the chimera loop play important roles, as minor changes in the loop allows an acyl-CoA synthetase to 'escape' acetylation by *Rp*Pat (214). This indicates that although 'acetylation motifs' may suggest a protein is controlled by RLA, each substrate should be validated experimentally, as structural elements outside of the motif can affect the ability of the acetyltransferase to recognize and acetylate the target.

ROLE OF RLA IN MAINTAINING METABOLIC HOMEOSTASIS

Acetyl-CoA, Energy Charge, NAD^+, and cAMP Link RLA to Central Metabolism

Both components of the RLA system (acylation and deacylation) involve the essential coenzymes CoA and NAD^+. Acylation requires acyl-CoA thioesters, connecting this process to CoA homeostasis, carbon load, and energy charge, while the sirtuin-catalyzed deacylation reaction requires NAD^+, an indicator of high energy levels in the cell. Acylation is further regulated by metabolic cofactors in acetyltransferases such as the *Mycobacterium* Pat proteins, which respond to cAMP levels, an indicator of the quality of carbon source available in the cell. As a result, RLA modifies proteins in response to the metabolic state of the cell.

Acetylation and acetyl-CoA levels. Bacterial protein acetyltransferases use acetyl-CoA as a substrate, linking protein acetylation to acetyl-CoA levels, which are regulated by the metabolic activity of the cell. The two-domain Pat homologues *Se*Pat, *Ec*Pka, *Rp*Pat, and *Sl*PatA have large regulatory domains that bind acetyl-CoA to allosterically regulate acetyltransferase activity (72). Acetyl-CoA is a metabolite linked to many pathways including carbon utilization (*e.g.* glycolysis), the tricarboxylic acid (TCA) cycle, the acetate kinase/phosphotransacetylase pathway, and fatty acid biosynthesis / degradation (Fig. 2.15).

Although some insights into the reasons why AMP-forming acyl-CoA synthetases are regulated by RLA have been reported (see below), there may be a number of other reasons why cells control this class of enzymes so carefully. Not all acyl-CoA synthetases are regulated by acetylation. In prokaryotes, data have been reported about the propionylation of propionyl-CoA synthetase (PrpE), a modification that affects the same lysine as acetylation does, also abolishing the activity of the enzyme (56). The use of RLA to control acyl-CoA synthetases by acetylation or propionylation is not unique to Gamma-proteobacteria, since there is abundant evidence of the same type of control happening in the Alpha-proteobacterium *R. palustris*. The common theme here is that RLA helps maintain a balance in the intracellular acetyl-CoA (or propionyl-CoA) pools, while an acyl-CoA synthetase (MatB) that contributes to the succinyl-CoA pool is not under RLA control (28, 214). It is possible that acetylation of these AMP-forming acyl-CoA synthetases may control CoA homeostasis by preventing depletion of CoA or build-up of acetyl-CoA or propionyl-CoA.

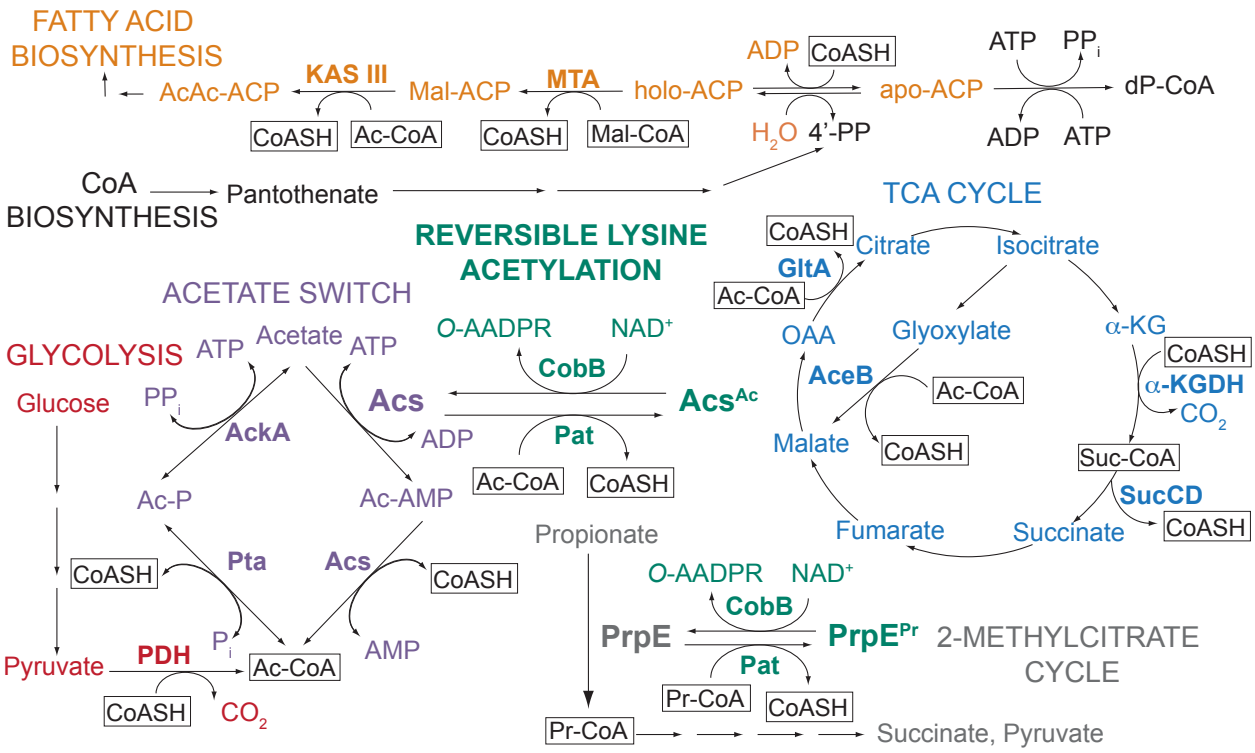

Figure 2.15. CoA homeostasis. Schematic of the contributions of CoA and acetyl-CoA to cellular metabolism. CoASH, Coenzyme A; Ac-CoA, acetyl-CoA, *O*-AADPR, *O*-acetyl-ADP-ribose; Ac-P, acetyl-phosphate; Ac-AMP, acetyl-AMP, PPi, pyrophosphate; Pr-CoA, propionyl-CoA; α-KG, alpha-ketoglutarate; OAA, oxaloacetate; Suc-CoA, succinyl-CoA; dP-CoA, dephospho-Coenzyme A.

Possible effects on CoA homeostasis. Coenzyme A (CoA) is an essential metabolic cofactor and CoA homeostasis is important for cell survival. As an acyl carrier group, CoA activates the carbonyl groups of carboxylic acids, including fatty acids and amino acids. The resulting thioester bond increases the electrophilicity of the carbonyl carbon, facilitating nucleophilic attacks, thus making the carbonyl carbon more prone to react with thiolates, hydroxyl, and amino groups (217, 218). Reactive acyl-CoA thioesters are used by ~ 4% of all known enzymes, which catalyze over 100 reactions involved in diverse cellular processes, including the TCA cycle, fatty-acid degradation, and fatty-acid, amino-acid, and secondary-metabolite biosynthesis (219, 220) (Fig. 2.15). Due to both limiting substrate availability and allosteric regulation of central metabolic enzymes, CoASH and acyl-CoA control metabolic flux through glycolysis and the TCA cycle (221-227).

CoASH, acetyl-CoA, succinyl-CoA, and malonyl-CoA comprise the bulk of the CoA pool (228). Availability of nutrients, phase of growth, and environmental conditions all affect the CoA pool and can cause the balance of acyl-CoA species to alter by more than an order of magnitude in a matter of minutes (220, 229-231). For example, acetyl-CoA is the major species during exponential growth on glucose (300 μM), while CoASH is the predominant species during growth on acetate (100 μM) (228).

Because CoASH and acyl-CoA availability affect many cellular processes, an imbalance in CoA homeostasis results in profound consequences on cellular metabolism. For example, depletion of CoA stalls protein synthesis and reduces the supply of acyl carrier protein (ACP). Protein synthesis is stalled by depletion of CoA due to the lack of available acetyl-CoA as well as inhibition of the TCA cycle and production of amino-acid precursors (232). Reduced levels of ACP limits fatty-acid biosynthesis, ultimately resulting in reduced phospholipid synthesis (232-

234). Due to the deleterious effects on the cell caused by an imbalance in CoA homeostasis, there must be tight control over both the total CoA pool, as well as the relative concentrations of the various CoA species, in response to the metabolic status of the cell. Given that the RLA system recycles acylated CoAs, this could be a mechanism for the maintenance of CoA homeostasis.

Effect of RLA on energy charge. Insights into why acyl-CoA synthetases are under RLA control have been reported in *S. enterica* (179). From this work, the authors learned that, in this bacterium, an imbalance in the protein acetyltransferase (*Se*Pat):sirtuin deacetylase (*Se*CobB) ratio has a profound effect on cell growth under conditions that depend on the activity of acetyl-CoA synthetase (*Se*Acs), *i.e.* ≤10 mM acetate as the sole source of carbon and energy. Results from experiments where *Se*Pat was ectopically synthesized under the control of an inducible promoter showed, that incremental levels of *Se*Pat eventually arrested growth because the energy charge of the cell was lowered to a level (0.17) that could not support growth. The depletion of ATP and the concomitant production of AMP was determined to be the reason for the drop in energy charge. That is the cell did not have enough ATP to convert AMP to ADP so the ATPase could synthesize more ATP, thus restoring the energy charge of the cell.

Deacetylation and NAD^+ levels. Sirtuins require NAD^+ as a co-substrate, linking deacetylation to the availability of NAD^+ in the cell. NAD^+ is the oxidized form of NADH, an important electron donor to the electron transport system, which generates the proton motive force that drives the synthesis of ATP by the membrane-bound ATPase. When bacteria are grown in conditions with differing nutritional and oxygen availability, the NAD^+ pools have greater variation compared to the NADH pools (130). This suggests that the NAD^+ pool is (i) dynamic and (ii) an important reporter of cellular carbon and energy status. For example, growth

conditions that generate high NAD^+ levels, like aerobic respiration, could cause an increase in the deacetylation of sirtuin targets. A recent report provided evidence of a new and unprecedented role for NAD^+ in cell physiology. Cahová *et al* presented experimental evidence supporting the idea that bacteria stabilize RNA molecules by capping their 5' end with NAD^+ (235). Whether NAD^+-capped RNAs are substrates for sirtuins is an intriguing possibility that should be explored.

Regulation of protein acetylation by cAMP. In *E. coli*, cAMP is involved in catabolite repression, a process in which cells preferentially use glucose and only utilize other available carbon sources once glucose has been depleted. The global transcriptional regulator, Crp mediates this cAMP-dependent response (236). In mycobacteria, cAMP not only plays a role in basic physiology, it acts as a secondary messenger and is involved in re-routing host signaling during infection (237). Notably, *M. tuberculosis* has 15 adenylate cyclase enzymes for production of cAMP, whereas *E. coli* only has one (CyaA) [reviewed in (238)]. The adenylate cyclases of *M. tuberculosis* are allosterically activated by signals like low pH (239, 240), bicarbonate / CO_2 (241), and saturated fatty acids (242), which occur during the course of infection.

While cAMP concentrations do not fluctuate with addition of glucose to the medium, cAMP availability does increase ~50-fold during macrophage infection (237). For *M. tuberculosis* to enter a non-replicating persister or 'quiescent' state during chronic infection requires a significant downshift in metabolism, which is thought to be achieved by diverting acetyl-CoA away from the TCA cycle, toward synthesis of triacylglycerides (243). Mycobacteria accumulate and store triacylglycerides during stress conditions, although their role is not fully understood.

In *M. tuberculosis*, cAMP is integral to the control of the RLA system through the allosteric regulation of the acetyltransferase, *Mt*PatA. It is possible that Mycobacteria may use cAMP availability to adjust flux through AMP-forming acyl-CoA synthetases, the targets of *Ms*PatA (192). Taken together, it is also conceivable that *M. tuberculosis* would down-regulate Acs activity as a mechanism to reduce the available acetyl-CoA pool in order to slow down cellular metabolism during chronic infection.

Cellular Stress and RLA

Mammalian sirtuins have been reported to play a role in cellular protection by promoting positive effects on processes like DNA repair, cell survival, and stress resistance [reviewed in (244)]. Recent studies have shown that this effect is also conserved in bacteria.

Deletion of the *E. coli* sirtuin deacetylase (*Ec*CobB) increases acetylation levels in the cell, which was shown to increase resistance to both heat and oxidative stress (245). This same study performed whole-transcriptome analysis of a Δ*cobB* strain and found many stress related systems were repressed in this mutant, including genes related to heat shock, osmotic stress, acid resistance, cold shock, and carbon starvation (245). These data provided compelling evidence that RLA is a mechanism used by cells to respond to environmental stressors.

An acetylome study of *M. tuberculosis* identified 10% of the enzymes involved in fatty acid biosynthesis were acetylated (143). Fatty acid biosynthesis in this organism plays a role in colony morphology and biofilm formation. The authors demonstrated that deletion of the sirtuin deacetylase in this organism (MRA_1161) resulted in a more granular morphology, a decrease in biofilm formation, and increased resistance to heat stress (143). These studies further support the hypothesis that RLA is a mechanism for protection again environmental stresses.

TRANSCRIPTIONAL REGULATION OF GENES ENCODING RLA ENZYMES

While the field is beginning to identify acetyltransferases, partner deacetylases, and protein targets, as well as distinguish structural determinants needed for recognition and enzyme regulation, much remains unknown about the transcriptional regulation of the genes encoding the components of the RLA systems.

Regulation of RLA Genes in *Escherichia coli*

The *pka* gene, which encodes the protein acetyltransferase of *E. coli*, has a similar expression profile to that of *acs*, one of its target substrates (177). When *E. coli* grows in certain conditions (i. e. glucose minimal medium), the TCA cycle cannot process acetyl-CoA quickly enough and instead utilizes an overflow pathway to excrete acetate. This acetate pool is later assimilated via Acs and utilized by the cell when glucose is depleted (246).

This "acetate switch" is mediated in part by the expression of *acs*, which is low during exponential phase but increases dramatically in late exponential and early stationary phases (247). Expression of *acs* is controlled by several transcription factors including the nucleoid proteins Fis and IHF, as well as Crp (177, 248). Interestingly, the *E. coli* protein acetyltransferase *pka* has a similar expression profile to its target, *acs,* during growth on glucose (177). Transcription of *pka* is also activated by Crp in response to cAMP levels (177). The activation of *pka* and *acs* expression by Crp may represent a regulatory mimic of the direct cAMP-dependent activation of GNAT activity observed in mycobacteria. At present, it appears that the *cobB* gene encoding the sirtuin in *E. coli* is constitutively expressed and is not dependent on cAMP levels (177).

Multiple Isoforms of the CobB Deacetylase are Present in *Salmonella enterica*

In *S. enterica,* the CobB sirtuin exists as two isoforms, due to the presence of two independent start codons that are read in the same open reading frame. This results in the production of a long isoform ($CobB_L$, 273 a.a), and a short isoform ($CobB_S$, 236 a.a.), which lacks 37 of the amino acids present in $CobB_L$ (249). Interestingly, both $CobB_L$ and $CobB_S$ isoforms are active, although $CobB_S$ is the dominant isoform *in vivo* and is produced at ~10-fold higher levels (249). The presence of the dual start codons is not limited to *S. enterica*, and is found throughout the enterobacteria. The physiological relevance of $CobB_L$ and $CobB_S$ and their contribution to RLA is currently unknown.

CONCLUSIONS

RLA is an emerging field in prokaryotes that is advancing by leaps and bounds through the use of high-throughput and detailed mechanistic studies in a variety of organisms. Validation of ideas obtained through global 'omics' approaches is key to improving our understanding of the role of RLA. GNAT protein acetyltransferases and their cognate protein deacetylases have been identified in bacteria, archaea, and eukaryotes. The abundance of GNATs in cells of all domains of life is a strong indicator of the relevance of these enzymes to life. Although the physiological role of the majority of these enzymes remains unknown, and the elucidation of their function is a challenge to cell physiologists, efforts to advance this research area will likely provide valuable insights into the strategies used by cells to cope with metabolic stress.

FOOTNOTES

RLA, reversible lysine acetylation; PTM, post-translational modification; HAT, histone acetyltransferase; Co-ASH, Coenzyme A; Ac-CoA, acetyl-CoA; GNAT, Gcn5-related *N*-acetyltransferase; Pat, protein acetyltransferase; Acs, acetyl-CoA synthetase; CobB, NAD^+-dependent sirtuin deacetylase; *O*-AADPR, *O*-acyl-ADP-ribose; HDAC, histone deacetylase; NUDIX, nucleoside diphosphate linked to X; SILAC, stable isotope labeling with amino acids in cell culture; *Ec*, *Escherichia coli*; *Se*, *Salmonella enterica*; *Sl*, *Streptomyces lividans*; *Bs*, *Bacillus subtilis*; *Ms*, *Mycobacterium smegmatis*; *Mt*, *Mycobacterium tuberculosis*; *Ss*, *Sulfolobus solfataricus*; *Rp*, *Rhodopseudomonas palustris*, *Bx*, *Burkholderia xenovorans*.

ACKNOWLEDGEMENTS

This work was supported by USPHS grant R01 GM062203 to J.C.E.-S. We would like to thank Dr. Heidi Crosby, Dr. Alex Tucker, and Chelsey VanDrisse for critical reading and feedback during the drafting stages of this review.

REFERENCES

1. **Walsh CT, Garneau-Tsodikova S, Gatto GJ, Jr.** 2005. Protein posttranslational modifications: the chemistry of proteome diversifications. *Angew. Chem. Int. Ed. Engl.* **44:**7342-7372.
2. **Phillips DM.** 1963. The presence of acetyl groups of histones. *J. Biochem.* **87:**258-263.
3. **Jarrell KF, Ding Y, Meyer BH, Albers SV, Kaminski L, Eichler J.** 2014. *N*-Linked glycosylation in archaea: a structural, functional, and genetic analysis. *Microbiol. Mol. Biol. Rev.* **78:**304-341.

4. **Zverina EA, Lamphear CL, Wright EN, Fierke CA.** 2012. Recent advances in protein prenyltransferases: substrate identification, regulation, and disease interventions. *Curr. Opin. Chem. Biol.* **16:**544-552.

5. **Rivera C, Gurard-Levin ZA, Almouzni G, Loyola A.** 2014. Histone lysine methylation and chromatin replication. *Biochim. Biophys. Acta.* **1839:**1433-1439.

6. **Gould N, Doulias PT, Tenopoulou M, Raju K, Ischiropoulos H.** 2013. Regulation of protein function and signaling by reversible cysteine *S*-nitrosylation. *J. Biol. Chem.* **288:**26473-26479.

7. **Kennelly PJ.** 2014. Protein Ser/Thr/Tyr phosphorylation in the Archaea. *J. Biol. Chem.* **289:**9480-9487.

8. **Cousin C, Derouiche A, Shi L, Pagot Y, Poncet S, Mijakovic I.** 2013. Protein-serine/threonine/tyrosine kinases in bacterial signaling and regulation. *FEMS. Microbiol. Lett.* **346:**11-19.

9. **Weinert BT, Scholz C, Wagner SA, Iesmantavicius V, Su D, Daniel JA, Choudhary C.** 2013. Lysine succinylation is a frequently occurring modification in prokaryotes and eukaryotes and extensively overlaps with acetylation. *Cell. Rep.* **4:**842-851.

10. **Rieser E, Cordier SM, Walczak H.** 2013. Linear ubiquitination: a newly discovered regulator of cell signalling. *Trends Biochem. Sci.* **38:**94-102.

11. **Muller MP, Albers MF, Itzen A, Hedberg C.** 2014. Exploring adenylylation and phosphocholination as post-translational modifications. *Chembiochem.* **15:**19-26.

12. **Van Meter M, Mao Z, Gorbunova V, Seluanov A.** 2011. Repairing split ends: SIRT6, mono-ADP ribosylation and DNA repair. *Aging*. **3:**829-835.

13. **Paquette N, Conlon J, Sweet C, Rus F, Wilson L, Pereira A, Rosadini CV, Goutagny N, Weber AN, Lane WS, Shaffer SA, Maniatis S, Fitzgerald KA, Stuart L, Silverman N.** 2012. Serine/threonine acetylation of TGFbeta-activated kinase (TAK1) by Yersinia pestis YopJ inhibits innate immune signaling. *Proc. Natl. Acad. Sci. USA*. **109:**12710-12715.

14. **Stuecker TN, Hodge KM, Escalante-Semerena JC.** 2012. The missing link in coenzyme A biosynthesis: PanM (formerly YhhK), a yeast GCN5 acetyltransferase homologue triggers aspartate decarboxylase (PanD) maturation in *Salmonella enterica*. *Mol. Microbiol.* **84:**608-619.

15. **Stuecker TN, Tucker AC, Escalante-Semerena JC.** 2012. PanM, an acetyl-Coenzyme A sensor required for maturation of *L*-aspartate decarboxylase (PanD). *MBio.* **3:**e00158-00112.

16. **Cui W, Shi Z, Fang Y, Zhou L, Ding N, Zhou Z.** 2014. Significance of Arg3, Arg54, and Tyr58 of *L*-aspartate alpha-decarboxylase from *Corynebacterium glutamicum* in the process of self-cleavage. *Biotechnol. Lett.* **36:**121-126.

17. **Helbig AO, Gauci S, Raijmakers R, van Breukelen B, Slijper M, Mohammed S, Heck AJ.** 2010. Profiling of *N*-acetylated protein termini provides in-depth insights into the N-terminal nature of the proteome. *Mol. Cell Proteomics.* **9:**928-939.

18. **Helsens K, Van Damme P, Degroeve S, Martens L, Arnesen T, Vandekerckhove J, Gevaert K.** 2011. Bioinformatics analysis of a *Saccharomyces cerevisiae N*-terminal proteome provides evidence of alternative translation initiation and post-translational *N*-terminal acetylation. *J. Proteome Res.* **10:**3578-3589.

19. **Sterner DE, Berger SL.** 2000. Acetylation of histones and transcription-related factors. *Microbiol. Mol. Biol. Rev.* **64:**435-459.

20. **Khorasanizadeh S.** 2004. The nucleosome: from genomic organization to genomic regulation. *Cell.* **116:**259-272.

21. **Gu W, Roeder RG.** 1997. Activation of p53 sequence-specific DNA binding by acetylation of the p53 C-terminal domain. *Cell.* **90:**595-606.

22. **Yang XJ, Seto E.** 2008. Lysine acetylation: codified crosstalk with other posttranslational modifications. *Mol. Cell.* **31:**449-461.

23. **Starai VJ, Celic I, Cole RN, Boeke JD, Escalante-Semerena JC.** 2002. Sir2-dependent activation of acetyl-CoA synthetase by deacetylation of active lysine. *Science.* **298:**2390-2392.

24. **Starai VJ, Escalante-Semerena JC.** 2004. Identification of the protein acetyltransferase (Pat) enzyme that acetylates acetyl-CoA synthetase in *Salmonella enterica*. *J. Mol. Biol.* **340:**1005-1012.

25. **Soppa J.** 2010. Protein acetylation in archaea, bacteria, and eukaryotes. *Archaea.* **2010:**pii: 820681.

26. **Kouzarides T.** 2007. Chromatin modifications and their function. *Cell.* **128:**693-705.

27. **Glozak MA, Sengupta N, Zhang X, Seto E.** 2005. Acetylation and deacetylation of non-histone proteins. *Gene.* **363:**15-23.

28. **Crosby HA, Pelletier DA, Hurst GB, Escalante-Semerena JC.** 2012. System-wide studies of *N*-lysine acetylation in *Rhodopseudomonas palustris* reveal substrate specificity of protein acetyltransferases. *J. Biol. Chem.* **287:**15590-15601.

29. **Starai VJ, Takahashi H, Boeke JD, Escalante-Semerena JC.** 2003. Short-chain fatty acid activation by acyl-coenzyme A synthetases requires SIR2 protein function in *Salmonella enterica* and *Saccharomyces cerevisiae*. *Genetics.* **163:**545-555.

30. **Gardner JG, Grundy FJ, Henkin TM, Escalante-Semerena JC.** 2006. Control of acetyl-coenzyme A synthetase (AcsA) activity by acetylation/deacetylation without NAD(+) involvement in *Bacillus subtilis*. *J. Bacteriol.* **188:**5460-5468.

31. **Tucker AC, Escalante-Semerena JC.** 2013. Acetoacetyl-CoA synthetase activity is controlled by a protein acetyltransferase with unique domain organization in *Streptomyces lividans*. *Mol. Microbiol.* **87:**152-167.

32. **Hubbert C, Guardiola A, Shao R, Kawaguchi Y, Ito A, Nixon A, Yoshida M, Wang XF, Yao TP.** 2002. HDAC6 is a microtubule-associated deacetylase. *Nature.* **417:**455-458.

33. **Kim GW, Yang XJ.** 2011. Comprehensive lysine acetylomes emerging from bacteria to humans. *Trends Biochem. Sci*. **36:**211-220.

34. **Xiong Y, Guan KL.** 2012. Mechanistic insights into the regulation of metabolic enzymes by acetylation. *J. Cell. Biol.* **198:**155-164.

35. **Lin YY, Lu JY, Zhang J, Walter W, Dang W, Wan J, Tao SC, Qian J, Zhao Y, Boeke JD, Berger SL, Zhu H.** 2009. Protein acetylation microarray reveals that NuA4 controls key metabolic target regulating gluconeogenesis. *Cell.* **136:**1073-1084.

36. **Lv L, Li D, Zhao D, Lin R, Chu Y, Zhang H, Zha Z, Liu Y, Li Z, Xu Y, Wang G, Huang Y, Xiong Y, Guan KL, Lei QY.** 2011. Acetylation targets the M2 isoform of pyruvate kinase for degradation through chaperone-mediated autophagy and promotes tumor growth. *Mol. Cell.* **42:**719-730.

37. **Hallows WC, Yu W, Denu JM.** 2012. Regulation of glycolytic enzyme phosphoglycerate mutase-1 by Sirt1 protein-mediated deacetylation. *J. Biol. Chem.* **287:**3850-3858.

38. **LeDizet M, Piperno G.** 1987. Identification of an acetylation site of *Chlamydomonas* alpha-tubulin. *Proc. Natl. Acad. Sci. USA.* **84:**5720-5724.

39. **Kouzarides T.** 2000. Acetylation: a regulatory modification to rival phosphorylation? *EMBO. J.* **19:**1176-1179.

40. **Tanner KG, Langer MR, Denu JM.** 2000. Kinetic mechanism of human histone acetyltransferase P/CAF. *Biochemistry.* **39:**11961-11969.

41. **Tanner KG, Langer MR, Kim Y, Denu JM.** 2000. Kinetic mechanism of the histone acetyltransferase GCN5 from yeast. *J. Biol. Chem.* **275:**22048-22055.

42. **Marmorstein R, Roth SY.** 2001. Histone acetyltransferases: function, structure, and catalysis. *Curr. Opin. Genet. Dev.* **11:**1555-1561.

43. **Berndsen CE, Albaugh BN, Tan S, Denu JM.** 2007. Catalytic mechanism of a MYST family histone acetyltransferase. *Biochemistry.* **46:**623-629.

44. **Thompson PR, Kurooka H, Nakatani Y, Cole PA.** 2001. Transcriptional coactivator protein p300. Kinetic characterization of its histone acetyltransferase activity. *J. Biol. Chem.* **276:**33721-33729.

45. **Yan Y, Barlev NA, Haley RH, Berger SL, Marmorstein R.** 2000. Crystal structure of yeast Esa1 suggests a unified mechanism for catalysis and substrate binding by histone acetyltransferases. *Mol. Cell.* **6:**1195-1205.

46. **Yan Y, Harper S, Speicher DW, Marmorstein R.** 2002. The catalytic mechanism of the ESA1 histone acetyltransferase involves a self-acetylated intermediate. *Nat. Struct. Biol.* **9:**862-869.

47. **Liu X, Wang L, Zhao K, Thompson PR, Hwang Y, Marmorstein R, Cole PA.** 2008. The structural basis of protein acetylation by the p300/CBP transcriptional coactivator. *Nature.* **451:**846-850.

48. **Wang L, Tang Y, Cole PA, Marmorstein R.** 2008. Structure and chemistry of the p300/CBP and Rtt109 histone acetyltransferases: implications for histone acetyltransferase evolution and function. *Curr. Opin. Struct. Biol.* **18:**741-747.

49. **Rojas JR, Trievel RC, Zhou J, Mo Y, Li X, Berger SL, Allis CD, Marmorstein R.** 1999. Structure of *Tetrahymena* GCN5 bound to coenzyme A and a histone H3 peptide. *Nature.* **401:**93-98.

50. **Dutnall RN, Tafrov ST, Sternglanz R, Ramakrishnan V.** 1998. Structure of the histone acetyltransferase Hat1: a paradigm for the GCN5-related *N*-acetyltransferase superfamily. *Cell.* **94:**427-438.

51. **Clements A, Rojas JR, Trievel RC, Wang L, Berger SL, Marmorstein R.** 1999. Crystal structure of the histone acetyltransferase domain of the human PCAF transcriptional regulator bound to coenzyme A. *EMBO. J.* **18:**3521-3532.

52. **Lin Y, Fletcher CM, Zhou J, Allis CD, Wagner G.** 1999. Solution structure of the catalytic domain of GCN5 histone acetyltransferase bound to coenzyme A. *Nature.* **400:**86-89.

53. **Vetting MW, Carvalho LPSd, Yu M, Hegde SS, Magnet S, Roderick SL, Blanchard JS.** 2005. Structure and functions of the GNAT superfamily of acetyltransferases. *Arch. Biochem. Biophys.* **433:**212-226.

54. **Dyda F, Klein DC, Hickman AB.** 2000. GCN5-related *N*-acetyltransferases: a structural overview. *Annu. Rev. Biophy. Biomol. Struc.* **29:**81-103.

55. **Hodawadekar SC, Marmorstein R.** 2007. Chemistry of acetyl transfer by histone modifying enzymes: structure, mechanism and implications for effector design. *Oncogene.* **26:**5528-5540.

56. **Garrity J, Gardner JG, Hawse W, Wolberger C, Escalante-Semerena JC.** 2007. N-lysine propionylation controls the activity of propionyl-CoA synthetase. *J. Biol. Chem.* **282:**30239-30245.

57. **Cheng Z, Tang Y, Chen Y, Kim S, Liu H, Li SS, Gu W, Zhao Y.** 2009. Molecular characterization of propionyllysines in non-histone proteins. *Mol. Cell. Proteomics.* **8:**45-52.

58. **Berndsen CE, Denu JM.** 2008. Catalysis and substrate selection by histone/protein lysine acetyltransferases. *Curr. Opin. Struct. Biol.* **18:**682-689.

59. **Marsh VL, Peak-Chew SY, Bell SD.** 2005. Sir2 and the acetyltransferase, Pat, regulate the archaeal chromatin protein, Alba. *J. Biol. Chem.* **280:**21122-21228.

60. **Thao S, Escalante-Semerena JC.** 2011. Control of protein function by reversible N(epsilon)-lysine acetylation in bacteria. *Curr. Opin. Microbiol.* **14:**200-204.

61. **Wright GD, Ladak P.** 1997. Overexpression and characterization of the chromosomal aminoglycoside 6'-*N*-acetyltransferase from *Enterococcus faecium*. *Antimicrob. Agents Chemother.* **41:**956-960.

62. **Wolf E, Vassilev A, Makino Y, Sali A, Nakatani Y, Burley SK.** 1998. Crystal structure of a GCN5-related *N*-acetyltransferase: *Serratia marcescens* aminoglycoside 3-*N*-acetyltransferase. *Cell.* **94:**439-449.

63. **Davies J, Wright GD.** 1997. Bacterial resistance to aminoglycoside antibiotics. *Trends Microbiol.* **5:**234-240.

64. **Chen Y, Sprung R, Tang Y, Ball H, Sangras B, Kim S, Falck JR, Peng J, Gu W, Zhao Y.** 2007. Lysine propionylation and butyrylation are novel post-translational modifications in histones. *Mol. Cell. Proteomics.* **6:**8211-8829.

65. **Leemhuis H, Packman LC, Nightingale KP, Hollfelder F.** 2008. The human histone acetyltransferase P/CAF is a promiscuous histone propionyltransferase. *Chembiochem.* **9:**499-503.

66. **Feng L, Wang W, Cheng J, Ren Y, Zhao G, Gao C, Tang Y, Liu X, Han W, Peng X, Liu R, Wang L.** 2007. Genome and proteome of long-chain alkane degrading *Geobacillus thermodenitrificans* NG80-2 isolated from a deep-subsurface oil reservoir. *Proc. Natl. Acad. Sci. USA.* **104:**5602-5607.

67. **Neuwald AF, Landsman D.** 1997. GCN5-related histone *N*-acetyltransferases belong to a diverse superfamily that includes the yeast SPT10 protein. *Trends Biochem. Sci.* **22:**154-155.

68. **Liang W, Deutscher MP.** 2012. Post-translational modification of RNase R is regulated by stress-dependent reduction in the acetylating enzyme Pka (YfiQ). *RNA.* **18:**37-41.

69. **Crosby HA, Heiniger EK, Harwood CS, Escalante-Semerena JC.** 2010. Reversible *N*(ε)-lysine acetylation regulates the activity of acyl-CoA synthetases involved in

anaerobic benzoate catabolism in *Rhodopseudomonas palustris*. Mol. Microbiol. **76:**874-888.

70. **Thao S, Escalante-Semerena JC.** 2012. A positive selection approach identifies residues important for folding of *Salmonella enterica* Pat, an *N*(ε)-lysine acetyltransferase that regulates central metabolism enzymes. *Res. Microbiol.* **163:**427-435.

71. **Tucker AC, Taylor KC, Rank KC, Rayment I, Escalante-Semerena JC.** 2014. Insights into the specificity of lysine acetyltransferases. *J. Biol. Chem.* **289:**36249-36262.

72. **Thao S, Escalante-Semerena JC.** 2011. Biochemical and thermodynamic analyses of *Salmonella enterica* Pat, a multidomain, multimeric *N*(ε)-lysine acetyltransferase involved in carbon and energy metabolism. *MBio*. **2:**e00216-00211.

73. **Mackay DT, Botting CH, Taylor GL, White MF.** 2007. An acetylase with relaxed specificity catalyses protein *N*-terminal acetylation in *Sulfolobus solfataricus*. *Mol. Microbiol.* **64:**1540-1548.

74. **Brent MM, Iwata A, Carten J, Zhao K, Marmorstein R.** 2009. Structure and biochemical characterization of protein acetyltransferase from *Sulfolobus solfataricus*. *J. Biol. Chem.* **284:**19412-19419.

75. **Glasemacher J, Bock AK, Schmid R, Schönheit P.** 1997. Purification and properties of acetyl-CoA synthetase (ADP-forming), an archaeal enzyme of acetate formation and ATP synthesis, from the hyperthermophile *Pyrococcus furiosus*. *Eur. J. Biochem.* **244:**561-567.

76. **Shikata K, Fukui T, Atomi H, Imanaka T.** 2007. A novel ADP-forming succinyl-CoA synthetase in *Thermococcus kodakaraensis* structurally related to the archaeal nucleoside diphosphate-forming acetyl-CoA synthetases. *J. Biol. Chem.* **282:**26963-26970.

77. **Sánchez LB, Galperin MY, Muller M.** 2000. Acetyl-CoA synthetase from the amitochondriate eukaryote Giardia lamblia belongs to the newly recognized superfamily of acyl-CoA synthetases (Nucleoside diphosphate-forming). *J. Biol. Chem.* **275:**5794-5803.

78. **Gardner JG, Escalante-Semerena JC.** 2008. Biochemical and mutational analyses of AcuA, the acetyltransferase enzyme that controls the activity of the acetyl coenzyme a synthetase (AcsA) in *Bacillus subtilis*. *J. Bacteriol.* **190:**5132-5136.

79. **Marsh VL, Peak-Chew SY, Bell SD.** 2005. Sir2 and the acetyltransferase, Pat, regulate the archaeal chromatin protein, Alba. *J. Biol. Chem.* **280:**21122-21128.

80. **Hu LI, Lima BP, Wolfe AJ.** 2010. Bacterial protein acetylation: the dawning of a new age. *Mol. Microbiol.* **77:**15-21.

81. **Weinert BT, Iesmantavicius V, Wagner SA, Scholz C, Gummesson B, Beli P, Nystrom T, Choudhary C.** 2013. Acetyl-phosphate is a critical determinant of lysine acetylation in *E. coli*. *Mol. Cell.* **51:**265-272.

82. **Cumberlidge AG, Isono K.** 1979. Ribosomal protein modification in *Escherichia coli.* I. A. mutant lacking the *N*-terminal acetylation of protein S5 exhibits thermosensitivity. *J. Mol. Biol.* **131:**169-189.

83. **Isono K, Isono S.** 1980. Ribosomal protein modification in *Escherichia coli*. II. Studies of a mutant lacking the *N*-terminal acetylation of protein S18. Mol. *Gen. Genet.* **177:**645-651.

84. **Fukuchi J, Kashiwagi K, Takio K, Igarashi K.** 1994. Properties and structure of spermidine acetyltransferase in *Escherichia coli*. *J. Biol. Chem.* **269:**22581-22585.

85. **Hung MN, Rangarajan E, Munger C, Nadeau G, Sulea T, Matte A.** 2006. Crystal structure of TDP-fucosamine acetyltransferase (WecD) from *Escherichia coli*, an enzyme required for enterobacterial common antigen synthesis. *J. Bacteriol.* **188:**5606-5617.

86. **Marvil DK, Leisinger T.** 1977. *N*-acetylglutamate synthase of *Escherichia coli*: purification, characterization, and molecular properties. *J. Biol. Chem.* **252:**3295-32303.

87. **Kazakov T, Kuznedelov K, Semenova E, Mukhamedyarov D, Datsenko KA, Metlitskaya A, Vondenhoff GH, Tikhonov A, Agarwal V, Nair S, Van Aerschot A, Severinov K.** 2014. The RimL transacetylase provides resistance to translation inhibitor microcin C. *J. Bacteriol.* **196:**3377-3385.

88. **Ikeuchi Y, Kitahara K, Suzuki T.** 2008. The RNA acetyltransferase driven by ATP hydrolysis synthesizes N^4-acetylcytidine of tRNA anticodon. *EMBO. J.* **27:**2194-2203.

89. **Yoshikawa A, Isono S, Sheback A, Isono K.** 1987. Cloning and nucleotide sequencing of the genes *rimI* and *rimJ* which encode enzymes acetylating ribosomal proteins S18 and S5 of *Escherichia coli* K12. *Mol. Gen. Genet.* **209:**481-488.

90. **Tanaka S, Matsushita Y, Yoshikawa A, Isono K.** 1989. Cloning and molecular characterization of the gene *rimL* which encodes an enzyme acetylating ribosomal protein L12 of *Escherichia coli* K12. *Mol. Gen. Genet.* **217:**289-293.

91. **Hentchel KL, Escalante-Semerena JC.** 2015. In *Salmonella enterica*, the Gcn5-related acetyltransferase MddA (formerly YncA) acetylates methionine sulfoximine and methionine sulfone, blocking their toxic effects. *J. Bacteriol.* **197:**314-325.

92. **Liang W, Malhotra A, Deutscher MP.** 2011. Acetylation regulates the stability of a bacterial protein: growth stage-dependent modification of RNase R. *Mol. Cell.* **44:**160-166.

93. **Leibowitz MJ, Soffer RL.** 1970. Enzymatic modification of proteins. 3. Purification and properties of a leucyl, phenylalanyl transfer ribonucleic acid protein transferase from *Escherichia coli*. *J. Biol. Chem.* **245:**2066-2073.

94. **Tobias JW, Shrader TE, Rocap G, Varshavsky A.** 1991. The *N*-end rule in bacteria. *Science*. **254:**1374-1377.

95. **Nozaki S, Webb ME, Niki H.** 2012. An activator for pyruvoyl-dependent l-aspartate alpha-decarboxylase is conserved in a small group of the gamma-proteobacteria including *Escherichia coli*. *Micro. Open Acc.* **1:**298-310.

96. **Monteiro DC, Rugen MD, Shepherd D, Nozaki S, Niki H, Webb ME.** 2012. Formation of a heterooctameric complex between aspartate alpha-decarboxylase and its cognate activating factor, PanZ, is CoA-dependent. *Biochem. Biophys. Res. Commun.* doi:10.1016/j.bbrc.2012.08.084.

97. **Sauve AA, Wolberger C, Schramm VL, Boeke JD.** 2006. The biochemistry of sirtuins. *Annu. Rev. Biochem.* **75:**435-465.

98. **Tsang AW, Escalante-Semerena JC.** 1998. CobB, a new member of the SIR2 family of eucaryotic regulatory proteins, is required to compensate for the lack of nicotinate mononucleotide:5,6-dimethylbenzimidazole phosphoribosyltransferase activity in *cobT* mutants during cobalamin biosynthesis in *Salmonella typhimurium* LT2. *J. Biol. Chem.* **273:**31788-31794.

99. **Frye RA.** 2000. Phylogenetic classification of prokaryotic and eukaryotic Sir2-like proteins. *Biochem. Biophys. Res. Commun.* **273:**793-798.

100. **Marmorstein R.** 2001. Structure of histone deacetylases: insights into substrate recognition and catalysis. *Structure*. **9:**1127-1233.

101. **Lombardi PM, Cole KE, Dowling DP, Christianson DW.** 2011. Structure, mechanism, and inhibition of histone deacetylases and related metalloenzymes. *Curr. Opin. Struct. Biol.* **21:**735-743.

102. **Smith BC, Denu JM.** 2007. Acetyl-lysine analog peptides as mechanistic probes of protein deacetylases. *J. Biol. Chem.* **282:**37256-37265.

103. **Zhou Y, Zhang H, He B, Du J, Lin H, Cerione RA, Hao Q.** 2012. The bicyclic intermediate structure provides insights into the desuccinylation mechanism of human sirtuin 5 (SIRT5). *J. Biol. Chem.* **287:**28307-28314.

104. **Park J, Chen Y, Tishkoff DX, Peng C, Tan M, Dai L, Xie Z, Zhang Y, Zwaans BM, Skinner ME, Lombard DB, Zhao Y.** 2013. SIRT5-mediated lysine desuccinylation impacts diverse metabolic pathways. *Mol. Cell.* **50:**919-930.

105. **Peng C, Lu Z, Xie Z, Cheng Z, Chen Y, Tan M, Luo H, Zhang Y, He W, Yang K, Zwaans BM, Tishkoff D, Ho L, Lombard D, He TC, Dai J, Verdin E, Ye Y, Zhao Y.** 2011. The first identification of lysine malonylation substrates and its regulatory enzyme. *Mol. Cell. Proteomics.* **10:**M111 012658.

106. **Osborne B, Cooney GJ, Turner N.** 2014. Are sirtuin deacylase enzymes important modulators of mitochondrial energy metabolism? *Biochim. Biophys. Acta.* **1840:**1295-1302.

107. **He W, Newman JC, Wang MZ, Ho L, Verdin E.** 2012. Mitochondrial sirtuins: regulators of protein acylation and metabolism. *Trends Endocrinol Metab.* **23:**467-476.

108. **Lin SJ, Guarente L.** 2003. Nicotinamide adenine dinucleotide, a metabolic regulator of transcription, longevity and disease. *Curr. Opin. Cell. Biol.* **15:**241-246.

109. **Denu JM.** 2003. Linking chromatin function with metabolic networks: Sir2 family of NAD(+)-dependent deacetylases. *Trends Biochem. Sci.* **28:**41-48.

110. **Moazed D.** 2001. Enzymatic activities of Sir2 and chromatin silencing. *Curr. Opin. Cell. Biol.* **13:**232-238.

111. **Blander G, Guarente L.** 2004. The sir2 family of protein deacetylases. *Annu. Rev. Biochem.* **73:**417-435.

112. **Rowen JW, Kornberg A.** 1951. The phosphorolysis of nicotinamide riboside. *J. Biol. Chem.* **193:**497-507.

113. **Zhao K, Harshaw R, Chai X, Marmorstein R.** 2004. Structural basis for nicotinamide cleavage and ADP-ribose transfer by NAD^+-dependent Sir2 histone/protein deacetylases. *Proc. Natl. Acad. Sci. USA*. **101:**8563-8568.

114. **Sauve AA, Celic I, Avalos J, Deng H, Boeke JD, Schramm VL.** 2001. Chemistry of gene silencing: The mechanism of $NAD(^+)$-dependent deacetylation reactions. *Biochemistry*. **40:**15456-15463.

115. **Smith JS, Brachmann CB, Celic I, Kenna MA, Muhammad S, Starai VJ, Avalos JL, Escalante-Semerena JC, Grubmeyer C, Wolberger C, Boeke JD.** 2000. A phylogenetically conserved NAD^+-dependent protein deacetylase activity in the Sir2 protein family. *Proc. Natl. Acad. Sci. USA*. **97:**6658-6663.

116. **Tanner KG, Landry J, Sternglanz R, Denu JM.** 2000. Silent information regulator family of NAD-dependent histone/protein deacetylases generates a unique product, 1-*O*-acetyl-ADP-ribose. *Proc. Natl. Acad. Sci. USA*. **97:**14178-14182.

117. **Sauve AA.** 2010. Sirtuin chemical mechanisms. *Biochim. Biophys. Acta.* **1804:**1591-1603.

118. **Borra MT, O'Neill FJ, Jackson MD, Marshall B, Verdin E, Foltz KR, Denu JM.** 2002. Conserved enzymatic production and biological effect of *O*-acetyl-ADP-ribose by silent information regulator 2-like NAD^+-dependent deacetylases. *J. Biol. Chem.* **277:**12632-12641.

119. **Jackson MD, Denu JM.** 2002. Structural identification of 2'- and 3'-*O*-acetyl-ADP-ribose as novel metabolites derived from the Sir2 family of beta-NAD^+-dependent histone/protein deacetylases. *J. Biol. Chem.* **277:**18535-18544.

120. **Grubisha O, Rafty LA, Takanishi CL, Xu X, Tong L, Perraud AL, Scharenberg AM, Denu JM.** 2006. Metabolite of SIR2 reaction modulates TRPM2 ion channel. *J. Biol. Chem.* **281:**14057-14065.

121. **Rafty LA, Schmidt MT, Perraud AL, Scharenberg AM, Denu JM.** 2002. Analysis of *O*-acetyl-ADP-ribose as a target for Nudix ADP-ribose hydrolases. *J. Biol. Chem*. **277:**47114-47122.

122. **Ono T, Kasamatsu A, Oka S, Moss J.** 2006. The 39-kDa poly(ADP-ribose) glycohydrolase ARH3 hydrolyzes *O*-acetyl-ADP-ribose, a product of the Sir2 family of acetyl-histone deacetylases. *Proc. Natl. Acad. Sci. USA*. **103:**16687-166891.

123. **Schmidt MT, Smith BC, Jackson MD, Denu JM.** 2004. Coenzyme specificity of Sir2 protein deacetylases: implications for physiological regulation. *J. Biol. Chem.* **279:**40122-40129.

124. **Guarente L.** 2005. Calorie restriction and SIR2 genes-Towards a mechanism. *Mech. Ageing Dev*. **126:**923-928.

125. **Porcu M, Chiarugi A.** 2005. The emerging therapeutic potential of sirtuin-interacting drugs: from cell death to lifespan extension. *Trends Pharmacol. Sci.* **26:**94-103.

126. **Bitterman KJ, Anderson RM, Cohen HY, Latorre-Esteves M, Sinclair DA.** 2002. Inhibition of silencing and accelerated aging by nicotinamide, a putative negative regulator of yeast sir2 and human SIRT1. *J. Biol. Chem.* **277:**45099-45107.

127. **Avalos JL, Bever KM, Wolberger C.** 2005. Mechanism of sirtuin inhibition by nicotinamide: Altering the NAD($^+$) cosubstrate specificity of a Sir2 enzyme. *Mol. Cell.* **17:**855-868.

128. **Sauve AA, Schramm VL.** 2003. Sir2 regulation by nicotinamide results from switching between base exchange and deacetylation chemistry. *Biochemistry*. **42:**9249-9256.

129. **Jackson MD, Schmidt MT, Oppenheimer NJ, Denu JM.** 2003. Mechanism of nicotinamide inhibition and transglycosidation by Sir2 histone/protein deacetylases. *J. Biol. Chem.* **278:**50985-50998.

130. **Wimpenny JWT, Firth A.** 1972. Levels of nicotinamide adenine dinucleotide and reduced nicotinamide adenine dinucleotide in facultative bacteria and the effect of oxygen. *J. Bacteriol.* **111:**24-32.

131. **Lin H, Vadali RV, Bennett GN, San KY.** 2004. Increasing the acetyl-CoA pool in the presence of overexpressed phosphoenolpyruvate carboxylase or pyruvate carboxylase enhances succinate production in *Escherichia coli*. *Biotechnol. Prog.* **20:**1599-1604.

132. **Fulco M, Schiltz RL, Iezzi S, King MT, Zhao P, Kashiwaya Y, Hoffman E, Veech RL, Sartorelli V.** 2003. Sir2 regulates skeletal muscle differentiation as a potential sensor of the redox state. *Mol. Cell.* **12:**51-62.

133. **Yuan H, Marmorstein R.** 2012. Structural basis for sirtuin activity and inhibition. *J. Biol. Chem.* **287:**42428-42435.

134. **Sanders BD, Jackson B, Marmorstein R.** 2009. Structural basis for sirtuin function: What we know and what we don't. *Biochim. Biophys. Acta.* **1804**:1604-1616.

135. **Chakrabarty SP, Balaram H.** 2010. Reversible binding of zinc in *Plasmodium falciparum* Sir2: structure and activity of the apoenzyme. *Biochim. Biophys. Acta*. **1804:**1743-1750.

136. **Iwabata H, Yoshida M, Komatsu Y.** 2005. Proteomic analysis of organ-specific post-translational lysine-acetylation and -methylation in mice by use of anti-acetyllysine and -methyllysine mouse monoclonal antibodies. *Proteomics.* **5:**4653-4664.

137. **Kim SC, Sprung R, Chen Y, Xu Y, Ball H, Pei J, Cheng T, Kho Y, Xiao H, Xiao L, Grishin NV, White M, Yang XJ, Zhao Y.** 2006. Substrate and functional diversity of lysine acetylation revealed by a proteomics survey. *Mol. Cell.* **23:**607-618.

138. **Schwer B, Eckersdorff M, Li Y, Silva JC, Fermin D, Kurtev MV, Giallourakis C, Comb MJ, Alt FW, Lombard DB.** 2009. Calorie restriction alters mitochondrial protein acetylation. *Aging Cell.* **8:**604-606.

139. **Zhao S, Xu W, Jiang W, Yu W, Lin Y, Zhang T, Yao J, Zhou L, Zeng Y, Li H, Li Y, Shi J, An W, Hancock SM, He F, Qin L, Chin J, Yang P, Chen X, Lei Q, Xiong Y, Guan KL.** 2010. Regulation of cellular metabolism by protein lysine acetylation. *Science.* **327:**1000-1004.

140. **Falb M, Aivaliotis M, Garcia-Rizo C, Bisle B, Tebbe A, Klein C, Konstantinidis K, Siedler F, Pfeiffer F, Oesterhelt D.** 2006. Archaeal *N*-terminal protein maturation commonly involves *N*-terminal acetylation: a large-scale proteomics survey. *J. Mol. Biol.* **362:**915-924.

141. **Yu BJ, Kim JA, Moon JH, Ryu SE, Pan JG.** 2008. The diversity of lysine-acetylated proteins in *Escherichia coli*. *J. Microbiol. Biotechnol*. **18:**1529-1536.

142. **Zhang J, Sprung R, Pei J, Tan X, Kim S, Zhu H, Liu CF, Grishin NV, Zhao Y.** 2009. Lysine acetylation is a highly abundant and evolutionarily conserved modification in *Escherichia coli*. *Mol. Cell. Proteomics.* **8:**215-225.

143. **Liu F, Yang M, Wang X, Yang S, Gu J, Zhou J, Zhang XE, Deng J, Ge F.** 2014. Acetylome analysis reveals diverse functions of lysine acetylation in *Mycobacterium tuberculosis*. *Mol. Cell. Proteomics.* **12:**3352-3366.

144. **Xing S, Poirier Y.** 2012. The protein acetylome and the regulation of metabolism. *Trends Plant Sci.* **17:**423-430.

145. **Miao J, Lawrence M, Jeffers V, Zhao F, Parker D, Ge Y, Sullivan WJ, Jr., Cui L.** 2013. Extensive lysine acetylation occurs in evolutionarily conserved metabolic pathways and parasite-specific functions during *Plasmodium falciparum* intraerythrocytic development. *Mol. Microbiol.* **89:**660-675.

146. **Jeffers V, Sullivan WJ, Jr.** 2012. Lysine acetylation is widespread on proteins of diverse function and localization in the protozoan parasite *Toxoplasma gondii. Eukaryot. Cell*. **11:**735-742.

147. **Choudhary C, Kumar C, Gnad F, Nielsen ML, Rehman M, Walther T, Olsen JV, Mann M.** 2009. Lysine acetylation targets protein complexes and co-regulates major cellular functions. *Science***. 325:**834-840.

148. **Zhu H, Klemic JF, Chang S, Bertone P, Casamayor A, Klemic KG, Smith D, Gerstein M, Reed MA, Snyder M.** 2000. Analysis of yeast protein kinases using protein chips. *Nat. Genet.* **26:**283-289.

149. **Thao S, Chen CS, Zhu H, Escalante-Semerena JC.** 2010. N(epsilon)-Lysine acetylation of a bacterial transcription factor inhibits its DNA-binding activity. *PLOS ONE*. **5:**e15123.

150. **Chen Y, Colak G, Zhao Y.** 2013. SILAC-based quantification of Sirt1-responsive lysine acetylome. *Methods Mol. Biol.* **1077:**105-120.

151. **Baeza J, Dowell JA, Smallegan MJ, Fan J, Amador-Noguez D, Khan Z, Denu JM.** 2014. Stoichiometry of site-specific lysine acetylation in an entire proteome. *J. Biol. Chem.* **289:**21326-21338.

152. **Kuhn ML, Zemaitaitis B, Hu LI, Sahu A, Sorensen D, Minasov G, Lima BP, Scholle M, Mrksich M, Anderson WF, Gibson BW, Schilling B, Wolfe AJ.** 2014. Structural, kinetic and proteomic characterization of acetyl phosphate-dependent bacterial protein acetylation. *PLOS ONE*. **9:**e94816.

153. **Wang Q, Zhang Y, Yang C, Xiong H, Lin Y, Yao J, Li H, Xie L, Zhao W, Yao Y, Ning ZB, Zeng R, Xiong Y, Guan KL, Zhao S, Zhao GP.** 2010. Acetylation of metabolic enzymes coordinates carbon source utilization and metabolic flux. *Science*. **327:**1004-1007.

154. **Kim D, Yu BJ, Kim JA, Lee YJ, Choi SG, Kang S, Pan JG.** 2013. The acetylproteome of Gram-positive model bacterium *Bacillus subtilis*. *Proteomics*. **13:**1726-1736.

155. **Wu X, Vellaichamy A, Wang D, Zamdborg L, Kelleher NL, Huber SC, Zhao Y.** 2013. Differential lysine acetylation profiles of *Erwinia amylovora* strains revealed by proteomics. *J. Proteomics.* **79:**60-71.

156. **Zhang Y, Wu ZX, Wan XL, Liu P, Zhang JB, Ye Y, Zhao YM, Tan MJ.** 2014. Comprehensive profiling of lysine acetylome in *Staphylococcus aureus*. *Sci. China Chem.* **57:**732-738.

157. **Lee DW, Kim DI, Lee YJ, Kim JA, Choi JY, Kang S, Pan JG.** 2013. Proteomic analysis of acetylation in thermophilic *Geobacillus kaustophilus*. *Proteomics*. **13:**2278-2282.

158. **Pan J, Ye Z, Cheng Z, Peng X, Wen L, Zhao F.** 2014. Systematic analysis of the lysine acetylome in *Vibrio parahemolyticus*. *J. Proteome Res.* **13:**3294-3302.

159. **Okanishi H, Kim K, Masui R, Kuramitsu S.** 2013. Acetylome with structural mapping reveals the significance of lysine acetylation in *Thermus thermophilus*. *J. Proteome Res.* **12:**3952-3968.

160. **van Noort V, Seebacher J, Bader S, Mohammed S, Vonkova I, Betts MJ, Kuhner S, Kumar R, Maier T, O'Flaherty M, Rybin V, Schmeisky A, Yus E, Stulke J, Serrano L, Russell RB, Heck AJ, Bork P, Gavin AC.** 2012. Cross-talk between phosphorylation and lysine acetylation in a genome-reduced bacterium. *Mol. Syst. Biol.* **8:**571.

161. **Liao G, Xie L, Li X, Cheng Z, Xie J.** 2014. Unexpected extensive lysine acetylation in the trump-card antibiotic producer *Streptomyces roseosporus* revealed by proteome-wide profiling. *J. Proteomics.* **106:**260-2699.

162. **Zhang K, Zheng S, Yang JS, Chen Y, Cheng Z.** 2013. Comprehensive profiling of protein lysine acetylation in *Escherichia coli*. *J. Proteome Res.* **12:**844-851.

163. **Guan KL, Xiong Y.** 2011. Regulation of intermediary metabolism by protein acetylation. *Trends Biochem. Sci.* **36:**108-116.

164. **Karanam B, Jiang L, Wang L, Kelleher NL, Cole PA.** 2006. Kinetic and mass spectrometric analysis of p300 histone acetyltransferase domain autoacetylation. *J. Biol. Chem.* **281:**40292-402301.

165. **Yang C, Wu J, Sinha SH, Neveu JM, Zheng YG.** 2012. Autoacetylation of the MYST Lysine Acetyltransferase MOF. *J. Biol. Chem.* **287:**34917-34926.

166. **Barak R, Yan J, Shainskaya A, Eisenbach M.** 2006. The chemotaxis response regulator CheY can catalyze its own acetylation. *J. Mol. Biol.* **359:**251-265.

167. **Crosby HA, Escalante-Semerena JC.** 2014. The acetylation motif in AMP-forming acyl coenzyme A synthetases contains residues critical for acetylation and recognition by the protein acetyltransferase Pat of *Rhodopseudomonas palustris*. *J. Bacteriol.* **196:**1496-1504.

168. **You D, Yao LL, Huang D, Escalante-Semerena JC, Ye BC.** 2014. Acetyl-CoA synthetase is acetylated on multiple lysine residues by a protein acetyltransferase with single GNAT domain in *Saccharopolyspora erythraea*. *J. Bacteriol.* **196:**3169-3178.

169. **Starai VJ, Escalante-Semerena JC.** 2004. Acetyl-coenzyme A synthetase (AMP forming). *Cell. Mol. Life Sci.* **61:**2020-2030.

170. **Karan D, David JR, Capy P.** 2001. Molecular evolution of the AMP-forming Acetyl-CoA synthetase. *Gene*. **265:**95-101.

171. **Ingram-Smith C, Smith KS.** 2007. AMP-forming acetyl-CoA synthetases in Archaea show unexpected diversity in substrate utilization. *Archaea*. **2:**95-107.

172. **Gulick AM.** 2009. Conformational dynamics in the acyl-CoA synthetases, adenylation domains of non-ribosomal peptide synthetases, and firefly luciferase. *ACS. Chem. Biol.* **4:**811-827.

173. **Brown TD, Jones-Mortimer MC, Kornberg HL.** 1977. The enzymic interconversion of acetate and acetyl-coenzyme A in *Escherichia coli*. *J. Gen. Microbiol.* **102:**327-336.

174. **Wu R, Cao J, Lu X, Reger AS, Gulick AM, Dunaway-Mariano D.** 2008. Mechanism of 4-chlorobenzoate:coenzyme A ligase catalysis. *Biochemistry*. **47:**8026-8039.

175. **Branchini BR, Murtiashaw MH, Magyar RA, Anderson SM.** 2000. The role of lysine 529, a conserved residue of the acyl-adenylate- forming enzyme superfamily, in firefly luciferase. *Biochemistry*. **39:**5433-5440.

176. **Hallows WC, Lee S, Denu JM.** 2006. Sirtuins deacetylate and activate mammalian acetyl-CoA synthetases. *Proc. Natl. Acad. Sci. USA.* **103:**10230-10235.

177. **Castano-Cerezo S, Bernal V, Blanco-Catala J, Iborra JL, Canovas M.** 2011. cAMP-CRP co-ordinates the expression of the protein acetylation pathway with central metabolism in *Escherichia coli*. *Mol. Microbiol*. **82:**1110-1128.

178. **Xu H, Hegde SS, Blanchard JS.** 2011. Reversible acetylation and inactivation of *Mycobacterium tuberculosis* acetyl-CoA synthetase is dependent on cAMP. *Biochemistry*. **50:**5883-5892.

179. **Chan CH, Garrity J, Crosby HA, Escalante-Semerena JC.** 2011. In *Salmonella enterica*, the sirtuin-dependent protein acylation/deacylation system (SDPADS) maintains energy homeostasis during growth on low concentrations of acetate. *Mol. Microbiol.* **80:**168-183.

180. **Lima BP, Antelmann H, Gronau K, Chi BK, Becher D, Brinsmade SR, Wolfe AJ.** 2011. Involvement of protein acetylation in glucose-induced transcription of a stress-responsive promoter. *Mol. Microbiol.* **81:**1190-1204.

181. **Lima BP, Thanh Huyen TT, Basell K, Becher D, Antelmann H, Wolfe AJ.** 2012. Inhibition of acetyl phosphate-dependent transcription by an acetylatable lysine on RNA polymerase. *J. Biol. Chem.* **287:**32147-32160.

182. **Gardner JG, Escalante-Semerena JC.** 2009. In *Bacillus subtilis*, the sirtuin protein deacetylase encoded by the *srtN* gene (formerly *yhdZ*), and functions encoded by the *acuABC* genes control the activity of acetyl-CoA synthetase. *J. Bacteriol.* **191:**1749-1755.

183. **Grundy FJ, Waters DA, Takova TY, Henkin TM.** 1993. Identification of genes involved in utilization of acetate and acetoin in *Bacillus subtilis*. *Mol. Microbiol.* **10:**259-271.

184. **Huang M, Oppermann-Sanio FB, Steinbuchel A.** 1999. Biochemical and molecular characterization of the *Bacillus subtilis* acetoin catabolic pathway. *J. Bacteriol*. **181:**3837-3841.

185. **Seow KT, Meurer G, Gerlitz M, Wendt-Pienkowski E, Hutchinson CR, Davies J.** 1997. A study of iterative type II polyketide synthases, using bacterial genes cloned from soil DNA: a means to access and use genes from uncultured microorganisms. *J. Bacteriol.* **179:**7360-7368.

186. **Courtois S, Cappellano CM, Ball M, Francou FX, Normand P, Helynck G, Martinez A, Kolvek SJ, Hopke J, Osburne MS, August PR, Nalin R, Guerineau M, Jeannin P, Simonet P, Pernodet JL.** 2003. Recombinant environmental libraries provide access to microbial diversity for drug discovery from natural products. *Appl. Environ. Microbio*l. **69:**49-55.

187. **McMahon MD, Guan C, Handelsman J, Thomas MG.** 2012. Metagenomic analysis of *Streptomyces lividans* reveals host-dependent functional expression. *Appl. Environ. Microbiol.* **78:**3622-3629.

188. **Chater KF.** 2006. *Streptomyces* inside-out: a new perspective on the bacteria that provide us with antibiotics. *Philos. Trans. R. Soc. Lond. B. Biol. Sci.* **361:**761-768.

189. **Mitchell CA, Tucker AC, Escalante-Semerena JC, Gulick AM.** 2015. The structure of *S. lividans* acetoacetyl-CoA synthetase shows a novel interaction between the *C*-terminal extension and the *N*-terminal domain. *Proteins.* **83:**575-581.

190. **Mikulik K, Felsberg J, Kudrnacova E, Bezouskova S, Setinova D, Stodulkova E, Zidkova J, Zidek V.** 2012. CobB1 deacetylase activity in *Streptomyces coelicolor*. *Biochem. Cell. Biol.* **90:**179-187.

191. **Nambi S, Basu N, Visweswariah SS.** 2010. Cyclic AMP-regulated protein lysine acetylases in mycobacteria. *J. Biol. Chem*. **285:**24313-24323.

192. **Nambi S, Gupta K, Bhattacharya M, Ramakrishnan P, Ravikumar V, Siddiqui N, Thomas AT, Visweswariah SS.** 2013. Cyclic AMP-dependent protein lysine acylation in mycobacteria regulates fatty acid and propionate metabolism. *J. Biol. Chem.* **288**.

193. **Nambi S, Badireddy S, Visweswariah SS, Anand GS.** 2012. Cyclic AMP-induced conformational changes in mycobacterial protein acetyltransferases. *J. Biol. Chem.* **287:**18115-18129.

194. **Lee HJ, Lang PT, Fortune SM, Sassetti CM, Alber T.** 2012. Cyclic AMP regulation of protein lysine acetylation in *Mycobacterium tuberculosis*. *Nat. Struct. Mol. Biol.* **19:**811-818.

195. **O'Toole R, Williams HD.** 2003. Universal stress proteins and *Mycobacterium tuberculosis*. *Res. Microbiol.* **154:**387-392.

196. **Escalante-Semerena JC.** 2010. *N*(ε)-Lysine acetylation control conserved in all three domains of life. *Microbes. Infect.* **5:**340-344.

197. **Hase T, Wakabayashi S, Matsubara H, Kerscher L, Oesterhelt D, Rao KK, Hall DO.** 1978. Complete amino acid sequence of *Halobacterium halobium* ferredoxin containing an *N* epsilon-acetyllysine residue. *J. Biochem.* **83:**1657-1670.

198. **Sandman K, Reeve JN.** 2005. Archaeal chromatin proteins: different structures but common function? Curr. *Opin. Microbiol.* **8:**656-661.

199. **Forbes AJ, Patrie SM, Taylor GK, Kim YB, Jiang L, Kelleher NL.** 2004. Targeted analysis and discovery of posttranslational modifications in proteins from methanogenic archaea by top-down MS. *Proc. Natl. Acad. Sci. USA.* **101:**2678-2683.

200. **Bell SD, Botting CH, Wardleworth BN, Jackson SP, White MF.** 2002. The interaction of Alba, a conserved archaeal chromatin protein, with Sir2 and its regulation by acetylation. *Science*. **296:**148-151.

201. **Wardleworth BN, Russell RJ, Bell SD, Taylor GL, White MF.** 2002. Structure of Alba: an archaeal chromatin protein modulated by acetylation. *EMBO J.* **21:**4654-4662.

202. **Guo R, Xue H, Huang L.** 2003. Ssh10b, a conserved thermophilic archaeal protein, binds RNA *in vivo. Mol. Microbiol.* **50:**1605-1615.

203. **Majdalani N, Gottesman S.** 2005. The Rcs phosphorelay: a complex signal transduction system. *Annu. Rev. Microbiol.* **59:**379-405.

204. **Huang YH, Ferrieres L, Clarke DJ.** 2006. The role of the Rcs phosphorelay in Enterobacteriaceae. *Res. Microbiol*. **157:**206-212.

205. **Hu LI, Chi BK, Kuhn ML, Filippova EV, Walker-Peddakotla AJ, Basell K, Becher D, Anderson WF, Antelmann H, Wolfe AJ.** 2013. Acetylation of the response regulator RcsB controls transcription from a small RNA promoter. *J. Bacteriol.* **195:**4174-4886.

206. **Barak R, Prasad K, Shainskaya A, Wolfe AJ, Eisenbach M.** 2004. Acetylation of the chemotaxis response regulator CheY by acetyl-CoA synthetase purified from *Escherichia coli*. *J. Mol. Biol.* **342:**383-401.

207. **Ramakrishnan R, Schuster M, Bourret RB.** 1998. Acetylation at Lys-92 enhances signaling by the chemotaxis response regulator protein CheY. *Proc. Natl. Acad. Sci. USA*. **95:**4918-4923.

208. **Liarzi O, Barak R, Bronner V, Dines M, Sagi Y, Shainskaya A, Eisenbach M.** 2010. Acetylation represses the binding of CheY to its target proteins. *Mol. Microbiol.* **76:**932-943.

209. **Li R, Gu J, Chen YY, Xiao CL, Wang LW, Zhang ZP, Bi LJ, Wei HP, Wang XD, Deng JY, Zhang XE.** 2010. CobB regulates *Escherichia coli* chemotaxis by deacetylating the response regulator CheY. *Mol. Microbiol.* **76:**1162-1174.

210. **Yan J, Barak R, Liarzi O, Shainskaya A, Eisenbach M.** 2008. *In vivo* acetylation of CheY, a response regulator in chemotaxis of *Escherichia coli*. *J. Mol. Biol.* **376:**1260-1271.

211. **Barak R, Welch M, Yanovsky A, Oosawa K, Eisenbach M.** 1992. Acetyladenylate or its derivative acetylates the chemotaxis protein CheY *in vitro* and increases its activity at the flagellar switch. *Biochemistry.* **31:**10099-11107.

212. **Fraser ME, James MN, Bridger WA, Wolodko WT.** 1999. A detailed structural description of *Escherichia coli* succinyl-CoA synthetase. *J. Mol. Biol.* **285:**1633-1653.

213. **Tucker AC, Escalante-Semerena JC.** 2014. Determinants within the *C*-terminal domain of *Streptomyces lividans* acetyl-CoA synthetase that block acetylation of its active site lysine *in vitro* by the protein acetyltransferase (Pat) enzyme. *PLOS ONE.* **9:**e99817.

214. **Crosby HA, Rank KC, Rayment I, Escalante-Semerena JC.** 2012. Structure-guided expansion of the substrate range of methylmalonyl-CoA synthetase (MatB) of *Rhodopseudomonas palustris*. *Appl. Environ. Microbiol.* **78:**6619-6629.

215. **Crosby HA, Rank KC, Rayment I, Escalante-Semerena JC.** 2012. Structural insights into the substrate specificity of the protein acetyltransferase *Rp*Pat: identification of a loop critical for recognition by *Rp*Pat. *J. Biol. Chem.* **287:**41392-41404.

216. **Bains J, Boulanger MJ.** 2007. Biochemical and structural characterization of the paralogous benzoate CoA ligases from *Burkholderia xenovorans* LB400: defining the entry point into the novel benzoate oxidation (box) pathway. *J. Mol. Biol.* **373:**965-977.

217. **Bhaumik P, Koski MK, Glumoff T, Hiltunen JK, Wierenga RK.** 2005. Structural biology of the thioester-dependent degradation and synthesis of fatty acids. *Curr. Opin. Struct. Biol.* **15:**621-628.

218. **Skonberg C, Olsen J, Madsen KG, Hansen SH, Grillo MP.** 2008. Metabolic activation of carboxylic acids. *Expert Opin. Drug Metab. Toxicol.* **4:**425-438.

219. **Berg P.** 1956. Acyl adenylates: An enzymatic mechanism of acetate activation. *J. Biol. Chem.* **222:**991-1013.

220. **Leonardi R, Zhang Y, Rock C, Jackowski S.** 2005. Coenzyme A: back in action. *Prog. Lipid Res.* **44:**125-153.

221. **Brass EP.** 1994. Overview of coenzyme A metabolism and its role in cellular toxicity. *Chem. Biol. Interact.* **90:**203-214.

222. **El-Mansi M.** 2005. Free CoA-mediated regulation of intermediary and central metabolism: an hypothesis which accounts for the excretion of alpha-ketoglutarate during aerobic growth of *Escherichia coli* on acetate. *Res. Microbiol.* **156:**874-879.

223. **El-Mansi M, Cozzone AJ, Shiloach J, Eikmanns BJ.** 2006. Control of carbon flux through enzymes of central and intermediary metabolism during growth of *Escherichia coli* on acetate. *Curr. Opin. Microbiol.* **9:**173-179.

224. **Guest JR, Miles JS, Roberts RE, Woods SA.** 1985. The fumarase genes of *Escherichia coli*: location of the *fumB* gene and discovery of a new gene (*fumC*). *J. Gen. Microbiol.* **131:**2971-2984.

225. **Guest JR.** 1979. Anaerobic growth of *Escherichia coli* K12 with fumarate as terminal electron acceptor. Genetic studies with menaquinone and fluoroacetate-resistant mutants. *J. Gen. Microbiol.* **115:**259-271.

226. **Izui K, Taguchi M, Morikawa M, Katsuki H.** 1981. Regulation of *Escherichia coli* phosphoenolpyruvate carboxylase by multiple effectors *in vivo*. II. Kinetic studies with a reaction system containing physiological concentrations of ligands. *J. Biochem.* **90:**1321-1331.

227. **Sanwal BD.** 1970. Allosteric controls of amphilbolic pathways in bacteria. *Bacteriol. Rev.* **34:**20-39.

228. **Vallari DS, Rock CO.** 1985. Pantothenate transport in *Escherichia coli*. *J. Bacteriol.* **162:**1156-1161.

229. **Vallari DS, Jackowski S.** 1988. Biosynthesis and degradation both contribute to the regulation of coenzyme A content in *Escherichia coli. J. Bacteriol.* **170:**3961-3966.

230. **Chohnan S, Furukawa H, Fujio T, Nishihara H, Takamura Y.** 1997. Changes in the size and composition of intracellular pools of nonesterified coenzyme A and coenzyme A thioesters in aerobic and facultatively anaerobic bacteria. *Appl. Environ. Microbiol.* **63:**553-560.

231. **Chohnan S, Izawa H, Nishihara H, Takamura Y.** 1998. Changes in size of intracellular pools of coenzyme A and its thioesters in *Escherichia coli* K-12 cells to various carbon sources and stresses. *Biosci. Biotech. Biochem.* **62:**1122-1128.

232. **Jackowski S, Rock CO.** 1986. Consequences of reduced intracellular coenzyme A content in *Escherichia coli*. *J. Bacteriol.* **166:**866-871.

233. **Keating DH, Carey MR, Cronan JE, Jr.** 1995. The unmodified (apo) form of *Escherichia coli* acyl carrier protein is a potent inhibitor of cell growth. *J. Biol. Chem.* **270:**22229-22235.

234. **Keating DH, Zhang Y, Cronan JE, Jr.** 1996. The apparent coupling between synthesis and posttranslational modification of *Escherichia coli* acyl carrier protein is due to inhibition of amino acid biosynthesis. *J. Bacteriol.* **178:**2662-2667.

235. **Cahová H, Winz M, Hofer K, Nubel G, Jaschke A.** 2015. NAD captureSeq indicates NAD as a bacterial cap for a subset of regulatory RNAs. *Nature*. **519:**374-377.

236. **Kolb A, Busby S, Buc H, Garges S, Adhya A.** 1993. Transcriptional regulation by cAMP and its receptor protein. *Ann. Rev. Biochem.* **62:**749-795.

237. **Bai G, Schaak DD, McDonough KA.** 2009. cAMP levels within *Mycobacterium tuberculosis* and *Mycobacterium bovis* BCG increase upon infection of macrophages. *FEMS Immunol. Med. Microbiol.* **55:**68-73.

238. **Bai G, Knapp GS, McDonough KA.** 2011. Cyclic AMP signalling in mycobacteria: redirecting the conversation with a common currency. *Cell. Microbiol.* **13:**349-358.

239. **Findeisen F, Linder JU, Schultz A, Schultz JE, Brugger B, Wieland F, Sinning I, Tews I.** 2007. The structure of the regulatory domain of the adenylyl cyclase Rv1264 from *Mycobacterium tuberculosis* with bound oleic acid. *J. Mol. Biol.* **369:**1282-1295.

240. **Tews I, Findeisen F, Sinning I, Schultz A, Schultz JE, Linder JU.** 2005. The structure of a pH-sensing mycobacterial adenylyl cyclase holoenzyme. *Science*. **308:**1020-1023.

241. **Cann MJ, Hammer A, Zhou J, Kanacher T.** 2003. A defined subset of adenylyl cyclases is regulated by bicarbonate ion. *J. Biol. Chem.* **278:**35033-35038.

242. **Abdel Motaal A, Tews I, Schultz JE, Linder JU.** 2006. Fatty acid regulation of adenylyl cyclase Rv2212 from *Mycobacterium tuberculosis* H37Rv. *FEMS J.* **273:**4219-4228.

243. **Baek SH, Li AH, Sassetti CM.** 2011. Metabolic regulation of mycobacterial growth and antibiotic sensitivity. *PLOS Biol.* **9:**e1001065.

244. **Michan S, Sinclair D.** 2007. Sirtuins in mammals: insights into their biological function. *Biochem. J.* **404:**1-13.

245. **Ma Q, Wood TK.** 2011. Protein acetylation in prokaryotes increases stress resistance. *Biochem. Biophys. Res. Commun.* **410:**846-851.

246. **Wolfe AJ.** 2005. The acetate switch. *Microbiol. Mol. Biol. Rev.* **69:**12-50.

247. **Kumari S, Beatty CM, Browning DF, Busby SJ, Simel EJ, Hovel-Miner G, Wolfe AJ.** 2000. Regulation of acetyl coenzyme A synthetase in *Escherichia coli*. *J. Bacteriol.* **182:**4173-4179.

248. **Browning DF, Beatty CM, Sanstad EA, Gunn KE, Busby SJ, Wolfe AJ.** 2004. Modulation of CRP-dependent transcription at the *Escherichia coli acs*P2 promoter by nucleoprotein complexes: anti-activation by the nucleoid proteins FIS and IHF. *Mol. Microbiol.* **51:**241-254.

249. **Tucker AC, Escalante-Semerena JC.** 2010. Biologically active isoforms of CobB sirtuin deacetylase in *Salmonella enterica* and *Erwinia amylovora*. *J. Bacteriol.* **192:**6200-6208.

250. **Hulmes DJ.** 1992. The collagen superfamily - diverse structures and assemblies. *Essays Biochem.* **27:**49-67.

251. **Errey JC, Blanchard JS.** 2006. Functional annotation and kinetic characterization of PhnO from *Salmonella enterica*. *Biochemistry*. **45:**3033-3039.

252. **Davies AM, Tata R, Beavil RL, Sutton BJ, Brown PR.** 2007. *L*-Methionine sulfoximine, but not phosphinothricin, is a substrate for an acetyltransferase (gene PA4866) from *Pseudomonas aeruginosa*: structural and functional studies. *Biochemistry.* **46:**1829-1839.

253. **Gutierrez A, Elez M, Clermont O, Denamur E, Matic I.** 2011. *Escherichia coli* YafP protein modulates DNA damaging property of the nitroaromatic compounds. *Nucleic Acids Res.* **39:**4192-4201.

CHAPTER 3

DECIPHERING THE REGULATORY CIRCUITRY THAT CONTROLS REVERSIBLE LYSINE ACETYLATION IN *SALMONELLA ENTERICA*[2]

[2]Hentchel K.L., Thao S., Intile P.J., and J.C. Escalante-Semerena. 2015. *mBio*. Accepted. Reprinted here with permission from the publisher.

ABSTRACT

In *Salmonella enterica*, the reversible lysine acetylation (RLA) system is comprised of the protein acetyltransferase (Pat) and sirtuin deacetylase (CobB). RLA controls the activities of many proteins, including the acetyl-CoA synthetase (Acs), by modulating the degree of Acs acetylation. We report that IolR, a *myo*-inositol catabolism repressor, activates the expression of genes encoding components of the RLA system. *In vitro* evidence shows that the IolR protein directly regulates *pat* expression. An *iolR* mutant strain displayed a growth defect in minimal medium containing 10 mM acetate, a condition in which RLA function is critical to control Acs activity. Increased levels of Pat, CobB, or Acs activity reversed the growth defect, suggesting the Pat:CobB ratio in an *iolR* strain is altered and that such a change affects the level of acetylated, inactive Acs. Results of *in vitro* assays showed an ~25% decrease in Acs activity in cell-free extracts of the mutant *iolR* strain relative a strain carrying the wild-type *iolR* allele. An *iolR* mutant strain displayed decreased expression of *pat, cobB*, and *acs*, and glucose differentially regulated expression of *pat*, *cobB*, and *acs*. The catabolite repressor protein (Crp) positively regulated expression of *pat* while having no effect on *cobB*.

IMPORTANCE

Reversible lysine acylation (RLA) is used by cells of all domains of life to modulate the function of proteins involved in diverse processes. Work herein begins to outline the regulatory circuitry that integrates the expression of genes encoding enzymes that control the activity of a central metabolic enzyme in C2 metabolism. Genetic analyses revealed subtle effects on RLA that greatly impacted the growth behavior of the cell. This work provides the first insights into the complexities of the system responsible for controlling RLA at the transcriptional level.

INTRODUCTION

Reversible lysine acetylation (RLA) is a posttranslational regulatory mechanism present in all domains of life (1). RLA allows an organism to rapidly and reversibly modulate the biological activity of proteins involved in carbon utilization, transcription, translation, and stress responses (2-5) by modulating the acetylation state of epsilon amino group of lysyl residues critical for function [reviewed in (6)]. In the last decade, studies have provided insights into how the RLA system works in diverse prokaryotes (3, 7-10). In *S. enterica* the RLA system is comprised of a protein acetyltransferase (Pat) of the Gcn5 *N*-acetyltransferase (GNAT) family, and a NAD^+-consuming sirtuin deacetylase (CobB) (2) (Fig. 3.1). Relevant to this work is the RLA control of acetyl-CoA synthetase (Acs), an AMP-forming CoA ligase involved in acetate utilization (11). Pat is responsible for the acetylation and inactivation of Acs (2), while removal of the acetyl moiety of Acs^{Ac} by the CobB deacetylase reactivates Acs (12). RLA-dependent regulation of Acs is imperative, as uncontrolled Acs results in growth arrest by depletion of ATP pools (8).

In addition to post-translational regulation, expression of *acs* is controlled by several transcriptional regulators (13). While the regulatory region of *cobB* in *S. enterica* has been examined to some extent (14), the transcriptional regulation of genes encoding the enzymes of the RLA system (*pat*, *cobB*) has not been investigated. It has been shown that the catabolite repressor protein (Crp) regulates the *E. coli pat* homologue (*pka*) (15), although a role for Crp regulation of *pat* in *S. enterica* has not been reported.

In this work a genetic approach was used to identify *S. enterica* genes whose products affected the *pat* promoter (P_{pat}). We show that inactivation of *iolR* (*stm4417*), encoding an RpiR-like transcriptional repressor, decreased *pat* expression (16). RpiR-like regulators are involved in sugar catabolism and can function as activators and repressors (17, 18). In *S. enterica*, *Bacillus*

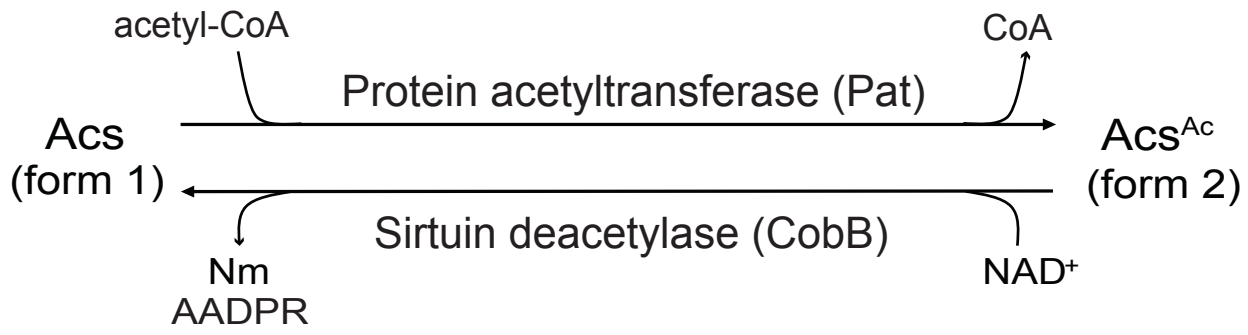

Figure 3.1. Reversible Lysine Acetylation (RLA) in *S. enterica*. Activity of the AMP-forming acetyl-CoA synthetase (Acs) is post-translationally modified by the protein acetyltransferase Pat. This modification is reversible by the activity of the NAD^+-consuming class III sirtuin deacetylase, CobB. *O*-AADPR, *O*-acetyl ADP ribose; Nm, nicotinamide.

subtilis, *Corynebacterium glutamicum*, and *Sinorhizobium meliloti*, IolR negatively regulates expression of the *myo*-inositol utilization operon (16, 19). *myo*-Inositol (cyclohexane-1,2,3,4,5,6-hexol) is an abundant cyclic polyol in soil and its utilization as a sole carbon source depends on the presence of a large number of genes organized as a genomic island (16), which is present in γ-proteobacteria, α-proteobacteria, and Gram-positive bacteria (20-26).

Here we present *in vivo* evidence that IolR activates *pat* expression in *S. enterica*, and that IolR binds to the *pat* promoter *in vitro*. We also report that *acs* and *cobB* are transcriptionally activated by IolR, which places the reversible lysine acetylation system of *S. enterica* under IolR control. Significantly, an *iolR* mutant strain displayed a growth defect in minimal medium containing 10 mM acetate, which we suggest is due to an imbalance of active (non-acetylated) / inactive (acetylated) Acs ratio caused by changes in *pat* and *cobB* expression in the absence of IolR. Lastly, we show that Crp, a global regulator of carbon metabolism, regulates *pat* and *acs* expression in *S. enterica*. To our knowledge, this is the first report of global, integrative transcriptional control of genes encoding the enzymes of the RLA system in *S. enterica* and its effect on carbon metabolism.

RESULTS

IolR regulates* pat *expression. A genetic screen was used to identify genes whose functions affected the expression of *pat,* the gene encoding the protein acetyltransferase in *S. enterica*. Changes in *pat* expression were monitored in strain JE7449, which carried a chromosomal *pat*::MudJ (*lacZ*$^+$ *kan*$^+$) reporter (hereafter *pat-lacZ*$^+$; Table 3.1). This strain was transduced to tetracycline resistance (Tc^R) via a P22 lysate grown on a pool of ~100,000 strains, each of which assumed to contain one Tn*10*d(*tet*$^+$) element randomly inserted in the genome. Tc^R derivatives of

the *pat-lacZ*$^+$ reporter strain (~20,000) were screened for changes in β-galactosidase activity, leading to the identification of two colonies that were less blue than the parental strain. The DNA sequence flanking the Tn*10*d(*tet*$^+$) elements located both insertions within *iolR* (*stm4417*), the gene encoding the repressor of the *myo*-inositol utilization (*iol*) genes. No other insertions affecting *pat* expression were identified in the screen. To confirm that the *iolR*::Tn*10*d(*tet*$^+$) element was responsible for the reduced expression of the *pat-lacZ*$^+$ reporter, phage P22 grown on the original *iolR*::Tn*10*d(*tet*$^+$) *pat-lacZ*$^+$ strain was used to transduce strain JE7449 (*pat-lacZ*$^+$) to Tc^R. The reconstructed *iolR*::Tn*10*d(*tet*$^+$) *pat-lacZ*$^+$ strain (JE10535) displayed the same reduction in *pat-lacZ*$^+$ expression as measured in the original mutant strain (data not shown).

To independently confirm the effect of IolR on *pat* expression, an *iolR*::*cat*$^+$ mutation was introduced into strain JE7449 (*pat-lacZ*$^+$). Measurements of β-galactosidase activity of the *pat-lacZ*$^+$ *iolR*::*cat*$^+$ strain (JE10714) during growth in nutrient broth (NB) showed a reproducible ~2-fold decrease in *pat* promoter (P_{pat}) activity relative to that in the *pat-lacZ*$^+$ *iolR*$^+$ strain (Fig. 3.2A). Complementation analysis with an *iolR* copy provided *in trans* restored *pat* expression to wild type level (Fig. 3.2B). The effect of IolR on *pat* expression was confirmed using qRT-PCR, and showed a 5-fold down-regulation of the *pat* transcript in an *iolR*::*cat*$^+$ strain compared to wild type (Fig. 3.2C). From these data we concluded that the decrease in *pat* expression was due to the absence of IolR. The effect of IolR on *pat* expression was tested on acetate (10 mM) and *myo*-inositol (55 mM). In the absence of IolR, *pat-lacZ*$^+$ expression decreased 1.4-fold on acetate (Fig. 3.3A) and 1.3-fold on *myo*-inositol (Fig. 3.3B), compared to the *iolR*$^+$ strain.

Table 3.1. Strains and plasmids used in this study

Strain	Genotype	Reference/source
TR6583	*metE205 ara-9*	K. Sanderson via J. Roth
Derivatives of TR6583		
JE2845	*cobB1206*::MudJ[b]	Laboratory collection
JE4637	pACS3	Laboratory collection
JE7449	*pat10*::MudJ	Laboratory collection
JE7758	Δ*acs2*	Laboratory collection
JE9912	Δ*acs2* / pACS7	Laboratory collection
JE10040	pBAD30[c]	Laboratory collection
JE10535	*pat10*::MudJ *iolR52*::Tn*10*d(*tet*)[d]	
JE10713	*iolR51*::*cat*	
JE10714	*pat10*::MudJ *iolR51*::*cat*	
JE10727	*pat10*::MudJ *iolR51*::*cat* / pBAD30	
JE10728	*pat10*::MudJ *iolR51*::*cat* / pIOLR1	
JE14413	D*iolR53*	
JE14962	*iolR*::*cat* / pACS3	
JE14972	*cobB1206*::MudJ *iolR51*::*cat*	
JE16466	*crp892*::*cat*	
JE16596	Δ*acs2 iolR51*::*cat* / pACS7	
JE16743	*pat10*::MudJ *crp892*::*cat*	
JE16744	*pat10*::MudJ D*iolR51 crp892*::*cat*	
JE16771	*pat10*::MudJ *crp892*::*cat* / pBAD30	
JE16843	*cobB1206*::MudJ *iolR51*::*cat* / pBAD30	
JE16844	*cobB1206*::MudJ *iolR51*::*cat* / pIOLR1	
JE16934	*iolR51*::*cat* / pBAD30	
JE16935	*iolR51*::*cat* / pIOLR1	
JE17322	*pat10*::MudJ *crp892*::*cat* / pCRP2	
JE18891	*iolR51*::*cat* / pCOBB8	
JE18927	*iolR51*::*cat* / pPAT27	
JE19811	*pat10*::MudJ *iolR51*::*cat* / pPAT27	
***E. coli* strains**		
E. coli C41(lDE3)	*ompT hsdS* (r_B m_B) *gal* (λDE3) including at least one non-characterized mutation	{Miroux, 1996 #20626; Rocco, 2008 #11866}
Plasmids		
pIOLR1	*iolR* cloned into pBAD30[c]	
pIOLR3	*iolR* cloned into pTEV6[e]	
pCRP2	*crp* cloned into pBAD30[c]	
pCRP3	*crp* cloned into pTEV16[f]	
pACS3	P_{acs} cloned into pFZY1[g]	Laboratory collection
pACS7	*acs* cloned into pBAD30[c]	Laboratory collection
pACS33	*acs* cloned into pTEV5[h]	Laboratory collection
pCOBB8	*cobB* cloned into pBAD30[c]	Laboratory collection
pPAT27	*pat* cloned into pBAD30[c]	Laboratory collection
pPAT8	*pat* cloned into pTEV6[e]	Laboratory collection

[a] All strains and plasmids were constructed during the course of this work, unless otherwise stated
[b] MudJ is an abbreviation of MudI1734 (*lacZ*$^+$ *kan*$^+$) {Castilho, 1984 #11544}

[c] pBAD30 refers to a cloning vector described in {Guzman, 1995 #11361}
[d] Tn*10*d(*tet*) is an abbreviation of Tn*10*D*16*D*17* {Way, 1984 #21272}
[e] pTEV6 is an overexpression vector described in {Rocco, 2008 #11866}
[f] pTEV16 is a modified version of pTEV5 with BspQ1 restriction sites (C. M. VanDrisse and J. C. Escalante-Semerena, unpublished data)
[g] pFZY1 is a vector containing a promoterless *lacZ* fusion {Koop, 1987 #3238}
[h] pTEV5 is an overexpression vector described in {Rocco, 2008 #11866}

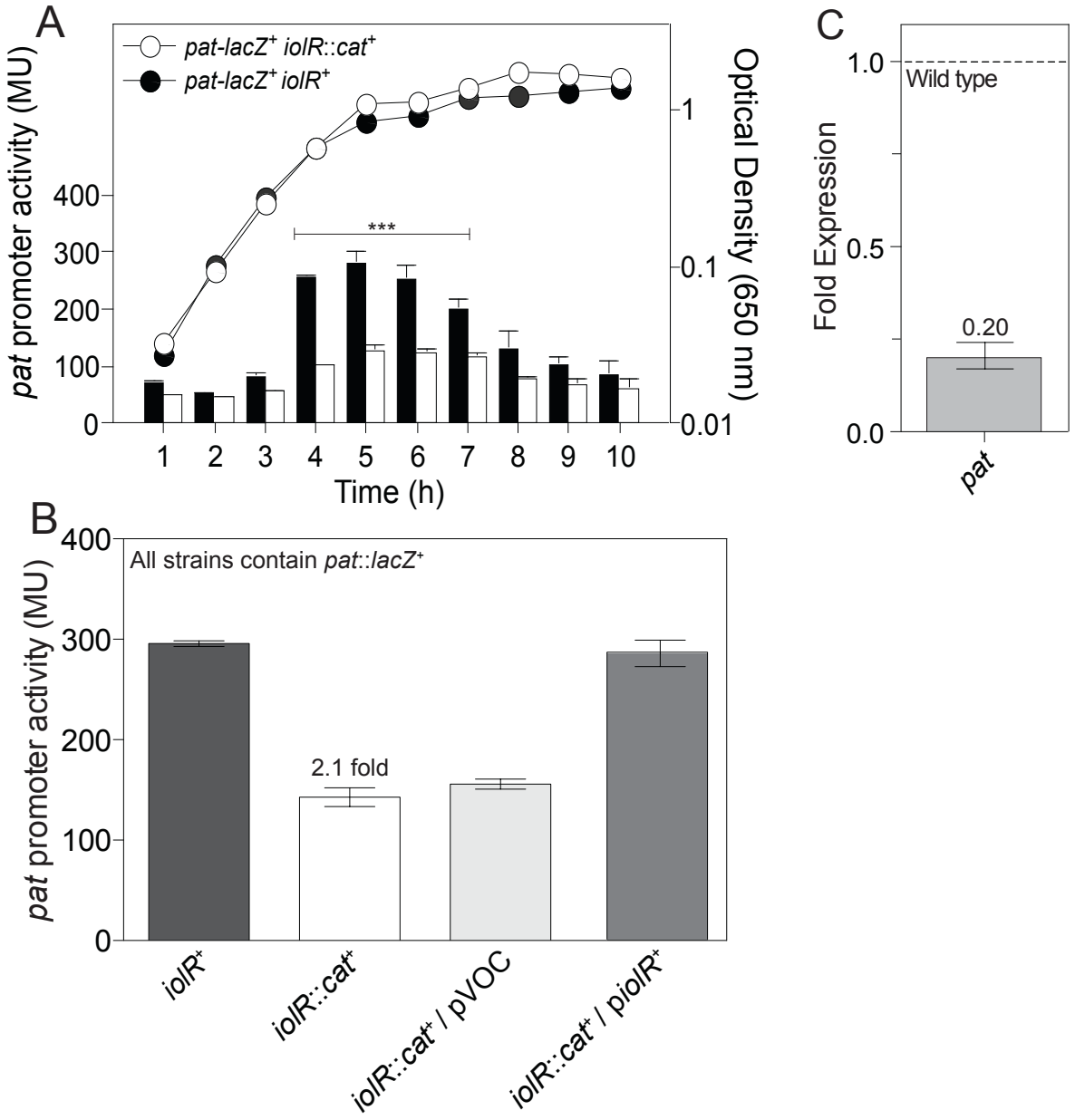

Figure 3.2. IolR activates *pat* expression *in vivo*. Activity of a *pat-lacZ*$^+$ chromosomal operon fusion was assessed in the presence (JE7449) or absence (JE10714) of *iolR* to measure *pat* promoter activity *in vivo* (A, B). Cell cultures were grown at 37°C in NB medium. The data presented are the average of two independent experiments from individual cultures performed in triplicate. Error bars represent standard deviation. Unpaired t test gave a P value of 0.0004 (A). C. qRT-PCR showed a 5-fold down-regulation in *pat* activity in an *iolR* strain relative to the *iolR*$^+$ strain. Wild-type transcript level is set at 1, indicated by the dashed line. Error bars represent standard deviation.

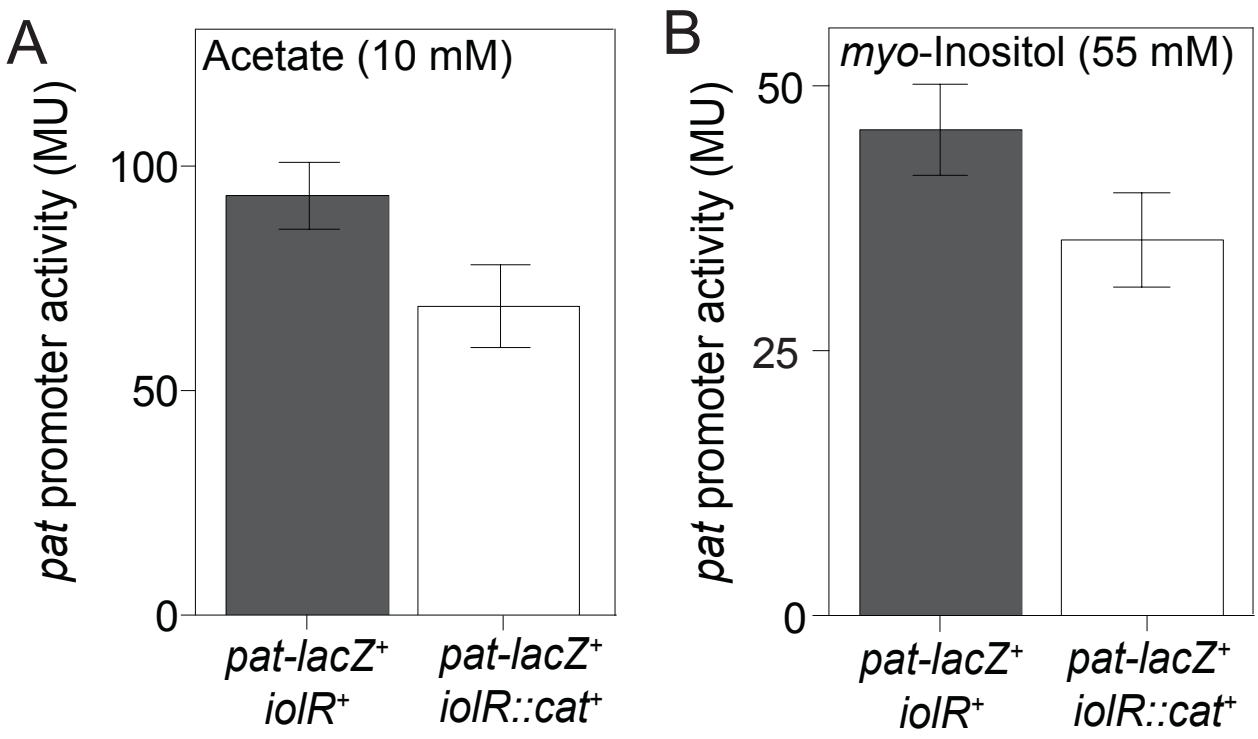

Figure 3.3. Expression of *pat* on acetate and *myo*-inositol. Cultures were grown in NCE minimal medium with acetate (10 mM; panel A), or *myo*-inositol (55 mM; panel B). β-Galactosidase activity was measured at mid-log phase. Assays were determined in duplicate from three biological replicates.

Pat does not acetylate IolR, and is not required during growth on* myo-*inositol. IolR represses the expression of genes encoding *myo*-inositol degrading enzymes (16, 33), and it was surprising to find that IolR may also play a role in the activation of genes comprising the RLA system. We considered the possibility of a regulatory system in which Pat would control the DNA binding activity of IolR via acetylation, as reported for Pat and the *E. coli* transcription factor RcsB (3). However, we did not obtain any experimental evidence of Pat-dependent regulation of IolR function under conditions in which acetyl-CoA synthetase (Acs), a bona fide Pat substrate (12), was acetylated (Fig. 3.4).

Consistent with the above-mentioned observation, we determined no difference in growth rate of the *pat-lacZ*$^+$ *iolR*::*cat*$^+$ to a strain carrying the wild-type *pat* and *iolR* alleles when grown on *myo*-inositol (Fig. 3.5). However, the *pat-lacZ*$^+$ *iolR*$^+$ strain consistently showed a slight but reproducible delay in the onset of growth. As reported by others (16), we observed that the onset of growth of the *iolR*::*cat*$^+$ strain occurred substantially earlier than that of a strain carrying the wild-type *iolR* allele, an observation consistent with the lack of repression of the *myo*-inositol genomic island in a strain devoid of the IolR repressor (Fig. 3.5).

IolR is a tetramer. To study the role of IolR regulation of *pat*, the IolR protein was isolated to 96% homogeneity (Fig. 3.6). The oligomeric state of IolR was determined using FPLC gel filtration analysis (Fig. 3.6). Under the conditions tested, IolR eluted ~24 min after injection, a retention time consistent with the behavior of a protein whose mass was approximately ~134 kDa when compared to elution times of molecular mass standards. Since the predicted molecular mass of IolR was 31 kDa, it was concluded that IolR was either a dimer of dimers or a tetramer.

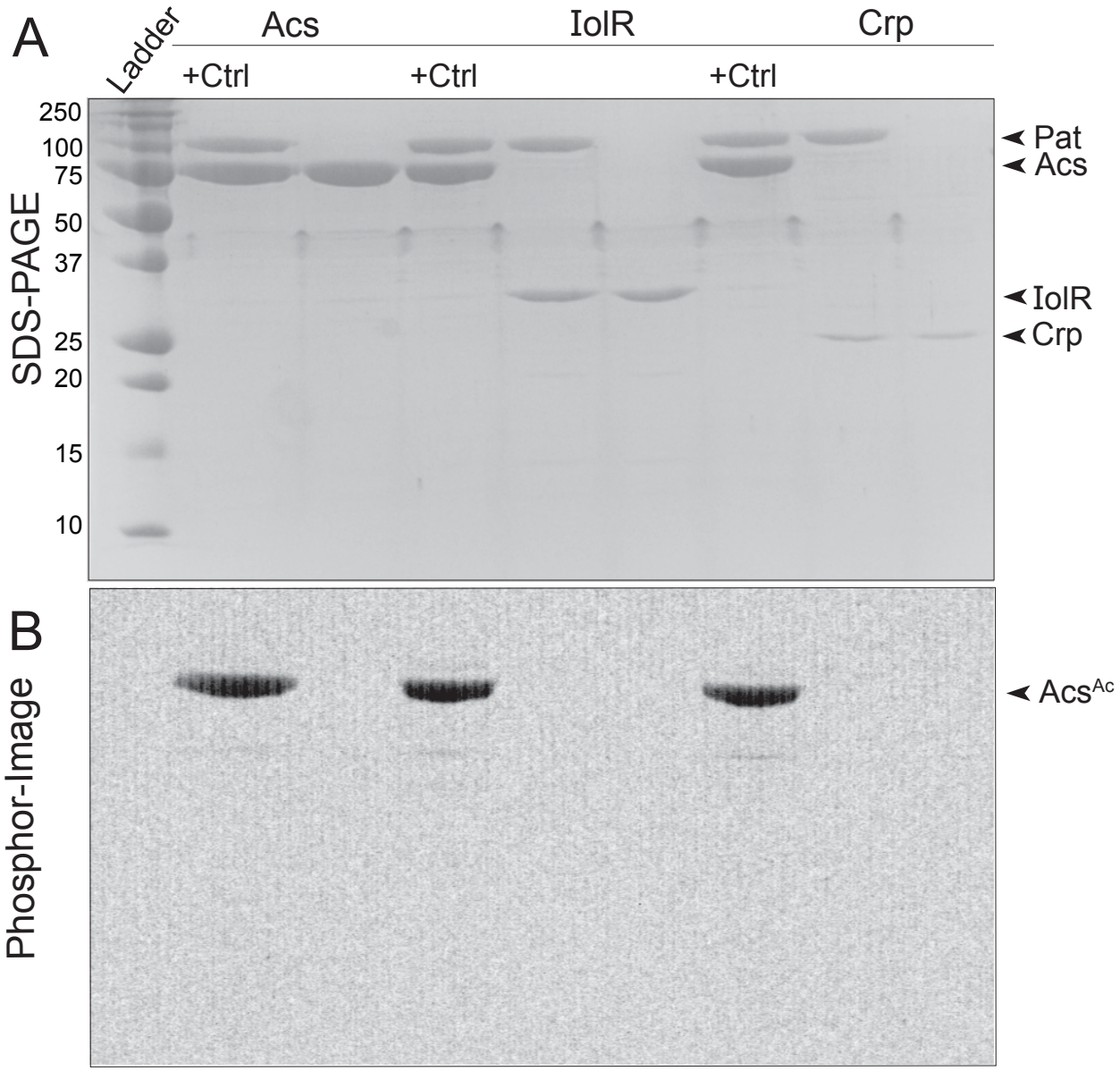

Figure 3.4. Pat does not acetylate IolR or Crp. An *in vitro* acetylation assay using [1-^{14}C] Ac-CoA was used to test Pat-dependent acetylation of IolR or Crp. Acs was used as a positive control. Reactions were analyzed SDS-PAGE and stained with Coomassie Blue to visualize proteins (A). Transfer of the acetyl group was visualized by phosphor-imaging (B). +Ctrl, positive control.

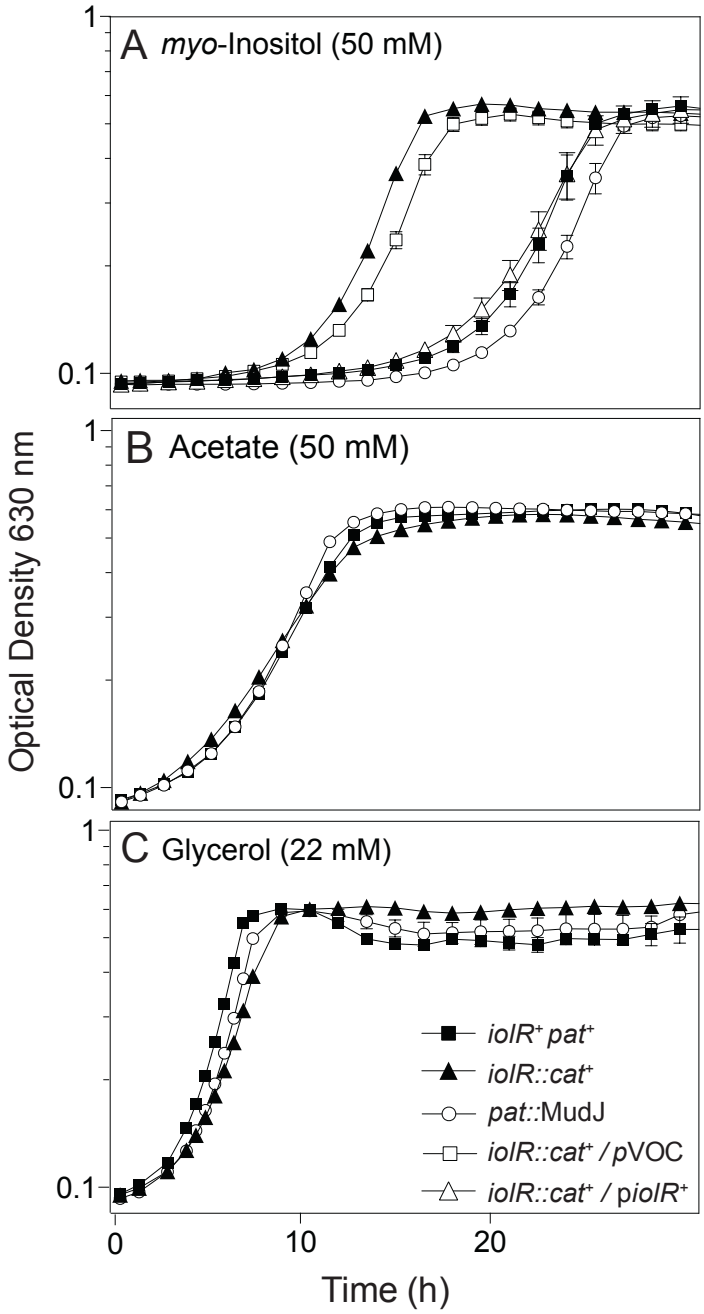

Figure 3.5. Growth study controls. Growth of *S. enterica* strains in NCE minimal medium with (A) *myo*-inositol (50 mM), (B) acetate (50 mM), and (C) glycerol (22 mM). Growth curves were performed using a Powerwave XS2 microplate reader (Bio-Tek Instruments) at 37°C with shaking in triplicate in three independent experiments. Strains analyzed: *iolR*$^+$ *pat*$^+$ (JE6583), *iolR*::*cat*$^+$ (JE10713), *iolR*::*cat*$^+$ / pVOC (JE16934), *iolR*::*cat*$^+$ / p*iolR*$^+$ (JE16935), and *pat*::MudJ (JE7449). Plasmids were induced with 100 μM *L*-(+)-arabinose. Error bars represent standard deviation. pVOC, vector-only control. Symbols shown in panel C apply to all panels.

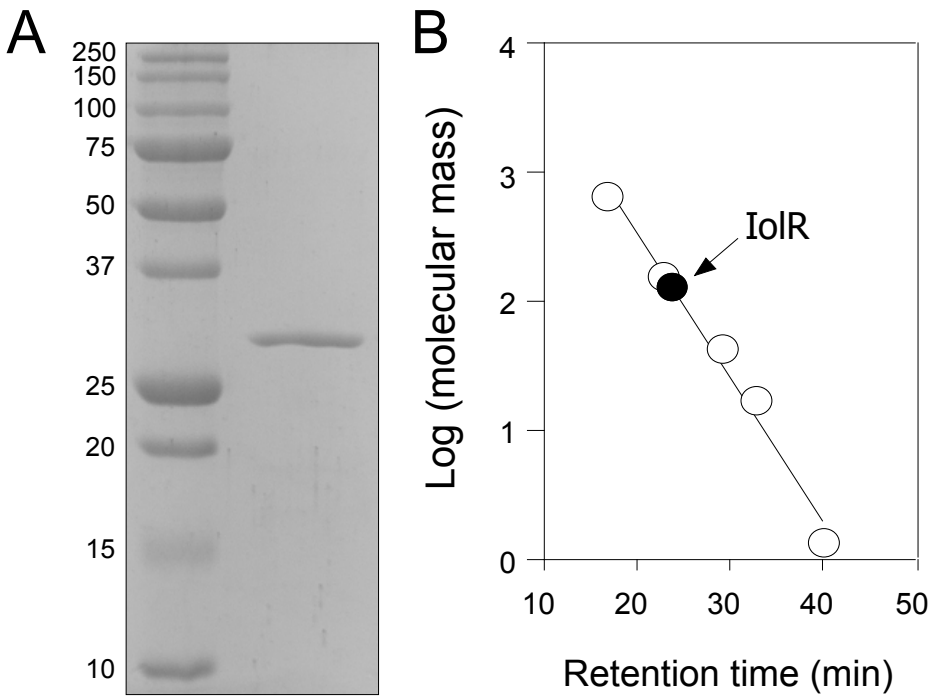

Figure 3.6. IolR is a tetramer. (A) *S. enterica* IolR protein (30.8 kDa) was purified using nickel affinity purification. An SDS-PAGE gel shows molecular size standards (kDa) (lane 1) and purified IolR protein (lane 2), purified to 96% homogeneity. (B) The molecular mass of IolR (closed circle) in solution was estimated by gel filtration. Molecular mass standards (open circles) are thyroglobulin (bovine; 670 kDa), γ-globulin (bovine; 158 kDa), ovalbumin (chicken; 44 kDa), myoglobin (horse; 17 kDa) and vitamin B_{12} (1.35 kDa).

***IolR binds to the* pat *promoter (P_{pat})* in vitro.** Electrophoretic mobility shift assays (EMSAs) were performed to determine if the effect of the IolR regulator on *pat* expression was the result of direct binding of IolR to P_{pat}. Experimental promoter analysis data was used to identify the transcription start site (TSS, www.imib-wuerzburg.de/research/salmonella) (34). To probe for the specificity of the interaction between IolR and P_{pat}, we added a non-specific competitor DNA P_{argS}, previously used to study IolR binding (16). Increasing concentrations of IolR shifted the P_{pat} probe, but not the P_{argS} probe, a result that supported the conclusion that IolR directly and specifically interacted with the P_{pat}, (Fig. 3.7A). Increasing amounts of IolR protein titrated against a fixed amount of the P_{pat} DNA probe without the presence of P_{argS} also yielded increased amounts of IolR/P_{pat} complex (Fig. 3.7B). IolR did not shift the mobility of P_{argS} until a molar excess of 50x protein was reached, indicative of non-specific binding of IolR to P_{argS} (Fig. 3.7C). Previous studies by others showed that IolR negatively regulates the transcription of its own promoter, P_{iolR} (16). Using P_{iolR} (175 nt) as a positive control with the presence of the competitor probe P_{argS}, we confirmed the reported specificity of IolR for its promoter (16) (Fig. 3.7D). The P_{pat} and P_{iolR} probes each shifted at similar molar excess concentrations of IolR, supporting the conclusion that IolR directly and specifically interacted with P_{pat}.

***Region of the* pat *promoter recognized by IolR*.** We performed DNA-footprinting analysis to identify the region within the *pat* promoter recognized by IolR. A 6FAM-5'-labeled 382-nucleotide probe containing the P_{pat} was incubated with varying concentrations of IolR protein or bovine serum albumin (negative control). After incubation and subsequent DNase digestion and purification of the DNA, samples were analyzed as described under *Materials and Methods*. Electropherogram overlays comparing IolR and BSA (negative control) and putative binding

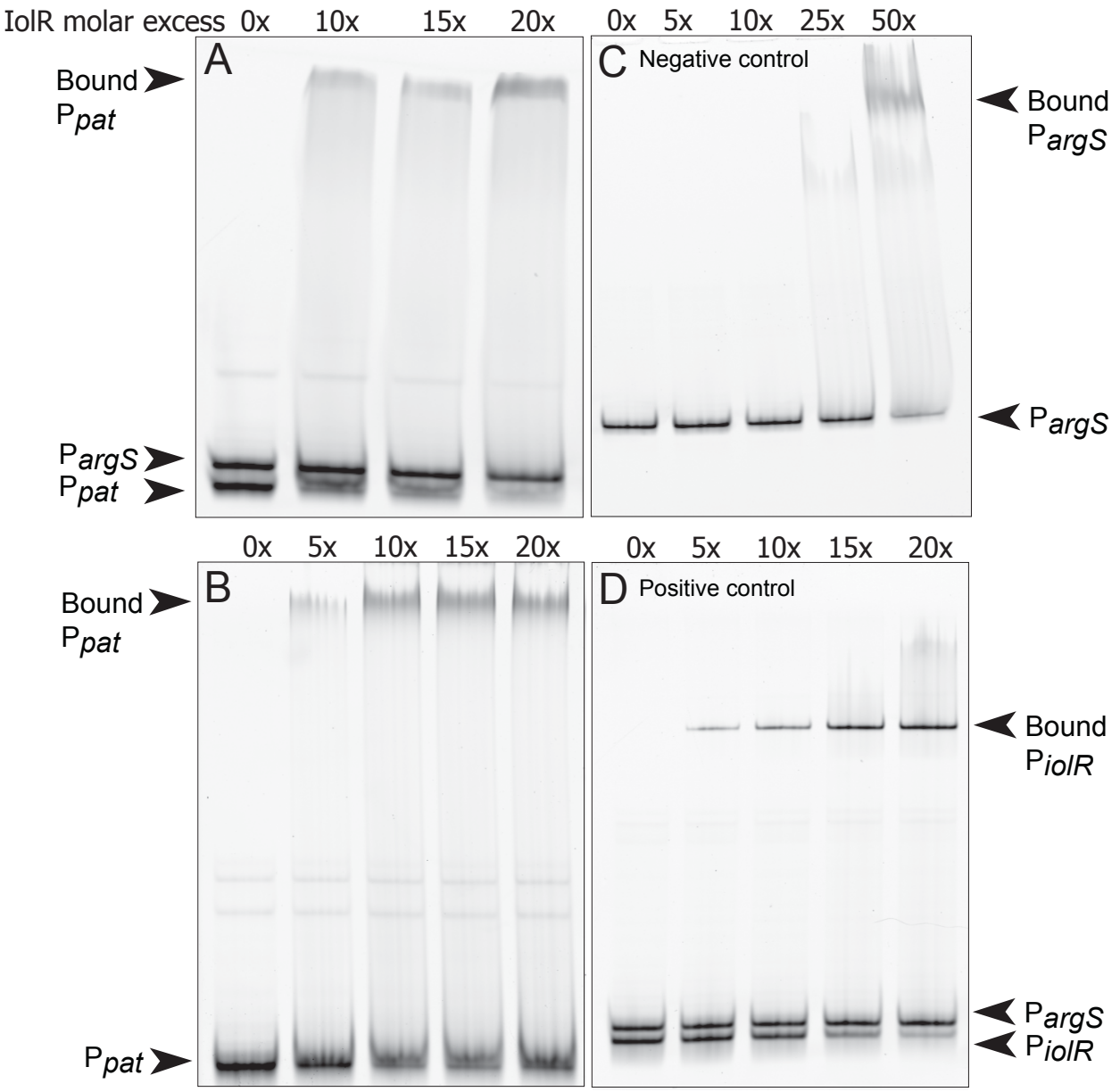

Figure 3.7. IolR binds to the *pat* promoter region. Binding of IolR to the 6FAM-5'-labeled *pat* promoter (P_{pat}, 150 nt, 51 nM) was analyzed by electrophoretic mobility shift assays in the presence of increasing concentrations of IolR. (A) P_{pat} and competitor DNA, (P_{argS}, 196 nt), were incubated together to show binding specificity of IolR to P_{pat}. (B) The P_{pat} probe alone was incubated at varying concentrations of IolR. (C) Competitor DNA P_{argS} was incubated with increasing concentrations of IolR to determine at what point non-specific binding interactions occur. (D) The interaction between IolR and P_{iolR} (175 nt) was performed as a known binding control and incubated in the presence of competitor DNA, P_{argS}. Protein concentration shown is in molar excess to probe (pmol). EMSAs were performed in triplicate.

sites were analyzed by aligning the sequenced probe data (data not shown). Data presented in figure 3.8 show a region of protection of P_{pat} from nucleotides -112 to -70 relative to the predicted transcription start site (Fig. 3.8A). Experimental promoter analysis data from Kroger *et al* was used to identify the transcription start site (www.imib-wuerzburg.de/research/salmonella) (34) (Fig. 3.8B). A region of hypersensitivity was seen at position -112, an indicator of DNA bending as the result of the binding of a transcriptional regulator, causing an exposed site susceptible to increased cleavage by DNase. A control was performed in which the amount of IolR was doubled in the reaction (10 μg). With this increase in protein concentration we expected an increase in signal intensity, as seen in figure 3.8A.

Previous studies aimed at examining the regulation of the *iol* genomic island in *S. enterica* by IolR repression did not identify a conserved binding site (16, 35). The intent of the DNA-footprinting analysis was to compare the binding region of IolR within P_{pat} to promoter regions regulated by IolR, with the idea of determining a consensus IOLR-binding region. While unable to determine a consensus site, the data confirmed the direct interaction between IolR and P*pat*.

IolR binds to the region of P_{pat} identified by DNA footprinting. A 45-nt probe corresponding to the protected region of P_{pat} identified as the IolR-binding region was used to validate the DNA-footprinting experiments. A 6FAM-5'-P_{pat45} 45-nt probe was generated by annealing complementary primers and the binding of IolR to this region was examined. Data presented show that IolR binds to the 45-nt probe, confirming that the IolR-binding site is located within this region (Fig. 3.9). The reason for the presence of signals of higher molecular mass complexes is unclear. Possible explanations include the absence of a ligand sensed by IolR, or the formation of higher order IolR multimers.

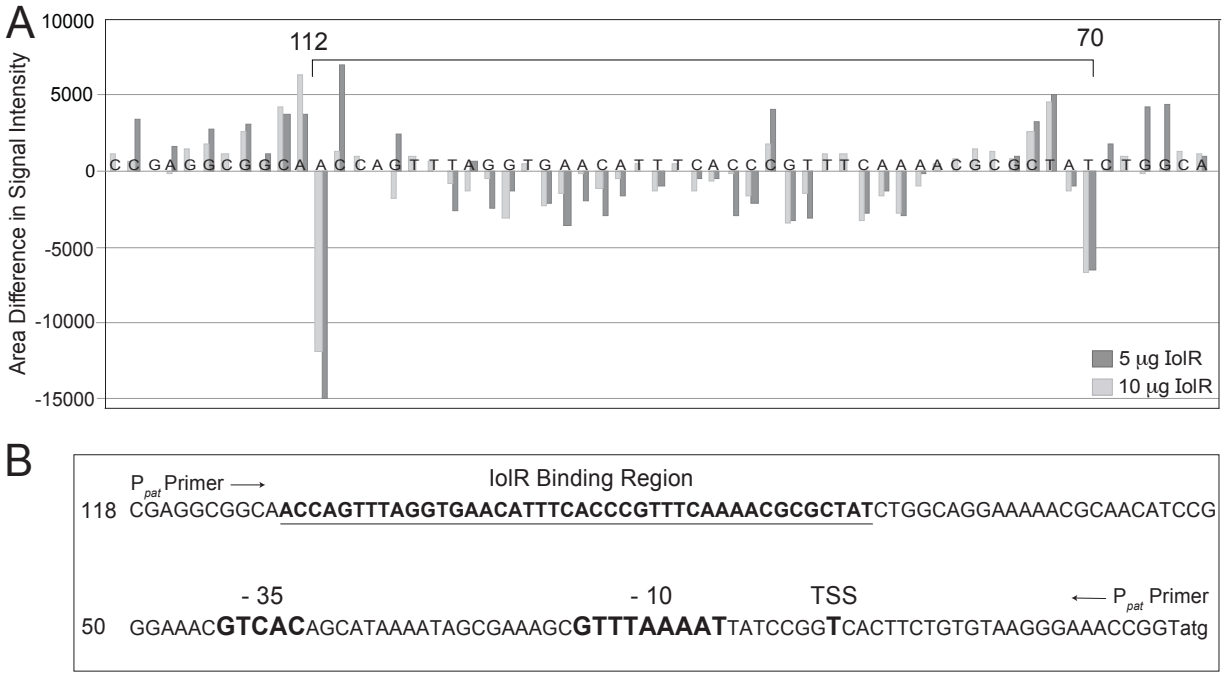

Figure 3.8. IolR protein binds *pat* promoter at position -112 to -70. (A) DNA-footprinting analysis by capillary electrophoresis was used to define the IolR binding region on the *pat* promoter (P_{pat}). On the graph, negative values represent an area of protection, bars indicate concentration of IolR protein (5 μg dark gray, 10 μg light gray), and bar heights represent the area difference between the IolR sample and the negative control (BSA). DNA-footprinting was performed and analyzed in two independent experiments. (B) Work by Kroger *et al.* (34) was used to identify the *pat* transcriptional start site (TSS).

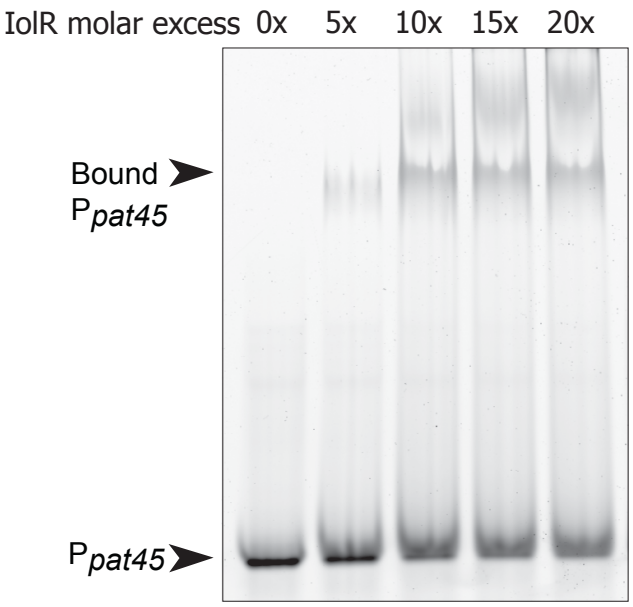

Figure 3.9. IolR protein binds to the P_{pat} 45-nt probe. Electrophoretic mobility shift assays were used to validate the binding region identified by footprinting experiments. A 6FAM-5'-labeled 45-nt probe of the *pat* promoter region, P_{pat} (166 nM), corresponding to the identified binding region was incubated with increasing concentrations of IolR protein. Protein concentration shown is in molar excess to probe. EMSAs were performed in triplicate.

The absence of IolR impairs growth on 10 mM acetate. Growth of an *iolR*::*cat*$^+$ strain was inhibited on 10 mM acetate, with a growth rate three times slower (doubling time = 36 h; Fig. 3.10A, solid triangles) than that of strain carrying the wild-type *iolR* allele (doubling time = 11 h; Fig. 3.10A, solid squares). Growth of the *iolR*::*cat*$^+$ strain was restored when *iolR* was expressed ectopically (Fig. 3.10A, open triangles), indicating the growth defect was due to the absence of IolR. A similar growth defect was reported for an *iolR* mutant strain of *C. glutamicum*, but this observation was not investigated (33). No growth differences were observed for the *iolR*$^+$ *pat*$^+$, *iolR*::*cat*$^+$, or *pat*::MudJ strains when grown on 50 mM acetate or glycerol (Fig. 3.5C, D).

Because the observed phenotype on 10 mM acetate correlated with lower levels of *pat* expression, we hypothesized that increases in the expression of *pat* under the control of an IolR-independent promoter would restore growth of the *iolR*::*cat*$^+$ strain on 10 mM acetate. Indeed, the *iolR*::*cat*$^+$ strain grew almost as well as the *iolR*$^+$ strain when *pat* was expressed *in trans* (Fig. 3.10B, inverted triangles). An increase in the level of inducer (10-100 μM) compromised growth of the *iolR*::*cat*$^+$ / p*pat*$^+$ strain. The negative effect of higher *pat* expression was not surprising since increased Pat levels are known to increase the level of acetylated, inactive Acs (8).

The phenotype of the* iolR *strain is caused by an imbalance in the Pat:CobB ratio, which affects Acs activity. In *S. enterica*, Pat and CobB control Acs activity (6). Given that *pat* expression decreased in the *iolR*::*cat*$^+$ strain, we hypothesized that the absence of IolR created an imbalance in the Pat:CobB ratio that favored Pat activity, thus a decrease in Acs activity due to Acs acetylation. We reasoned that such loss of Acs activity could be counteracted in several ways. Firstly, inactivation of *pat* in the *iolR* strain would block Acs acetylation, and should restore growth. Indeed, the poor growth of the *iolR* strain on 10 mM acetate (Fig. 3.10C, solid

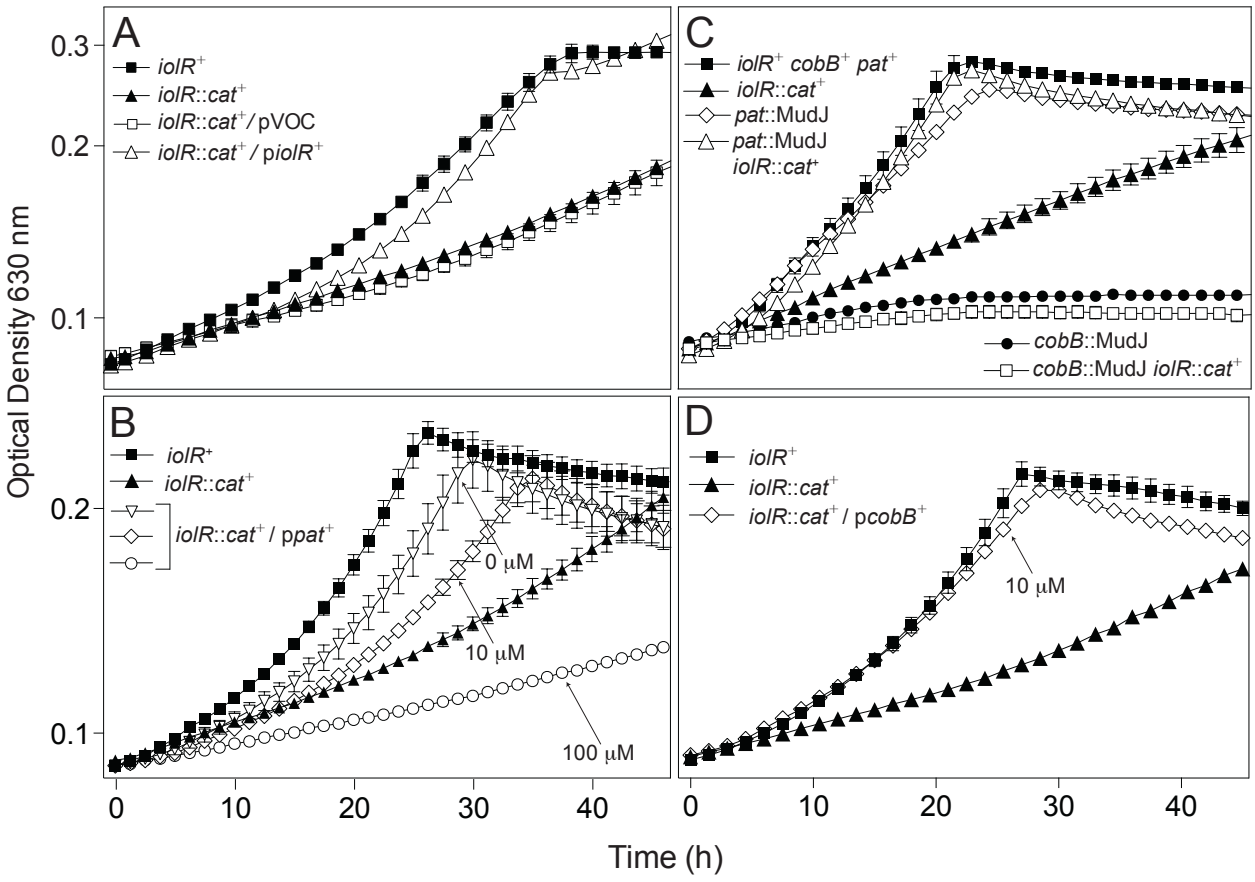

Figure 3.10. An *iolR* strain has a growth defect on 10 mM acetate. Growth of *S. enterica* strains was examined in NCE minimal medium containing 10 mM acetate. Expression of *iolR* was induced using 100 μM *L*-(+)-arabinose, *cobB* expression was induced with 10 μM *L*-(+)-arabinose, and *pat* expression was induced with various concentrations of inducer, as indicated. Growth curves were performed using a Powerwave XS2 microplate reader (Bio-Tek Instruments) at 37°C with shaking in triplicate in three independent experiments. Strains analyzed: *iolR*$^+$ (JE6583), *iolR*::*cat*$^+$ (JE10713), *iolR*::*cat*$^+$ / pVOC (JE16934), *iolR*::*cat*$^+$ / p*iolR*$^+$ (JE16935), *pat*::MudJ (JE7449), *pat*::MudJ *iolR*::*cat*$^+$ (JE10714), *cobB*::MudJ (JE2845), *cobB*::MudJ *iolR*::*cat*$^+$ (JE14972), *iolR*::*cat*$^+$ / p*pat*$^+$ (JE18927), and *iolR*::*cat*$^+$ / p*cobB*$^+$ (JE18891). Error bars represent standard deviation. pVOC, vector-only control.

triangles) was reversed when *pat* was inactivated (Fig. 3.10C, open triangles). As expected, a *cobB* strain failed to grow on 10 mM acetate because acetylated Acs could not be reactivated by deacetylation (Fig. 3.10C, solid circles). Although inactivation of *iolR* presumably reduced Pat levels in the *cobB* strain (by lowering the expression of *pat*), the reduced level was apparently sufficient to keep Acs acetylated (i.e., inactive), thus growth was not restored (Fig. 3.10C, open squares). Additionally, inactivation of *pat* in an otherwise wild-type background had minimal effect on growth likely caused by an excess of Acs activity due to CobB deacetylation (2).

Secondly, if the net result of the change in Pat:CobB ratio in the *iolR*::*cat*$^{+}$ strain was an increase in acetylated, inactive Acs, an increase the level of CobB sirtuin deacetylase in the *iolR*::*cat*$^{+}$ strain would restore Acs to its active, deacetylated state, and consequently growth on 10 mM acetate would occur. This prediction was confirmed, as shown in figure 3.10D.

Thirdly, if the growth defect of the *iolR*::*cat*$^{+}$ strain on 10 mM acetate was caused by a change in the level of Acs activity, it followed that overexpression of *acs* in the Δ*acs iolR*::*cat*$^{+}$ strain would restore growth on 10 mM acetate. Results obtained using control strains are shown and as expected, the Δ*acs* strain failed to grow on 10 mM acetate (Fig. 3.11A, inverted triangles), and growth was restored by expression of *acs in trans* (Fig. 3.11A, circles). Shown in figure 3.11B is the effect of ectopic synthesis of Acs^{WT} in the Δ*acs iolR*::*cat*$^{+}$ strain. Wild-type growth of the Δ*acs iolR*::*cat*$^{+}$ strain on 10 mM acetate was observed upon induction of *acs* expression (20 μM *L*-(+)-arabinose) (Fig. 3.11B, circles). Unsurprisingly, excessive levels of Acs (100 μM *L*-(+)-arabinose) (Fig. 3.5, open squares) had a deleterious effect on growth, as reported elsewhere (8).

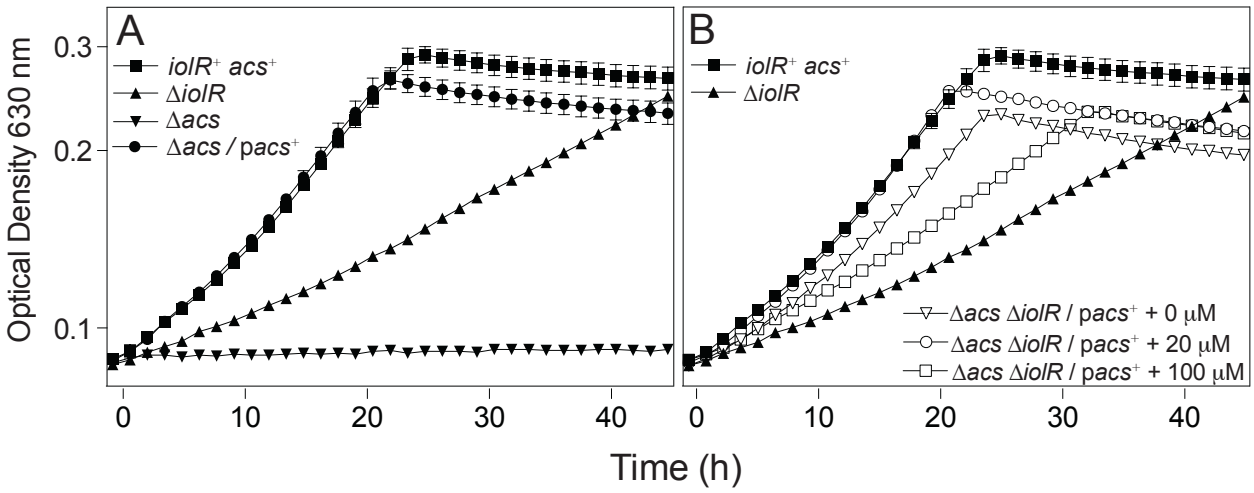

Figure 3.11. Induction of *acs* expression restores growth of an *iolR* strain on 10 mM acetate. Growth of an *iolR*::*cat*$^+$ strain containing *acs* expressed ectopically under the control of an *L*-(+)-arabinose-inducible promoter was examined in minimal medium containing acetate (10 mM). Control strains are shown in (A). The effects of *acs* induction are shown in (B). Growth curves were performed using a Powerwave XS2 microplate reader (Bio-Tek Instruments) at 37°C with shaking in triplicate in three independent experiments. Strains analyzed: *iolR*$^+$ (JE6583), *iolR*::*cat*$^+$ (JE10713), Δ*acs* (JE7758), Δ*acs* / p*acs*$^+$ (JE9912), Δ*acs iolR::cat*$^+$ / p*acs*$^+$ (JE16596). Expression of *acs* was induced with 0 μM (open triangles), 20 μM (open circles), or 100 μM (black circles (A), open squares (B)). Error bars represent standard deviation.

Activity of Acs is decreased in an* iolR*::*cat$^+$ *strain. If the growth phenotype of the *iolR*::*cat*$^+$ strain on acetate was due to lower Acs activity, we should be able to detect differences in Acs activity in cell-free extracts. Indeed, a reproducible and statistically significant reduction (~25%) in Acs activity was found in cell-free extracts of the *iolR*::*cat*$^+$ strain relative to extracts of the *iolR*$^+$ strain (Fig. 3.12).

***IolR controls expression of* acs *and* cobB.** Since ectopic expression of *acs* restored growth of the *iolR*::*cat*$^+$ mutant, we surmised that *acs* expression was lower in the mutant than in the wild-type strain. To address this possibility we used an *acs-lacZ*$^+$ reporter fusion to determine whether IolR was also involved in the regulation of *acs* in *S. enterica.* Since alterations in *pat* expression were likely to affect CobB levels, we also used a *cobB-lacZ*$^+$ fusion to assess the effect of the absence of IolR on *cobB* expression. Data obtained from experiments with the above-mentioned transcriptional reporters support the idea that IolR somehow activated expression of both genes (Fig. 3.13). In the absence of IolR, expression of *acs* (Fig. 3.13A) and *cobB* (Fig. 3.13B) was reduced on average by 40% (*acs*) or 22% (*cobB*), respectively. The effect of IolR on *acs* and *cobB* expression was confirmed using qRT-PCR, and showed a >2-fold and >3-fold down-regulation, respectively, of the transcripts in an *iolR*::*cat*$^+$ strain compared to wild type (Fig. 3.13C). At present, it is unclear whether the effect of IolR on Acs and CobB levels is direct or indirect.

Glucose differentially affects* pat, cobB, *and* acs *expression. Due to the previously established role of the catabolite repressor protein (Crp) in the regulation of the *E. coli pat* homologue (*pka*) (15) we examined the effect of catabolite repression on genes encoding the RLA system, ± *iolR*.

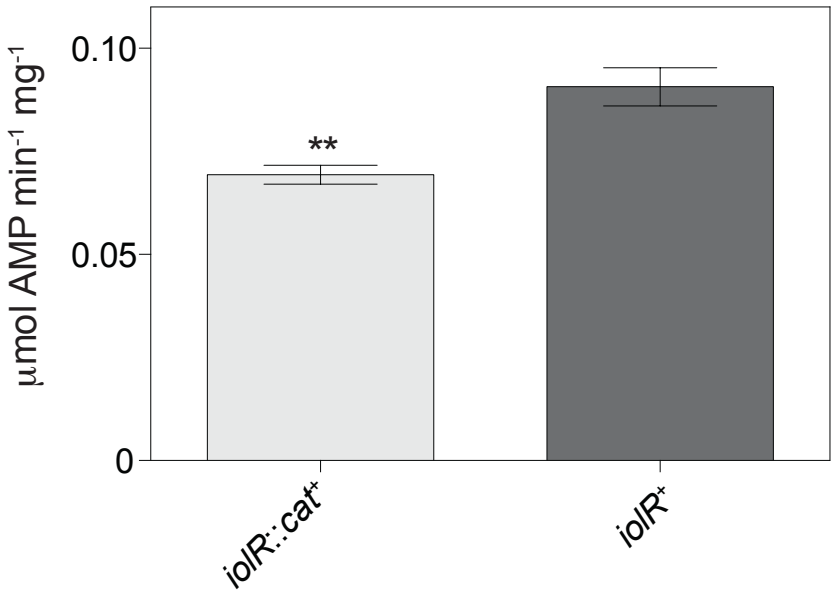

Figure 3.12. Activity of acetyl-CoA synthetase (Acs). The activity of Acs from whole cell extracts of an *iolR*$^+$ or *iolR*::*cat*$^+$ strain grown on acetate (10 mM) was measured using a coupled NADH-consuming spectrophotometric assay (36). The strains analyzed: *iolR*$^+$ (JE6583) and *iolR*::*cat*$^+$ (JE10713). Samples were analyzed in triplicate. Error bars represent standard deviation. Unpaired t test gave a P value of 0.002.

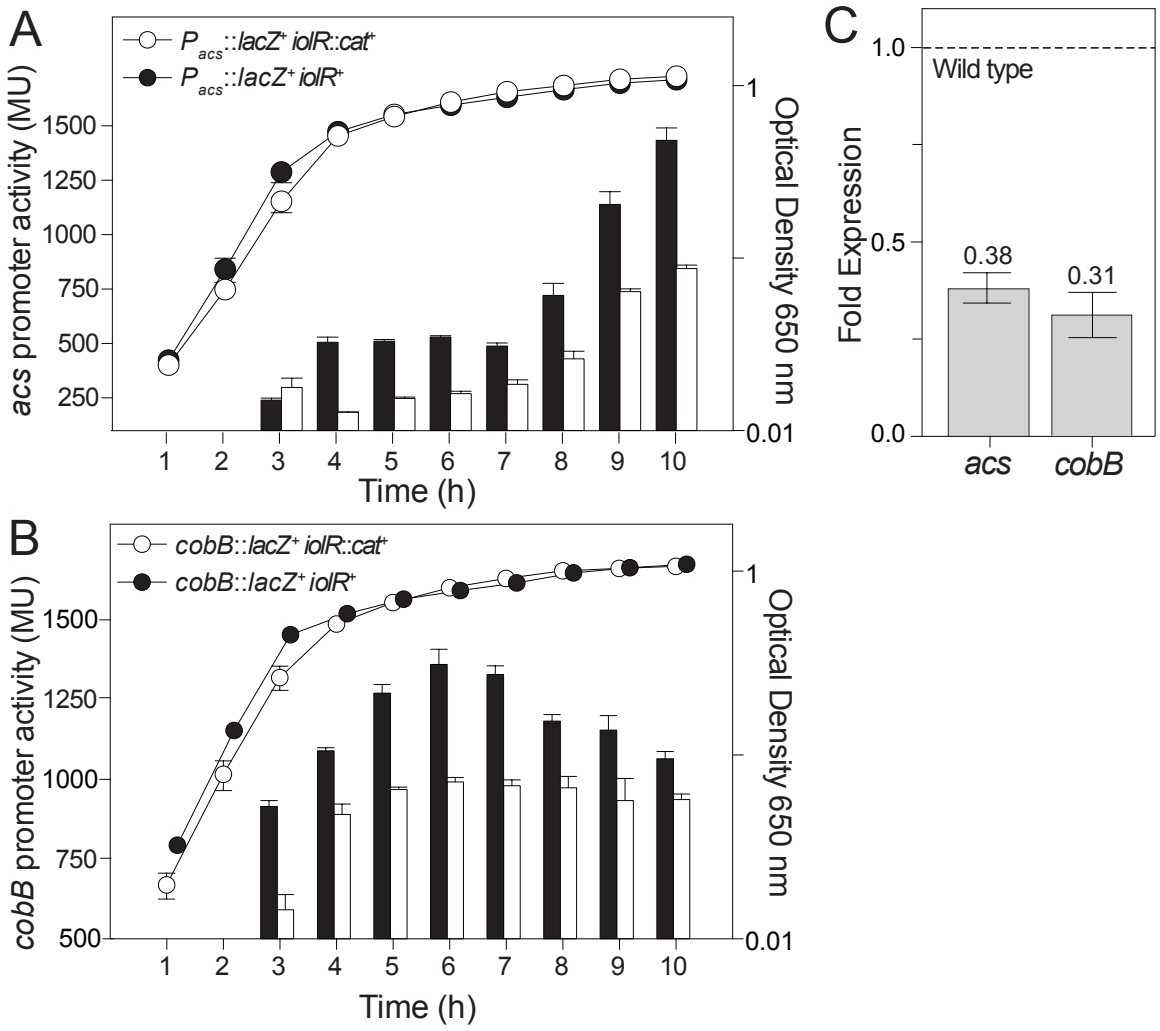

Figure 3.13. IolR controls expression of *acs* and *cobB*. Activity of *acs-lacZ*$^+$ and *cobB-lacZ*$^+$ reporters was assessed in backgrounds ± *iolR* to measure P_{acs} and P_{cobB} activity. Cultures were grown at 37°C in NB medium (A, B). Optical density (650 nm) and β-galactosidase activity (420 nm) were measured hourly. The data were obtained from individual cultures performed in triplicate. Error bars represent standard deviation. Strains analyzed: *cobB*::MudJ (JE2845), *cobB*::MudJ *iolR*::*cat*$^+$ (JE14972), pACS3 P_{acs}^+ (JE4637), and *iolR*::*cat*$^+$ / pACS3 P_{acs}^+ (JE14962). C. qRT-PCR showed a 2.6-fold down-regulation in *acs* activity, and a 3-fold decrease in *cobB* activity in an *iolR* strain relative to the *iolR*$^+$ strain. Wild-type transcript level is set at 1, indicated by the dashed line. Error bars represent standard deviation.

Expression of *pat* in cells grown in NB + glucose medium was reduced ~ 2-fold relative to the expression of *pat* in cells grown in NB lacking glucose (Fig. 3.14, compare black bars). This suggested that *pat* expression was subjected to catabolite repression, an idea that was further explored. Regardless of the presence of glucose in the medium, the absence of IolR reduced *pat-lacZ*$^{+}$ expression 30-40% (Fig. 3.14A). The absence of IolR had a small but reproducible negative effect (~20%) on *cobB* expression in the absence of glucose, an effect that was magnified to ~40% when glucose was added (Fig. 3.14B). Significantly, in contrast to *pat* expression, the expression of *cobB* increased ~30% when glucose was added, suggesting that unlike *pat,* expression of *cobB* was not subject to catabolite repression (Fig. 3.14B, black bars).

In *E. coli,* Crp, controls the expression of *acs* (37). Consistent with the idea that in *S. enterica* *acs* expression is controlled by catabolite repression, transcription of *acs* was reduced 80% when glucose was present (Fig. 3.14C, compare black bars). IolR function also appeared to be important for the activation of *acs* in medium devoid of glucose, with ~50% reduction in *acs* expression in the *iolR*::*cat*$^{+}$ strain relative to the wild-type (Fig 3.14C, NB medium). In the presence of glucose, expression of *acs* ± *iolR* was very similar (Fig. 3.14C, NB + glucose).

Crp activates* pat *expression. The effect of Crp on *pat* expression was examined in cultures grown in NB + ribose (10 mM). P_{pat} activity in the Δ*iolR crp*::*cat*$^{+}$ strain was 2.5-fold lower than the P_{pat} activity measured in a strain containing wild-type *iolR* and *crp* alleles (Fig. 3.15). This decrease in activity was similar to the one measured in a strain lacking *iolR*, and was restored when *crp* was provided *in trans*. P_{pat} activity was slightly lower in the Δ*iolR crp*::*cat*$^{+}$ strain compared to strains lacking only *crp* or *iolR* (Fig. 3.15). Collectively, the data indicated that Crp was required for wild-type levels of *pat* expression in *S. enterica*. Pat-dependent acetylation of Crp was tested; however, the data indicate that Pat does not acetylate Crp (Fig. 3.4).

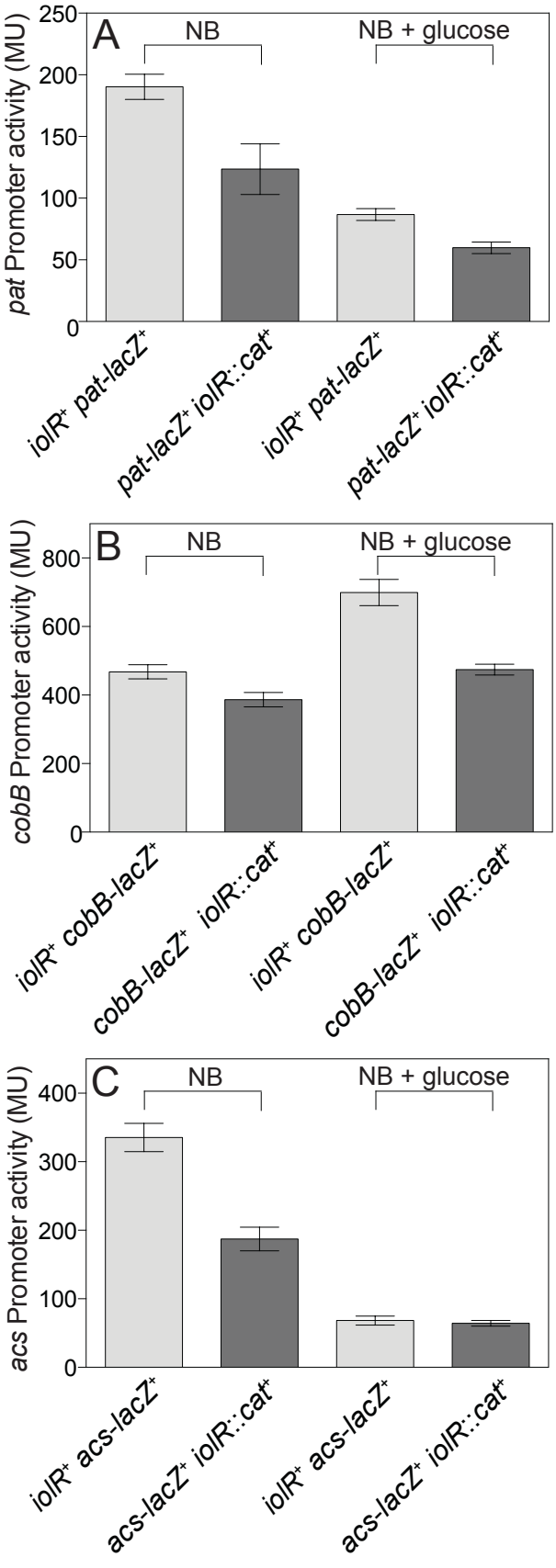
A
NB
NB + glucose
pat Promoter activity (MU)
250
200
150
100
50
0
iolR+ pat-lacZ+
pat-lacZ+ iolR::cat+
iolR+ pat-lacZ+
pat-lacZ+ iolR::cat+
B
NB
NB + glucose
cobB Promoter activity (MU)
800
600
400
200
0
iolR+ cobB-lacZ+
cobB-lacZ+ iolR::cat+
iolR+ cobB-lacZ+
cobB-lacZ+ iolR::cat+
C
NB
NB + glucose
acs Promoter activity (MU)
400
300
200
100
0
iolR+ acs-lacZ+
acs-lacZ+ iolR::cat+
iolR+ acs-lacZ+
acs-lacZ+ iolR::cat+

Figure 3.14. Glucose differentially controls expression of *pat*, *cobB*, and *acs*. Cultures were grown at 37°C in NB medium ± glucose (10 mM). Optical density (650 nm) and β-galactosidase activity (420 nm) were measured at mid-log phase (OD_{650} ~0.7) to assay for *pat* and *cobB* promoter activity in a *pat-lacZ*$^+$ or *cobB-lacZ*$^+$ strain backgrounds ± *iolR*. The data are the average of two independent experiments from individual cultures performed in triplicate. Strains analyzed: *pat*::MudJ (JE7449), *pat*::MudJ *iolR*::*cat*$^+$ (JE10714), *cobB*::MudJ (JE2845), *cobB*::MudJ *iolR*::*cat*$^+$ (JE14972), pACS3 P_{acs} (JE4637), and *iolR*::*cat*$^+$ / pACS3 P_{acs} (JE14962). Error bars represent standard deviation.

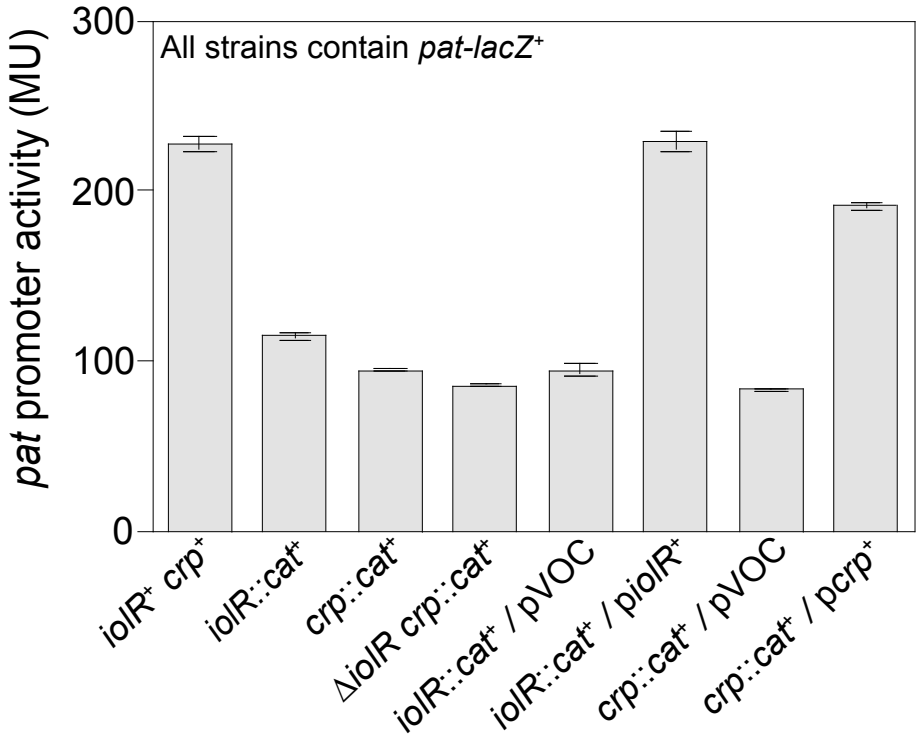

Figure 3.15. Crp activates *pat* expression. Cultures were grown at 37°C in NB medium with ribose (10 mM). Optical density (650 nm) and β-galactosidase activity (420 nm) were measured at the peak of *pat* expression (OD_{650} ~0.7) to assay for *pat* promoter activity in a *pat-lacZ*$^+$ strain background. Plasmids were induced with *L*-(+)-arabinose (100 μM). The data presented are the average of two independent experiments from individual cultures performed in triplicate. Strains analyzed: *pat*::MudJ (JE7449), *pat*::MudJ *iolR*::*cat*$^+$ (JE10714), *pat*::MudJ *crp*::*cat*$^+$ (JE16743), *pat*::MudJ Δ*iolR crp*::*cat*$^+$ (JE16744), *pat*::MudJ *iolR*::*cat*$^+$ / pVOC (JE10727), *pat*::MudJ *iolR*::*cat*$^+$ / pIOLR1 (JE10728), *pat*::MudJ *crp*::*cat*$^+$ / pVOC (JE16771), and *pat*::MudJ *crp*::*cat*$^+$ / p*crp*$^+$ (JE17322). Error bars represent standard deviation. pVOC, vector-only control.

DISCUSSION

In* S. enterica, *IolR regulates the RLA system. The chief finding from the studies reported herein is that the IolR protein controls and integrates the expression of *pat*, *cobB*, and *acs* (Figs. 2, 8). Although we do not yet understand the molecular details of how IolR integrates the expression of the above-mentioned genes, collectively our *in vivo* genetic evidence supporting this claim is compelling (Figs. 5, 6). Furthermore, *in vitro* data obtained support the conclusion that IolR directly interacts with the *pat* promoter (Figs. 3, 4). Whether or not the effect of IolR on *cobB* and *acs* expression is direct remains to be determined.

IolR function is needed for growth on 10 mM acetate, which require RLA and Acs. IolR function is necessary for optimal growth on 10 mM acetate (Fig. 3.10) and the growth defect of an *iolR* strain suggests that IolR regulation of *pat* and *cobB* impacts the levels of Acs activity in the cell (Fig. 3.13). This conclusion is supported by data showing that the ectopic expression of *acs* complements growth of an *iolR* strain (Fig. 3.11). The subtle effects of the absence of IolR on *pat, cobB,* and *acs* expression make it difficult to determine the precise magnitude of the changes in Pat, CobB and Acs protein levels, and in the case of Acs there is also a need to distinguished between acetylated vs. non-acetylated protein. Our attempts to gain insights into these changes using Western blot analysis were unsuccessful due to the lack of required sensitivity to define the magnitude of the predicted changes (data not shown). However, the lower levels of Acs activity present in cell-extracts of the *iolR* strain (Fig. 3.12) support our conclusions.

The differentially repressive effect of glucose on* pat *and* cobB *expression is needed to ensure sufficient activation of acetate by Acs. The differential effect that glucose has on the expression of *pat* and *cobB* (Fig. 3.14) can be explained by considering the acetogenic nature of

glucose. During glucose catabolism, excess acetyl-CoA is diverted through the acetate kinase (AckA) / phosphotransacetylase (Pta) pathway yielding ATP via substrate-level phosphorylation and releasing CoA, which is needed by the pyruvate dehydrogenase to make more acetyl-CoA. In *S. enterica,* the assimilation of glucose-derived acetate is known to require the functions of AckA/Pta and Acs. Notably, during growth on glucose less Acs is made because Crp cannot fully activate *acs* expression when cAMP levels are low (38). One plausible way the cell can ensure that the limited amount of Acs made by the cell in the presence of glucose supplies enough acetyl-CoA to support growth is to lower the expression of *pat* while increasing *cobB* expression (Fig. 3.14). By so doing, less Acs becomes acetylated, and whatever Acs is acetylated is reactivated by the higher levels of CobB deacetylase made under these conditions. Given that *pat* expression is reduced whenever IolR or Crp are not made, it was surprising to find out that the absence of both regulators did not have an additive effect on *pat* expression (Fig. 3.15). This result could simply reflect the basal level of *pat* expression, or possibly, a more complex regulatory network in which Crp affects regulation of *iolR.* Such an idea would not be unprecedented, since in *B. subtilis*, the *iol* operon, including *iolR*, is under the control of catabolite repression (39).

Why does IolR activate expression of the RLA system? The dual regulatory role of IolR as a repressor of *iol* genes and an activator of *pat*, *cobB*, and *acs* is intriguing. The ability of IolR to function as an activator is not unprecedented. A report in *C. glutamicum* demonstrated that IolR activates expression of *pck* (encodes phosphoenolpyruvate carboxykinase) (33). IolR also regulates *srfJ*, a type-III secretion effector protein, in *Salmonella* (40), a result that is not surprising as *srfJ* lies within the *iol* genomic island, which is regulated by IolR.

Under conditions where acetate and *myo*-inositol are simultaneously present in the environment, the cell needs to integrate their metabolism. In thinking about this issue one must consider that acetate and *myo*-inositol are catabolized at substantially different rates, as acetate enters central metabolism as soon as it is converted into acetyl-CoA. In contrast, *myo*-inositol degradation requires the generation of a signal that upon binding to IolR lifts repression of the *iol* genes and synthesis of *myo*-inositol-degrading enzymes can occur. Generation of the signal needed to transcribe the *iol* genes is apparently an extensive process (Fig. 3.5A, comparing the differences in lag phases between the $iolR^+$ and *iolR* strains). The use of IolR to integrate *myo*-inositol and acetate metabolism would be an efficient way to generate as much acetyl-CoA for anabolic purposes as possible while maintaining the capability of modulating the activity of the RLA system for the purpose of controlling the level of Acs activity.

Is* myo-*inositol utilization regulated by RLA? Recently, the total population of acetylated proteins (acetylome) of the *myo*-inositol utilizing bacteria *B. subtilis* and *Erwinia amylovora* were reported (9, 10). Notably, two enzymes involved in the degradation of *myo*-inositol, the malonate semialdehyde dehydrogenase (IolA) and carbohydrate kinase (IolC) were amongst the acetylated proteins identified. It is unclear whether the activity of IolA and/or IolC is controlled by RLA in either organism or in *S. enterica*. If any Iol proteins are under RLA control, it could provide a link between IolR regulation of RLA and RLA involvement in *myo*-inositol utilization.

MATERIALS AND METHODS

Culture media and chemicals. Nutrient broth (NB, Difco) containing NaCl (85 mM) was used as rich medium. The minimal medium used was no-carbon essential (NCE) minimal medium (41) containing $MgSO_4$ (1 mM), Wolfe's trace minerals (1x) (42), and carbon source

[acetate (10 or 50 mM), glycerol (22 mM), or *myo*-inositol (50 mM)]. Antibiotics were added at following concentrations: tetracycline, 20 μg ml^{-1}; chloramphenicol 20 μg ml^{-1}; kanamycin, 50 μg ml^{-1}; and ampicillin, 100 μg ml^{-1}. When added, 5-bromo-4-chloro-3-indolyl-β-D-galactopyranoside (X-gal) was present at 40 μg ml^{-1} and the calcium chelator ethyleneglycol tetraacetic acid (EGTA) was present at 10 mM. Chemicals were purchased from Sigma-Aldrich.

Bacterial strains. All strains studied were derivatives of *S. enterica* serovar Typhimurium strain LT2 (unless noted, Table 3.1). Tn*10*d(*tet*$^+$) refers to the transposase-defective mini-Tn*10* (Tn*10*Δ*16*Δ*17*) (31); MudJ (refers to MudI1734) was used to generate a strain carrying the MudJ (*kan*$^+$ *lacZ*$^+$) element under the control of the *pat* promoter (29). The MudJ element inactivated the gene at the same time that it fused the expression of *lacZ* to the promoter of choice, either P_{pat} or P_{cobB}. All primers used in this study are listed in Table 3.2 (IDT, Coralville, Iowa).

Strains carrying a deletion of *iolR* or *crp* were constructed following described protocols (43). To construct the *iolR* and *crp* deletions in strain JE7449 (*pat*::MudJ), P22 phage was propagated using strain JE10713 (*iolR*::*cat*$^+$), or strain JE16466 (*crp*::*cat*$^+$) and used to transduce strain JE7449 to chloramphenicol resistance. Bacteriophage P22-mediated transductions were performed as described (44), using the high-frequency general transducing mutant of bacteriophage P22 HT105/1 *int-210* (45). Phage-free, phage-sensitive transductants were isolated on non-selective green indicator plates as described (46).

Plasmid construction. Plasmids are listed in Table 3.1. To construct the arabinose-inducible *iolR* plasmid (pIOLR1), the 834-bp *iolR* allele from *S. enterica* and its ribosome-binding site (849 bp total) were amplified and inserted pBAD30 (30) using primers *Eco*RI and *Xba*I restrictions sites (pBAD30 *iolR* 5' and pBAD30 *iolR* 3'). Primers were synthesized at the Biotechnology Center of the University of Wisconsin-Madison. To construct the plasmid for the

Table 3.2. Primers used in this study

Primer Name	Primer Sequence
Strain construction	
iolR – 5'DEL	5'-TGCTAATATGGTTATTTACGAAATTTTCGTTCTATTAGAGTATCATGCATGGTGTAGGCTGGAGCTGCTTC-3'
iolR – 3'DEL	5'- TTCACCACAATGCCGATGATCGCTAAATACGATCATCGGCTTGTTTTTTTACATATGAATATCCTCCTTAG-3'
crp – 5'DEL	5'-GCTCTGGAGACAGCTTATAACAGAGGATAACCGCGCATGGTGTAGGCTGGAGCTGCTTC-3'
crp – 3'DEL	5'-AAATGGCGCATGATAAAACGCGCCATTCTGACGGAATTACATATGAATATCCTCCTTAG-3'
Cloning	
pBAD30 *iolR* 5'	5'-AAAAAAGAATTCATTAGAGTATCATGCATGTCTAAACAT-3'
pBAD30 *iolR* 3'	5'-AAAAAATCTAGATTACTCCGTCGCCAGCGCCAGTGAAA-3'
pTEV6 *iolR* 5'	5'-AAAAAAGGTACCATGTCTAAACATCAAACTCAACT-3'
pTEV6 *iolR* 3'	5'-AAAAAAAAGCTTTTACTCCGTCGCCAGCGCCA-3'
pBAD30 *crp* 5'	5'-GAATTCGCTAGCCCAAAAAAACGG-3'
pBAD30 *crp* 3'	5'-AAGCTTGGCTGTTTTGGCGGATGA-3'
pTEV16 *crp* 5'	5'-NNGCTCTTCNAGCATGGTGCTTGGCAAACCGCAAACAG-3'
pTEV16 *crp* 3'	5'-NNGCTCTTCNTTATTAACGGGTGCCGTAGACGACGA-3'
EMSA and DNA footprinting	
P_{pat} 150 FAM [a]	5'-CGAGGCGGCAACCAGTTTA-3'
P_{pat} 150 Rev	5'-CATACCGGTTTCCCTTACACA-3'
P_{iolR} 175 FAM	5'-CTGATCCTGTCGCATTTATG-3'
P_{iolR} 175 Rev	5'-CATGCATGATACTCTAATAGAACG-3'
P_{pat} 45 FAM	5'-CAACCAGTTTAGGTGAACATTTCACCCGTTTCAAAACGCGCTATCT-3'
P_{pat} 45	5'-CAACCAGTTTAGGTGAACATTTCACCCGTTTCAAAACGCGCTATCT-3'
P_{pat} 45 Rev	5'-AGATAGCGCGTTTTGAAACGGGTGAAATGTTCACCTAAACTGGTTG-3'
P_{pat} 382 FAM	5'-CCCGAAGCACGTAAAATGTT-3'
P_{pat} 382 Rev	5'-TTCATTGATGCGCCAATCAC-3'
qRT-PCR	
acs qRT-PCR F'	ACCGACTCACTGCCAAAAAC
acs qRT-PCR R'	CTTCGAGCAGTTTCTCCACC
cobB qRT-PCR F'	CTGTCGATGGCGGATATTTT
cobB qRT-PCR R'	GGCCGTAGTGCTTCTCTTCA
pat qRT-PCR F'	GATTTTGACGCGCTTATGGT
pat qRT-PCR R'	CTGAATAGCCGTCTTGCCTC
gyrA qRT-PCR F'	AACACCCATGACACCATCCT
gyrA qRT-PCR R'	GGTGATACGTTCGTTGGCTT

[a] fluorophore 6-carboxyfluorescein (6FAM)

overexpression of *iolR* (pIOLR3), the gene was inserted into plasmid pTEV6 (28) using *Kpn*I and *Hin*dIII restriction sites (pTEV6 *iolR* 5') and (pTEV6 *iolR* 3'). The resulting overexpression plasmid, pIOLR3, directed the synthesis of IolR protein with an *N*-terminal hexahistidine-maltose-binding protein (His_6-MBP) tag cleavable by tobacco etch virus (TEV) protease (47). The polymerase incomplete primer extension (PIPE) cloning method (48) was used to construct the arabinose-inducible plasmid for the expression of *crp* (pCRP2). The 633-bp *crp* gene from *S. enterica* and its ribosome-binding site (643-bp total) were amplified using primers (pBAD30 *crp* 5') and (pBAD30 *crp* 3'). Plasmid pTEV5 (28), which directs the synthesis of the protein with a cleavable *N*-terminal hexahistidine tag, was engineered with BspQI restriction sites (pTEV16, C. M. VanDrisse & J. C. Escalante-Semerena, unpublished data, (49)), and used for overexpression of CRP, using primers (pTEV16 *crp* 5') and (pTEV16 *crp* 3') (pCRP3). DNA sequencing was used to verify the cloned sequences in all plasmids.

Isolation of Tn10d(tet$^+$) insertion in iolR. A pool of ~100,000 *S. enterica* strains each assumed to contain one Tn*10*d(*tet*$^+$) element randomly inserted in the chromosome was generated as described (50). A P22 lysate grown on this pool of strains was used to transduce recipient strain JE7449 (*metE ara pat*::MudJ) to tetracycline resistance (Tc^R) on NB agar plates containing X-gal and EGTA. Colonies displaying altered coloration were freed of phage and P22 phage lysates were generated to use as donors in crosses with the parental JE7449 strain. The location of the insertion was determined in the reconstructed strains by sequencing the DNA flanking the Tn*10*d(*tet*$^+$) element using a PCR-based protocol with degenerate primers (51). DNA sequencing was performed using BigDye® Terminator v3.1 protocols (Applied Biosystems).

Growth studies. Cultures were grown overnight at 37°C in NB and used to inoculate medium with (5% v/v) in a volume of 200 µl per well of a 96-well plate. NCE minimal medium containing $MgSO_4$ (1 mM), Wolfe's trace minerals (1x), and carbon source [acetate (10 mM, 50 mM), glycerol (22 mM), or *myo*-inositol (50 mM)] was used. Plasmids were induced with *L*-(+)-arabinose, as described. Plates were incubated at 37°C in a Powerwave Microplate Reader (Bio-Tek Instruments). Data were analyzed using Prism v6 (GraphPad) software.

β-Galactosidase assays. β-Galactosidase activities were determined as described (52). Three independent overnight cultures were grown in NB + ampicillin, sub-cultured (1:100, v/v) into 200 ml of medium + ampicillin and induced with 100 µM *L*-(+)-arabinose. Cultures were grown at 37°C in NB, NB + ribose (10 mM), NB + glucose (10 mM), acetate (10 mM), or *myo*-inositol (55 mM) medium. Acetate cultures were inoculated with 2.5% (v/v) of overnight culture.

qRT-PCR. Cultures of strains JE10713 (*iolR*::*cat*$^+$) and JE6583 (*iolR*$^+$) were grown in NB to an OD_{600} of 0.6. RNA extraction was performed as described (53). cDNA synthesis was performed using iScript cDNA synthesis kit (Bio-Rad). qRT-PCR reactions were performed using Fast SYBR® Green Master Mix (Thermo Fischer) and a 7500 Fast Real-Time PCR System (Applied Biosystems).

Overproduction and purification of proteins. Plasmid pIOLR3 and pCRP3 were transformed into *E. coli* C41(λDE3), and overnight cultures sub-cultured 1:100 (v/v, inoculum/medium) into 4 L of LB and ampicillin (150 µg ml^{-1}). Cultures were grown at 37°C with shaking to an OD_{600} of 0.6, induced with isopropyl-β-D-thiogalactopyranoside (IPTG, 1 mM), and shaken overnight at 28°C. Cells were harvested by centrifugation at 8,394 × *g* for 15 min at 4°C. Cell lysate was re-suspended in bind buffer A [4-(2-hydroxyethyl)-1-piperazineethanesulfonic acid (HEPES) buffer (50 mM, pH 7.5), NaCl (500 mM) and imidazole (20 mM)] plus lysozyme (1 mg ml^{-1}),

DNase I (25 μg ml^{-1}) and protease inhibitor phenylmethanesulfonyl fluoride (PMSF, 0.5 mM)]. Cells were lysed by sonication for 2 min (2 s, 50% duty, setting 4) in 30 s intervals on ice using a 550 Sonic Dismembrator (Fisher Scientific). Clarified cell lysates were obtained after centrifugation for 45 min at 4°C at 43,667 × *g*.

IolR Purification: Protein was resolved using ÄKTA FPLC system (GE Healthcare) equipped with a HisTrap 10 mL column. After loading the protein, the column was washed with 7 column volumes (CV) of bind buffer, followed by 10 CV of wash buffer [HEPES buffer (50 mM, pH 7.5), NaCl (500 mM), and imidazole (40 mM)]. rTEV-cleavable His_6-MBP tagged IolR eluted off the column using a 30 min linear gradient of elution buffer [HEPES buffer (50 mM, pH 7.5), NaCl (500 mM), and imidazole (500 mM)]. To cleave the His_6-MBP tag from IolR, recombinant His_6-TEV protease (rTEV) was purified as described (47), and added to the His_6-MBP-IolR solution containing dithiothreitol (DTT, 1 mM) at a 1:100 [rTEV:tagged IolR] ratio for 3 h at RT. Cleaved IolR protein was dialyzed against dialysis buffer A [HEPES (50 mM, pH 7.5), NaCl (500 mM), and *tris*(2-carboxyethyl)phosphine hydrochloride (TCEP, 0.5 mM)] and EDTA (0.5 mM). The second purification was carried out using the purification described above, and un-tagged IolR eluted off the column during the wash step. IolR was dialyzed in dialysis buffer B [HEPES (50 mM, pH 7.5), NaCl (350 mM), and 20% (v/v) glycerol], followed by dialysis buffer C [HEPES (50 mM, pH 7.5), NaCl (250 mM) and 20% (v/v) glycerol], and lastly into storage buffer A [HEPES (50 mM, pH 7.5), NaCl (150 mM) and 20% (v/v) glycerol]. IolR was drop-frozen in liquid nitrogen and stored at -80°C. The IolR protein was purified to 96% homogeneity as determined using Total Lab v2005 software.

Crp Purification: Protein was loaded onto a 1 ml HisPur™ Ni-NTA resin column (Thermo Scientific) at 4°C, pre-equilibrated with binding buffer. The Ni^+ column was washed first with

bind buffer. Followed by that His_6-tagged Crp eluted in the same buffer system that contained 500 mM imidazole. Protein cleaved with rTEV (1:50 mg:mg ratio) for 3 hr at 25°C, then dialyzed at 4°C against dialysis buffer A, dialysis buffer B, and dialysis buffer C, as described above. Cleaved protein ran over equilibrated column (Crp eluted in flow-through), followed by 10 CV bind buffer, 5 CV of wash buffer, and 5 CV of elution buffer. Protein was dialyzed at 4°C against dialysis buffer E [50 mM HEPES, 400 NaCl (pH 7.0)], dialysis buffer F [50 mM HEPES, and 250 NaCl (pH 7.0)], and storage buffer B [50mM HEPES, 150 NaCl, and 20% glycerol (pH 7.0)]. Crp was drop-frozen in liquid nitrogen and stored at -80°C.

Analytical gel filtration. Experiments were performed at 4°C with a 0.5 ml/min flow rate. Per run, a sample volume of 100 μl containing 150 μg of IolR was injected onto a Superdex 200 HR 10/30 gel filtration column (GE Healthcare) attached to an ÄKTA FPLC system that was equilibrated with HEPES (50 mM, pH 7.5) containing NaCl (500 mM). A calibration standard containing a mixture of molecular masses (Bio-Rad Laboratories; vitamin B_{12} (1.35 kDa), equine myoglobin (17 kDa), chicken ovalbumin (44 kDa), bovine γ-globulin (158 kDa), and thyroglobulin (670 kDa)) was used to generate a standard curve. Analysis was performed using UNICORN v4.11 software. Data were graphed and analyzed using Prism v6 (GraphPad) software. Typical linear regression analyses of the standard curves yielded r^2 values of 0.98.

DNA-binding assays. Electrophoretic mobility shift DNA-binding assays were performed using probes with a fluorophore 6-carboxyfluorescein (6FAM) attached at the 5' prime end. Probes were generated by PCR amplification from the *S. enterica* chromosome. The probe containing the putative promoter region of *pat* (P_{pat}, 150 nt) was generated using a 6FAM-5'-labeled primer P_{pat} 150 FAM and 3' primer P_{pat} 150 Rev. The positive control probe P_{iolR} (175 nt) was generated using primers 6FAM-5'-labeled (P_{iolR} 175 FAM) and 3' primer (P_{iolR} 175 Rev).

The negative control probe P_{argS} (196 nt) was generated using the primers described elsewhere (35). Probes were purified with the Wizard® SV Gel and PCR Clean-Up System (Promega). Reactions (10 μl) contained 6FAM-5'-labeled probe (50 ng), Tris-HCl buffer (50 mM, pH 7.5), KCl (50 mM), $MgCl_2$ (10 mM), EDTA (0.5 mM), glycerol (10%, v/v), and IolR protein [shown in molar excess to probe (2.5-10 pmol)]. Reactions were incubated at 22°C for 45 min and resolved on a Criterion 10% native polyacrylamide gel (BioRad) in 0.5X Tris-borate-EDTA buffer (TBE, pH 8.3; Tris-HCl (45 mM), boric acid (45 mM), EDTA (1 mM)). The signal was detected using a Typhoon Trio+ Variable Mode Imager (GE Healthcare) with ImageQuant v5.2 software.

DNA-footprinting analysis. The *pat* promoter (P_{pat}) was amplified from *S. enterica* genomic DNA using 6-FAM-5'-labeled primer (P_{pat} 382 FAM) and 3' primer (P_{pat} 382 Rev). Appropriate digestion levels were tested using varying concentrations of both fluorescently labeled probe and DNase. Reactions contained varying amounts of IolR or bovine serum albumin (BSA, negative control), Tris-HCl (50 mM, pH 7.5), KCl (50 mM), $MgCl_2$ (10 mM), EDTA (0.5 mM), glycerol (10%, v/v), and incubated for 10 min at 25°C. The labeled DNA probe (120 ng) was added to the reaction and incubated for 20 min at 25°C, followed by addition of DNase for 5 min at 25°C and heat-inactivated for 10 min at 78°C. Reaction mixtures were purified using the MinElute PCR Purification Kit (Qiagen). Samples were analyzed with an Applied Biosystems 3730 DNA Analyzer (Plant-Microbe Genomics Facility, Ohio State University) set to default run module for LIZ600 dye, with 0.1 μl of size standard (LIZ600), 0.5-1.0 μl of sample and 9 μl of HiDi per well. Electropherogram overlays comparing IolR and BSA as a negative control per condition were generated using GeneMapper v4.0 software and putative binding sites were analyzed by aligning the sequenced probe data (electropherogram data not shown; available upon request).

In vitro acetylation assay. Protein acetylation assays were performed as described, using radiolabeled [1-^{14}C] Ac-CoA (2, 7, 14). Briefly, reactions contained *Se*IolR or *Se*Crp (5 μM) with or without *Se*Pat (3 μM). *Se*Acs was used as a positive control. Laboratory stocks of purified *Se*Pat and *Se*Acs proteins were used in these studies. Reactions were resolved and visualized by SDS-PAGE. Radiolabeled proteins were visualized using a Typhoon Trio+ Variable Mode Imager (GE Healthcare) with ImageQuant v5.2 software.

Acetyl-CoA synthetase assay. Acs activity was measured using an NADH-consuming assay[53]. Cultures of the *iolR*$^+$ (JE6583) and *iolR*::*cat*$^+$ (JE10713) strains were grown in NCE minimal medium with acetate (10 mM) at 37°C with shaking to an OD_{600} of 0.2. Cell cultures were harvested by centrifugation at 6,000 x *g* for 30 min and cell pellets were stored at -80°C until used. Cell paste was re-suspended in HEPES buffer (pH 7.5), plus lysozyme (1 mg ml^{-1}), DNase I (25 μg ml^{-1}), phenylmethanesulfonyl fluoride (PMSF, 0.5 mM), and SIGMAFAST protease inhibitor cocktail tables (Sigma)]. Cells were lysed by sonication for 1 min (2 s, 50% duty, setting 80) on ice using a QSonica Q55 cell disruptor (QSonica LLC). Lysed cells were centrifuged at 16,000 x *g* at 4°C for 20 min. The lysed cell extract was concentrated and dialyzed simultaneously using Amicon ® Ultra concentrators (Millipore) with a 30 kD MWCO (Acs is ~72 kD), per the manufacturer's instructions. Samples were washed twice with 5 ml of HEPES buffer (pH 7.5), and total protein concentration was measured using a NanoDrop device (Thermo Scientific). *R*eactions contained HEPES buffer (50 mM, pH 7.5), TCEP (1 mM), ATP (2.5 mM) CoA (0.5 mM), $MgCl_2$ (5 mM), KCl (1 mM), phosphoenolpyruvate (PEP, 3 mM), NADH (0.1 mM), pyruvate kinase (1 U), myokinase (5 U), lactate dehydrogenase (1.5 U) and acetate (0.2 mM). Reactions were started by addition of the treated cell extract (50 μg). Absorbance at 340 nm was monitored in a 96-well plate using the

Spectramax Plus UV-visible spectrophotometer (Molecular Devices). Enzyme activity (of total protein concentration) was calculated as described [53]. Samples were analyzed in triplicate. Error bars represent standard deviation. Statistics were analyzed using unpaired t test (GraphPad Prism v6 software).

ACKNOWLEDGEMENTS

This work was supported by PHS grant R01-GM62203 to J.C.E.-S. S.T. was supported by the PHS Molecular Biosciences Training Grant T32-GM07215 and NRSA Predoctoral Fellowship F31-GM083668. We thank Chelsey M. VanDrisse, Flavia G. Costa, and Michael Ullmer for technical assistance and Michael Zianni (Plant-Microbe Genomic Facility, Ohio State University) for DNA footprinting analysis.

REFERENCES

1. **Smith JS, Brachmann CB, Celic I, Kenna MA, Muhammad S, Starai VJ, Avalos JL, Escalante-Semerena JC, Grubmeyer C, Wolberger C, Boeke JD.** 2000. A phylogenetically conserved NAD(+)-dependent protein deacetylase activity in the Sir2 protein family. *Proc. Natl. Aca. Sci. USA.* **97:**6658-6663.
2. **Starai VJ, Escalante-Semerena JC.** 2004. Identification of the protein acetyltransferase (Pat) enzyme that acetylates acetyl-CoA synthetase in *Salmonella enterica*. *J. Mol. Biol.* **340:**1005-1012.
3. **Thao S, Chen CS, Zhu H, Escalante-Semerena JC.** 2010. *N*(ε)-Lysine acetylation of a bacterial transcription factor inhibits its DNA-binding activity. *PLOS ONE.* **5:**e15123.

4. **Hu LI, Chi BK, Kuhn ML, Filippova EV, Walker-Peddakotla AJ, Basell K, Becher D, Anderson WF, Antelmann H, Wolfe AJ.** 2013. Acetylation of the response regulator RcsB controls transcription from a small RNA promoter. *J. Bacteriol.* **195:**4174-4886.

5. **Lima BP, Antelmann H, Gronau K, Chi BK, Becher D, Brinsmade SR, Wolfe AJ.** 2011. Involvement of protein acetylation in glucose-induced transcription of a stress-responsive promoter. *Mol. Microbiol.* **81:**1190-1204.

6. **Thao S, Escalante-Semerena JC.** 2011. Control of protein function by reversible *N*(ε)-lysine acetylation in bacteria. *Curr. Opin. Microbiol.* **14:**200-204.

7. **Crosby HA, Heiniger EK, Harwood CS, Escalante-Semerena JC.** 2010. Reversible *N* (ε)-lysine acetylation regulates the activity of acyl-CoA synthetases involved in anaerobic benzoate catabolism in *Rhodopseudomonas palustris*. *Mol. Microbiol.* **76:**874-888.

8. **Chan CH, Garrity J, Crosby HA, Escalante-Semerena JC.** 2011. In *Salmonella enterica*, the sirtuin-dependent protein acylation/deacylation system (SDPADS) maintains energy homeostasis during growth on low concentrations of acetate. *Mol. Microbiol.* **80:**168-183.

9. **Kim D, Yu BJ, Kim JA, Lee YJ, Choi SG, Kang S, Pan JG.** 2013. The acetylproteome of Gram-positive model bacterium *Bacillus subtilis*. *Proteomics.* **13:**1726-1736.

10. **Wu X, Vellaichamy A, Wang D, Zamdborg L, Kelleher NL, Huber SC, Zhao Y.** 2013. Differential lysine acetylation profiles of *Erwinia amylovora* strains revealed by proteomics. *J. Proteomics.* **79:**60-71.

11. **Starai VJ, Escalante-Semerena JC.** 2004. Acetyl-coenzyme A synthetase (AMP forming). *Cell Mol Life Sci* **61:**2020-2030.

12. **Starai VJ, Celic I, Cole RN, Boeke JD, Escalante-Semerena JC.** 2002. Sir2-dependent activation of acetyl-CoA synthetase by deacetylation of active lysine. *Science.* **298:**2390-2392.

13. **Browning DF, Beatty CM, Wolfe AJ, Cole JA, Busby SJ.** 2002. Independent regulation of the divergent *Escherichia coli nrfA* and *acs*P1 promoters by a nucleoprotein assembly at a shared regulatory region. *Mol. Microbiol.* **43:**687-701.

14. **Tucker AC, Escalante-Semerena JC.** 2010. Biologically active isoforms of CobB sirtuin deacetylase in *Salmonella enterica* and *Erwinia amylovora*. *J. Bacteriol.* **192:**6200-6208.

15. **Castano-Cerezo S, Bernal V, Blanco-Catala J, Iborra JL, Canovas M.** 2011. cAMP-CRP co-ordinates the expression of the protein acetylation pathway with central metabolism in *Escherichia coli*. *Mol. Microbiol.* **82:**1110-1128.

16. **Kroger C, Fuchs TM.** 2009. Characterization of the *myo*-inositol utilization island of *Salmonella enterica* serovar Typhimurium. *J. Bacteriol.* **191:**545-554.

17. **Sorensen KI, Hove-Jensen B.** 1996. Ribose catabolism of *Escherichia coli*: characterization of the *rpiB* gene encoding ribose phosphate isomerase B and of the *rpiR* gene, which is involved in regulation of *rpiB* expression. *J. Bacteriol.* **178:**1003-1011.

18. **Yamamoto H, Serizawa M, Thompson J, Sekiguchi J.** 2001. Regulation of the *glv* operon in *Bacillus subtilis*: YfiA (GlvR) is a positive regulator of the operon that is repressed through CcpA and Cre. *J. Bacteriol.* **183:**5110-5121.

19. **Yoshida K, Yamamoto Y, Omae K, Yamamoto M, Fujita Y.** 2002. Identification of two *myo*-inositol transporter genes of *Bacillus subtilis*. *J. Bacteriol.* **184:**983-991.

20. **Sundaram TK.** 1972. Regulation of *myo*-inositol catabolism in *Aerobacter aerogenes*. *J. Bacteriol.* **111:**284-286.

21. **Fawole MO.** 1976. Inositol dehydrogenase from *Serratia marcescens*. *Z. Allg. Mikrobiol.* **16:**327-328.

22. **Galbraith MP, Feng SF, Borneman J, Triplett EW, de Bruijn FJ, Rossbach S.** 1998. A functional *myo*-inositol catabolism pathway is essential for rhizopine utilization by *Sinorhizobium meliloti*. *Microbiology.* **144** 2915-2924.

23. **Fry J, Wood M, Poole PS.** 2001. Investigation of *myo*-inositol catabolism in *Rhizobium leguminosarum* bv. *viciae* and its effect on nodulation competitiveness. *MolPlant. Microbe Interact* .**14:**1016-1025.

24. **Kawsar HI, Ohtani K, Okumura K, Hayashi H, Shimizu T.** 2004. Organization and transcriptional regulation of *myo*-inositol operon in *Clostridium perfringens*. *FEMS. Microbiol. Lett*. **235:**289-295.

25. **Yebra MJ, Zuniga M, Beaufils S, Perez-Martinez G, Deutscher J, Monedero V.** 2007. Identification of a gene cluster enabling *Lactobacillus casei* BL23 to utilize *myo*-inositol. *Appl. Environ. Microbiol.* **73:**3850-3858.

26. **Mittal R, Peak-Chew SY, Sade RS, Vallis Y, McMahon HT.** 2010. The acetyltransferase activity of the bacterial toxin YopJ of *Yersinia* is activated by eukaryotic host cell inositol hexakisphosphate. *J. Biol. Chem.* **285:**19927-19934.

27. **Miroux B, Walker JE.** 1996. Over-production of proteins in *Escherichia coli*: mutant hosts that allow synthesis of some membrane proteins and globular proteins at high levels. *J. Mol. Biol.* **260:**289-298.

28. **Rocco CJ, Dennison KL, Klenchin VA, Rayment I, Escalante-Semerena JC.** 2008. Construction and use of new cloning vectors for the rapid isolation of recombinant proteins from *Escherichia coli*. *Plasmid.* **59:**231-237.

29. **Castilho BA, Olfson P, Casadaban MJ.** 1984. Plasmid insertion mutagenesis and *lac* gene fusion with mini-Mu bacteriophage transposons. *J. Bacteriol.* **158:**488-495.

30. **Guzman LM, Belin D, Carson MJ, Beckwith J.** 1995. Tight regulation, modulation, and high-level expression by vectors containing the arabinose PBAD promoter. *J. Bacteriol*. **177:**4121-4130.

31. **Way JC, Davis MA, Morisato D, Roberts DE, Kleckner N.** 1984. New Tn*10* derivatives for transposon mutagenesis and for construction of *lacZ* operon fusions by transposition. *Gene.* **32:**369-379.

32. **Koop AH, Hartley ME, Bourgeois S.** 1987. A low-copy-number vector utilizing beta-galactosidase for the analysis of gene control elements. *Gene.* **52:**245-256.

33. **Klaffl S, Brocker M, Kalinowski J, Eikmanns BJ, Bott M.** 2013. Complex regulation of the phosphoenolpyruvate carboxykinase gene *pck* and characterization of its GntR-type regulator IolR as a repressor of *myo*-inositol utilization genes in *Corynebacterium glutamicum*. *J. Bacteriol.* **195:**4283-4296.

34. **Kroger C, Dillon SC, Cameron AD, Papenfort K, Sivasankaran SK, Hokamp K, Chao Y, Sittka A, Hebrard M, Handler Kw, Colgan A, Leekitcharoenphon P, Langridge GC, Lohan AJ, Loftus B, Lucchini S, Ussery DW, Dorman CJ, Thomson**

NR, Vogel J, Hinton JC. 2012. The transcriptional landscape and small RNAs of *Salmonella enterica* serovar Typhimurium. *Proc. Natl. Acad. Sci. USA.* **109:**E1277-1286.

35. **Kroger C, Stolz J, Fuchs TM.** 2010. *myo*-Inositol transport by *Salmonella enterica* serovar Typhimurium. *Microbiology* .**156:**128-138.

36. **Garrity J, Gardner JG, Hawse W, Wolberger C, Escalante-Semerena JC.** 2007. *N*-lysine propionylation controls the activity of propionyl-CoA synthetase. *J. Biol. Chem.* **282:**30239-30245.

37. **Browning DF, Beatty CM, Sanstad EA, Gunn KE, Busby SJ, Wolfe AJ.** 2004. Modulation of CRP-dependent transcription at the *Escherichia coli acs*P2 promoter by nucleoprotein complexes: anti-activation by the nucleoid proteins FIS and IHF. *Mol. Microbiol.* **51:**241-254.

38. **Beatty CM, Browning DF, Busby SJ, Wolfe AJ.** 2003. Cyclic AMP receptor protein-dependent activation of the *Escherichia coli acs*P2 promoter by a synergistic class III mechanism. *J. Bacteriol.* **185:**5148-5157.

39. **Yoshida K, Kobayashi K, Miwa Y, Kang CM, Matsunaga M, Yamaguchi H, Tojo S, Yamamoto M, Nishi R, Ogasawara N, Nakayama T, Fujita Y.** 2001. Combined transcriptome and proteome analysis as a powerful approach to study genes under glucose repression in *Bacillus subtilis*. *Nucleic Acids Res.* **29:**683-692.

40. **Cordero-Alba M, Bernal-Bayard J, Ramos-Morales F.** 2012. SrfJ, a *Salmonella* type III secretion system effector regulated by PhoP, RcsB, and IolR. *J. Bacteriol.* **194:**4226-4236.

41. **Berkowitz D, Hushon JM, Whitfield HJ, Jr., Roth J, Ames BN.** 1968. Procedure for identifying nonsense mutations. *J. Bacteriol.* **96:**215-220.

42. **Balch WE, Wolfe RS.** 1976. New approach to the cultivation of methanogenic bacteria: 2-mercaptoethanesulfonic acid (HS-CoM)-dependent growth of *Methanobacterium ruminantium* in a pressurized atmosphere. *Appl. Environ. Microbiol.* **32:**781-791.

43. **Datsenko KA, Wanner BL.** 2000. One-step inactivation of chromosomal genes in *Escherichia coli* K-12 using PCR products. *Proc. Natl. Acad. Sci. USA.* **97:**6640-6645.

44. **Davis RW, Botstein D, Roth JR.** 1980. A manual for genetic engineering: advanced bacterial genetics. Cold Spring Harbor Laboratory Press, Cold Spring Harbor, NY.

45. **Schmieger H.** 1971. A method for detection of phage mutants with altered transducing ability. *Mol. Gen. Genet.* **110:**378-381.

46. **Chan RK, Botstein D, Watanabe T, Ogata Y.** 1972. Specialized transduction of tetracycline resistance by phage P22 in *Salmonella typhimurium*. II. Properties of a high-frequency-transducing lysate. *Virology.* **50:**883-898.

47. **Blommel PG, Fox BG.** 2007. A combined approach to improving large-scale production of tobacco etch virus protease. *Protein Expr. Purif.* **55:**53-68.

48. **Klock HE, Koesema EJ, Knuth MW, Lesley SA.** 2008. Combining the polymerase incomplete primer extension method for cloning and mutagenesis with microscreening to accelerate structural genomics efforts. *Prot-Struct. Funct. Bioinformat.* **71:**982-994.

49. **Galloway NR, Toutkoushian H, Nune M, Bose N, Momany C.** 2013. Rapid cloning for protein crystallography using Type IIS restriction enzymes. *Crys. Growth & Des.* **13:**2833-2839.

50. **Kleckner N, Roth J, Botstein D.** 1977. Genetic engineering *in vivo* using translocatable drug-resistance elements. New methods in bacterial genetics. *J. Mol. Biol* .**116:**125-159.

51. **Caetano-Anolles G.** 1993. Amplifying DNA with arbitrary oligonucleotide primers. *PCR Methods Appl.* **3:**85-94.

52. **Miller JH.** 1972. Assay of β-galactosidase, p 352-355, Experiments in Molecular Genetcis. Cold Spring Harbor Laboratory, Cold Spring Harbor, New York.

53. **Stead MB, Agrawal A, Bowden KE, Nasir R, Mohanty BK, Meagher RB, Kushner SR.** 2012. RNAsnap: a rapid, quantitative and inexpensive, method for isolating total RNA from bacteria. *Nucleic Acids Res.* **40:**e156.

CHAPTER 4

IN *SALMONELLA ENTERICA*, THE GCN5-RELATED ACETYLTRANSFERASE MDDA (FORMERLY YNCA) ACETYLATES METHIONINE SULFONE AND METHIONINE SULFOXIMINE, BLOCKING THEIR TOXIC EFFECTS[3]

[3]Hentchel K.L. and J.C. Escalante-Semerena. 2015. *J. Bacteriol*. 197:314-325.
Reprinted here with permission from the publisher.

ABSTRACT

Protein and small molecule acylation are widespread in nature. Many of the enzymes catalyzing acylation reactions belong to the Gcn5-related *N*-acetyltransferase family (GNAT, PF00583), named after the yeast Gcn5 protein. The genome of *Salmonella enterica* serovar Typhimurium LT2 encodes 26 GNATs, 11 of which have no known physiological role. Here we provide *in vivo* and *in vitro* evidence for the role of the MddA (Methionine derivative detoxifier A; formerly YncA) GNAT in the detoxification of oxidized forms of methionine, including methionine sulfoximine (MSX) and methionine sulfone (MSO). MSX and MSO inhibited growth of an *S. enterica* Δ*mddA* strain unless glutamine or methionine was present in the medium. We used an *in vitro* spectrophotometric assay and mass spectrometry to show that MddA acetylated MSX and MSO. An $mddA^{+}$ strain displayed biphasic growth kinetics in the presence of MSX and glutamine. Deletion of two amino acid transporters (GlnHPQ and MetNIQ) in a Δ*mddA* strain restored growth in the presence of MSX. Notably, MSO was transported by GlnHPQ, but not by MetNIQ. In summary, MddA is the mechanism used by *S. enterica,* to respond to oxidized forms of methionine, which MddA detoxifies by acetyl-CoA-dependent acetylation.

INTRODUCTION

The Gcn5 related *N*-acetyltransferase (GNAT, PF00583) superfamily of proteins (>10,000 members) is present in all domains of life. GNATs transfer the acetyl group from acetyl-CoA to proteins or small molecules (for reviews see (1, 2). Acetylation targets of GNATs include the *N*-termini of proteins (3, 4), aminoglycoside antibiotics (5), glutamate (6), spermidine (7), aminoalkylphosphonic acid (8), dTDP-fucosamine (9), and transfer RNAs (10). Some of the first bacterial GNATs characterized were the aminoglycoside *N*-acetyltransferases from *Enterococcus*

faecium (5) and *Serratia marcescens* (11), demonstrating GNAT-dependent acetylation and inactivation of antibiotics.

GNATs provide protection against a myriad of cellular stressors, and the number of stressors controlled by GNATs appears to correlate with the environment encountered by the cell. Therefore, the relevance of GNAT function to cell physiology varies amongst organisms. For example, *S. enterica* and *E. coli* each contain ~26 GNATs, yet actinomycetes such as *Streptomyces lividans* encode up to ~70 putative GNATs, suggesting that *S. lividans* occupies a more challenging habitat.

At present, there is limited to no information available on the cellular processes several putative *S. enterica* GNATs may affect. Not surprisingly, the signals that trigger the synthesis of GNATs, the transcription factors involved in sensing such signals, and the determinants of GNAT substrate specificity remain unknown.

In *S. enterica*, MddA (formerly YncA, STM1590) is a putative GNAT with no characterized function. Homology searches reveal the presence of MddA-like proteins in *Pseudomonas aeurginosa* (63% identity) and *Acinetobacter baylyi* (36% identity), and suggest a role for *Se*MddA in controlling the toxic effects of methionine sulfoximine (MSX) and methionine sulfone (MSO) (Fig. 4.1) (12, 13). Protein structures of *Se*MddA homologues have been solved in *P. aeurginosa* (PDB 2J8R) and *A. baylyi* (PDB 2JLM), showing these enzymes contain the structural core representative of members of the GNAT family (12-14). The *P. aeurginosa* MddA homologue was solved in complex with MSX and showed a conformational change in the active site upon binding to MSX (13).

MSX is similar in structure to phosphinothricin (PHO) (Fig. 4.1), and at least some MddA homologues have been incorrectly annotated as PHO acetyltransferases (12, 13), an activity

performed by the Bar acetyltransferase (15). The Bar protein is a GNAT of *Streptomyces* spp. involved in protection against a self-produced toxin Bialaphos, a natural herbicide consisting of the tripeptide PHO-Ala-Ala (16). The toxin is activated when PHO, a glutamate analogue, is cleaved from the peptide. Bialaphos is a potent herbicide and plants have been genetically engineered to be resistant by encoding the *bar* gene (15, 17). PHO and MSX both inhibit glutamine synthetase (GlnA), which converts glutamate to glutamine, and plays an important role in the regulation of nitrogen metabolism (18, 19).

MSX is found in the roots and seeds of members of the Connaraceae plant species, and has been identified to be toxic component of these plants (20). While this is the only example of natural occurring MSX, in the late 1940's MSX was identified as a toxic by-product in bleached flour (21-23). It was produced by addition of nitrogen trichloride, which reacted with wheat proteins in the flour. This had severe effects on individuals that consumed flour treated this way, and around 1950 this method of flour bleaching was discontinued. Researchers have hypothesized that long-time exposure to MSX in processed foods may account for an increase in neurodegenerative disorders in humans such as Alzheimer's disease, Parkinson's disease, and amyotrophic lateral sclerosis (ALS) (24, 25).

Here we present *in vivo* and *in vitro* evidence that *Se*MddA (methionine derivative detoxifier A) is necessary for survival of *S. enterica* in the presence of MSX and MSO, addition of glutamine or methionine prevents this toxicity, and that the *Se*MddA protein acetylates the amino moiety of MSX. We report that deletion of two amino acid transporters, MetNIQ and GlnHPQ, fully restores growth of a Δ*mddA* strain exposed to MSX. Our data also indicate transport of MSO differs from MSX, as MetNIQ cannot transport MSO. Taken together, these data demonstrate that *Se*MddA acetylates MSX and MSO, thereby blocking their toxic effects.

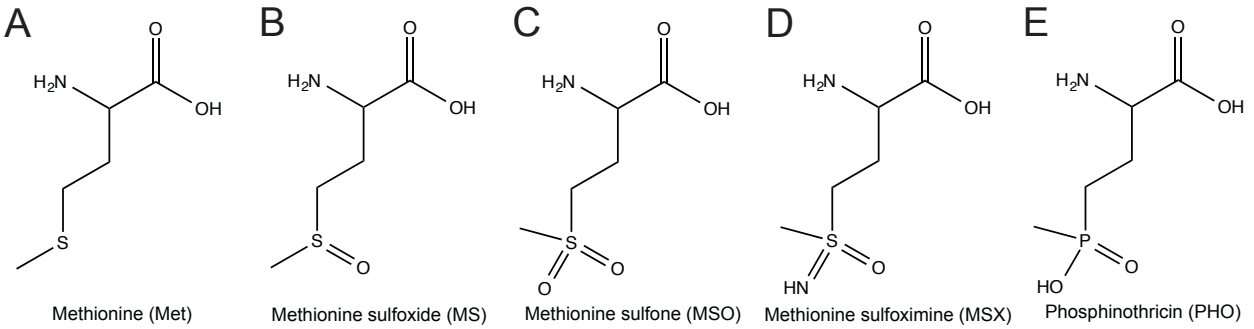

Figure 4.1. Chemical structures of methionine analogs. (A) methionine (Met); (B) methionine sulfoxide (MS); (C) methionine sulfone (MSO); (D) methionine sulfoximine (MSX); and (E) phosphinothricin (PHO).

MATERIALS AND METHODS

Culture media and chemicals. Nutrient broth (NB, Difco) containing NaCl (85 mM) was used as rich medium. The minimal medium used was no-carbon essential (NCE) minimal medium (26) containing $MgSO_4$ (1 mM), Wolfe's trace minerals (1x) (27), and glycerol (22 mM) as the sole source of carbon and energy. When used, antibiotics were added at the following concentrations: tetracycline, 20 μg ml^{-1}; kanamycin, 50 μg ml^{-1}; chloramphenicol, 20 μg ml^{-1}; and ampicillin, 100 μg ml^{-1}. When added to the medium, the calcium chelator ethyleneglycol tetraacetic acid (EGTA) was present at 10 mM, and X-gal was added to a final concentration of 40 μg ml^{-1}. All chemicals were purchased from Sigma-Aldrich unless noted otherwise; Kanamycin, ampicillin, NaCl, and 4-(2-hydroxyethyl)-1-piperazineethanesulfonic acid (HEPES, Fischer Scientific); *tris*(2-carboxyethyl)phosphine hydrochloride **(**TCEP, Soltec Ventures); isopropyl β-D-1-thiogalactopyranoside (IPTG, IBI Scientific); dithiothreitol (DTT, Gold BioTechnology); and [^{14}C-1]-Acetyl-CoA (Moravek).

Bacterial strains and primers. All strains are derivatives of *S. enterica* serovar Typhimurium strain LT2 (unless specified), and are listed in Table 4.1. Tn*10*d(*tet*$^{+}$) refers to the transposase-defective mini-Tn*10* (Tn*10*Δ*16*Δ*17*) (28). All primers used in this study were synthesized by IDT (Coralville, Iowa) and are listed in Table 4.2.

Phage transductions. P22 phage-mediated transduction crosses were performed as described previously (29), using the high-frequency general transducing mutant of bacteriophage P22 HT105/1 *int-210* (30, 31). Phage-free, phage-sensitive transductants were isolated on non-selective green indicator plates as described previously (32).

Table 4.1. Strains and plasmids used in this study.

Strain	Relevant genotype	Reference/source[a]
JE10079	*ara-9 mddA*$^+$	Laboratory strain
Derivatives of JE10079		
JE18333	*mddA1*::*cat*$^+$	
JE18543	*mddA1*::*cat*$^+$ / pNK972[b]	
JE18622	Δ*mddA2*	
JE18955	pMDD8	
JE18961	*mddA1*::*cat*$^+$ / pMDD8	
JE19029	*mddA1*::*cat*$^+$ / pMDD11	
JE19583	*metNI2703*::*kan*$^+$	
JE19730	Δ*mddA2 metNI2703*::*kan*$^+$	
JE20027	Δ*mddA2 glnP1561*::Tn*10*d(*tet*$^+$)[c]	
JE20064	*glnPQ1562*::*cat*$^+$	
JE20065	Δ*mddA2 glnPQ1562*::*cat*$^+$	
JE20067	Δ*mddA2 metNI2703*::*kan*$^+$ *glnPQ1562*::*cat*$^+$	
JE20073	Δ*mddA2 glnPQ1562*::*cat*$^+$ / pGLN2	
JE20329	Δ*mddA2 metNI2703*::*kan*$^+$ / pMETN1	
JE6583	*metE205 ara-9*	K. Sanderson via J. Roth
***E. coli* strains**		
E. coli C41(lDE3)	*ompT hsdS* (r_B m_B) *gal* λ (DE3) including at least one non-characterized mutation	(1, 2)
Plasmids		
pMDD7	*mddA*$^+$ cloned into pKLD66[d]	
pMDD8	*mddA*$^+$ cloned into pBAD24[e]	
pMDD10	*mddA3* cloned into pKLD66[d] (encodes MddA^{E82Q})	
pMDD11	*mddA3* cloned into pBAD24[e], (encodes MddA^{E82Q})	
pGLN2	*glnPQ*$^+$ cloned into pBAD24[e]	
pMETN1	*metNI*$^+$ cloned into pBAD24[e]	
pNK972	*tpn*$^+$ *bla*$^+$	(3)

[a] All strains and plasmids were constructed during the course of this work, unless otherwise stated
[b] pNK972 is a pBR332 derivative carrying the IS10transposase gene described in (3)
[c] Tn*10*d(*tet*$^+$) is an abbreviation of Tn*10*Δ*16*Δ*17* (4)
[d] pKLD66 is an overexpression vector described in (2)
[e] pBAD24 is a cloning vector described in (5)

Table 4.2. Primers used in this study.

Primer Name	Primer Sequence
Cloning	
5' *glnPQ* pBAD24	NNGCTCTTCNTTCATGCAGTTTGACTGGAGCGCCATCT
3' *glnPQ* pBAD24	NNGCTCTTCNTTATCAGGAGACGTGCTGTAAAAATTCC
5' *metNI* pBAD24	NNGCTCTTCNTTCATGATTAAACTTTCGAATATTACCA
3' *metNI* pBAD24	NNGCTCTTCNTTATTACTTATGCGTGACAGCCCTGACG
5' *mddA* pBAD24	NNGCTCTTCNTTCATGACGATTCGCTTTGCCGATAAAG
3' *mddA* pBAD24	NNGCTCTTCNTTATCAGCAGGCGTCCGGCGCGGCGTGT
5' *mddA* pTEV16	NNGCTCTTCNAGCATGACGATTCGCTTTGCCGATAAAG
3' *mddA* pTEV16	NNGCTCTTCNTTATCAGCAGGCGTCCGGCGCGGCGTGT
Mutagenesis	
5' *mddA* G244C	GTTTTCGCTATACCGTCCAGCACTCGGTTTATGTTC
3' *mddA* G244C	GAACATAAACCGAGTGCTGGACGGTATAGCGAAAAC
Strain deletions	
5' *glnPQ* DEL	TGACTATTTACACCACGGTAACAGGAACGACATATGGTGTAGGCTGGAGCTGCTTC
3' *glnPQ* DEL	CCCTTCCTGCCGCAGGGCTGGAAGGGCGATATCTCACATATGAATATCCTCCTTAG
5' *metNI* DEL	CTCCGCTCATTTCATTACGATAATAAAGAATCAATGGTGTAGGCTGGAGCTGCTTC
3' *metNI* DEL	TTTCCTTAATGAGTATTTGTGTTGTGTTTAACGTTACATATGAATATCCTCCTTAG
5' *mddA* DEL	TATCGTAAACATTCCCTGGGGTTCCCTATGGTGTAGGCTGGAGCTGCTTC
3' *mddA* DEL	AAAAGATGAGCGTC GCGACTGGTTCATCACATATGAATATCCTCCTTAG

Construction of gene deletions. Strains carrying in-frame deletions of each gene of interest were constructed following the protocol established for *E. coli* (33). Briefly, PAGE-purified primers with 36 bp of homology with the 5' and 3' ends of the gene of interest (IDT, Coralville, Iowa) were used to amplify the *cat*$^+$ or *kan*$^+$ cassette from template plasmid pKD3 or pKD4, respectively. PCR products were analyzed on a 1% agarose gel, purified using the Wizard® SV Gel and PCR Clean-Up System (Promega), per the manufacturer's protocol, followed by subsequent construction of the deletion of the gene as described in the original protocol (33). PCR was used to confirm the insertion of the *cat*$^+$ or *kan*$^+$ amplicons compared to the wild type allele size. All mutations were re-constructed in the appropriate strain background using P22 phage-mediated transduction crosses. Briefly, P22 phage was propagated on a strain containing an allele of interest. P22 lysates were generated from these strains to transduce the original recipient strain to the appropriate antibiotic resistance, yielding a re-constructed strain with the allele of interest (Table 4.1).

Plasmid construction. All plasmids used in this work are listed in Table 4.1. The cloning method using unique BspQ1 restriction sites as published previously (34) was used to construct all plasmids in this study unless otherwise stated. DNA sequencing (Georgia Genomics Facility, UGA) was used to verify all plasmids constructed in this study. Each gene of interest was amplified from *S. enterica* sv. Typhimurium LT2 genomic DNA.

Genes of interest (*mddA*$^+$, *glnPQ*$^+$, *metNI*$^+$) were cloned into the *L*-(+)-arabinose inducible vector pBAD24 (35) engineered to contain BspQ1 sites (C. M. VanDrisse & J. C. Escalante-Semerena, unpublished data). The resulting plasmids (pMDD8, pGLN2, and pMETN1) were used in complementation studies.

Plasmid pTEV5 (36), which directs the synthesis of the protein with a cleavable *N*-terminal hexahistidine tag, was modified to contain BspQ1 restriction sites. The resulting plasmid was named pTEV16 (C. M. VanDrisse & J. C. Escalante-Semerena, unpublished data), and used for overexpression of *Se*MddA^{WT} (pMDD7).

Site-directed mutagenesis was performed using primers designed from PrimerX (available at http://www.bioinformatics.org/primerx/) to mutate the predicted catalytic residue of *Se*MddA^{WT}, glutamate (E82), to a non-catalytic glutamine residue (Q82), to construct a catalytic variant (*Se*MddA^{E82Q}) in both the complementation (pMDD11) and overexpression vectors (pMDD10).

Growth behavior analyses. Starter cultures were grown overnight at 37°C with shaking in nutrient broth containing the appropriate drug marker and used to inoculate fresh medium (1% v/v) in a volume of 200 μl per well of a 96-well plate with appropriate antibiotics. Strains containing plasmids were induced with varying concentrations of *L*-(+)-arabinose, as described in figure legends. Additional chemicals such as glutamine, methionine, MSX, MSO, or PHO were added at concentrations indicated in figures and figure legends. Plates were incubated at 37°C with shaking for 20-48 h in a microplate reader (Bio-Tek Instruments). Growth curves were performed in triplicate in three independent experiments, with a representative growth curve shown. Data were analyzed using Prism v6 (GraphPad) analytical software. Error bars represent the standard deviation.

Overproduction and purification of the* Se*MddA^{WT}* *and* Se*MddA^{E82Q}* *proteins. Vectors encoding *Se*MddA^{WT} (pMDD7) and *Se*MddA^{E82Q} (pMDD10) were transformed into *E. coli* C41(λDE3). Overnight cultures of the transformants were sub-cultured (1:100 (v/v, inoculum:medium)) into 1 L of LB containing ampicillin (100 μg ml^{-1}). Cultures were grown at 37°C with shaking to an OD_{600} of 0.6, induced with IPTG (1 mM), and shaken overnight at

~28°C. Cells were harvested by centrifugation at 6,000 x *g* for 15 min at 4°C. The collected cell paste was re-suspended in binding buffer A [HEPES buffer (50 mM, pH 7.5) containing NaCl (500 mM) and imidazole (20 mM)] plus lysozyme (1 mg ml^{-1}), DNAse I (25 µg ml^{-1}) and protease inhibitor phenylmethanesulfonyl fluoride (PMSF, 0.5 mM)]. Cells were lysed by sonication for 1 min (2 sec, 50% duty) for 2 rounds on ice using a 550 Sonic Dismembrator (Fisher Scientific) at setting 4. Clarified cell lysates were obtained after centrifugation for 45 min at 4°C at 43,667 x *g* followed by filtration of the supernatant through a 0.45 µm filter (Millipore). Samples were loaded onto a 2 ml HisPur™ Ni-NTA resin column (Thermo Scientific) at 4°C, pre-equilibrated with binding buffer. His_6-tagged *Se*MddA proteins eluted with buffer B (HEPES buffer (50 mM, pH 7.5) containing NaCl (500 mM) and imidazole (500 mM)] following a wash step in the same buffer system with a lower amount of imidazole (40 mM).

To cleave the tag, His_6-TEV protease (rTEV) was purified as described (37), and cleavage of tagged *Se*MddA proteins was performed as follows: rTEV was added to the eluted protein supplemented with DTT (1 mM) at a 1:100 protease:tagged mg protein ratio, and the mixture was incubated at room temperature for 3 h. Proteins were dialyzed at 4°C in buffer C [HEPES buffer (50 mM, pH 7.5) containing NaCl (500 mM), *tris*(2-carboxyethyl)phosphine hydrochloride (TCEP, 0.5 mM)], and ethylenediaminetetraacetic acid (EDTA, 0.5 mM). Dialyzed, cleaved protein was reloaded onto the column and were eluted using a 40 mM imidazole wash step, followed by an imidazole wash (500 mM, which allowed separation of the untagged (*Se*$MddA^{WT}$ or *Se*$MddA^{E82Q}$) from tagged (His_6-TEV protease) protein. *Se*$MddA^{WT}$ and *Se*$MddA^{E82Q}$ eluted from the column during the wash step. The proteins were stored in HEPES buffer (50 mM, pH 7.2) containing NaCl (100 mM), *tris*(2-carboxyethyl)phosphine

hydrochloride (TCEP, 0.5 mM)) and glycerol (10% v/v), drop-frozen in liquid nitrogen, and stored at -80°C. Both proteins were purified to 99% homogeneity as determined using Total Lab v2005 software.

Analytical gel filtration. Experiments were performed at 4°C. Per run, a sample volume of 500 µl of 100 µg of *Se*MddA^{WT} or *Se*MddA^{E82Q} protein was injected onto a Superdex 200 HR 10/30 gel filtration column (GE Healthcare) attached to an ÄKTA purifier FPLC system that was equilibrated with buffer D [HEPES (50 mM, pH 7.4) and NaCl (100 mM)]. A calibration standard containing a mixture of molecular masses ranging from 1.35 to 670 kDa (Bio-Rad) was used to generate a standard curve to determine the molecular mass. The standards mixtures contained vitamin B_{12} (1.35 kDa), equine myoglobin (17 kDa), chicken ovalbumin (44 kDa), bovine γ-globulin (158 kDa), and thyroglobulin (670 kDa). A flow rate of 0.5 ml min^{-1} was used to develop the column and elution peak analysis was performed using UNICORN v4.11 software. Data were graphed and analyzed using Prism v6 (GraphPad) analytical software. Linear regression analyses of the standard curves yielded r^2 values of 0.98.

Thin layer chromatography. Reaction mixtures included HEPES buffer (50 mM, pH 7.0), containing TCEP (1 mM), [1-^{14}C]-Ac-CoA or [1-^{14}C]-Pro-CoA (20 µM), substrate (0.5 mM), and *Se*MddA^{WT} or *Se*MddA^{E82Q} (1 µg). Reactions were incubated at 37°C for 30 minutes, spotted onto a polyester backed silica gel plate (Whatman Ltd), and developed in a chamber pre-equilibrated with a mobile phase of *n*-butanol, acetic acid, and dH_2O (3:1:1). TLC plates were incubated for 3-4 h, dried, and developed with a phosphor screen overnight. The resulting phosphor-image was detected using a Typhoon Trio+ Variable Mode Imager (GE Healthcare) with ImageQuant v5.2 software.

Spectrophotometric enzyme activity assay. Specific activities of *Se*MddA^{WT} and *Se*MddA^{E82Q} were measured using a continuous spectrophotometric assay that employed 5,5'-dithiobis-(2-nitrobenzoic acid) (DTNB, Ellman's reagent) as a reporter of free sulfhydryl groups (38, 39). Reaction mixtures contained HEPES buffer (50 mM, pH 7.2) containing Ac-CoA or Pro-CoA (100 μM), amine substrate (150 μM), DTNB (0.3 mM) and *Se*MddA^{WT} or *Se*MddA^{E82Q} protein (500 ng). Reactions were incubated for 5 min at 30°C in a Spectramax 384 Plus (Molecular Devices). Absorbance was measured continuously at 412 nm using SoftMax Pro v6.2 software. Data graphing and analysis was performed using Prism v6 software. Activity assays were performed in technical duplicate in three independent experiments.

Synthesis and identification of acetyl-methionine sulfoximine and acetyl-methionine sulfone. To confirm the location of acetylation of MSX and MSO, acetyl-MSX and acetyl-MSO were generated enzymatically. Reaction components included acetyl-CoA (1 mM), MSX or MSO (0.5 mM), *Se*MddA^{WT} (20 μg), and ammonium bicarbonate (20 mM) in a reaction volume of 500 μl. A no-enzyme control reaction was also performed. Reactions were incubated at 37°C for 2 h. *Se*MddA^{WT} was removed from the reaction mixture by filtration using Amicon® Ultra centrifugal filters (Millipore) with a 3K molecular weight cut-off, according to manufacturer's protocol. Samples were concentrated in a Vacufuge plus speed vacuum (Eppendorf) at 30°C, and resuspended in 50% acetonitrile, 50% dH_2O with 1% formic acid. The identity of acetyl-MSX and acetyl-MSO was confirmed by mass spectrometry (Protein and Mass Spectrometry Facility, UGA). ESI-MS was performed after sample dilution in acetonitrile and run on an Esquire 3000 Plus (Bruker) Ion Trap Mass Spectrometer at 0.3 ml/h.

Isolation of a Tn*10*d*(tet$^+$) *insertion in an* mddA*::*cat$^+$ *strain by transposon mutagenesis. To identify mutations that allow for growth of an *mddA*::*cat*$^+$ strain in the presence of MSX, a

mutagenesis screen using Tn*10*d(*tet*$^+$) transposons was utilized. To obtain a phage pool lacking the *mddA* gene, a transposition experiment was performed by transducing a P22 phage stock carrying a pool of Tn*10*d(*tet*$^+$) transposons inserted throughout the *S. enterica* genome into an *mddA*::*cat*$^+$ strain containing a plasmid carrying a transposase (JE18543). This was done to prevent recovery of growth due to repair of the *mddA*::*cat*$^+$ deletion. Transduction reactions were plated on NB plates containing tetracycline (20 μg ml^{-1}) to select for transposon insertion. An estimated total of 61,308 colonies were pooled, resulting in ~13.5x coverage of the *S. enterica* genome.

A P22 lysate grown on this pool of strains was used to transduce strain *mddA*::*cat*$^+$ (JE18333) to tetracycline resistance (20 μg ml^{-1}) on NB plates, followed by replica printing onto NCE minimal medium plates containing glycerol (22 mM) and MSX (10 μM). Colonies arising on the selection plates were freed of phage, patched onto NB plates, incubated for 4-6 h at 37°C, and replica printed to several selection plates including NB with tetracycline (20 μg ml^{-1}), NB with chloramphenicol (20 μg ml^{-1}), and NCE minimal medium with MSX (10 μM). Mutants that grew in all of these conditions were freed of phage and P22 lysates were generated. The resulting phage lysate was used as a donor in crosses with parental *mddA*::*cat*$^+$ strain (JE18333). Transductions were plated on NB with tetracycline, selecting for the transposon, and after 24 h of growth at 37°C replica printed to plates containing MSX (10 μM) to confirm the phenotype.

The location of the insertion on the chromosome was determined in the re-constructed strain by sequencing the DNA flanking the Tn*10*d(*tet*$^+$) element using a PCR-based protocol. A DNA product was amplified with degenerate primers and primers derived from the Tn*10*d(*tet*$^+$) insertion sequences as reported previously (40) and used as template for sequencing reactions.

DNA sequencing was performed using BigDye® Terminator v3.1 protocols (Applied Biosystems) and the reactions were analyzed at the University of Georgia Genomics Facility.

RESULTS

Methionine sulfoximine (MSX) and methionine sulfone (MSO) inhibit growth of an* mddA*::*cat$^+$ *strain. We examined the ability of an *S. enterica mddA*::*cat*$^+$ strain (JE18333) to grow in the presence of MSX or MSO (Fig. 4.2). In the absence of MSX or MSO, no growth differences were observed between the *mddA*$^+$ and *mddA*::*cat*$^+$ strains in either rich or minimal media (data not shown). Addition of MSX (10 μM) caused complete growth inhibition of the *mddA*::*cat*$^+$ strain in minimal medium (Fig. 4.2A, solid diamonds). The same concentration of MSX did not have any effect on the growth of the *mddA*$^+$ strain (Fig. 4.2A, inverted solid triangles). The observed effects were different when strains were grown in rich medium. Under these conditions MSX partially inhibited growth of the *mddA*::*cat*$^+$ strain, and only when the MSX concentration was at least 50 μM (Fig. 4.2B, solid triangles).

Addition of methionine sulfone (MSO, 50 μM) also negatively affected growth of the *mddA*::*cat*$^+$ strain relative to that of the *mddA*$^+$ in minimal medium, but was less severe than the effect caused by MSX (Fig. 4.2C, solid triangles). A short delay in the onset of exponential growth was observed for the *mddA*::*cat*$^+$ strain in rich medium containing 200 μM MSO (Fig. 4.2D, solid triangles).

Se*MddA activity blocks the negative effects of MSX and MSO*. We performed *in vivo* experiments to determine whether or not *Se*MddA played a role in circumventing the toxic effects of MSX and MSO. For this purpose, plasmid pMDD8 (*mddA*$^+$) was introduced into the *mddA*::*cat*$^+$ strain (JE18333), yielding strain JE18961. As a control, an inactive variant of

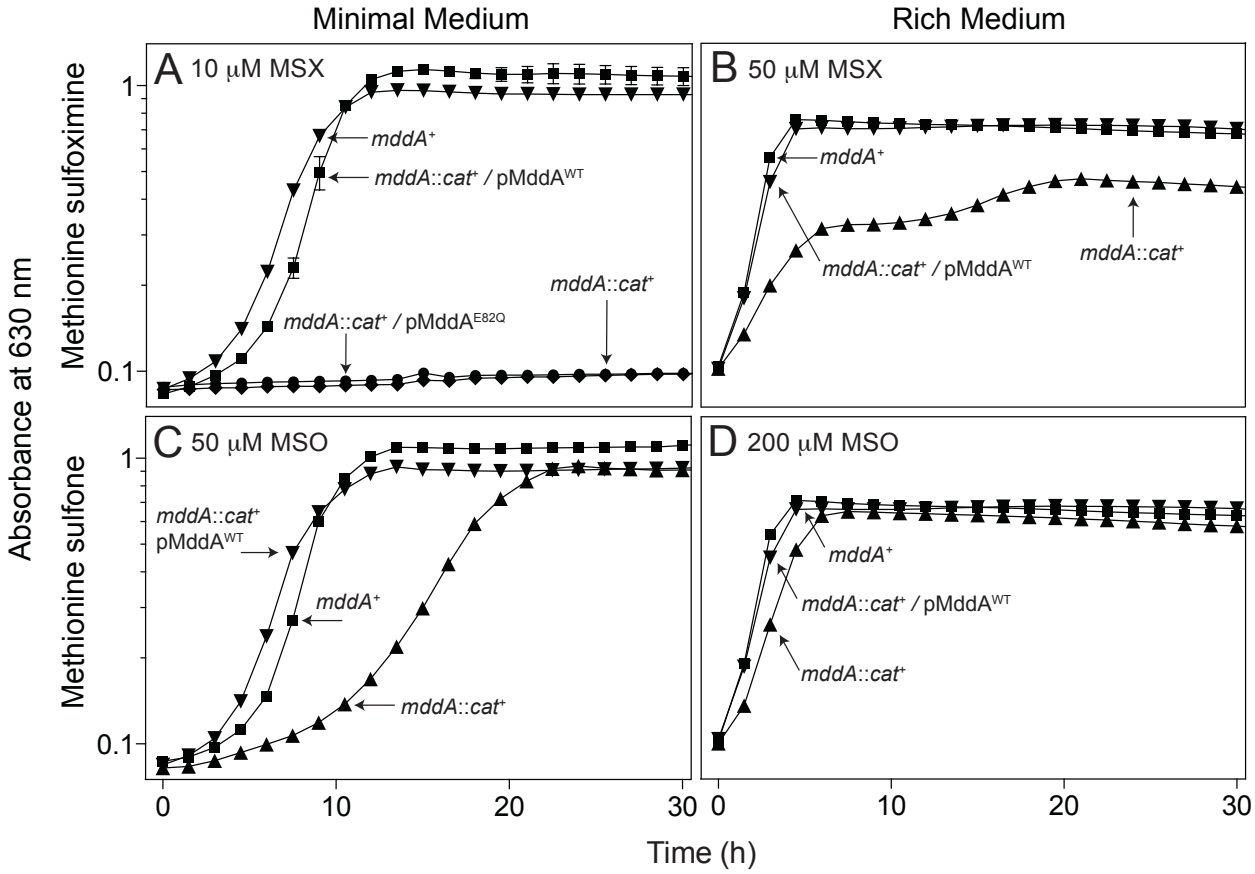

Figure 4.2. MSX and MSO inhibit growth of an *mddA*::*cat*$^+$ strain. Growth of *S. enterica* *mddA*$^+$ and *mddA*::*cat*$^+$ strains was examined in the presence of MSX (10 μM or 50 μM) or MSO (50 μM or 100 μM) as indicated. Non-essential E (NCE) minimal medium with glycerol (22 mM) or nutrient broth were used in these experiments. Growth curves were performed using a microplate reader (Bio-Tek Instruments) as described under *Materials and Methods*. The following strains were analyzed: *mddA*$^+$ (JE10079), *mddA*::*cat*$^+$ (JE18333), *mddA*::*cat*$^+$ / pMDD8 *mddA*$^+$ (JE18961), and *mddA*::*cat*$^+$ / pMDD11 *mddA*$^+$ (encoding *Se*MddA^{E82Q}) (JE19029). Error bars represent standard deviation.

*Se*MddA was constructed by site-directed mutagenesis, in which the predicted catalytic residue E82 was changed to Q82 (*Se*MddA^{E82Q}). The presence of plasmid pMDD11 encoding the *Se*MddA^{E82Q} variant did not restore growth of the *mddA*::*cat*$^{+}$ strain in the presence of MSX (Fig. 4.2A, solid circles). However, the wild-type *mddA*$^{+}$ allele *in trans* (pMDD8) supported growth of the *mddA*::*cat*$^{+}$ strain in the presence MSX or MSO (Fig. 4.2A, solid squares; Fig. 4.2D, inverted solid triangles). It should be noted that at higher levels of inducer, *i.e.* ≥250 μM (*L*-(+)-arabinose), an *mddA*::*cat*$^{+}$ strain synthesizing the *Se*MddA^{E82Q} variant grew in medium containing MSX (10 μM), albeit with an extended lag phase, indicating that *Se*MddA^{E82Q} retained some catalytic activity (Fig. 4.3).

***High levels of MSX are inhibitory to wild-type* S. enterica.** An increase in the lag phase of a culture of the *mddA*$^{+}$ strain (JE10079) was seen at higher levels of MSX (20-50 μM). However, the strain grew at the same rate observed in medium devoid of MSX, and reached the same optical density of a culture unexposed to MSX (Fig. 4.4A). The effect of MSX in rich medium was notably different as the *mddA*$^{+}$ strain showed no inhibition when the MSX concentration was at 500 μM (data not shown), and only partial inhibition of growth occurred at 1 mM (Fig. 4.4B, solid triangles). In sharp contrast, as stated previously, no growth of the *mddA*::*cat*$^{+}$ strain was observed in the presence of as low as 10 μM MSX in minimal medium (Fig 4.4C), however, in rich medium, growth of the *mddA*::*cat*$^{+}$ strain was only abolished at a concentration of 1 mM MSX (Fig 4.4D, inverted solid triangles). High concentrations (*e.g.* 200 μM) of other methionine derivatives such as methionine sulfoxide (MS) and buthionine sulfoximine (BSX) did not affect the growth rate of either the *mddA*$^{+}$ or *mddA*::*cat*$^{+}$ strains in minimal medium (doubling time: + MS 1.4, 1.5, respectively; + BSX 1.6, 1.7, respectively).

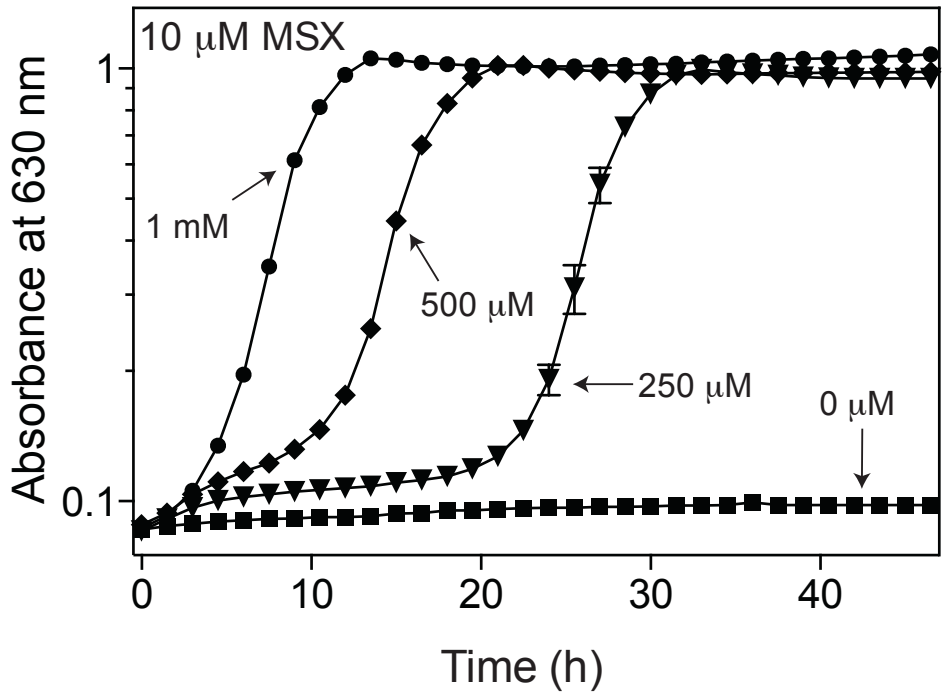

Figure 4.3. High levels of MddA^{E82Q} variant allow an *mddA1*::*cat*$^{+}$ strain to grow in the presence of MSX. Growth of the *S. enterica* strain *mddA1*::*cat*$^{+}$ / pMDD11 *(*encodes MddA^{E82Q}) in NCE minimal medium (glycerol, 22 mM) was examined in the presence of MSX (10 μM) and increasing concentrations of inducer (*L*-(+)-arabinose; 250 μM, 500 μM, and 1000 μM), as indicated. Growth curves were performed using a microplate reader (Bio-Tek Instruments) as described under *Materials and Methods*. The strain analyzed was JE19029 (*mddA1*::*cat*$^{+}$ / pMDD11 *mddA3*$^{+}$, which encodes MddA^{E82Q}). Error bars represent standard deviation.

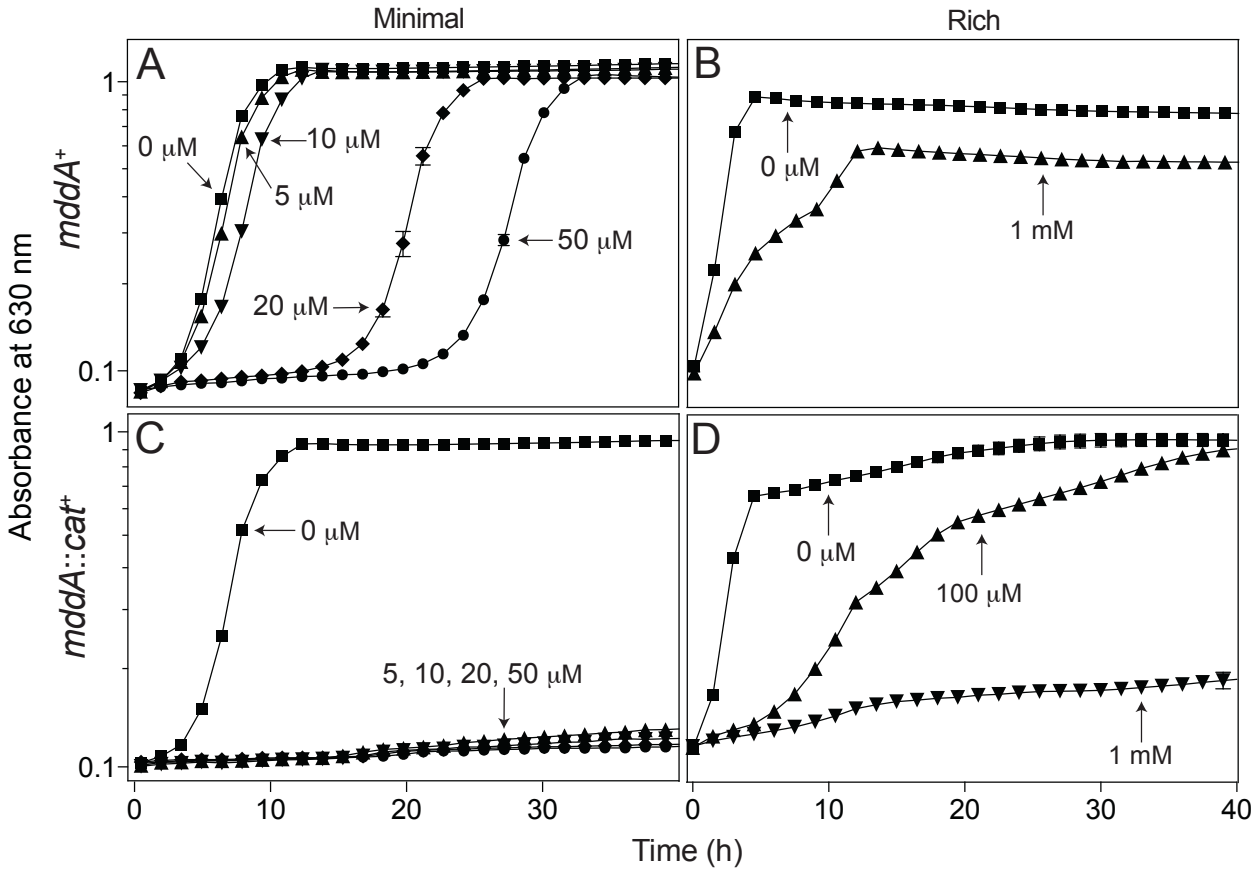

Figure 4.4. The effect of increasing MSX concentration on *mddA*$^+$ and *mddA*::*cat*$^+$ strains is detrimental to growth. Growth of the *S. enterica* strains *mddA*$^+$ and *mddA1*::*cat*$^+$ was examined with increasing concentrations of MSX, as indicated. The minimal medium used was NCE minimal medium with glycerol (22 mM) and the rich medium used was nutrient broth. Growth curves were performed using a microplate reader (Bio-Tek Instruments) as described under *Materials and Methods*. The following strains were analyzed: *mddA*$^+$ (JE10079) and *mddA1*::*cat*$^+$ (JE18333). Error bars represent standard deviation.

Se*MddA* does not block the inhibitory effects of *phosphinothricin (PHO)*. Addition of PHO (100 μM) was inhibitory to *S. enterica* growth, however, both the *mddA* and *mddA*::*cat*$^+$ strains were equally affected, indicating that the deleterious effect of PHO could not be blocked by *Se*MddA (Fig. 4.5). At present, it is unclear whether PHO is acetylated in *S. enterica*, and if so, which acetyltransferase catalyzes the reaction.

The inhibition of a* S. enterica mddA*::*cat$^+$ *strain by MSX or MSO is alleviated by the addition of glutamine or methionine. Glutamate analogues, such as MSX and MSO, inhibit glutamine synthetase (GlnA), which catalyzes the ATP-dependent condensation of glutamate with ammonia to produce glutamine. GlnA function is essential in nitrogen metabolism and MSX has been shown to bind tightly to the enzyme, causing irreversible inhibition of activity (41, 42). This inhibition is partially resolved by the addition of the product, glutamine, bypassing the requirement for GlnA (43). When glutamine (200 μM) was present in the culture medium, an *mddA*::*cat*$^+$ strain exposed to MSX (10 μM) resulted in a modest increase in growth yield, plateauing at OD_{630} ~0.2 (Fig 4.6A). The addition of higher concentrations of glutamine (*i.e.* 500 and 1000 μM) correlated with higher growth yields (Fig. 4.6A), suggesting that saturation of the GlnA active site with glutamine outcompeted binding of the inhibitor.

Growth of an *mddA*::*cat*$^+$ strain exposed to MSO (50 μM) was restored to wild type levels with higher levels of glutamine (*i.e.* 500 and 1000 μM) in the medium (Fig. 4.6C). Addition of glutamine to a *mddA*::*cat*$^+$ strain exposed to either MSX or MSO in rich medium allowed the strain to grow at a rate similar to that of the *mddA*$^+$ strain, and reached a similar growth yield compared to wild type levels (Fig. 4.7). It is clear that MSX and MSO inhibit GlnA activity (41, 44-48), however, it is less clear whether these compounds are inhibiting other cellular processes that could account for the observed growth phenotypes.

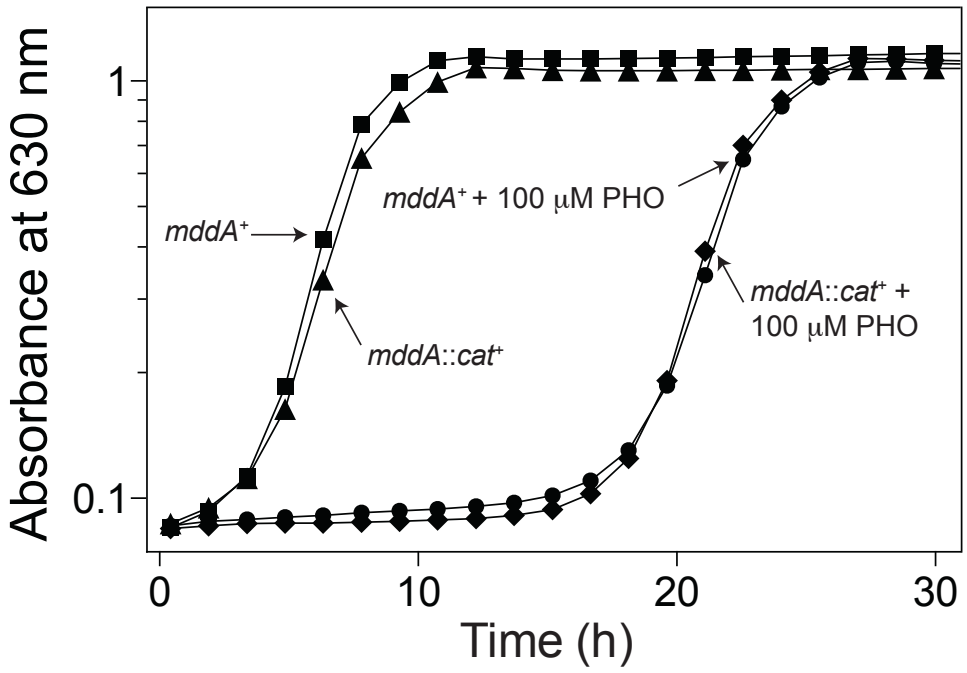

Figure 4.5. *Se*MddA does not prevent growth inhibition by PHO. Growth of the *S. enterica* strains *mddA*$^+$ and *mddA*::*cat*$^+$ was examined with or without PHO (100 μM). NCE minimal medium supplemented with glycerol (22 mM) was used in these experiments. Growth curves were performed using a microplate reader (Bio-Tek Instruments) as described under *Materials and Methods*. The following strains were analyzed: *mddA*$^+$ (JE10079) and *mddA*::*cat*$^+$ (JE18333). Error bars represent standard deviation.

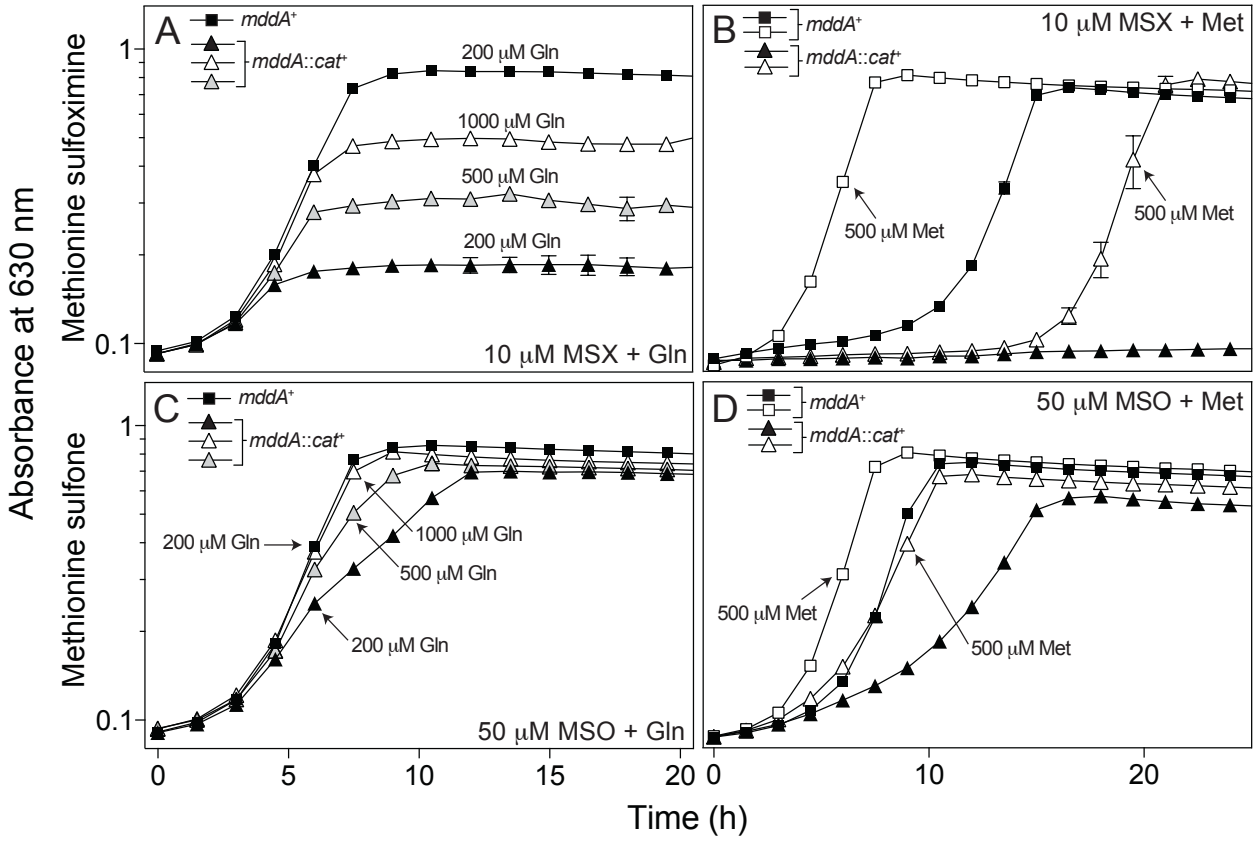

Figure 4.6. Glutamine and methionine counteract the deleterious effects of MSX and MSO on growth in the absence of MddA. Growth of *S. enterica mddA*$^+$ and *mddA*::*cat*$^+$ strains was examined in the presence of MSX (10 μM) and MSO (50 μM), with the addition of glutamine (200 μM, black triangles and squares; 500 μM, gray triangles; 1000 μM, white triangles) or methionine (500 μM, white squares and triangles) to the medium. NCE minimal medium supplemented with glycerol (22 mM) was used in these experiments. Growth curves were performed using a microplate reader (Bio-Tek Instruments) as described under *Materials and Methods*. The following strains were analyzed: *mddA*$^+$ (JE10079) and *mddA*::*cat*$^+$ (JE18333). Error bars represent standard deviation.

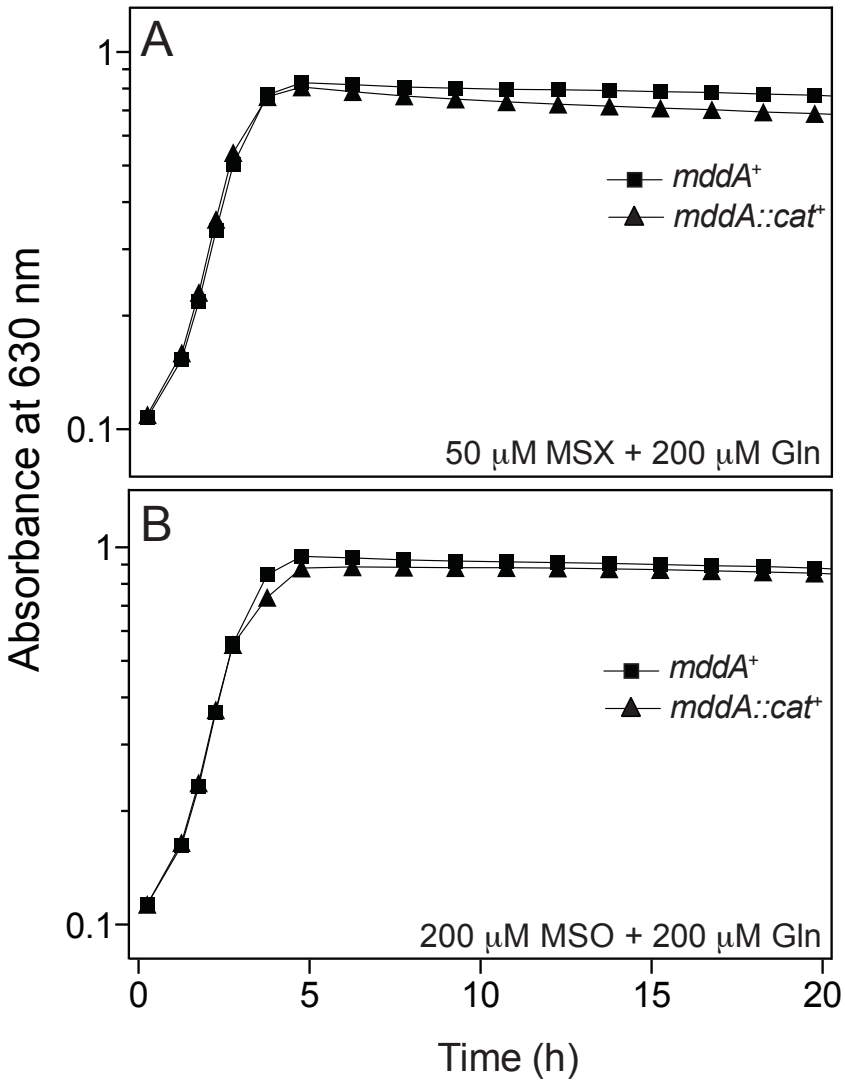

Figure 4.7. Addition of glutamine fully restores growth of an *mddA* strain exposed to MSX and MSO in rich medium. Growth of the *S. enterica* strains *mddA*$^+$ and *mddA1*::*cat*$^+$ was examined with (A) MSX (50 μM) and (B) MSO (100 μM), with the addition of glutamine (200 μM). The medium used was nutrient broth. Growth curves were performed using a microplate reader (Bio-Tek Instruments) as described under *Materials and Methods*. The following strains were analyzed: *mddA*$^+$ (JE10079) and *mddA1*::*cat*$^+$ (JE18333). Error bars represent standard deviation.

Previous work showed that the addition of methionine to wild type *S. enterica* exposed to MSX restored growth (for wild type cultures within 8 h), possibly alleviating toxicity by competing with the uptake of MSX (43). The growth behavior of *mddA*$^{+}$ and *mddA*::*cat*$^{+}$ strains in medium containing methionine (500 μM) and MSX (10 μM), or MSO (50 μM), was investigated (Fig. 4.6B, 4.6D). Addition of methionine improved the growth of a *mddA*::*cat*$^{+}$ strain exposed to MSX, but not to wild type levels. Methionine also decreased MSX toxicity in the *mddA*$^{+}$ strain, resulting in cultures reaching stationary phase ~10 h sooner than cultures growing in the presence of MSX and the absence of methionine (Fig. 4.6B). When MSO was used in lieu of MSX, growth of *mddA*::*cat*$^{+}$ was restored to wild type levels when methionine was added to the culture medium (Fig. 4.6D).

Se*MddA is a dimer in solution.* *Se*MddA^{WT} is a 516-residue, 19.2-kDa protein. *Se*MddA^{WT} and the *Se*MddA^{E82Q} catalytic variant were isolated to 99% homogeneity using Ni-affinity chromatography (see *Materials and Methods*) (Fig. 4.8A). To determine the oligomeric state of the proteins in solution, FPLC gel filtration analysis was performed using commercially available molecular mass standards. Under the conditions tested, *Se*MddA^{WT} and *Se*MddA^{E82Q} eluted ~30 min after injection. The retention time was consistent for a protein whose mass was approximately 40-kDa, when compared to the elution times of molecular mass standards. Since the calculated molecular mass *Se*MddA^{WT} was approximately 19-kDa, we inferred that the *Se*MddA^{WT} was a dimer in solution (Fig. 4.8B). The oligomeric state of *Se*MddA was consistent with MddA homologues from *P. aeurginosa* (PA4866) and *A. baylyi* (ACIAD1637) (12, 13).

Se*MddA^{WT} acetylates toxic methionine derivatives.* Thin layer chromatography (TLC) was used to identify the substrate(s) of *Se*MddA^{WT}. An *in vitro* activity assay was used to monitor the *Se*MddA-dependent transfer the ^{14}C-labeled acetyl moiety from [^{14}C-2]-acetyl-CoA to putative

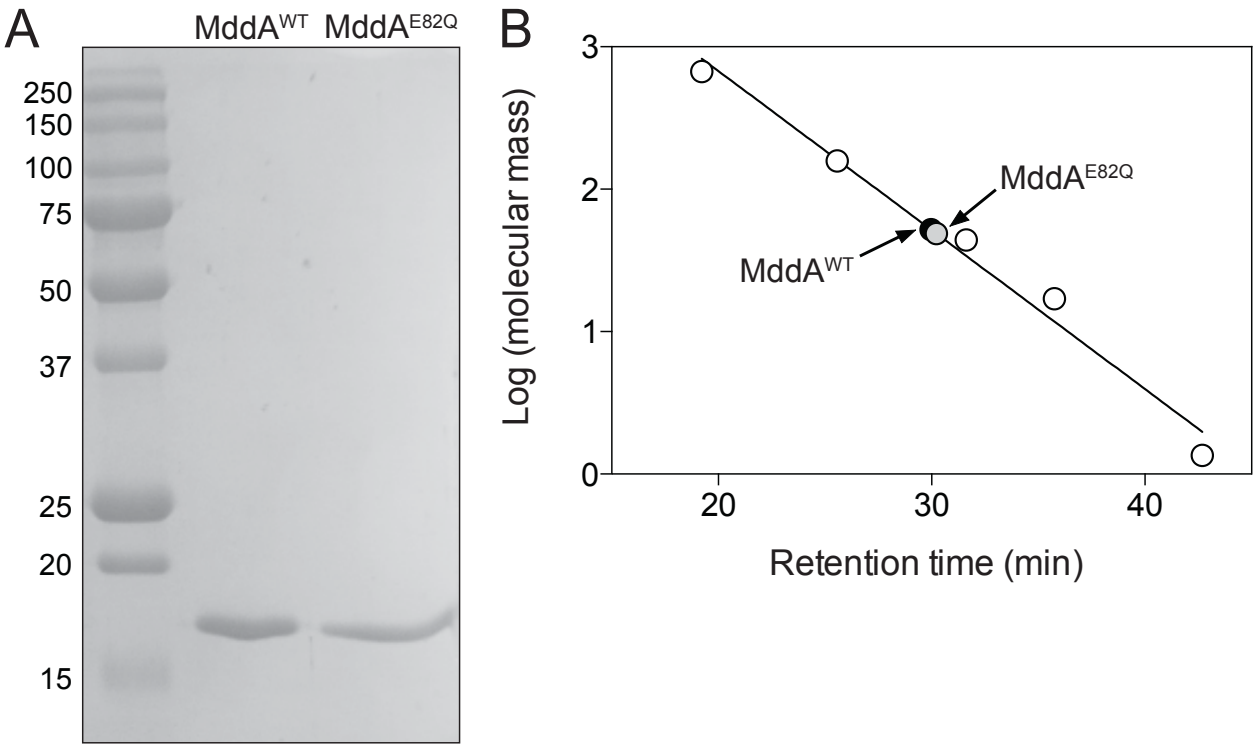

Figure 4.8. *Se*MddA is a dimer in solution. (A) *Se*MddA^{WT} and the catalytic variant *Se*MddA^{E82Q} (~19-kDa) were purified using a two-step nickel affinity purification. An SDS-PAGE gel shows the molecular mass standards (kDa) (lane 1), purified *Se*MddA^{WT} protein (lane 2), and purified *Se*MddA^{E82Q} (lane 3). Both proteins purified to >99% homogeneity. (B) The molecular mass of *Se*MddA^{WT} (black circle) and *Se*MddA^{E82Q} (gray circle) in solution was estimated by gel filtration chromatography as described under *Materials and Methods*. Molecular mass standards (open circles) are thyroglobulin (bovine; 670-kDa), γ-globulin (bovine; 158-kDa), ovalbumin (chicken; 44-kDa), myoglobin (horse; 17-kDa) and vitamin B_{12} (1.35-kDa).

substrates that were analogous in structure to MSX (see *Materials and Methods*). Phosphor imaging showed *Se*MddA^{WT}-dependent acetylation of MSX, MSO, methionine sulfoxide (MS), buthionine sulfoximine (BSX), methionine, and glutamine (Fig. 4.9). Transfer of the radiolabel was not seen when PHO, glutamate, or arginine were used as substrates (Fig. 4.9). To examine the specificity of the *Se*MddA^{WT} protein to acetylate the substrates identified by TLC, a spectrophotometric assay using 5,5'-dithiobis-2-nitrobenzoic acid (DTNB, Ellman's reagent), was utilized to measure the specific activity of *Se*MddA^{WT} for each substrate (see *Materials and methods*) (Table 4.3). *Se*MddA^{WT} had increased activity for MSX (24 ± 0.5) and MSO (23 ± 0.1) μmol CoA min^{-1} mg^{-1}. The other compounds tested (MS, BSX, methionine, and glutamine) were poor substrates for the enzyme compared to MSX, under the conditions tested, with specific activities of ~0.5-2 μmol CoA min^{-1} mg^{-1} (data not shown).

Activity of the *Se*MddA^{E82Q} catalytic variant (negative control) was reduced by >20-fold (1 ± 0.5) compared to *Se*MddA^{WT} (Table 4.3). Although the activity of *Se*MddA^{E82Q} was substantially decreased *in vitro*, the residual activity observed may account for the growth of an *mddA*::*cat*$^{+}$ strain containing a plasmid encoding *Se*MddA^{E82Q} in medium with MSX (10 μM) at high levels of induction (250-1000 μM *L*-(+)-arabinose) (Fig. 4.3).

GNATs can transfer not only acetyl groups but also longer acyl groups (*e.g.* propionyl, succinyl) to their substrates, and several reports demonstrate the physiological relevance of this modification (49, 50). The ability of *Se*MddA^{WT} to propionylate its substrates was also examined. *Se*MddA^{WT} propionylated MSX (14 ± 2.3) and MSO (15 ± 0.1) μmol min^{-1} mg^{-1}, but the specific activities were lower the one observed when acetyl-CoA was used as the acyl donor (Table 4.3). These data indicate that, although *Se*MddA^{WT} has propionylation activity, acetyl-CoA is the preferred co-substrate under the conditions tested.

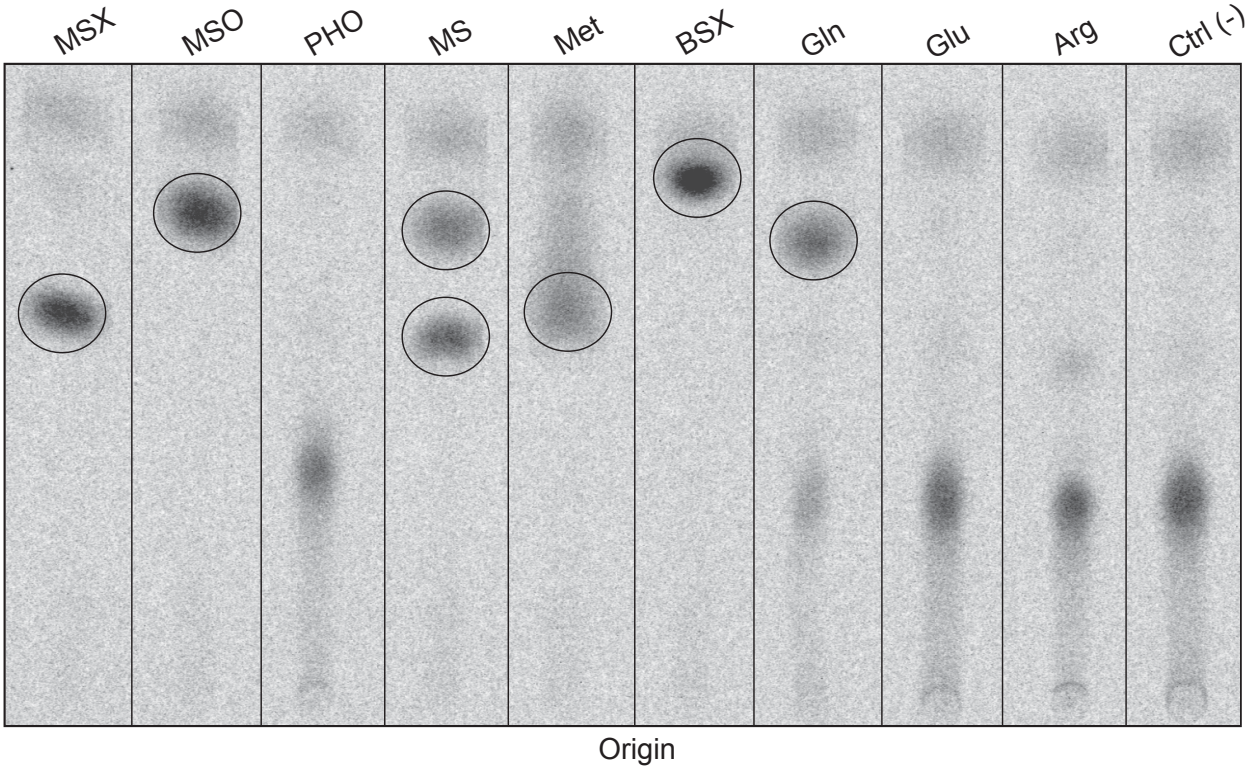

Figure 4.9. *Se*MddA^{WT} acetylates methionine derivatives. The substrate specificity of *Se*MddA^{WT} was examined using thin layer chromatography. Reactions included 1 µg of *Se*MddA^{WT} or *Se*MddA^{E82Q} (neg. ctrl), [1-^{14}C]-acetyl-CoA, and 0.5 mM of substrate. After exposure of the TLC plate to a phosphor screen the resulting image was detected using a Typhoon Trio+ Variable Mode Imager (GE Healthcare).

Table 4.3. Kinetic Parameters[a] for *S. enterica* MddA^{WT}.

Substrate	$K_{M(app)}$ (μM)	$k_{cat(app)}$ (s^{-1})	k_{cat}/K_M (M^{-1} s^{-1})
MSX	576.3 ± 89	34.5 ± 2.0	6.0 x 10^4
MSO	229.5 ± 56	30.6 ± 1.7	1.3 x 10^5
Acetyl-CoA	155.7 ± 41	23.4 ± 1.4	1.5 x 10^5

[a] Values represent average mean ± standard deviation

Table 4.3. *Se*MddA^{WT} acetylates MSX and MSO. Specific activity of the *Se*MddA^{WT} protein for MSX and MSO was measured using a spectrophotometric assay described under *Materials and Methods*. Both acetyl-CoA and propionyl-CoA were tested as acyl donors. The catalytic variant *Se*MddA^{E82Q} was used as negative control. Experiments were performed in technical duplicates in three independent experiments. Values represent specific activity (μmol of CoA produced per min per mg of protein); ± standard deviation for each substrate.

Location of acetylation of MSX and MSO. To confirm the location of acetylation of MSX and MSO, acetyl-MSX and acetyl-MSO were generated enzymatically (see *Materials and Methods*), and the structures resolved by mass spectrometry (Protein and Mass Spectrometry Facility, UGA). Signals for the predicted masses of acetylated MSX (221 *m/z*) and acetylated MSO (222 *m/z*) were observed using ESI MS (data not shown). LC/MS/MS of the acetyl-MSX signal resulted in a strong peak at 142 *m/z* (data not shown), indicative of the acetyl group being located at the carboxy end of the molecule.

S. enterica *cannot use MSX or acetyl-MSX as a source of methionine*. To try to understand the fate of Ac-MSX, the ability of this compound to be utilized by *S. enterica* as a methionine source was tested. A methionine auxotroph (JE6583, *metE mddA*$^+$) was grown in minimal medium that lacked methionine (negative control), contained methionine (positive control; 100 μM), MSX (100 μM), or methionine and MSX (100 μM each). Growth was only observed when methionine was present (Fig. 4.10). These results indicated that neither MSX nor its acetylated form, as the strain was *mddA*$^+$, could be utilized by *S. enterica* to generate methionine, or at least not to levels high enough to restore growth of the methionine auxotroph.

An* mddA$^+$ *strain displays biphasic growth at higher MSX concentrations with the addition of glutamine. Growth of the *mddA*$^+$ strain (JE10079) exposed to MSX with the addition of glutamine (200 μM) was examined at varying concentrations of MSX (50-200 μM). Under these conditions, cultures of the *mddA*$^+$ strain exhibited biphasic growth, with the initial growth onset occurring at the same time, followed by a plateau with an increasing lag phase. The observed lag in growth correlated with higher concentrations of MSX when greater than 5 μM MSX (Fig. 4.11A). Interestingly, after the onset of growth the growth rate for all conditions was similar [doubling time: 1.4 (5 μM), 2.1 (50 μM), 2.4 (100 μM), 3.2 (200 μM)].

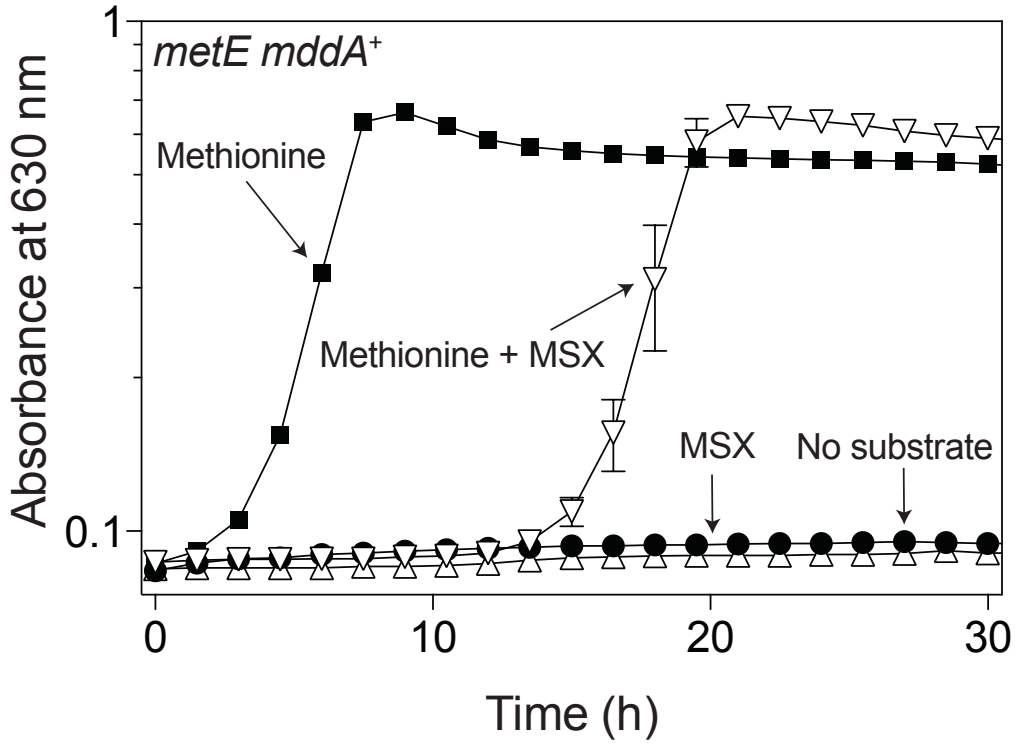

Figure 4.10. Neither MSX nor acetyl-MSX permits growth of a methionine auxotroph in *S. enterica*. Growth of an *S. enterica* strain auxotrophic for methionine (*metE mddA*$^+$) was tested in NCE minimal medium (glycerol, 22 mM) in the absence of methionine, methionine (100 μM), MSX (100 μM), or methionine and MSX (100 μM each). Growth curves were performed using a microplate reader (Bio-Tek Instruments) as described under *Materials and Methods*. The strain analyzed was *metE205 mddA*$^+$ (JE6583). Error bars represent standard deviation.

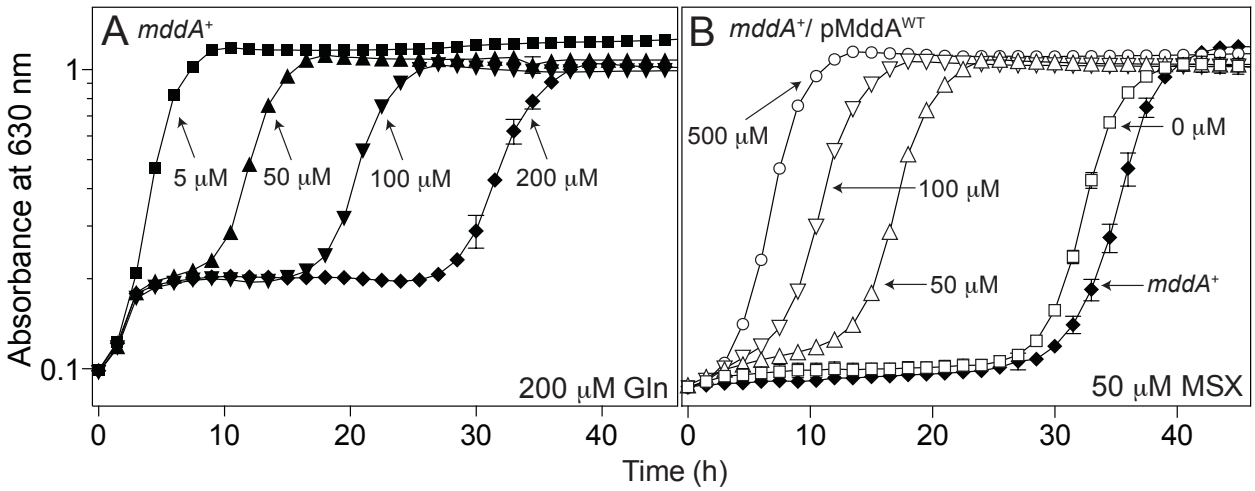

Figure 4.11. An *mddA*$^+$ strain exhibits biphasic growth in minimal medium containing glutamine and MSX. (A) Growth of the *S. enterica mddA*$^+$ strain in NCE minimal medium supplemented with glycerol (22 mM) was examined in the presence of glutamine (200 μM) and increasing concentrations of MSX (5-200 μM), as indicated. The strain analyzed was *mddA*$^+$ (JE10079). (B) Growth of the *S. enterica mddA*$^+$ / pMDD8 *mddA*$^+$ strain was examined in the same medium in the presence of MSX (50 μM) and increasing concentrations of inducer (*L*-(+)-arabinose, 50-500 μM), as indicated. The strain analyzed was *mddA*$^+$ / pMDD8 *mddA*$^+$ (JE18955). Growth curves were performed using a microplate reader (Bio-Tek Instruments) as described under *Materials and Methods*. Error bars represent standard deviation.

Ectopic overexpression of* mddA$^+$ *provides resistance to higher concentrations of MSX. A *mddA*$^+$ strain carrying *mddA*$^+$ on an plasmid under the control of an inducible promoter (JE18961) was grown in minimal medium with MSX (50 μM) and varying levels of inducer (50-500 μM *L*-(+)-arabinose). At higher concentrations of inducer, cultures of strain JE18961 grew with shorter lag times when compared to the non-induced control (Fig. 4.11B). These data were consistent with the idea that increased *Se*MddA protein levels provided greater protection against the toxic effects of MSX.

Identification of genetic loci whose functions are required for MSX toxicity. We took a genetic approach to find loss-of-function derivatives of a *mddA*::*cat*$^+$ (JE18333) strain that grew in the presence of MSX (10 μM). For this purpose, a P22 phage lysate grown on a pool of *S. enterica mddA*::*cat*$^+$ strains carrying Tn*10*d(*tet*$^+$) elements randomly inserted in the chromosome was used as donor to transduce the strain *mddA*::*cat*$^+$ to tetracycline resistance (for details see *Materials and Methods*). Tetracycline-resistant (Tet^R) colonies were replica printed onto minimal medium supplemented with glycerol (22 mM), tetracycline (20 μg ml^{-1}), and MSX (10 μM). Strains that grew this condition were analyzed further. To confirm that growth of the *mddA*::*cat*$^+$ strain was due to the inheritance of a Tn*10*d(*tet*$^+$) element, P22 phage was grown on these strains to generate a phage lysate that was used as donor to transduce the original *mddA*::*cat*$^+$ recipient strain to Tet^R. After freeing the reconstructed strain from phage, the location of the transposon insertion was identified by arbitrary PCR and subsequent DNA sequencing (40).

One of ~50,000 Tet^R colonies grew on medium containing MSX after re-construction. The transposon insertion in this strain was located within the *glnP* gene (insertion at bp 384 out of 660), which encodes the membrane component subunit of the glutamine ABC transporter GlnHPQ (Fig. 4.12A). The re-constructed *mddA*::*cat*$^+$ *glnP*::Tn*10*d(*tet*$^+$) strain (JE20027) grew

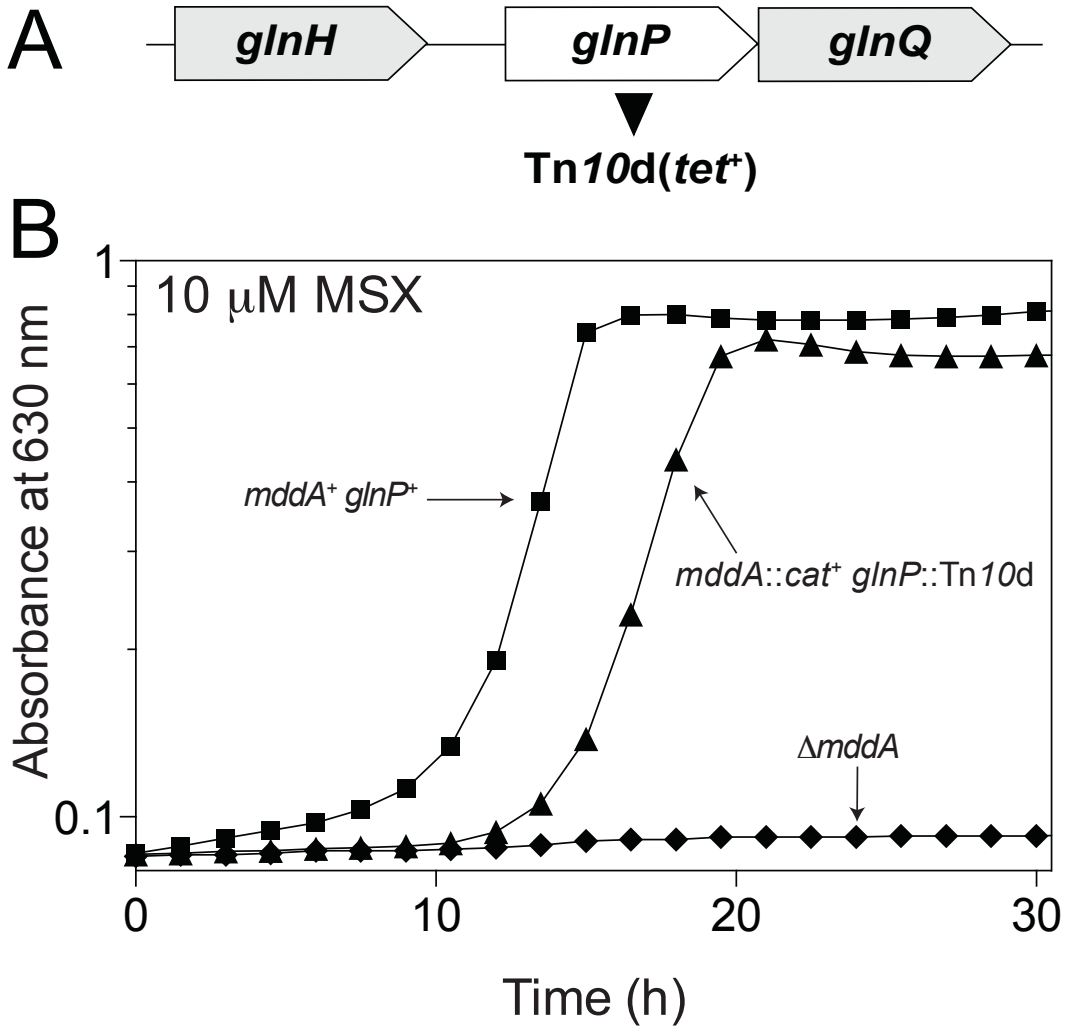

Figure 4.12. Growth of the *mddA*::*cat*$^+$ *glnP*::Tn*10*d strain in the presence of MSX. (A) Transposon mutagenesis (Tn*10*d(*tet*$^+$)) of an *mddA*::*cat*$^+$ strain identified that inactivation of the *glnHPQ* (glutamine permease) restored growth in the presence of MSX (10 μM). (B) Growth of the reconstructed *S. enterica mddA1*::*cat*$^+$ *glnP1561*::Tn*10*d strain identified in the mutagenesis screen was examined in NCE minimal medium supplemented with glycerol (22 mM) and MSX (10 μM). Growth curves were performed using a microplate reader (Bio-Tek Instruments) as described under *Materials and Methods*. The following strains were analyzed: *mddA*$^+$ *glnP*$^+$ (JE10079), Δ*mddA2* (JE18622), and *mddA1*::*cat*$^+$ *glnP1561*::Tn*10*d (JE20027). Error bars represent standard deviation.

on minimal medium containing MSX (10 μM) (Fig. 4.12B, solid triangles). Identification of this mutant was not surprising, as the amino acid transporters MetNIQ (methionine permease) and GlnHPQ (glutamine permease) are responsible for transporting MSX in *S. enterica*. To our knowledge, transport of MSO has not been investigated (51).

Deletion of two amino acid transport systems relieves MSX toxicity. A deletion of *glnP* in combination with *glnQ* (ATP-binding subunit, strain JE20064) was constructed to ensure that the cell was devoid of transporter. Growth of the *mddA*$^+$ and Δ*mddA* strains in the absence of GlnPQ was examined in medium containing MSX (20 μM) (Fig. 4.13A). A *glnPQ*::*cat*$^+$ strain (JE20064) exposed to MSX reached stationary phase faster than the wild type strain (~10 h) (Fig. 4.13A, inverted solid triangles). A Δ*mddA glnPQ*::*cat*$^+$ strain (JE20065) displayed an increased lag phase compared to the wild-type strain, but once the culture started growing it did so at a rate similar to that of the *glnPQ mddA*$^+$ strain (Fig. 4.13A, open diamonds). Ectopic synthesis of *glnPQ* in the Δ*mddA glnPQ*::*cat*$^+$ strain (JE20073) restored the transport of MSX and abolished growth in medium containing MSX (Fig. 4.13A, open circles).

Transport of MSX has been examined in *S. enterica* in relation to the transport of amino acids (Met) (52, 53). These studies demonstrated that the uptake of MSX and methionine sulfoxide was inhibited when both glutamine permease (GlnHPQ) and methionine permease (MetNIQ) were blocked. As seen in figure 3.13B, growth of a Δ*mddA glnPQ*::*cat*$^+$ *metNI*::*kan*$^+$ strain (JE20067) lacking both transporters was examined in the presence MSX. Strain JE20067 grew better than the wild-type strain, with no observed lag when MSX was added to the medium (Fig. 4.13B, open squares). The Δ*mddA metNI*::*kan*$^+$ strain behaved similarly to Δ*mddA glnPQ*::*cat*$^+$ strain (Fig. 4.13B, open diamonds).

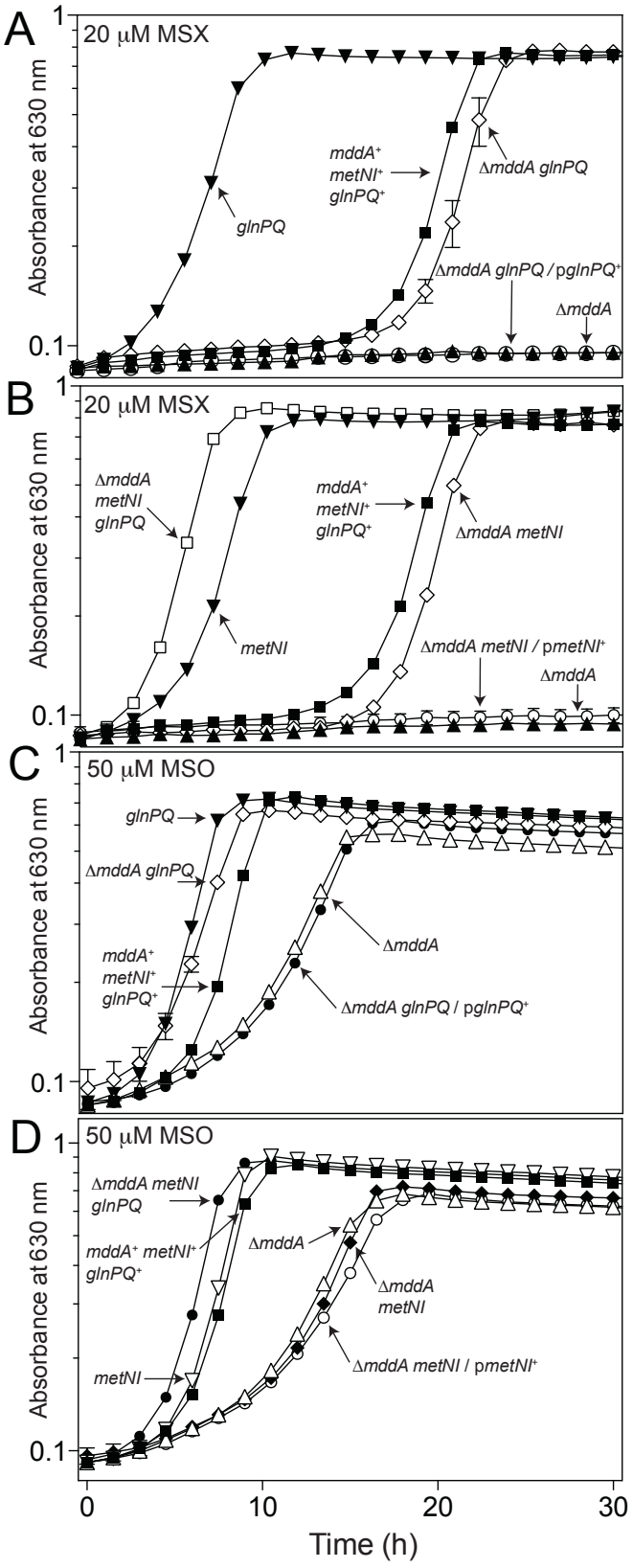
A
20 μM MSX
Absorbance at 630 nm
1
0.1
mddA+ metNI+ glnPQ+
ΔmddA glnPQ
glnPQ
ΔmddA glnPQ / pglnPQ+
ΔmddA
B
20 μM MSX
ΔmddA metNI glnPQ
mddA+ metNI+ glnPQ+
ΔmddA metNI
metNI
ΔmddA metNI / pmetNI+
ΔmddA
C
50 μM MSO
glnPQ
ΔmddA glnPQ
ΔmddA
mddA+ metNI+ glnPQ+
ΔmddA glnPQ / pglnPQ+
D
50 μM MSO
ΔmddA metNI glnPQ
ΔmddA
mddA+ metNI+ glnPQ+
ΔmddA metNI
metNI
ΔmddA metNI / pmetNI+
0
10
20
30
Time (h)

Figure 4.13. Deletion of two amino acid transporters (GlnHPQ, MetNIQ) restores growth of a Δ*mddA* strain exposed to MSX and MSO. (A, B, C, D) Growth of *S. enterica mddA*$^+$ and Δ*mddA* strains with or without the glutamine permease (*glnPQ*) or methionine permease (*metNI*) was examined in the presence of MSX (20 μM) or MSO (50 μM) in NCE minimal medium with glycerol (22 mM). Plasmids were induced with 10 μM *L*-(+)-arabinose. Growth curves were performed using a microplate reader (Bio-Tek Instruments) as described under *Materials and Methods*. The following strains were analyzed: *mddA*$^+$ *glnPQ*$^+$ *metNI*$^+$ (JE10079), Δ*mddA* (JE18622), *glnPQ*::*cat*$^+$ (JE20064), Δ*mddA glnPQ*::*cat*$^+$ (JE20065), *metNI*::*kan*$^+$ (JE19583), Δ*mddA metNI*::*kan*$^+$ (JE19730), Δ*mddA metNI*::*kan*$^+$ *glnPQ*::*cat*$^+$ (JE20067), Δ*mddA glnPQ*::*cat*$^+$ / pGLN2 *glnPQ*$^+$ (JE20073), and Δ*mddA metNI*::*kan*$^+$ / pMETN1 *metNI*$^+$ (JE20329). Error bars represent standard deviation.

Ectopic synthesis of MetNI in the Δ*mddA metNI*::*kan*$^+$ strain background also failed to support growth in the presence of MSX, confirming that GlnHPQ and MetNIQ transport MSX into the cell, and that deletion of these two systems supports growth of an *mddA* strain on medium containing MSX (Fig. 4.13B, open circles). It is interesting to note that in either the Δ*mddA glnPQ*::*cat*$^+$ or the Δ*mddA metNI*::*cat*$^+$, growth occurred at a rate similar to the *mddA*$^+$ strain with only a longer lag phase.

MSO is transported by GlnHPQ but not by MetNIQ. Similar growth experiments using the above-mentioned strains were carried out with the addition of MSO (50 μM) to investigate the transport of MSO (Fig. 4.13C, 4.13D). A deletion of *glnPQ* in a Δ*mddA* strain background (JE20065) restored growth to wild-type levels (Fig. 4.13C, open diamonds), indicating a decrease in the amount of MSO being transported into the cell. This effect was reversed when *glnPQ*$^+$ were expressed *in trans* (Fig. 4.13C, solid circles).

Surprisingly, the kinetics of growth of the Δ*mddA*$^+$ *metNI*::*kan*$^+$ strain (JE19730; Fig. 4.13D, solid diamonds) and Δ*mddA* strain (JE18622; Fig. 4.13D, open triangles) in the presence of MSO were very similar, demonstrating that deletion of the methionine transporter did not prevent sufficiently inhibitory levels of MSO from entering the cell. Expression of *metNI*$^+$ *in trans* in the Δ*mddA*$^+$ *metNI*::*kan*$^+$ strain (JE20329; Fig. 4.13D open circles) resulted in growth that was similar to that of the Δ*mddA* strain (Fig. 4.13D, open triangles). Taken together, these results imply that unlike MSX and methionine sulfoxide, MSO is not transported through the methionine permease.

DISCUSSION

Se*MddA is necessary for cell survival in the presence of MSX in minimal but not rich medium conditions.* On minimal medium, *S. enterica* strains lacking MddA cannot grow in the presence of MSX; however, in rich medium a higher concentration (5x) of MSX is needed to observe even a delay in growth (Fig. 4.2). This raises the question as to what enzymes or metabolites are present under rich medium conditions that help prevent MSX toxicity in the absence of MddA. One explanation could be differences in the availability of glutamine or methionine in rich *versus* minimal medium, since the addition of these compounds restore growth of a Δ*mddA* strain in the presence of MSX (Fig. 4.6). Other possibilities include increased expression of *glnA* (the gene encoding the enzyme known to be affected by MSX) or the presence of antioxidant compounds, in rich medium conditions.

Se*MddA does not acetylate phosphinothricin (PHO).* *Se*MddA and its homologues have been annotated as PHO acetyltransferases (like the Bar protein of *Streptomyces* spp.), an activity that MddA homologues in several organisms do not posses (12, 13). Although PHO is inhibitory to *S. enterica* when present at 100 μM, it is clear that the deleterious effect of PHO is affected by the absence or presence of MddA (Fig. 4.5). In contrast, our data support the conclusion that a physiological role of MddA in *S. enterica* is to block the harmful effects of oxidized methionine derivatives such as methionine sulfoximine (MSX) and methionine sulfone (MSO) (Fig. 4.2, 4.11, Table 4.3).

The fact that *Se*MddA can acetylate MSX and MSO, but not PHO, suggests a relative high degree of specificity of the enzyme for structural analogues to its *bona fide* substrates (Fig. 4.2, 4.5). There are, however, examples of homologues of the *Streptomyces* Bar protein that efficiently acetylate PHO and MSX. Such homologues are found in *Streptomyces hygroscopicus*

and *Rhodococcus* spp. (19, 54). Whether PHO is acetylated by another *S. enterica* GNAT remains an open question.

Expression of mddA is induced in response to MSX. In the presence of glutamine with increasing concentrations of MSX, an *mddA*$^+$ strain grows biphasically. Clearly, the addition of glutamine allows for the initial onset of growth, but at a certain point the cell either runs out of available glutamine, or GlnA is inhibited by MSX, leading to growth arrest (Fig. 4.11). Not surprisingly, the higher the concentration of MSX, the longer growth arrest lasts. We hypothesize that during growth arrest there may be an increase in the expression of *mddA*$^+$ in response to the level of MSX. Once the latter is acetylated and rendered innocuous, the cell can resume growth, a conclusion that is supported by the fact that growth rates remain similar as soon as growth is restored.

How does a strain devoid of MddA and either transporter grow in the presence of MSX? On the basis of growth data presented (Fig. 4.12, 4.13), we conclude that a deletion of only one of the MSX transport systems still allows inhibitory concentrations of MSX into the cell, which raises the question of how the *mddA glnPQ* and *mddA metNI* strains can survive the toxic effects of MSX. A plausible explanation is the existence of an enzyme with *Se*MddA-like activity whose k_{cat} for MSX is slower than that of *Se*MddA, but sufficient to support growth under such conditions. Examples of redundant functions in cells are not rare [*e.g.* MetE, MetH (methionine synthases); PurN, PurT (glycinamide ribonucleotide transformylase), etc]). It should also be noted that mutations in GlnA have been characterized which prevent MSX binding and inhibition while retaining activity (55, 56). It is also interesting to note that the while both MSX and methionine sulfoxide are transported through the methionine permease, MetNIQ, our data

indicate that the structural analogue MSO is not (Fig. 4.13), shedding light on the specificity of the MetNIQ transporter.

Why does* Se*MddA acetylate oxidized methionine derivatives? There is precedent for the role of GNATs in detoxifying toxic compounds (5, 11), by using acetylation as a means to inactivate antibiotics. While our data clearly demonstrate that MddA of *S. enterica* can prevent the deleterious effects of MSX and MSO (Fig. 4.2, 4.11), it is less clear what environmental conditions expose *S. enterica* to MSX and MSO.

MSX has been identified in processed foods (1940's) and naturally occurs in the roots and stems of some plant species (20). It is also possible that these compounds are produced as a consequence of the host response and reactive nitrogen or oxygen species (57), or synthesized endogenously as a by-product of a normal metabolic process (58), which would not be unprecedented for *S. enterica*. Oxidation of methionine residues of proteins can generate methionine sulfoxide, but no studies looking at protein oxidation have detected the production of MSO (59-61). Although the source of MSX and MSO are currently unknown, MddA function is necessary for *S. enterica* growth when these compounds are present. Future studies aim to understand the role of acetylation with respect to environmental stressors.

ACKNOWLEDGEMENTS

The authors have declared that no competing interests exist. This work was supported by USPHS grant R01 GM062203 to J.C.E.-S. We thank James N. Workman and Rachel Burckhardt for technical assistance.

REFERENCES

1. **Thao S, Escalante-Semerena JC.** 2011. Control of protein function by reversible *N*(ε)-lysine acetylation in bacteria. *Curr. Opin. Microbiol.* **14:**200-204.
2. **Bernal V, Castano-Cerezo S, Gallego-Jara J, Ecija-Conesa A, de Diego T, Iborra JL, Canovas M.** 2014. Regulation of bacterial physiology by lysine acetylation of proteins. *N. Biotechnol.* 31:586-95.
3. **Tanaka S, Matsushita Y, Yoshikawa A, Isono K.** 1989. Cloning and molecular characterization of the gene *rimL* which encodes an enzyme acetylating ribosomal protein L12 of *Escherichia coli* K12. *Mol. Gen. Genet.* **217:**289-293.
4. **Yoshikawa A, Isono S, Sheback A, Isono K.** 1987. Cloning and nucleotide sequencing of the genes *rimI* and *rimJ* which encode enzymes acetylating ribosomal proteins S18 and S5 of *Escherichia coli* K12. *Mol. Gen. Genet.* **209:**481-488.
5. **Wright GD, Ladak P.** 1997. Overexpression and characterization of the chromosomal aminoglycoside 6'-*N*-acetyltransferase from *Enterococcus faecium*. *Antimicrob. Agents Chemother.* **41:**956-960.
6. **Marvil DK, Leisinger T.** 1977. *N*-acetylglutamate synthase of *Escherichia coli*: purification, characterization, and molecular properties. *J. Biol. Chem.* **252:**3295-32303.
7. **Fukuchi J, Kashiwagi K, Takio K, Igarashi K.** 1994. Properties and structure of spermidine acetyltransferase in *Escherichia coli*. *J. Biol. Chem.* **269:**22581-22585.
8. **Errey JC, Blanchard JS.** 2006. Functional annotation and kinetic characterization of PhnO from *Salmonella enterica*. *Biochemistry*. **45:**3033-3039.

9. **Hung MN, Rangarajan E, Munger C, Nadeau G, Sulea T, Matte A.** 2006. Crystal structure of TDP-fucosamine acetyltransferase (WecD) from *Escherichia coli*, an enzyme required for enterobacterial common antigen synthesis. *J. Bacteriol.* **188:**5606-5617.

10. **Ikeuchi Y, Kitahara K, Suzuki T.** 2008. The RNA acetyltransferase driven by ATP hydrolysis synthesizes N4-acetylcytidine of tRNA anticodon. *Embo J.* **27:**2194-2203.

11. **Wolf E, Vassilev A, Makino Y, Sali A, Nakatani Y, Burley SK.** 1998. Crystal structure of a GCN5-related *N*-acetyltransferase: *Serratia marcescens* aminoglycoside 3-N-acetyltransferase. *Cell.* **94:**439-449.

12. **Davies AM, Tata R, Snape A, Sutton BJ, Brown PR.** 2009. Structure and substrate specificity of acetyltransferase ACIAD1637 from *Acinetobacter baylyi* ADP1. *Biochimie.* **91:**484-489.

13. **Davies AM, Tata R, Beavil RL, Sutton BJ, Brown PR.** 2007. *L*-Methionine sulfoximine, but not phosphinothricin, is a substrate for an acetyltransferase (gene PA4866) from *Pseudomonas aeruginosa*: structural and functional studies. *Biochemistry.* **46:**1829-1839.

14. **Vetting MW, Carvalho LPSd, Yu M, Hegde SS, Magnet S, Roderick SL, Blanchard JS.** 2005. Structure and functions of the GNAT superfamily of acetyltransferases. *Arch. Biochem. Biophys.* **433:**212-226.

15. **Deblock M, Botterman J, Vandewiele M, Dockx J, Thoen C, Gossele V, Movva NR, Thompson C, Vanmontagu M, Leemans J.** 1987. Engineering herbicide resistance in plants by expression of a detoxifying enzyme. *EMBO J.* **6:**2513-2518.

16. **Ogawa Y, Tsuruoka T, Inoue S, Niida T.** 1973. Studies on a new antibiotic SF-1293. II. Chemical structure of antibiotic SF-1293. *Sci. Rep. Meijii Kaisha*. **13:**42-48.

17. **Murakami T, Anzai H, Imai S, Satoh A, Nagaoka K, Thompson CJ.** 1986. The bialaphos biosynthetic genes of *Streptomyces-Hygroscopicus* - Molecular-cloning and characterization of the gene-cluster. *Mol. Gen. Genet.* **205:**42-50.

18. **Circello BT, Eliot AC, Lee JH, van der Donk WA, Metcalf WW.** 2010. Molecular cloning and heterologous expression of the dehydrophos biosynthetic gene cluster. *Chem. Biol.* **17:**402-411.

19. **Maughan SC, Cobbett CS.** 2003. Methionine sulfoximine, an alternative selection for the bar marker in plants. *J. Biotech.* **102:**125-128.

20. **Jeannoda VL, Rakoto-Ranoromalala DA, Valisolalao J, Creppy EE, Dirheimer G.** 1985. Natural occurrence of methionine sulfoximine in the Connaraceae family. *J. Ethnopharmacol.* **14:**11-17.

21. **Bentley HR, Booth RG, et al.** 1948. Action of nitrogen trichloride on proteins; production of toxic derivative. *Nature.* **161:**126.

22. **Bentley HR, Mc DE, et al.** 1949. Action of nitrogen trichloride (agene) on proteins; isolation of crystalline toxic factor. *Nature.* **164:**438.

23. **Bentley HR, Mc DE, et al.** 1949. Action of nitrogen trichloride on proteins; progress in the isolation of the toxic factor. *Nature.* **163:**675.

24. **Shaw CA, Bains JS.** 1998. Did consumption of flour bleached by the agene process contribute to the incidence of neurological disease? *Med. Hypotheses.* **51:**477-481.

25. **Blin M, Crusio WE, Hevor T, Cloix JF.** 2002. Chronic inhibition of glutamine synthetase is not associated with impairment of learning and memory in mice. *Brain res. bull.* **57:**11-15.

26. **Berkowitz D, Hushon JM, Whitfield HJ, Jr., Roth J, Ames BN.** 1968. Procedure for identifying nonsense mutations. *J. Bacteriol.* **96:**215-220.

27. **Balch WE, Wolfe RS.** 1976. New approach to the cultivation of methanogenic bacteria: 2-mercaptoethanesulfonic acid (HS-CoM)-dependent growth of *Methanobacterium ruminantium* in a pressurized atmosphere. *Appl. Environ. Microbiol.* **32:**781-791.

28. **Way JC, Davis MA, Morisato D, Roberts DE, Kleckner N.** 1984. New Tn*10* derivatives for transposon mutagenesis and for construction of LacZ operon fusions by transposition. *Gene*. **32:**369-379.

29. **Davis RW, Botstein D, Roth JR.** 1980. A manual for genetic engineering: advanced bacterial genetics. Cold Spring Harbor Laboratory Press, Cold Spring Harbor, NY.

30. **Schmieger H.** 1971. The fate of the bacterial chromosome in P22-infected cells of *Salmonella typhimurium*. *Mol. Gen. Genet.* **110:**238-244.

31. **Schmieger H, Backhaus H.** 1973. The origin of DNA in transducing particles in P22-mutants with increased transduction-frequencies (HT-mutants). *Mol. Gen. Genet.* **120:**181-190.

32. **Chan RK, Botstein D, Watanabe T, Ogata Y.** 1972. Specialized transduction of tetracycline resistance by phage P22 in *Salmonella typhimurium*. II. Properties of a high-frequency-transducing lysate. *Virology.* **50:**883-898.

33. **Datsenko KA, Wanner BL.** 2000. One-step inactivation of chromosomal genes in *Escherichia coli* K-12 using PCR products. *Proc. Natl. Acad. Sci. USA.* **97:**6640-6645.

34. **Galloway NR, Toutkoushian H, Nune M, Bose N, Momany C.** 2013. Rapid cloning for protein crystallography using Type IIS restriction enzymes. *Cryst. Growth Des.* **13:**2833-2839.

35. **Guzman LM, Belin D, Carson MJ, Beckwith J.** 1995. Tight regulation, modulation, and high-level expression by vectors containing the arabinose PBAD promoter. *J. Bacteriol.* **177:**4121-4130.

36. **Rocco CJ, Dennison KL, Klenchin VA, Rayment I, Escalante-Semerena JC.** 2008. Construction and use of new cloning vectors for the rapid isolation of recombinant proteins from *Escherichia coli*. *Plasmid.* **59:**231-237.

37. **Blommel PG, Fox BG.** 2007. A combined approach to improving large-scale production of tobacco etch virus protease. *Protein Expr. Purif.* **55:**53-68.

38. **Ellman GL, Courtney KD, Andres V, Jr., Feather-Stone RM.** 1961. A new and rapid colorimetric determination of acetylcholinesterase activity. *Biochem. Pharmacol.* **7:**88-95.

39. **Griffith KL, Wolf RE, Jr.** 2002. Measuring beta-galactosidase activity in bacteria: cell growth, permeabilization, and enzyme assays in 96-well arrays. *Biochem. Biophys. Res. Commun.* **290:**397-402.

40. **Caetano-Anolles G.** 1993. Amplifying DNA with arbitrary oligonucleotide primers. *PCR Methods Appl.* **3:**85-94.

41. **Ronzio RA, Rowe WB, Meister A.** 1969. Studies on mechanism of Inhibition of glutamine synthetase by methionine sulfoximine. *Biochemistry.* **8:**1066-1075.

42. **Liaw SH, Eisenberg D.** 1994. Structural model for the reaction mechanism of glutamine synthetase, based on five crystal structures of enzyme-substrate complexes. *Biochemistry.* **33:**675-681.

43. **Steimerv K, Brenchley J.** 1974. Characterization of *Salmonella typhimurium* strains sensitive and resistant to methionine sulfoximine. *J. Bacteriol.* **119:**848-856.

44. **Wedler FC, Sugiyama Y, Fisher KE.** 1982. Catalytic Cooperativity and Subunit Interactions in *Escherichia coli* Glutamine Synthetase - Binding and Kinetics with Methionine Sulfoximine and Related Inhibitors. *Biochemistry.* **21:**2168-2177.

45. **Rowe WB, Ronzio RA, Meister A.** 1969. Inhibition of glutamine synthetase by methionine sulfoximine. Studies on methionine sulfoximine phosphate. *Biochemistry.* **8:**2674-2680.

46. **Crespo JL, Guerrero MG, Florencio FJ.** 1999. Mutational analysis of Asp51 of *Anabaena azollae* glutamine synthetase. D51E mutation confers resistance to the active site inhibitors *L*-methionine-*DL*-sulfoximine and phosphinothricin. *Eur. J. Biochem.* **266:**1202-1209.

47. **Brenchley J.** 1973. Effect of methionine sulfoximine and methionine sulfone on glutamate synthesis in *Klebsiella aerogenes*. *J. Bacteriol.* **114:**666-673.

48. **Rowe WB, Meister A.** 1973. Studies on inhibition of glutamine synthetase by methionine sulfone. *Biochemistry.* **12:**1578-1582.

49. **Berndsen CE, Albaugh BN, Tan S, Denu JM.** 2007. Catalytic mechanism of a MYST family histone acetyltransferase. *Biochemistry.* **46:**623-629.

50. **Garrity J, Gardner JG, Hawse W, Wolberger C, Escalante-Semerena JC.** 2007. *N*-lysine propionylation controls the activity of propionyl-CoA synthetase. *J. Biol. Chem.* **282:**30239-30245.

51. **Betteridge PR, Ayling PD.** 1975. The role of methionine transport-defective mutations in resistance to methionine sulphoximine in *Salmonella typhimurium*. *Mol. Gen. Genet.* **138:**41-52.

52. **Kadner RJ.** 1977. Transport and utilization of *D*-methionine and other methionine sources in *Escherichia coli*. *J. Bacteriol.* **129:**207-216.

53. **Ayling PD.** 1981. Methionine sulfoxide is transported by high-affinity methionine and glutamine transport systems in *Salmonella typhimurium*. *J. Bacteriol.* **148:**514-520.

54. **Wu GB, Yuan MR, Wei L, Zhang Y, Lin YJ, Zhang LL, Liu ZD.** 2014. Characterization of a novel cold-adapted phosphinothricin *N*-acetyltransferase from the marine bacterium *Rhodococcus sp* strain YM12. *J. Mol. Catal. B-Enzym.* **104:**23-28.

55. **Carroll P, Waddell SJ, Butcher PD, Parish T.** 2011. Methionine sulfoximine resistance in *Mycobacterium tuberculosis* is due to a single nucleotide deletion resulting in increased expression of the major glutamine synthetase, GlnA1. *Microbial drug resistance.* **17:**351-355.

56. **Miller ES, Brenchley JE.** 1981. *L*-Methionine *SR*-sulfoximine-resistant glutamine-synthetase from mutants of *Salmonella-Typhimurium*. *J. Biol. Chem.* **256:**1307-1312.

57. **Winter SE, Thiennimitr P, Winter MG, Butler BP, Huseby DL, Crawford RW, Russell JM, Bevins CL, Adams LG, Tsolis RM, Roth JR, Baumler AJ.** 2010. Gut

inflammation provides a respiratory electron acceptor for *Salmonella*. *Nature.* **467:**426-4269.

58. **Lambrecht JA, Schmitz GE, Downs DM.** 2013. RidA proteins prevent metabolic damage inflicted by PLP-dependent dehydratases in all domains of life. *MBio.* **4:**e00033-00013.

59. **Cabiscol E, Piulats E, Echave P, Herrero E, Ros J.** 2000. Oxidative stress promotes specific protein damage in *Saccharomyces cerevisiae*. *J. Biol. Chem.* **275:**27393-27398.

60. **Drazic A, Winter J.** 2014. The physiological role of reversible methionine oxidation. *Bba-Proteins Proteom.* **1844:**1367-1382.

61. **Stadtman ER, Moskovitz J, Levine RL.** 2003. Oxidation of methionine residues of proteins: Biological consequences. *Antioxid. Redox. Sign.* **5:**577-582.

CHAPTER 5

PROBING SUBSTRATE SPECIFICITY OF PHOSPHINOTHRICIN ACETYLTRANSFERASE HOMOLOGUES IN *DEINOCOCCUS RADIODURANS* AND *GEOBACILLUS KAUSTOPHILUS*[4]

[4]Hentchel K.L., VanDrisse C.M., and J.C. Escalante-Semerena. To be submitted to *Appl. Environ. Microbiol*.

ABSTRACT

Acetylation of small molecules is widespread and used as a mechanism to detoxify harmful chemicals. Many of the enzymes catalyzing acetylation reactions belong to the Gcn5 *N*-acetyltransferase (GNAT) family. *Streptomyces* species utilize a GNAT, named Bar, to acetylate and detoxify a self-produced toxin, phosphinothricin (PPT). Many Bar homologues, such as MddA from *Salmonella enterica*, were previously annotated incorrectly as PPT acetyltransferases, but instead have been shown acetylate the toxic structural homologues methionine sulfoximine (MSX) and methionine sulfone (MSO). These findings raise questions as to the substrate selectivity and function of putatively annotated PPT acetyltransferases. Here we provide evidence for the specificity of Bar homologues from *Deinococcus radiodurans* and *Geobacillus kaustophilus*, each of which contain two genes annotated to encode PPT acetyltransferases (*Dr*1057, *Dr*1182; and *Gk*0593, *Gk*2920). Previous work with *S. enterica* demonstrated that MddA was required for growth in medium containing MSX or MSO. Growth studies using an *S. enterica mddA1*::*cat*$^{+}$ strain as a heterologous host revealed that ectopic expression of *D. radiodurans* and *G. kaustophilus* Bar homologues showed specificity in their ability to restore growth of an *mddA* strain in the presence of MSX and MSO. In wild-type *S. enterica*, synthesis of *Dr*1182, *Gk*0593, and *Gk*2920 blocked the inhibitory effect of PPT. Results of *in vitro* activity assays confirmed *in vivo* results, demonstrating selectivity among the enzymes annotated as PPT acetyltransferases. Here, we describe a genetic method to test substrate specificity of annotated PPT acetyltransferases.

INTRODUCTION

The Gcn5 *N*-acetyltransferase (GNAT, PF00583) superfamily of proteins is present in all domains of life and catalyze the transfer of the acetyl group of acetyl-CoA to proteins or small molecules (for review see (1)). These enzymes were first discovered to acetylate and inactivate aminoglycoside antibiotics (2-6) and protect against several cellular stressors (7-10), providing a precedent for the role of GNAT-mediated detoxification via acetylation. Previous work has shown a subset of GNAT enzymes annotated as phosphinothricin (PPT) acetyltransferases protect the cell against toxic amino acid derivatives, including PPT, methionine sulfoximine (MSX), and methionine sulfone (MSO) (7, 8, 11-14) (Fig. 5.1).

PPT is a component of a potent toxin known as Bialaphos, a tripeptide (phosphinothricyl-alanyl-alanine) produced by *Streptomyces* species. (15). The toxic effect occurs when PPT, a glutamate analogue, is cleaved from the tripeptide. PPT causes growth inhibition by irreversibly binding to the glutamine synthetase (GlnA) enzyme, responsible for the conversion of glutamate to glutamine using ATP and ammonium (16, 17). A GNAT of *Streptomyces* species, known as Bar (also Pat for phosphinothricin acetyltransferase), is responsible for the acetylation and detoxification of the self-produced PPT toxin *in vivo* (14). Once acetylated, acetyl-PPT can no longer bind to and inhibit GlnA. Bialaphos is a potent natural herbicide and plants have been genetically engineered to be resistant by encoding the *bar* gene (14, 18).

A subgroup of GNATs have been classified as PPT acetyltransferases based on sequence similarity at the protein level to *Streptomyces* Bar. Some Bar homologues have been incorrectly annotated as PPT acetyltransferases, including *Pseudomonas aeurginosa* PITA (PA4866), *Acinetobacter baylyi* (ACIAD1637) and *Salmonella enterica* MddA (STM1590) (8, 12). Instead, these enzymes acetylate the toxic analogues MSX and MSO, which also inhibit GlnA function.

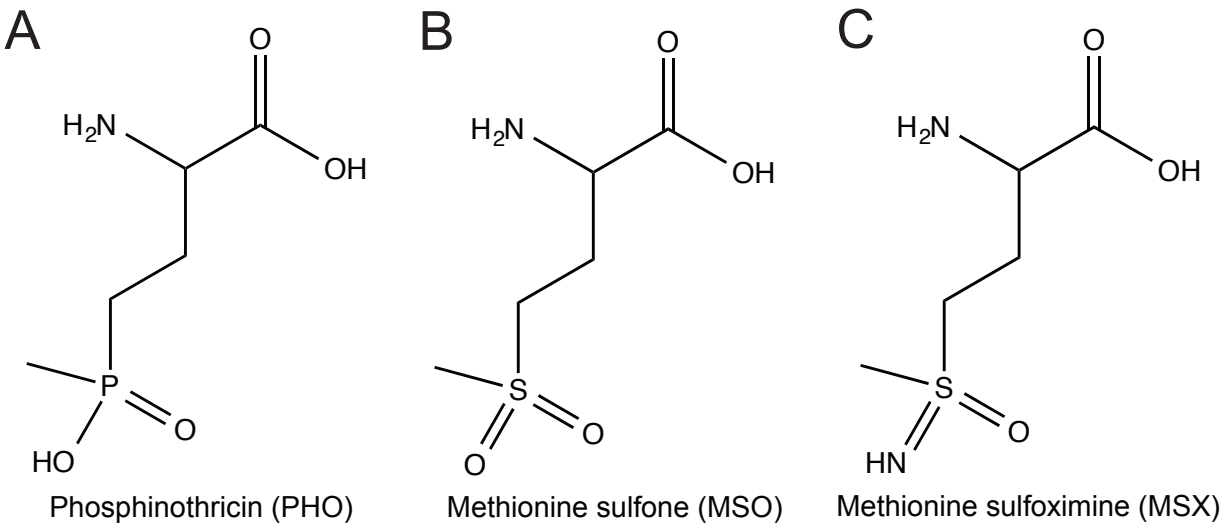

Figure 5.1. Chemical structure of PPT analogues. (A) Phosphinothricin (PPT); (B) Methionine sulfone (MSO); and (C) Methionine sulfoximine (MSX).

Here we present *in vivo* and *in vitro* data characterizing putative PPT acetyltransferases from *Geobacillus kaustophilus* and *Deinococcus radiodurans*. Using *S. enterica* as a heterologous host we assayed for function of the PPT acetyltransferases in an *S. enterica mddA* mutant or wild-type strain in conditions containing MSX, MSO, or PPT. Significantly, enzyme activity *in vitro* correlated with the observed growth phenotypes. Taken together, these data demonstrate varying specificity of these enzymes for MSX, MSO, and PPT. These data provide a potential model to assay for PPT acetyltransferase specificity.

MATERIALS AND METHODS

Culture media and chemicals. The minimal medium used in this study was no-carbon essential (NCE) minimal medium (19) containing $MgSO_4$ (1 mM), Wolfe's trace minerals (1x) (20), and glycerol (22 mM) as the sole source of carbon and energy. When used, antibiotics were added at the following concentrations: chloramphenicol (20 $\mu g\ ml^{-1}$), ampicillin (100 $\mu g\ ml^{-1}$). All chemicals were purchased from Sigma-Aldrich unless noted otherwise; Ampicillin, NaCl, and 4-(2-hydroxyethyl)-1-piperazineethanesulfonic acid (HEPES, Fischer Scientific); isopropyl β-D-1-thiogalactopyranoside (IPTG, IBI Scientific); and dithiothreitol (DTT, Gold BioTechnology).

Bacterial strains. All strains studied were derivatives of *S. enterica* serovar Typhimurium strain LT2 (unless specified), and are listed in Table 5.1. All primers used in this study were synthesized by IDT (Coralville, Iowa) and are listed in Table 5.2.

Plasmid construction for complementation and overexpression. All plasmids used in this work are listed in Table 5.1. The cloning method using unique BspQI restriction sites as

Table 5.1. Strains and plasmids used in this study.

Strain	Relevant genotype	Reference/source[a]
JE10079	*ara-9 mddA*$^{+}$	Laboratory strain
Derivatives of JE10079		
JE18333	*mddA*::*cat*$^{+}$	(7)
JE18961	*mddA*::*cat*$^{+}$ / pMDD8	(7)
JE20780	pDR1182-2	
JE20781	*mddA*::*cat*$^{+}$ / pDR1182-2	
JE20782	pGK0593-2	
JE20783	*mddA*::*cat*$^{+}$ / pGK0593-2	
JE20857	pDR1057-2	
JE20858	*mddA*::*cat*$^{+}$ / pDR1057-2	
JE20864	*mddA*::*cat*$^{+}$ / pVOC	
JE20865	*mddA*::*cat*$^{+}$ / pGK2920-2	
JE20866	pGK2920-2	
JE20973	pVOC	
***E. coli* strains**		
E. coli C41(lDE3)	*ompT hsdS* (r_B m_B) *gal* λ (DE3) including at least one non-characterized mutation	(22, 23)
Plasmids		
pMDD7	*mddA*$^{+}$ cloned into pKLD66[b]	(7)
pMDD8	*mddA*$^{+}$ cloned into pBAD24[c]	(7)
pDR1057-1	*Dr1057*$^{+}$ cloned into pKLD66[b]	
pDR1057-2	*Dr1057*$^{+}$ cloned into pBAD24[c]	
pDR1057-3	*Dr*1057* cloned into pBAD24[c] (Encodes *Dr*1057^{N114Q})	
pDR1057-4	*Dr1057** cloned into pKLD66[b] (Encodes *Dr*1057^{N114Q})	
pDR1182-1	*Dr1182*$^{+}$ cloned into pKLD66[b]	
pDR1182-2	*Dr1182*$^{+}$ cloned into pBAD24[c]	
pGK0593-1	*Gk0593*$^{+}$ cloned into pKLD66[b]	
pGK0593-2	*Gk0593*$^{+}$ cloned into pBAD24[c]	
pGK2920-1	*Gk2920*$^{+}$ cloned into pKLD66[b]	
pGK2920-2	*Gk2920*$^{+}$ cloned into pBAD24[c]	

[a] All strains and plasmids were constructed during the course of this work, unless otherwise stated

[b] pKLD66 is an overexpression vector described in (22) engineered with BspQ1 sites (C. M. VanDrisse and J. C. Escalante-Semerena, unpublished)

[c] pBAD24 is a cloning vector described in (23) engineered with BspQ1 sites (C. M. VanDrisse and J. C. Escalante-Semerena, unpublished)

Table 5.2. Primers used in this study.

Primer Name	Primer Sequence
Cloning	
5' *Dr1057* pBAD24	NNGCTCTTCNTTCATGCCGAGAGCGGCAACGCGCCCAT
5' *Dr1057* pTEV16	NNGCTCTTCNAGCATGCCGAGAGCGGCAACGCGCCCAT
3' *Dr1057* pVector	NNGCTCTTCNTTATCAGTCCTGTGCCAACGTCCGAACC
5' *Dr1182* pBAD24	NNGCTCTTCNTTCATGACCTCTGTCATTCGCCCCGCTG
5' *Dr1182* pTEV16	NNGCTCTTCNAGCATGACCTCTGTCATTCGCCCCGCTG
3' *Dr1182* pVector	NNGCTCTTCNTTATTAGCTCTCCTCGTCCAGCAGCAGT
5' *Gk0593* pBAD24	NNGCTCTTCNTTCATGAACATTCGTAGCTTTCGCAAAG
5' *Gk0593* pTEV16	NNGCTCTTCNAGCATGAACATTCGTAGCTTTCGCAAAG
3' *Gk0593* pVector	NNGCTCTTCNTTATCAGTCTATACCTACAACTGGACTG
5' *Gk2920* pBAD24	NNGCTCTTCNTTCTTGCGTAAACGGGCCGAGAAACGCG
5' *Gk2920* pTEV17	NNGCTCTTCNAGCTTGCGTAAACGGGCCGAGAAACGCG
3' *Gk2920* pVector	NNGCTCTTCNTTACTATACAAGCCGTTTGCCGACAATG
Mutagenesis	
5' *Dr1057* N114E	CCCGACCGCTACGAAGTCACGGTCAC
3' *Dr1057* N114E	GTGACCGTGACTTCGTAGCGGTCGGG

published previously (21) was used to construct all plasmids in this study and DNA sequencing (Georgia Genomics Facility, UGA) was used to verify all plasmids. Genes of interest were amplified from *D. radiodurans* R1, or *G. kaustophilus* HTA426, genomic DNA. *G. kaustophilus* HTA426 genomic DNA was from laboratory collection strains and *D. radiodurans* R1 genomic DNA was gift from John Batista (Louisiana State University).

Plasmid pKLD66 (22), which directs the synthesis of the protein with a cleavable *N*-terminal hexahistidine tag, was engineered with BspQI restriction sites (pTEV16, C. M. VanDrisse & Escalante-Semerena, unpublished data) and used for overexpression, resulting in plasmids pDR1057-2, pDR1182-1, pGK0593-1, and pGK2920-1.

Each gene of interest was cloned into the *L*-(+)-arabinose inducible vector pBAD24 (23) engineered with BspQI sites (C. M. VanDrisse & J. C. Escalante-Semerena, unpublished data) for complementation studies resulting in plasmids pDR1057-2, pDR1182-2, pGK0593-2, and pGK2920-2.

Site-directed mutagenesis was performed using primers designed from PrimerX (available at http://www.bioinformatics.org/primerx/) to mutate the asparagine (N) 114 of *Dr*1057^{WT} to a glutamate residue (Q114), to construct a catalytically active variant (*Dr*1057^{N114E}) in the pBAD24 overexpression vector (pDR1057-3).

Growth behavior analyses. Starter cultures were grown overnight at 37°C with shaking in nutrient broth containing the appropriate antibiotic and used to inoculate fresh medium (1% v/v, 200 µl per well) of a 96-well plate with appropriate antibiotics. Strains containing plasmids were induced with varying concentrations of *L*-(+)-arabinose, as described in figures and figure legends. Additional chemicals such as phosphinothricin (PPT), methionine sulfoximine (MSX), and methionine sulfone (MSO) were added at concentrations indicated in figures and figure

legends. Plates were incubated at 37°C with shaking for 20-48 h in a Powerwave Microplate Reader (Bio-Tek Instruments). Growth studies were performed in triplicate in three independent experiments, with a representative growth curve shown. Data were analyzed using Prism v6 (GraphPad) analytical software. Error bars represent the standard deviation.

Protein overproduction and purification. Plasmids encoding each gene of interest **(***Dr*1182, *Gk*0593, or *Gk*2920) were transformed into *E. coli* C41(λDE3). Overnight cultures of the transformants were sub-cultured (1:100 (v/v, inoculum:medium)) into 1 L of LB containing ampicillin (100 μg ml^{-1}). Cultures were grown at 37°C with shaking to an OD_{600} of 0.6, induced with IPTG (1 mM), and shaken overnight at ~28°C. Cells were harvested by centrifugation at 6,000 x *g* for 15 min at 4°C. The collected cell paste was re-suspended in binding buffer A [HEPES buffer (50 mM, pH 7.2) containing NaCl (500 mM) and imidazole (20 mM)] plus lysozyme (1 mg ml^{-1}), DNAse I (25 μg ml^{-1}) and protease inhibitor phenylmethanesulfonyl fluoride (PMSF, 0.5 mM)]. Cells were lysed by sonication for 1 min (2 sec, 50% duty) for 2 rounds on ice using a 550 Sonic Dismembrator (Fisher Scientific) at setting 4. Clarified cell lysates were obtained after centrifugation for 45 min at 4°C at 43,667 x *g* followed by filtration of the supernatant through a 0.45 μm filter (Millipore). Samples were loaded onto a 1 ml HisPur™ Ni-NTA resin column (Thermo Scientific) at 4°C, pre-equilibrated with binding buffer. The Ni^{+} column was washed first with buffer B (HEPES buffer (50 mM, pH 7.2) with NaCl (500 mM)) that contained 40 mM imidazole to remove nonspecifically bound proteins. Followed by that His_6-tagged proteins eluted in the same buffer system that contained 500 mM imidazole. Proteins were dialyzed at 4°C and stored in HEPES buffer (50 mM, pH 7.2) containing NaCl (100 mM), *tris*(2-carboxyethyl)phosphine hydrochloride (TCEP, 0.5 mM)) and glycerol (10% v/v), drop-frozen in liquid nitrogen, and stored at -80°C.

Mass spectrometry analysis. Protein bands of interest resolved by SDS-PAGE were excised and submitted to the Protein and Mass Spectrometry (PAMS) facility at the University of Georgia. After a trypsin digest the proteins were analyzed by MALDI mass finger printing an LC-MS/MS to determine protein identity and sequence.

Thin layer chromatography. Reactions were performed as described (7). Reaction mixtures included HEPES buffer (50 mM, pH 7.0), containing TCEP (1 mM), [1-^{14}C]-acetyl-CoA (20 μM), substrate (0.5 mM), and enzyme (*Dr*1057, *Dr*1182, *Gk*0593, or *Gk*2920; 1 μg). Reactions were incubated at 37°C for 30 min, spotted onto a polyester backed silica gel plate (Whatman Ltd), and developed in a chamber pre-equilibrated with a mobile phase of *n*-butanol, acetic acid, and dH_2O (3:1:1). After incubation TLC plates were developed with a phosphor screen overnight, and the resulting phosphor-image was detected using a Typhoon Trio+ Variable Mode Imager (GE Healthcare) with ImageQuant v5.2 software.

Activity assays. Reactions were performed as described (7), using a SpectraMax Plus 384 microplate spectrophotometer (Molecular Devices) equipped with SoftMax Pro v4 software was used for data acquisition. Assays were performed at 30°C in 100-μl volumes in 96-well microplates using a continuous spectrophotometric assay that employed 5,5'-dithiobis-(2-nitrobenzoic acid) (DTNB, Ellman's reagent) as a reporter of free sulfhydryl groups at 412 nm (24, 25). Reaction mixtures contained HEPES buffer (50 mM, pH 7.2), DTNB (0.3 mM), acetyl-CoA, protein of interest (*Dr*1057, *Dr*1182, *Gk*0593, or *Gk*2920), and substrate of interest (PPT, MSO, or MSX). Reactions were initiated by the addition of enzyme. A control containing enzyme but no acetyl-CoA was used to correct for the background. Data were acquired every 10 s over a 5 min time period. Data were collected using an average of a technical triplicate, in experimental triplicate. Reactions included HEPES (pH 7.5, 50 mM), protein of interest (0.5 μg),

acetyl-CoA (100 µM), and PPT, MSX, or MSO (150 µM), and DTNB (0.3 mM). Data was graphed using Prism v6 (GraphPad) analytical software. The molar extinction coefficient used for the concentration of the TNB^{2-} anion was 14,150 M^{-1} cm^{-1}.

Bioinformatic analyses. An alignment of the primary amino acid sequence of various PPT acetyltransferases was generated using the NCBI COBALT multiple alignment tool (http://www.st-va.ncbi.nlm.nih.gov/tools/cobalt/re_cobalt.cgi?). A phylogenetic tree was generated using FigTree software (http://tree.bio.ed.ac.uk/software/figtree/).

RESULTS

S. enterica *can be used as a heterologous host to screen activity of putative phosphinothricin (PPT) acetyltransferases* in vivo. Previous work from our lab characterized the annotated PPT acetyltransferase, MddA (formerly YncA, STM1590) from *S. enterica* (7). We demonstrated that this enzyme acetylated the methionine derivatives methionine sulfoximine (MSX) and methionine sulfone (MSO), but not PPT. Growth of an *S. enterica mddA1*::*cat*$^+$ strain is abolished when MSX is present (10 µM) and inhibited in the presence of MSO (50 µM), compared to the *mddA*$^+$ strain (Fig. 5.2) (7). The *mddA1*::*cat*$^+$ strain was used as a genetic tool to examine the ability of the *D. radiodurans* and *G. kaustophilus* putative PPT acetyltransferases to detoxify MSX or MSO *in vivo* when expressed *in trans*, by restoring growth to wild-type levels (Fig. 5.3). Control growth studies are shown in Figure 5.2. Expression of *Dr*1182 or *Gk*2920 *in trans* was able to restore growth of the *S. enterica mddA1*::*cat*$^+$ strain to wild-type levels at low levels of induction (10 µM *L*-(+) arabinose) in conditions with either MSX or MSO. Induction of *Gk*0593 was able to restore the growth defects only when expressed at high levels [MSX (1 mM), MSO (200 µM) *L*-(+) arabinose], indicating these may be poor substrates for the enzyme.

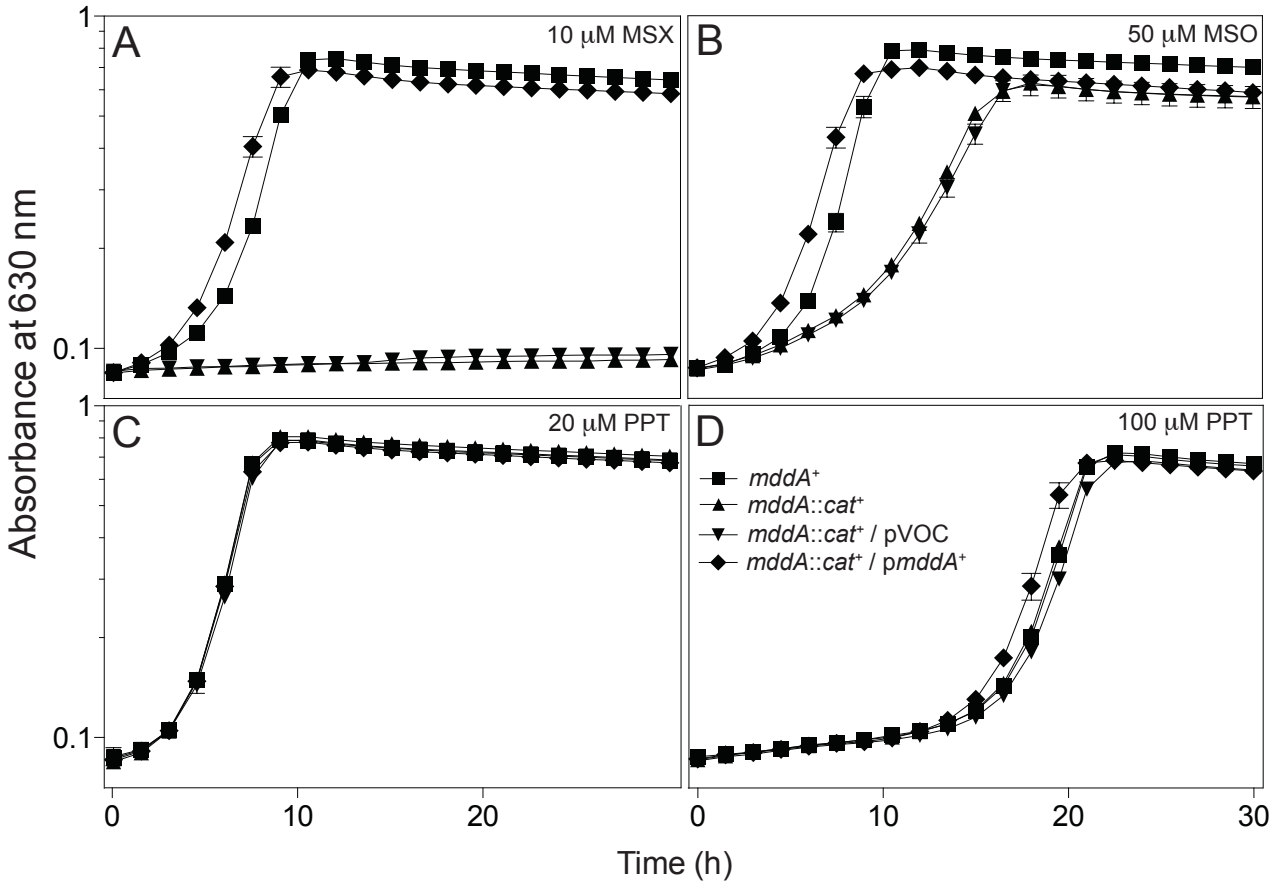

Figure 5.2. Growth of the *S. enterica mddA1*::*cat*$^+$ strain in conditions containing MSX, MSO, or PPT. Growth and complementation of the *S. enterica mddA1*::*cat*$^+$ strain in NCE minimal medium (glycerol, 22 mM) was examined in the presence of MSX (10 μM), MSO (50 μM), or PPT (20 or 100 μM). Vectors were induced with 10 μM of *L*-(+)-arabinose. Growth curves were performed using a microplate reader (Bio-Tek Instruments) as described under *Materials and Methods*. Strains analyzed: *ara-9* (JE10079), *ara-9 mddA1*::*cat*$^+$ (JE18333), *ara-9 mddA1*::*cat*$^+$ / pVOC (JE20864), *ara-9 mddA1*::*cat*$^+$ / pMDD8 *mddA*$^+$ (JE18961). Error bars represent standard deviation. pVOC, vector only control. Symbols in D apply to all panels.

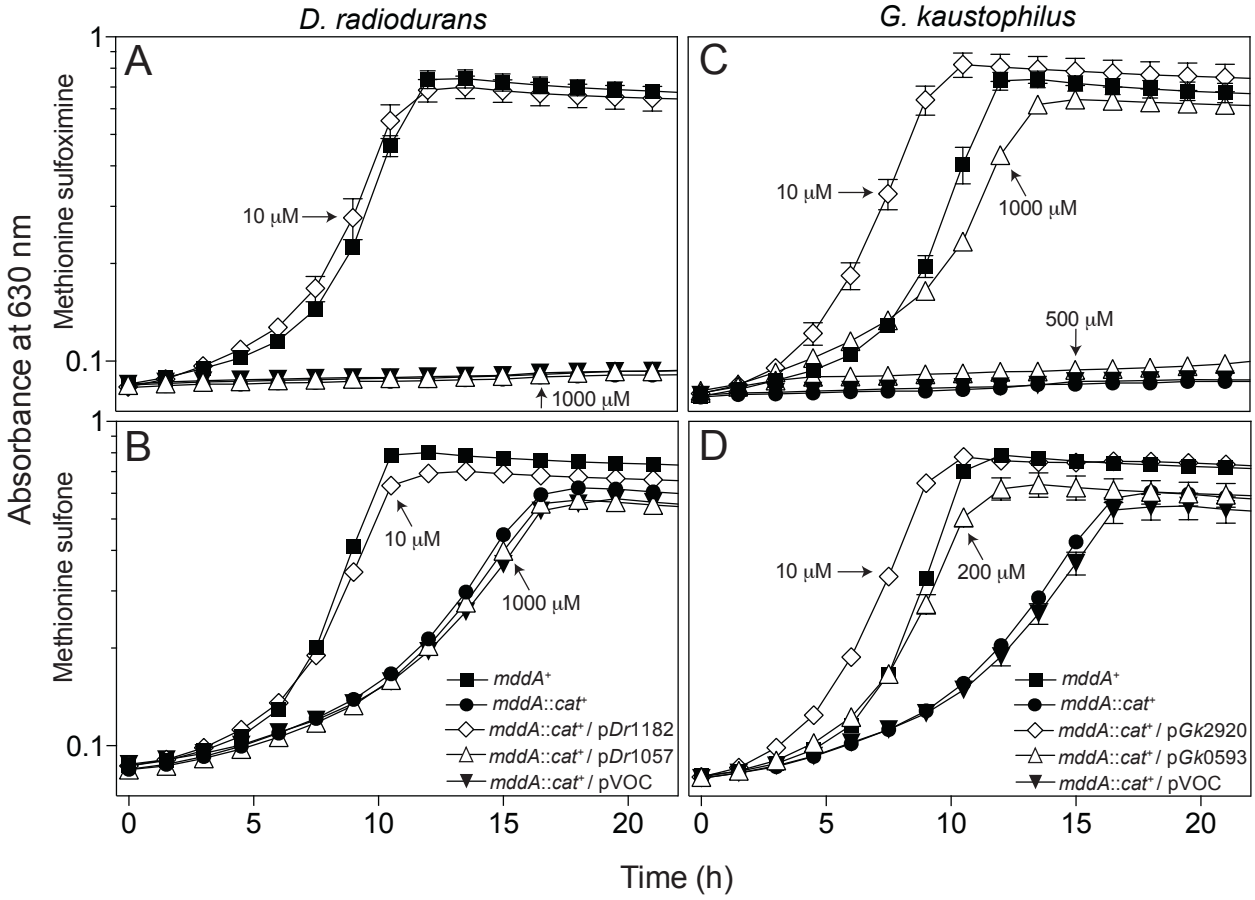

Figure 5.3. Complementation of annotated PPT acetyltransferases from *D. radiodurans* and *G. kaustophilus* in a heterologous host. Growth of an *S. enterica mddA1*::*cat*$^{+}$ strain carrying an *L*-(+)-arabinose inducible plasmid encoding *Dr*1057, *Dr*1182, *Gk*0593, or *Gk*2920 was examined in the presence of MSX (10 μM) or MSO (50 μM) in NCE minimal medium with glycerol (22 mM). Plasmids were induced with varying concentrations of *L*-(+)-arabinose (10-1000 μM), as indicated. Strains analyzed: *ara-9* (JE10079), *ara-9 mddA1*::*cat*$^{+}$ (JE18333), *ara-9 mddA1*::*cat*$^{+}$ / pVOC (JE20864), *ara-9 mddA1*::*cat*$^{+}$ / p*Dr*1057-2 (JE20858), *ara-9 mddA1*::*cat*$^{+}$ / p*Dr*1182-2 (JE20781), *ara-9 mddA1*::*cat*$^{+}$ / p*Gk*0593-2 (JE20783), *ara-9 mddA1*::*cat*$^{+}$ / p*Gk*2920-2 (JE20865). Growth curves were performed using a microplate reader (Bio-Tek Instruments) as described under *Materials and Methods*. Error bars represent standard deviation. pVOC, vector only control. Symbols in B apply to panels A and B; symbols in D apply to panels C and D.

*Dr*1057 was not able to complement the phenotype of the *mddA1*::*cat*$^{+}$ strain in either condition even at high levels of induction (1 mM *L*-(+) arabinose).

These data provide insights into the substrate specificity of the putative PPT acetyltransferases from *D. radiodurans* and *G. kaustophilus* when using *S. enterica* as a heterologous host to monitor growth in the presence of toxic compounds.

Increased expression provides protection against higher levels of MSO, MSO, and PPT. Growth of wild-type *S. enterica* is inhibited by MSX (20 μM), MSO (500 μM), and PPT (100 μM) when present at high concentrations (7). An *S. enterica mddA*$^{+}$ strain carrying p*Dr*1057, p*Dr*1182, p*Gk*0593, or p*Gk*2920 *in trans* under the control of an inducible promoter was grown in minimal medium with MSX (20 μM), MSO (500 μM), or PPT (100 μM), and varying levels of inducer (10-1000 μM *L*-(+)-arabinose). When induced, cultures expressing *Dr*1182 or *Gk*2920 grew with shorter lag times when compared to the wild-type *S. enterica* strain (Fig. 5.4). These data were consistent with the idea that increased protein levels provided greater protection against the toxic effects of MSX, MSO, and PPT. *Gk*0593 was able to completely reduce the lag phase of wild type *S. enterica* in conditions containing PPT at low induction (10 μM *L*-(+) arabinose) (Fig. 5.4E), but was not as efficient in providing protection against conditions including MSX or MSO, as a higher level of induction was needed to revert the *mddA1*::*cat*$^{+}$ growth defect (Fig. 5.4D, 5.4F). *Dr*1057 was unable to improve growth of the wild type *S. enterica* strain under any conditions even at high induction (1 mM *L*-(+) arabinose); indicating this protein does not acetylate these products under the conditions tested (Fig. 5.4A-C).

Functional analysis of the putative PPT acetyltransferases. Biochemical analysis of the putative PPT acetyltransferases was performed to better understand their substrate specificity (Fig. 5.5). Assays were carried out as described previously (7) using a SpectraMax Plus 384

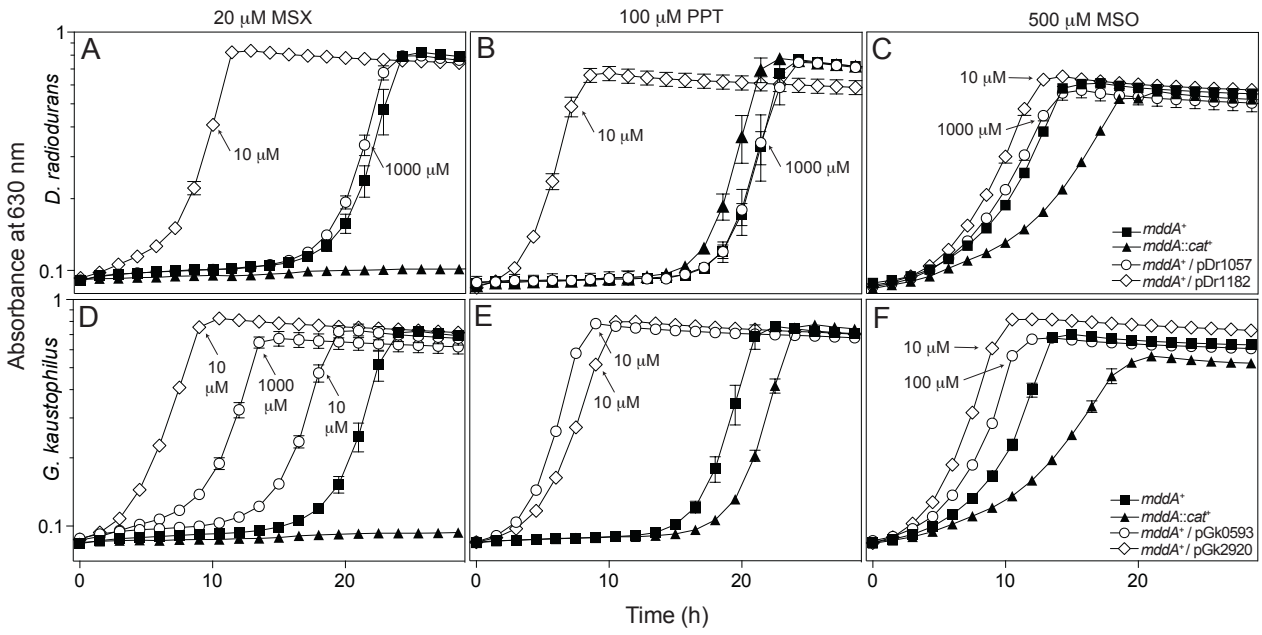

Figure 5.4. Overexpression provides resistance to higher levels of PPT, MSX, and MSO in a heterologous host. Growth of wild-type *S. enterica* (JE10079) carrying an *L*-(+)-arabinose inducible plasmid encoding *Dr*1057, *Dr*1182, *Gk*0593, or *Gk*2920 was examined in presence of PPT (100 μM), MSX (20 μM), or MSO (500 μM), in NCE minimal medium with glycerol (22 mM) with varying concentrations of *L*-(+)-arabinose (10-1000 μM), as indicated. Strains analyzed: *ara-9* (JE10079), *ara-9 mddA1*::*cat*$^{+}$ (JE18333), *ara-9* / pVOC (JE20973), *ara-9* / p*Dr*1057-2 (JE20857), *ara-9* / p*Dr*1182-2 (JE20780), *ara-9* / p*Gk*0593-2 (JE20782), and *ara-9* / p*Gk*2920-2 (JE20866). Growth curves were performed using a microplate reader (Bio-Tek Instruments) as described under *Materials and Methods*. Error bars represent standard deviation. pVOC, vector only control. Symbols in C apply to panels A-C; symbols in F apply to panels D-F.

microplate spectrophotometer (Molecular Devices). Assays were performed using a continuous spectrophotometric assay that employed 5,5'-dithiobis-(2-nitrobenzoic acid) (DTNB, Ellman's reagent) as a reporter of free sulfhydryl groups at 412 nm (24, 25). Reactions were initiated by the addition of enzyme (0.5 μg), and a control containing enzyme but no acetyl-CoA was used to correct for background. The *S. enterica* MddA acetyltransferase and a catalytically inactive variant, *Se*MddA^{E82Q}, were used as positive and negative controls, respectively, for MSX and MSO (7). The ability of the putative PPT acetyltransferases, *Dr*1057, *Dr*1182, *Gk*0593, or *Gk*2920, to acetylate MSX, MSO, or PPT was examined (Fig. 5.5). The *in vitro* acetylation activity of *Dr*1182 correlated with the obtained *in vivo* data demonstrating the enzyme can acetylate each of the three substrates tested, with higher activity seen when MSX or MSO were used as substrates (Fig. 5.5). The activity of *Gk*0593 also correlated with the observed phenotypes, and showed the enzyme acetylated all three substrates equally well, but overall with lower activity than observed with *Dr*1182 (Fig. 5.5).

Because Gk2920 was recalcitrant to purification, treated whole cell lysates containing the overexpressed enzyme were used to test activity. As a negative control, a treated whole cell lysate carrying an empty vector was used. These data show *Gk*2920 acetylates MSX and MSO, but had no activity for PPT (Fig. 5.5). Based on the *in vivo* data in which expression of *Gk*2920 *in trans* improved growth in conditions with PPT, this was an unexpected result. However, mass spectrometry analysis revealed the first 55 amino acids of the *N*-terminus of *Gk*2920 were being cleaved during overexpression at high protein concentrations by some unknown mechanism (data not shown). This cleavage could account for the ability of the enzyme to still acetylate MSX and MSO, but not PPT.

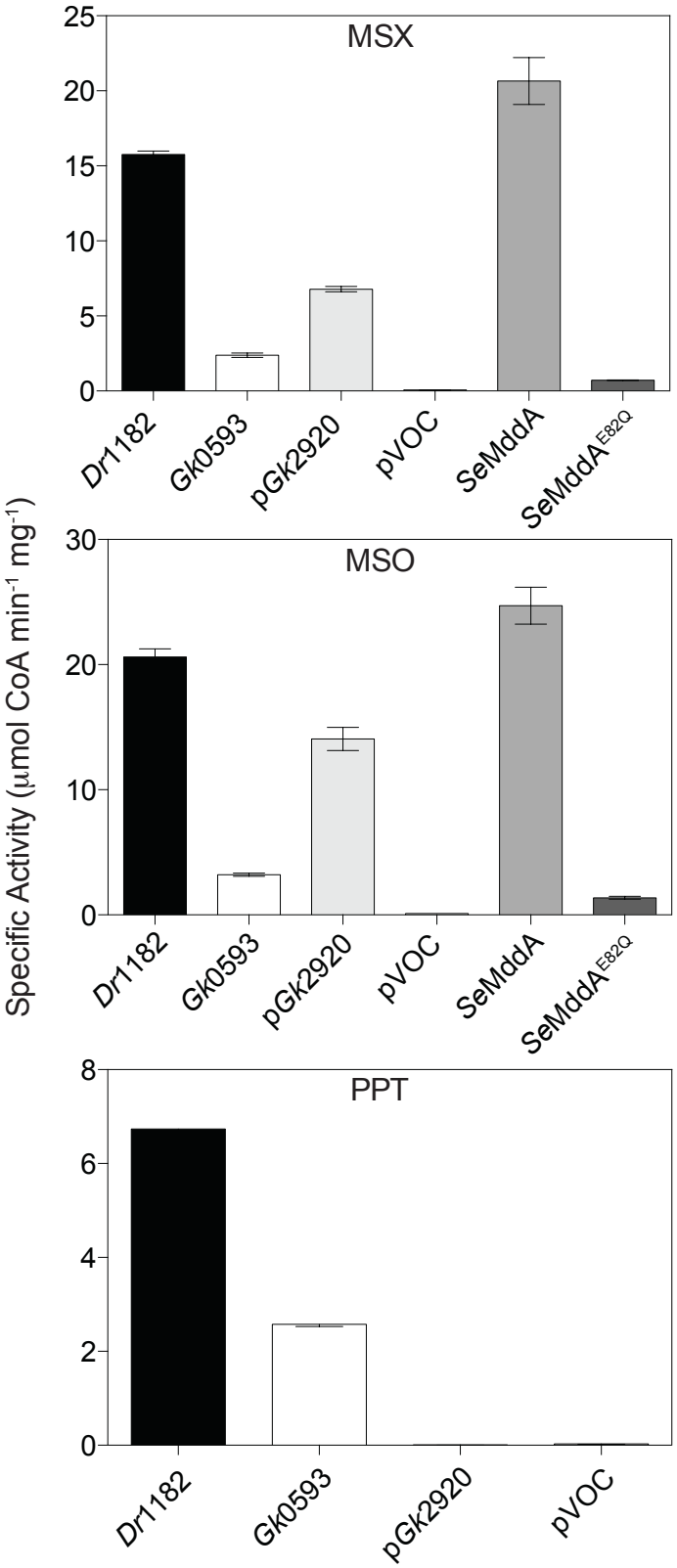
MSX
MSO
PPT
Specific Activity (µmol CoA min-1 mg-1)
Dr1182
Gk0593
pGk2920
pVOC
SeMddA
SeMddAE82Q

Figure 5.5. Substrate specificity of annotated PPT acetyltransferases. Specific activity of the annotated PPT acetyltransferases of *D. radiodurans* (*Dr*1182) and *G. kaustophilus* (*Gk*0593, *Gk*2920) for MSO, MSX, or PPT was measured using a spectrophotometric assay (see *Materials and Methods*).

Bioinformatic analyses of putative PPT acetyltransferases. An alignment was generated for putative PPT acetyltransferases across a range of bacterial species (NCBI COBALT Multiple Alignment Tool, Fig. 5.6A). Looking at the alignment of the catalytic glutamate residue, we discovered that Dr*1057* from *D. radiodurans*, which had no activity for MSX, MSO, or PPT under the conditions tested, lacked the catalytic glutamate, and instead encoded an asparagine. To determine if the loss of activity was due specifically to the lack of the glutamate residue, we engineered a variant of *Dr*1057 in which the asparagine residue was altered by site directed mutagenesis to a glutamate. Testing this variant *in trans* showed no restoration of an *mddA* mutant in conditions containing MSX or MSO and did not improve growth of the *S. enterica* wild type in conditions containing PPT (data not shown). Therefore we conclude that this enzyme is not lacking actively specifically due to the lack of the glutamate residue, and may have completely lost its ability to acetylate PPT and / or PPT analogues.

A phylogenetic tree was created comparing 19 PPT homologues (FigTree, Fig. 5.6B). We observed clustering of enzymes that acetylated MSX but not PPT, with the exception of *Dr*1182, which clustered more closely with the non-PPT utilizing enzymes. Organisms containing two annotated PPT acetyltransferases tend to be cluster separately in different nodes of the tree (*i.e. D. radiodurans, B. xenovorans,* and *G. kaustophilus*). A recent report examining the specificity of the two annotated PPT acetyltransferases from *P. putida,* which were also clustered in separate nodes of the tree, demonstrated that each enzyme was specific for either PPT or MSX (26). From *in vivo* data presented here for *G. kaustophilus* and *D. radiodurans*, we see that enzyme function overlaps and each of the two enzymes can acetylate both PPT and MSX, although to varying degrees.

A

```
Ab1637    QLLGFASWGSFRAFPAYKYTVEHSVYIHKDYRGLGLSKHLMNELIKRAVESEVHVMVGCI
BsYwnH    NVAAWISFETFYGRPAYNKTAEVSIYIDEACRGKGVGSYLLQEALRIAPNLGIRSLMAFI
BxA2261   RVIAWLSFSDFYGRPAYLRTAEVSIYLDESARGRGLGRQLLAASLAAAPALGIDTVLGFI
BxB1787   EVAGYCYATPYRPRAAYRNTIEDSIYVNDAYRGRGLGRVLLQALIERCETGPWRQMVAVI
Dr1057    KIVGFAGVTQWAGSHQP-DRYNVTVTVPPEHGRRGVGAVLAATVRTHLKERGAREVLAGA
Dr1182    TVLGFASYGTFREKPGYNGTVEHSVYIRDGQRGAGLGLALMERLIAEARAQHLHVMLGSV
Gk0593    GIQGWCKISKVSDRCVYEGVGEVSVYVRDVSRGKGVGKKLLQAMIKESEAKGFWTLTAGI
Gk2920    AVCAWLSFQSFYGRPAYRHTAEVSIYIAETHRGRGLGTKLLERAVERAPELGIKTLLGFI
Pa4866    EVLGYASYGDWRPFEGFRGTVEHSVYVRDDQRGKGLGVQLLQALIERARAQGLHVMVAAI
SaYncA    SVLGFATFGSFRPWPAYQYTIEHSIYVDASARGKGIASQLLQHLIVEAKAKGYRTLVAGI
SeMddA    VVTGYASFGDWRSFDGFRYTVEHSVYVHPAHQGKGLGRKLLSRLIDEARRCGKHVMVAGI
SlBar     EILGYATSSPYRAKPAYATSVETTVYVAPGAGGRGIGSLLYASLFDALAAEDLHRAYAGI
Sm1457    EVVGYASFGEWRAFDGYRHTVEHSVYVRADQRGGGIGRALMLELIDRAEALGKHVMIAGI
```

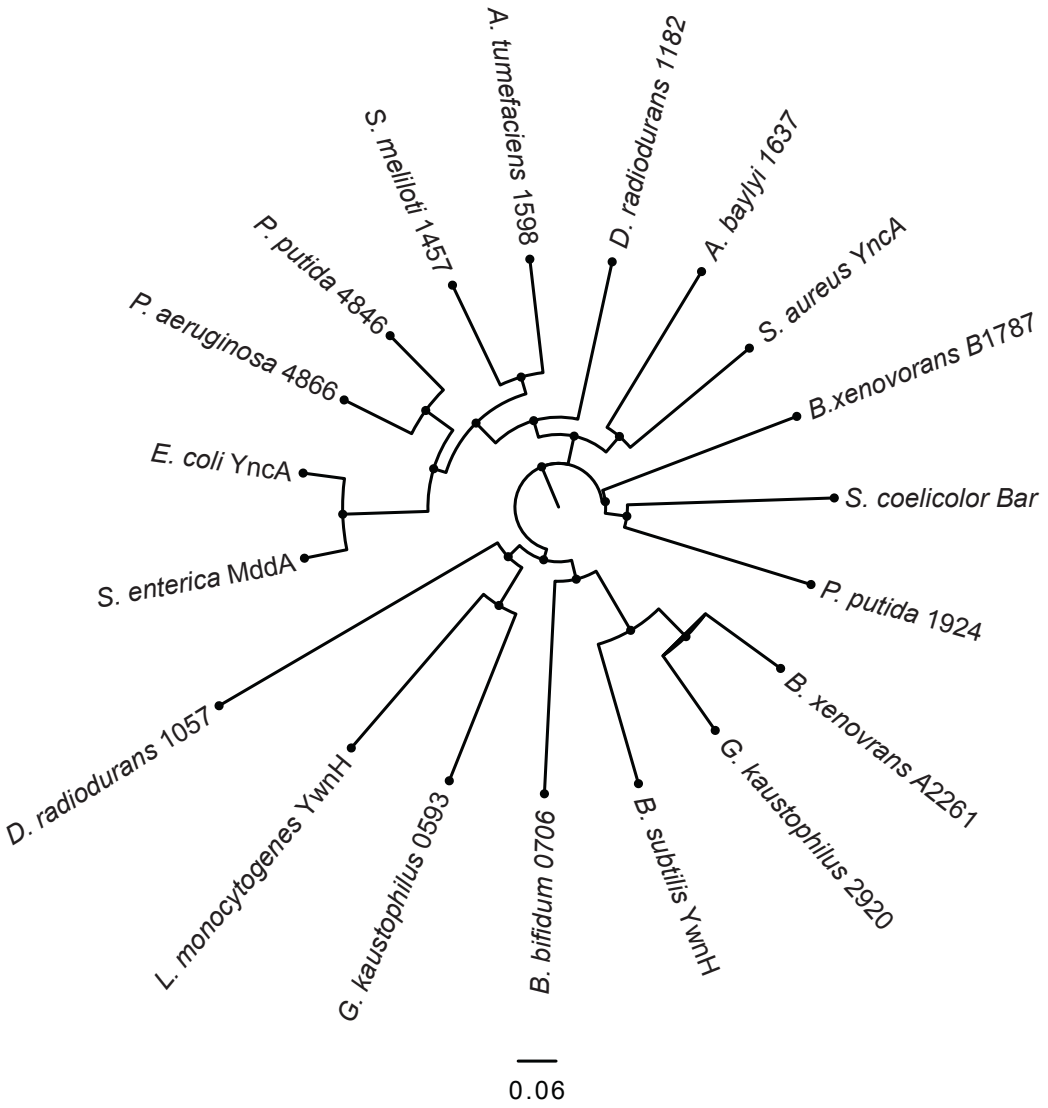

Figure 5.6. Bioinformatic analyses of annotated PPT acetyltransferases. (A) Alignments were generated using NCBI COBALT Multiple Alignment Tool. (B) A phylogenetic tree of 19 annotated PPT acetyltransferases was generated using FigTree. Legend: *Ab*, *Acinetobacter baylyi*; *Af*, *Agrobacterium fabrum*; *Bb*, *Bifidobacterium bifidum; Bs*, *Bacillus subtilis; Bx*, *Burkholderia xenovorans; Dr*, *Deinococcus radiodurans*; *Ec*, *Escherichia coli*; *Gk*, *Geobacillus kaustophilus*; *Lm Listeria monocytogenes*; *Pa*, *Pseudomonas aeurginosa*; *Pp*, *Pseudomonas putida*; *Sa*, *Staphylococcus aureus*; *Se*, *Salmonella enterica*; *Sc*, *Streptomyces coelicolor*; and *Sm*, *Sinorhizobium melloti*. *For *Dr*1057 only the sequence of the GNAT domain that aligned to the other putative PPT acetyltransferases (a.a. 1-180) was used for the phylogenetic tree.

DISCUSSION

Genes predicted to encode PPT acetyltransferases having varying specificities for PPT and the related analogues MSX and MSO. There is a pattern of enzymes annotated to be PPT acetyltransferases that do not retain this activity (7, 8, 12). The enzymes tested from *Geobacillus kaustophilus* and *Deinococcus radiodurans* exhibit varying degrees of specificity for the structurally related compounds MSX, MSO, and PPT (Fig. 5.3, 5.4, 5.5) (7, 8). More detailed mechanistic analyses are needed to verify the activity of this subclass of GNAT enzymes so that they are not misclassified based on sequence homology to Bar of *Streptomyces* species.

Why is there overlapping function? These studies raise question as to why an organism needs to encode multiple GNATs to combat the effects of PPT, MSX, and MSO. The only natural occurrence of MSX is from the members of the Connaraceae plant species, located in tropical regions around the world (27). MSX was also identified in the late 1940's as a toxic by-product in flour bleached with nitrogen trichloride (28-30). PPT would be a more pervasive threat in any soil condition where *Streptomyces* species were present. On average bacteria encode ~20-25 GNATs and it is interesting that some organisms encode multiple that are specific to these related toxic amino acid derivatives.

ACKNOWLEDGEMENTS

The authors have declared that no competing interests exist. This work was supported by USPHS grant R01-GM62203 to J.C.E.-S.

REFERENCES

1. **Thao S, Escalante-Semerena JC.** 2011. Control of protein function by reversible *N*(ε)-lysine acetylation in bacteria. *Curr. Opin. Microbiol.* **14:**200-204.
2. **Davies J, Wright GD.** 1997. Bacterial resistance to aminoglycoside antibiotics. *Trends Microbiol.* **5:**234-240.
3. **Wright GD, Ladak P.** 1997. Overexpression and characterization of the chromosomal aminoglycoside 6'-*N*-acetyltransferase from *Enterococcus faecium*. *Antimicrob. Agents Chemother*. **41:**956-960.
4. **Wolf E, Vassilev A, Makino Y, Sali A, Nakatani Y, Burley SK.** 1998. Crystal structure of a GCN5-related *N*-acetyltransferase: *Serratia marcescens* aminoglycoside 3-*N*-acetyltransferase. *Cell* **94:**439-449.
5. **Draker KA, Northrop DB, Wright GD.** 2003. Kinetic mechanism of the GCN5-related chromosomal aminoglycoside acetyltransferase AAC(6')-Ii from *Enterococcus faecium*: evidence of dimer subunit cooperativity. *Biochemistry.* **42:**6565-6574.
6. **Vetting MW, Magnet S, Nieves E, Roderick SL, Blanchard JS.** 2004. A bacterial acetyltransferase capable of regioselective *N*-acetylation of antibiotics and histones. *Chem. Biol.* **11:**565-573.
7. **Hentchel KL, Escalante-Semerena JC.** 2015. In *Salmonella enterica*, the Gcn5-related acetyltransferase MddA (formerly YncA) acetylates methionine sulfoximine and methionine sulfone, blocking their toxic effects. *J. Bacteriol.* **197:**314-325.
8. **Davies AM, Tata R, Beavil RL, Sutton BJ, Brown PR.** 2007. L-Methionine sulfoximine, but not phosphinothricin, is a substrate for an acetyltransferase (gene

PA4866) from *Pseudomonas aeruginosa*: structural and functional studies. *Biochemistry.* **46:**1829-1839.

9. **Carper SW, Willis DG, Manning KA, Gerner EW.** 1991. Spermidine acetylation in response to a variety of stresses in *Escherichia coli*. J Biol Chem **266:**12439-12441.

10. **Liang W, Malhotra A, Deutscher MP.** 2011. Acetylation regulates the stability of a bacterial protein: growth stage-dependent modification of RNase R. *Mol. Cell.* **44:**160-166.

11. **Davies AM, Tata R, Chauviac FX, Sutton BJ, Brown PR.** 2008. Structure of a putative acetyltransferase (PA1377) from *Pseudomonas aeruginosa*. *Acta Crystallogr. Sect. F Struct. Biol. Cryst. Commun.* **64:**338-342.

12. **Davies AM, Tata R, Snape A, Sutton BJ, Brown PR.** 2009. Structure and substrate specificity of acetyltransferase ACIAD1637 from *Acinetobacter baylyi* ADP1. *Biochimie.* **91:**484-489.

13. **Wu GB, Yuan MR, Wei L, Zhang Y, Lin YJ, Zhang LL, Liu ZD.** 2014. Characterization of a novel cold-adapted phosphinothricin *N*-acetyltransferase from the marine bacterium *Rhodococcus sp* strain YM12. *J. Mol. Catal. B-Enzym*. **104:**23-28.

14. **Deblock M, Botterman J, Vandewiele M, Dockx J, Thoen C, Gossele V, Movva NR, Thompson C, Vanmontagu M, Leemans J.** 1987. Engineering herbicide resistance in plants by expression of a detoxifying enzyme. *EMBO J.* **6:**2513-2518.

15. **Ogawa Y, Tsuruoka T, Inoue S, Niida T.** 1973. Studies on a new antibiotic SF-1293. II. Chemical structure of antibiotic SF-1293. *Sci. Rep. Meijii Kaisha.* **13:**42-48.

16. **Circello BT, Eliot AC, Lee JH, van der Donk WA, Metcalf WW.** 2010. Molecular cloning and heterologous expression of the dehydrophos biosynthetic gene cluster. *Chem. Biol.* **17:**402-411.

17. **Maughan SC, Cobbett CS.** 2003. Methionine sulfoximine, an alternative selection for the *bar* marker in plants. *J. of Biotech*. **102:**125-128.

18. **Murakami T, Anzai H, Imai S, Satoh A, Nagaoka K, Thompson CJ.** 1986. The bialaphos biosynthetic genes of *Streptomyces-Hygroscopicus* - Molecular-cloning and characterization of the gene-cluster. *Mol. Gen. Genet.* **205:**42-50.

19. **Berkowitz D, Hushon JM, Whitfield HJ, Jr., Roth J, Ames BN.** 1968. Procedure for identifying nonsense mutations. *J. Bacteriol.* **96:**215-220.

20. **Balch WE, Wolfe RS.** 1976. New approach to the cultivation of methanogenic bacteria: 2-mercaptoethanesulfonic acid (HS-CoM)-dependent growth of *Methanobacterium ruminantium* in a pressurized atmosphere. *Appl. Environ. Microbiol.* **32:**781-791.

21. **Galloway NR, Toutkoushian H, Nune M, Bose N, Momany C.** 2013. Rapid cloning for protein crystallography using Type IIS restriction enzymes. *Crystal. Growth Des.* **13:**2833-2839.

22. **Rocco CJ, Dennison KL, Klenchin VA, Rayment I, Escalante-Semerena JC.** 2008. Construction and use of new cloning vectors for the rapid isolation of recombinant proteins from *Escherichia coli*. *Plasmid*. **59:**231-237.

23. **Guzman LM, Belin D, Carson MJ, Beckwith J.** 1995. Tight regulation, modulation, and high-level expression by vectors containing the arabinose PBAD promoter. *J. Bacteriol.* **177:**4121-4130.

24. **Ellman GL, Courtney KD, Andres V, Jr., Feather-Stone RM.** 1961. A new and rapid colorimetric determination of acetylcholinesterase activity. *Biochem. Pharmacol.* **7:**88-95.

25. **Griffith KL, Wolf RE, Jr.** 2002. Measuring beta-galactosidase activity in bacteria: cell growth, permeabilization, and enzyme assays in 96-well arrays. *Biochem. Biophys. Res. Commun.* **290:**397-402.

26. **Paez-Espino AD, Chavarria M, de Lorenzo V.** 2015. The two paralogue *phoN* (phosphinothricin acetyl transferase) genes of *Pseudomonas putida* encode functionally different proteins. *Environ. Microbiol.*

27. **Jeannoda VL, Rakoto-Ranoromalala DA, Valisolalao J, Creppy EE, Dirheimer G.** 1985. Natural occurrence of methionine sulfoximine in the Connaraceae family. *J. Ethnopharmacol*. **14:**11-17.

28. **Bentley HR, Booth RG, et al.** 1948. Action of nitrogen trichloride on proteins; production of toxic derivative. *Nature*. **161:**126.

29. **Bentley HR, Mc DE, et al.** 1949. Action of nitrogen trichloride (agene) on proteins; isolation of crystalline toxic factor. *Nature*. **164:**438.

30. **Bentley HR, Mc DE, et al.** 1949. Action of nitrogen trichloride on proteins; progress in the isolation of the toxic factor. *Nature.* **163:**675.

31. **Miroux, B. and J.E. Walker.** 1996. Over-production of proteins in *Escherichia coli*: mutant hosts that allow synthesis of some membrane proteins and globular proteins at high levels. *J. Mol. Biol.* **260**: 289-298.

CHAPTER 6

CONCLUSIONS AND FUTURE DIRECTIONS

SUMMARY AND CONCLUSIONS

Overview. Acetylation of biomolecules (e.g. proteins and small molecules) is an important modification that can affect structure, DNA binding, and / or activity and is a conserved mechanism to rapidly modify cellular components in order to respond to environmental cues (1-5). The first portion of this work explored the transcriptional regulation of the reversible lysine acetylation system in *S. enterica*, providing the first example of a transcriptional regulator integrating the regulation of the RLA system with that of a target substrate, the acetyl-CoA synthetase (Hentchel *et al*, unpublished data). These studies demonstrated that slight perturbations in the ratios of the RLA components caused by mis-regulation drastically effected growth in conditions requiring a functional RLA system.

The second portion of this work focused on the characterization of GNAT enzymes annotated to encode phosphinothricin acetyltransferases. Phosphinothricin is a potent toxin produces by *Streptomyces* species and has important agricultural uses (6, 7). Characterization of the putative phosphinothricin acetyltransferase of *S. enterica*, MddA, revealed this enzyme did not have activity for phosphinothricin, but instead acetylated the closely related structural analogues methionine sulfoximine and methionine sulfone, which are toxic amino acid derivatives (8). The activities of other putative phosphinothricin acetyltransferases from *D. radiodurans*, *G. kaustophilus*, *B. xenovorans*, and *B. subtilis* were examined and revealed not only do certain

organisms encode multiple of these enzymes, but they have varying specificities for phosphinothricin, methionine sulfoximine, and methionine sulfone (Hentchel *et al*, unpublished data). These studies expand our understanding of the role of acetylation in cellular physiology.

IolR regulates the reversible lysine acetylation (RLA) system. Very little information is available on how the protein acetyltransferase (Pat) and protein deacetylase (CobB) of *S. enterica* are transcriptionally regulated (9). Work reported in Chapter 3 outlines the regulatory circuitry that integrates the expression of genes encoding the RLA system (*pat* and *cobB*), with that of their target substrate, acetyl-CoA synthetase (*acs*), and its impact on carbon metabolism (Hentchel *et al*, unpublished data). A mutagenesis screen identified IolR, a repressor of *myo*-inositol catabolism activated expression of *pat*. Genetic analyses revealed subtle effects on the RLA system that greatly impacted the growth behavior of the cell, due to the dysregulation of Acs by altering the levels of acetylated (inactive) vs. unacetylated (active) Acs. This work provides the first insights into the complexities of the system responsible for controlling RLA at the transcriptional level in *S. enterica* and how the cell regulates protein acetylation on various carbon sources.

MddA detoxifies methionine sulfoximine and methionine sulfone, but not phosphinothricin. GNATs have been shown to detoxify harmful compounds by acetylation (10-13). Work reported in Chapter 4 characterized a GNAT of *S. enterica*, MddA, responsible for the acetylation and detoxification of harmful amino acid derivatives (8). *In vivo* and *in vitro* analysis revealed MddA was necessary and sufficient for detoxification of methionine sulfoximine and methionine sulfone when present in the environment. Genetic and biochemical analyses identified ways in which MddA-deficient strains could prevent toxicity, including removal of the

methionine sulfoximine transport system, and the addition of exogenous amino acids. This work identified a mechanism of how *S. enterica* combats specific environment stresses.

S. enterica *can be used as a heterologous host to assay for function of putative phosphinothricin acetyltransferases*. Many putative phosphinothricin acetyltransferases are misannotated and instead, some of these enzymes have specificity for the phosphinothricin analogues methionine sulfoximine and methionine sulfone (8, 14, 15). In Chapter 5, the activities of putative phosphinothricin acetyltransferases from *D. radiodurans*, *G. kaustophilus*, *B. xenovorans*, and *B. subtilis* were determined using *S. enterica* as a heterologous host (Hentchel *et al*, unpublished data). This study provided the first example of using *S. enterica* to characterize the specificities of this subgroup of GNAT enzymes, and provided a model to predict functions of other putative phosphinothricin acetyltransferases.

FUTURE DIRECTIONS

Does IolR directly regulate the CobB deacetylase the acetyl-CoA synthetase? Our data show that IolR directly binds to and regulates the *pat* in *S. enterica* (Hentchel *et al*, unpublished data). While there is evidence that IolR also regulates expression of *acs* and *cobB*, the mechanism of this regulation is unclear (Hentchel *et al*, unpublished data). Gel shift assays need to be performed with IolR protein and the *acs* and *cobB* promoters to determine if IolR directly binds to and regulates these regions, or if there is another mechanism of indirect regulation. It has also been previously difficult to determine an IolR consensus site (16). If *acs* and *cobB* are directly regulated by IolR, DNA footprinting studies could be performed and these data added to previously known regulation targets could provide a framework for the development of an IolR consensus site.

Why is IolR needed to integrate the expression of the RLA system with that of its substrate, Acs? It is interesting that the repressor of *myo*-inositol catabolism (IolR) is responsible for activation of *pat*, *cobB*, and *acs* expression on various carbon sources. The data suggests that IolR is needed for full activation of the RLA system in growth containing low acetate, a condition in which activity of the RLA system is known to be important (Hentchel *et al*, unpublished data). Other data show that *pat* and *acs*, but not *cobB* expression are controlled in part by the catabolite repressor protein Crp. The link between carbon regulators and the RLA system needs further elucidation.

Is RLA function required for optimum growth on* myo-*inositol? Recently published acetylomes of *Bacillus subtilis* and *Erwinia amylovora* (17, 18) identified two enzymes involved in the degradation of *myo*-inositol, the malonate semialdehyde dehydrogenase (IolA) and carbohydrate kinase (IolC) amongst the acetylated proteins. It is not clear if the activity these

enzymes are under RLA control, but if so, it could provide a link between IolR regulation of RLA and RLA involvement in *myo*-inositol utilization.

How does* S. enterica *sense and respond to methionine sulfoximine? Preliminary work in *S. enterica* showed that the transcriptional regulators LRP and H-NS might play a role, either directly or indirectly, in the regulation of *mddA* (Hentchel *et al*, unpublished data). It is not known at this time if and how these regulators affect expression of *mddA*. Studies examining the cascade of events from sensing methionine sulfoximine in the environment to up-regulation of *mddA* expression need to be performed before we fully understand how the cell responds to this environmental stress.

What happens to acetylated MSX, MSO, and PPT? After acetylation by MddA, acetyl-methionine sulfoximine, acetyl-methionine sulfone, and acetyl-phosphinothricin can no longer bind to and inhibit glutamine synthetase and are effectively rendered non-toxic. It would be interesting to know what happens to these compounds after they are detoxified. It is doubtful there is a deacetylase present in the cell that deacetylates them, as removal of the acetyl moiety would cause growth inhibition via inactivation of glutamine synthetase to resume. It is possible once acetylated the acetylated compounds are (i) exported into the supernatant, or (ii) reused in some manner by the cell to recycle carbon. If acetyl-methionine sulfoximine or acetyl-methionine sulfone were somehow reused by the cell, the data indicate that free methionine is not the outcome, as growth of a methionine auxotroph cannot be restored by either acetylated or non-acetylated methionine sulfoximine or methionine sulfone (8).

Why do cells encode multiple phosphinothricin acetyltransferases? Organisms on average encode ~25 GNATs. It is perplexing that 2 of these 25 would be dedicated to the acetylation and detoxification of two closely related compounds, methionine sulfoximine and phosphinothricin.

Many soil-dwelling organisms could be exposed to the presence of phosphinothricin routinely, as the compound is produced by *Streptomyces* spp., which are prolific in the environment (19). However, it is not known where bacteria would be exposed to methionine sulfoximine or methionine sulfone. In the 1900's methionine sulfoximine was produced by the bleaching of flour by nitrogen trichloride, and is naturally produced by the *Connaraceae* plant species, only present in tropical locations (20-22) Oxidation of methionine residues typically results in production of methionine sulfoxide, not methionine sulfone (23-25). It is possible that a host response (nitric, oxidative stress responses) could generate these compounds *in vivo* (26), or that these compounds are present as the result of a normal metabolic pathway (27). However, none of these scenarios have been explored.

What are the structural differences that determine specificity of annotated phosphinothricin acetyltransferases? In order to fully understand the substrate specificity of the annotated phosphinothricin acetyltransferases, structural studies at the atomic level need to be performed. To date, there are crystal structures for this subclass of GNAT enzymes from *P. aeurginosa* and *A. baylyi* (14, 15). Comparisons of protein structure may allow us to determine how and why and particular GNAT annotated as a phosphinothricin acetyltransferase is able to acetylate specific compounds among closely related structural homologues. This in turn will allow us to properly predict and annotate the function of uncharacterized phosphinothricin acetyltransferases.

REFERENCES

1. **Smith JS, Brachmann CB, Celic I, Kenna MA, Muhammad S, Starai VJ, Avalos JL, Escalante-Semerena JC, Grubmeyer C, Wolberger C, Boeke JD.** 2000. A

phylogenetically conserved NAD(+)-dependent protein deacetylase activity in the Sir2 protein family. *Proc. Natl. Acad. Sci. USA*. **97:**6658-6663.

2. **Starai VJ, Escalante-Semerena JC.** 2004. Identification of the protein acetyltransferase (Pat) enzyme that acetylates acetyl-CoA synthetase in *Salmonella enterica*. *J. Mol. Biol.* **340:**1005-1012.

3. **Thao S, Chen CS, Zhu H, Escalante-Semerena JC.** 2010. *N*(ε)-Lysine acetylation of a bacterial transcription factor inhibits its DNA-binding activity. *PLOS ONE* **5:**e15123.

4. **Hu LI, Chi BK, Kuhn ML, Filippova EV, Walker-Peddakotla AJ, Basell K, Becher D, Anderson WF, Antelmann H, Wolfe AJ.** 2013. Acetylation of the response regulator RcsB controls transcription from a small RNA promoter. *J. Bacteriol.* **195:**4174-4886.

5. **Lima BP, Antelmann H, Gronau K, Chi BK, Becher D, Brinsmade SR, Wolfe AJ.** 2011. Involvement of protein acetylation in glucose-induced transcription of a stress-responsive promoter. *Mol. Microbiol.* **81:**1190-1204.

6. **Deblock M, Botterman J, Vandewiele M, Dockx J, Thoen C, Gossele V, Movva NR, Thompson C, Vanmontagu M, Leemans J.** 1987. Engineering herbicide resistance in plants by expression of a detoxifying enzyme. *EMBO J* **6:**2513-2518.

7. **Murakami T, Anzai H, Imai S, Satoh A, Nagaoka K, Thompson CJ.** 1986. The bialaphos biosynthetic genes of *Streptomyces-Hygroscopicus* - Molecular-cloning and characterization of the gene-cluster. *Mol. Gen. Genet.* **205:**42-50.

8. **Hentchel KL, Escalante-Semerena JC.** 2015. In *Salmonella enterica*, the Gcn5-related acetyltransferase MddA (formerly YncA) acetylates methionine sulfoximine and methionine sulfone, blocking their toxic effects. *J. Bacteriol.* **197:**314-325.

9. **Tucker AC, Escalante-Semerena JC.** 2010. Biologically active isoforms of CobB sirtuin deacetylase in *Salmonella enterica* and *Erwinia amylovora*. *J. Bacteriol.* **192:**6200-6208.

10. **Wright GD, Ladak P.** 1997. Overexpression and characterization of the chromosomal aminoglycoside 6'-*N*-acetyltransferase from *Enterococcus faecium*. *Antimicrob. Agents Chemother.* **41:**956-960.

11. **Davies J, Wright GD.** 1997. Bacterial resistance to aminoglycoside antibiotics. *Trends Microbiol.* **5:**234-240.

12. **Wolf E, Vassilev A, Makino Y, Sali A, Nakatani Y, Burley SK.** 1998. Crystal structure of a GCN5-related *N*-acetyltransferase: *Serratia marcescens* aminoglycoside 3-N-acetyltransferase. *Cell.* **94:**439-449.

13. **Draker KA, Northrop DB, Wright GD.** 2003. Kinetic mechanism of the GCN5-related chromosomal aminoglycoside acetyltransferase AAC(6')-Ii from *Enterococcus faecium*: evidence of dimer subunit cooperativity. *Biochemistry.* **42:**6565-6574.

14. **Davies AM, Tata R, Beavil RL, Sutton BJ, Brown PR.** 2007. *L*-Methionine sulfoximine, but not phosphinothricin, is a substrate for an acetyltransferase (gene PA4866) from *Pseudomonas aeruginosa*: structural and functional studies. *Biochemistry.* **46:**1829-1839.

15. **Davies AM, Tata R, Snape A, Sutton BJ, Brown PR.** 2009. Structure and substrate specificity of acetyltransferase ACIAD1637 from *Acinetobacter baylyi* ADP1. *Biochimie.* **91:**484-489.

16. **Kroger C, Stolz J, Fuchs TM.** 2010. *myo*-Inositol transport by *Salmonella enterica* serovar Typhimurium. *Microbiology.* **156:**128-138.

17. **Kim D, Yu BJ, Kim JA, Lee YJ, Choi SG, Kang S, Pan JG.** 2013. The acetylproteome of Gram-positive model bacterium *Bacillus subtilis*. *Proteomics.* **13:**1726-1736.

18. **Wu X, Vellaichamy A, Wang D, Zamdborg L, Kelleher NL, Huber SC, Zhao Y.** 2013. Differential lysine acetylation profiles of *Erwinia amylovora* strains revealed by proteomics. *J. Proteomics.* **79:**60-71.

19. **Ogawa Y, Tsuruoka T, Inoue S, Niida T.** 1973. Studies on a new antibiotic SF-1293. II. Chemical structure of antibiotic SF-1293. *Sci. Rep. Meijii. Kaisha.* **13:**42-48.

20. **Bentley HR, Booth RG, et al.** 1948. Action of nitrogen trichloride on proteins; production of toxic derivative. *Nature.* **161:**126.

21. **Jeannoda VL, Rakoto-Ranoromalala DA, Valisolalao J, Creppy EE, Dirheimer G.** 1985. Natural occurrence of methionine sulfoximine in the Connaraceae family. *J. Ethnopharmacol.* **14:**11-17.

22. **Bentley HR, Mc DE, et al.** 1949. Action of nitrogen trichloride on proteins; progress in the isolation of the toxic factor. *Nature.* **163:**675.

23. **Cabiscol E, Piulats E, Echave P, Herrero E, Ros J.** 2000. Oxidative stress promotes specific protein damage in *Saccharomyces cerevisiae*. *J. Biol. Chem.* **275:**27393-27398.

24. **Drazic A, Winter J.** 2014. The physiological role of reversible methionine oxidation. *BBA-Proteins Proteom*. **1844:**1367-1382.

25. **Stadtman ER, Moskovitz J, Levine RL.** 2003. Oxidation of methionine residues of proteins: Biological consequences. *Antioxid. Redox. Sign.* **5:**577-582.

26. **Winter SE, Thiennimitr P, Winter MG, Butler BP, Huseby DL, Crawford RW, Russell JM, Bevins CL, Adams LG, Tsolis RM, Roth JR, Baumler AJ.** 2010. Gut inflammation provides a respiratory electron acceptor for *Salmonella*. *Nature.* **467:**426-4269.

27. **Lambrecht JA, Schmitz GE, Downs DM.** 2013. RidA proteins prevent metabolic damage inflicted by PLP-dependent dehydratases in all domains of life. *MBio.* **4:**e00033-00013.